Department of Theoretical and Cosmos Physics
University of Granada

Effective Lagrangian Description of Physics Beyond the Standard Model and Electroweak Precision Tests

Jorge de Blas Mateo

Ph.D. Advisors:
Francisco del Águila Giménez
Manuel María Pérez-Victoria Moreno de Barreda

– May, 2010 –

Editor: Editorial de la Universidad de Granada
Autor: Jorge de Blas Mateo
D.L.: GR 3223-2010
ISBN: 978-84-693-4312-8

Departamento de Física Teórica y del Cosmos
Universidad de Granada

Descripción con Lagrangianos Efectivos de Física Más Allá del Modelo Estándar y Tests Electrodébiles de Precisión

Jorge de Blas Mateo

Directores:
Francisco del Águila Giménez
Manuel María Pérez-Victoria Moreno de Barreda

– Mayo de 2010 –

D. Francisco del Águila Giménez, Catedrático de Universidad, y D. Manuel María Pérez-Victoria Moreno de Barreda, Profesor Titular de Universidad,

CERTIFICAN: que la presente memoria, *Effective Lagrangian Description of Physics Beyond the Standard Model and Electroweak Precision Tests* (*Descripción con Lagrangianos Efectivos de Física Más Allá del Modelo Estándar y Tests Electrodébiles de Precisión*), ha sido realizada por D. Jorge de Blas Mateo bajo su dirección en el Departamento de Física Teórica y del Cosmos, así como que éste ha disfrutado de estancias en el extranjero, durante un periodo superior a tres meses, tanto en la división teórica del CERN (Suiza) como en el Instituto Superior Técnico de Lisboa (Portugal).

Granada, 20 de Mayo de 2010

Fdo: Francisco del Águila Giménez Manuel María Pérez-Victoria Moreno de Barreda

Contents

Introduction **1**

Introducción **5**

1 Effective field theories: The Standard Model and beyond **9**
1.1 The Standard Model of particle physics 9
1.2 The effective Lagrangian approach for the description of new physics 18
1.2.1 The dimension-six effective Lagrangian 23

2 Phenomenological implications of the dimension-six effective Lagrangian **27**
2.1 The effective Lagrangian after electroweak symmetry breaking 28
2.1.1 Scalar potential 28
2.1.2 Redefinition of gauge fields, coupling constants and vector boson masses. . 29
2.1.3 Fermion masses and rotation matrices 31
2.1.4 Neutral and charged current couplings I: Direct corrections 33
2.1.5 Neutral and charged current couplings II: Indirect corrections 35
2.1.6 Yukawa interactions 40
2.2 Corrections to electroweak precision observables 42
2.2.1 Z lineshape observables 42
2.2.2 W mass and width 45
2.2.3 Low-energy observables 46
2.2.4 Unitarity of the Cabibbo-Kobayashi-Maskawa matrix 51
2.2.5 Fermion pair production at LEP 2 52
2.3 Electroweak precision constraints on dimension-six operators 53

3 New matter fields: Extra spin-1/2 particles **61**
3.1 Extending the Standard Model with vector-like fermions 63
3.2 The effective Lagrangian for new fermions 65
3.3 The global fit for extra leptons 70
3.3.1 Numerical results 71
3.3.2 Large neutrino mixing and the Higgs mass 73
3.4 Conclusions 78

4 New interactions: Extra spin-1 particles **83**
4.1 General extra vector bosons 84
4.2 Effective description of new vector bosons 88
4.3 Limits on new vector bosons 89

4.3.1 Neutral singlet $\mathcal{B}$ . . . 91
4.3.2 Left-handed triplet: $\mathcal{W}$ . . . 94
4.3.3 Charged singlet: $\mathcal{B}^1$ . . . 95
4.3.4 Fermiophobic triplet: $\mathcal{W}^1$ . . . 96
4.3.5 Leptophilic vector: $\mathcal{L}$ . . . 96
4.3.6 Singlet vector leptoquarks: $\mathcal{U}^2$ and $\mathcal{U}^5$ . . . 98
4.3.7 Doublet vector leptoquarks: $\mathcal{Q}^1$ and $\mathcal{Q}^5$ . . . 98
4.3.8 Triplet vector leptoquark: $\mathcal{X}$ . . . 99
4.4 Several extra vectors . . . 99
4.4.1 Nonuniversal couplings and the bottom forward-backward asymmetry . . . 101
4.5 New vector bosons and the Higgs mass . . . 104
4.6 Conclusions . . . 104
4.7 Addendum: Operator coefficients in the effective Lagrangian . . . 107

5 Beyond the Standard Model dimension-six effective Lagrangian 115
5.1 The dimension-six effective Lagrangian with light right-handed neutrinos . . . 117
5.1.1 Contributions to precision observables . . . 118
5.2 Looking for right-handed neutrino signals at neutrino factories . . . 120
5.2.1 Electroweak precision data constraints on right-handed neutrino interactions 122
5.2.2 A simple Standard Model extension . . . 124
5.2.3 Neutrino factory predictions . . . 125
5.2.4 Further phenomenological implications . . . 127

Conclusions 129

Conclusiones 131

Appendices 133

A Experimental data and fit methodology 133
A.1 Experimental data . . . 133
A.2 The Standard Model fit . . . 136

List of figures 143

List of tables 147

Bibliography 151

Introduction

With the only exception of neutrino oscillations, the last decade experiments have confirmed the validity of the Standard Model of particle physics for the description of physical phenomena at energies below few hundred of GeV. In particular, with a precision in many cases of the order of 1‰, the electroweak precision data coming mainly from experiments performed at CERN and Tevatron have tested the model to the level of radiative corrections showing an excellent agreement. The model, however, is not completely satisfactory as it leaves too many open questions and suffers from several fine-tuning problems. This motivates our belief that new physics may complete it when we move to higher energies. In particular, if our understanding of electroweak symmetry breaking is correct, one would expect that new physics explaining why the electroweak scale is stable under quantum corrections must be present at energies of the order of the TeV. Many different scenarios have been proposed to address this question: supersymmetry, extra dimensions, composite or Little Higgs models, ... which, in turn, hold many different possible realizations. Irrespective of the nature of the new physics, this must be consistent with the existing electroweak precision data. Thus, within a given model a comparison of the extra corrections to the precision observables with the available data is required in order to test its viability. But, as emphasized before there are too many different scenarios and it is also possible that none of them is correct. Ultimately, given our ignorance about nature at high energies, a model-independent approach is a suitable choice for the analysis of the implications of new physics. On the other hand, the excellent agreement of the Standard Model predictions with the data does not leave too much room for new effects. This typically implies that the characteristic mass scale of the new particles is well above the energies where the experiments take place, as it is a rather general property of nature that high energy effects have little impact in the low energy physics. There is also the possibility that the new physics may come in the form of complex combinations of different particles in such a way that their effects approximately cancel, giving a small neat contribution to most of the precision observables and thus preserving, or hopefully improving, the agreement between the model predictions and the data. Therefore, an approach that allows to easily compare and combine the dominant effects of different types of new physics is very convenient.

Effective Field Theories offer a natural framework for studying physics beyond the Standard Model when the characteristic scale of the new particles is distinctively separated from the energies we have explored so far. If these heavy particles exist, even though they have not been directly produced, they can be exchanged as virtual states in physical processes and then result in observable effects. These new virtual effects are the ones that can be described by using an effective theory. Suppose we know the form of the high energy Lagrangian describing the observed light particles as well as a set of extra heavy fields. For the purpose of describing the physics at energies below the lowest threshold of the non-standard particles, one can integrate the heavy degrees of freedom out of the theory, and obtain an effective Lagrangian where the virtual effects of heavy modes are either absorbed in the renormalization of the existing operators of mass dimension $d \leq 4$ in

the Lagrangian for the light degrees or freedom, or encoded in the coefficients of an infinite set of new operators with mass dimensions $d > 4$. As higher dimensional operators come suppressed by inverse powers of the heavy mass scale, ordering such infinite set according to their dimensionality provides a systematic way of classifying the relevant effects of the new particles since the higher the scaling dimension of the operators, the more suppressed their effects. As we can only achieve a finite accuracy in the experimental data, in practice only a certain finite subset of the effective operators needs to be considered. For the accuracy of the current data, it suffices in general to use the effective Lagrangian up to dimension six. Another advantage of effective field theories is that they can be used for completely model-independent analyses, using only the light field content and the required symmetries, which in our context are both given by the Standard Model. Therefore, this approach combines the two qualities mentioned in the above paragraph: it is an excellent tool to isolate and compare the leading effects of different sources of new physics via their contributions to the higher dimensional operators, and it does not necessarily require to know the nature of the underlying theory, so it can be used for model-independent studies.

In this thesis we use effective Lagrangian techniques to perform a semi model independent analysis of physics beyond the Standard Model. Most of our attention is focused on the study of the effects resulting from the presence of new matter fields (heavy extra fermions with special attention to the case of new leptons) or new interactions (heavy extra vector fields), which are predicted in a large class of Standard Model extensions. We do not make any assumption regarding the underlying theory where these new particles may come from. In this sense, our results are model independent and therefore have a wide range of applicability, being of special interest for model building. In order to yield contributions to physical observables, the heavy particles must be coupled to the Standard Model ones. This requirement together with renormalizability as well as gauge invariance of such interactions allow us to classify all the possible additions according to their quantum numbers. We construct the most general Lagrangian that can be built assuming the Standard Model symmetries and using both the standard and the extra particles, and then integrate the latter out of the theory to find the corresponding effective Lagrangian. This is one of the results of this thesis: we provide general expressions for the coefficients of the operators in the dimension-six effective Lagrangian in terms of the couplings and masses of the extra particles. In the next step, we study the implications the extra virtual corrections would have on precision observables. As mentioned above, the data leaves small room for new physics. This reduces the dominant effects to be of the order of the experimental accuracy and then, together with our requirement that the new particles interact at tree level with the Standard Model ones, justifies to restrict ourselves to a leading tree-level approach for the computation of the extra corrections. All these results are finally used to extract the experimental restrictions on the parameter space describing the new physics, by confronting the theoretical predictions for the precision observables, including the new corrections, with the experimentally measured values. For that purpose, a global fit to the existing electroweak precision data is performed. A detailed discussion of the experimental data is also given in an appendix. The results of the fit are expressed in terms of limits on the values that the masses and couplings of the new particles can have. Obtaining these limits, as well as identifying "holes" in the data that could be eventually filled by some kind of new physics, is the main goal of this thesis. The constraints obtained here are of relevance for the simulation of the production and decay of the heavy particles at large colliders. This kind of analysis, however, lies beyond the scope of this thesis and we will restrict at most to a qualitative description of the implications of our results for the *Large Hadron Collider* or future lepton colliders.

Along most of this work we will deal with the implications of the "standard" effective Lagrangian, constructed by assuming no more than the Standard Model particles and symmetries. Extending the method to different scenarios is straightforward: it only requires to incorporate

additional light fields. This enlarges the number of operators that can be built at each order in the effective Lagrangian expansion. On the other hand, we can impose extra symmetries of the high energy theory, restricting the possible terms that can be written. While the latter has no limitation a priori, as long as the Standard Model symmetries become manifest at low energies, the absence of experimental confirmation on the existence of extra particles greatly constrains the freedom we have for enlarging the light spectrum. One possible extension is to consider the existence of light right-handed neutrino singlets, which would be necessary in order to explain neutrino masses if these were of Dirac type. These particles have no interactions within a minimal extension of the Standard Model, so they manifest only through neutrino masses, and are unobservable in laboratory experiments where the relevant energies are much larger. They may however come accompanied by some non-standard interactions if they arise from some more complicated extension, as it is the case of models with an enlarged gauge symmetry. Thus, the interesting question is whether these light right-handed neutrinos have further observable interactions beyond their masses, which motivates the study of the suggested effective Lagrangian extension. If sizable, it may be possible that these new interactions may result in observable effects that could eventually guide us in the search for these elusive particles. This is considered in the last part of this thesis which, in turn, closes our analysis on extra leptons.

The thesis is organized as follows:

In Chapter 1 the Standard Model is briefly reviewed, and the problems that suggest the presence of new physics are described. Then, the formalism of the effective Lagrangian approach for the study of an arbitrary extension of the model is presented, explaining all the hypotheses that will apply throughout the rest of this work, and establishing the notation for the operators relevant to our analysis.

Chapter 2 is devoted to a fully model-independent analysis of the phenomenology of the extension of the Standard Model with the new effective operators. We compute the corrections to the masses and couplings of the standard particles induced by the presence of the dimension-six operators in the Lagrangian after electroweak symmetry breaking. Then the resulting Lagrangian is used to compute the corrections to the electroweak precision observables which will enter in the global fits in the subsequent chapters. We also discuss here what operators can be actually constrained by the available precision data.

The analysis of the implications of the presence of new particles is covered by Chapters 3 and 4. Chapter 3 presents the analysis of the implications of new extra fermions in the spectrum, focussed in the case of new leptons. Chapter 4 covers the analysis of extra vector bosons. The effective Lagrangian corresponding to the integration of the heavy particles is computed, and the values of the coefficients of the dimension-six operators are reported. As announced, these results are used to perform a global fit to the electroweak precision data and to derive the existing experimental bounds on these new particles.

The last chapter of this thesis covers the corrections that must be applied to the "standard" effective Lagrangian approach used in the previous chapters in order to extend the formalism to describe the presence in the spectrum of light right-handed neutrinos. As an application of the method we explore the possibility of finding evidence of the existence of these particles at neutrino factories if some non-standard interactions are large enough. As we will see, this seems to be allowed by the data but requires a precise cancellation between different effects.

The main results of this Ph. D. thesis are finally summarized in the Conclusions. These are followed by one appendix where we explain the experimental data included in our fits as well as the methodology followed. Details of the Standard Model fit, used through out the discussion in the main text, are also given here.

The material contained in this thesis has lead to several publications. The analysis of the

implications of new leptons studied in Chapter 3 has been published in Refs. [1, 2, 3, 4]. For the new vectors discussed in Chapter 4 our studies have also lead to one publication [5]. Finally, the main discussion in Chapter 5 can be found in references [6, 7]. [1]

[1] My works with A. Falkowski, M. Pérez-Victoria and S. Pokorsky [8], and with P. Langacker, G. Paz and L-T. Wang [9] lie somewhat apart from the main topic of this thesis and have not been included here.

Introducción

Con la única excepción del descubrimiento de las oscilaciones de neutrinos, los experimentos realizados en las últimas décadas han confirmado la validez del Modelo Estándar de física de partículas para la descripción de los fenómenos físicos a energías por debajo de unos cientos de GeV. En particular, con una precisión en muchos casos del orden del 1‰, los datos electrodébiles de precisión obtenidos mayormente en los experimentos realizados en el CERN y en Tevatron han comprobado las predicciones del modelo al nivel de las correcciones cuánticas, encontrando un acuerdo excelente. El modelo, sin embargo, no es completamente satisfactorio ya que deja muchas cuestiones abiertas y padece de varios problemas de naturalidad. Esto motiva nuestra creencia en que debe haber nueva física a energías más altas. En particular, si la forma en que entendemos la rotura de la simetría electrodébil es correcta, esperamos que, a energías del order del TeV, haya nueva física que explique el por qué la escala electrodébil es estable frente a correcciones cuánticas. Varios tipos de escenarios han sido propuestos para intentar explicar esta cuestión: supersimetría, dimensiones extra, modelos de Higgs "pequeño" o compuesto, ..., cada uno de ellos con muchas realizaciones posibles. Independientemente de cual sea la naturaleza de la nueva física, ésta debe ser compatible con los datos electrodébiles de precisión de los que disponemos. De esta forma, de cara a comprobar la validez de un modelo dado, es necesario comprobar que las nuevas contribuciones a los observables de precisión están de acuerdo con los valores obtenidos experimentalmente. Para este propósito, dada la gran cantidad de modelos existentes, con la posibilidad de que ninguno sea el correcto, y, en última instancia, nuestra ignorancia acerca de la naturaleza a altas energías, el uso de una descripción independiente de modelo es una opción recomendable. Por otro lado, el excelente acuerdo de los datos con las predicciones del Modelo Estándar deja muy poco lugar para nuevos efectos. Esto implica típicamente que la escala de masa característica de las nuevas partículas debe ser considerablemente mayor que las energías a las que disponemos de datos, pues es una propiedad bastante general de la naturaleza que la física a una escala dada de energías tiene un impacto reducido a energías mucho menores. Otra posibilidad diferente es que la nueva física sea lo suficientemente compleja como para las contribuciones de distintas partículas cancelen de manera aproximada, dejando una contribución neta que permita preservar o incluso mejorar el acuerdo entra los datos y la teoría. Por lo tanto, un método de trabajo que permita comparar y combinar los efectos dominantes de diferentes tipos de nueva física resulta también muy conveniente.

Las teorías de campos efectivas ofrecen un marco de trabajo natural para el estudio de física más allá del Modelo Estándar en aquellos casos en los que la escala de masas de las nuevas partículas esté significativamente por encima de las energías que hemos explorado. Si tales partículas existen, aunque no han podido ser producidas directamente aún, pueden ser intercambiadas como estados virtuales en procesos físicos y por lo tanto pueden tener efectos observables. Este tipo de efectos virtuales son los que se pueden describir usando una teoría efectiva. Supongamos que conocemos la forma del Lagrangiano a altas energías que describe las interacciones de las partículas conocidas y de un conjunto dado de campos pesados. Si lo que nos interesa es la física a energías muy por

debajo del umbral de producción de las partículas extra, podemos integrar estas últimas de la teoría, obteniendo un nuevo Lagrangiano para los modos ligeros, donde los efectos virtuales de los modos pesados son reabsorvidos en la renormalización de los campos ligeros y sus acoplamientos, o aparecen en la forma de contribuciones a los coeficientes de un conjunto infinito de operadores con dimensiones de masa $d > 4$. Dado que estos últimos vienen suprimidos por potencias inversas de la escala de masas de las partículas pesadas, el ordenar los nuevos operadores de acuerdo a su dimensión es un método sistemático para clasificar los efectos de las nuevas partículas, ya que cuanto mayor sea la dimensión del operador más suprimidos estarán sus efectos. En consecuencia, dado que sólo podemos conseguir una precisión experimental finita, en la práctica sólo un subconjunto finito de los operadores efectivos es relevante. Para la precisión actual, en general es suficiente considerar el Lagrangiano efectivo hasta dimensión seis. Otra ventaja de las teorías de campos efectivas es que pueden usarse para estudios independientes de modelo, ya que para construir el Lagrangiano efectivo más general sólo necesitamos conocer el contenido de campos ligeros así como las simetrías de la teoría, y ambos vienen dados por los del Modelo Estándar. Por lo tanto, este método de trabajo combina las dos cualidades mencionadas en el parrafo anterior: es una herramienta excelente para aislar y comparar los efectos dominantes de diferentes tipos de nueva física a través de sus contribuciones a los operadores de dimensión superior, y no requiere necesariamente conocer la naturaleza de la teoría subyacente de manera que puede utilizarse para estudios independientes de modelo.

En esta tesis usamos técnicas de Lagrangianos efectivos para realizar análisis de física más allá del Modelo Estándar cuasi-independientes de modelo. La mayor parte de nuestra atención se centra en el estudio de los efectos resultantes de la presencia de nuevos campos de materia (nuevos fermiones pesados, con especial atención al caso de nuevos leptones) o nuevas interacciones (campos vectoriales masivos adicionales), los cuales son predichos por una clase amplia de extensiones del Modelo Estándar. No realizamos ninguna suposición adicional en relación a la teoría de donde estas partículas pudieran venir. En este sentido, nuestros resultados son independientes de modelo y tienen un amplio rango de aplicación. Para poder dar contribuciones a los observables físicos medidos hasta el momento, las partículas pesadas deben acoplarse a las del Modelo Estándar. Este requisito junto con la renormalizabilidad, así como la invariancia gauge de las interacciones, nos permite clasificar todos los casos posibles de acuerdo con los números cuánticos de las nuevas partículas. Para cada uno de ellos construimos el Lagrangiano más general compatible con las simetrías del Modelo Estándar y la extensión correspondiente del contenido de campos, e integramos los pesados de la teoría obteniendo el correspondiente Lagrangiano efectivo. Este es uno de los resultados de esta tesis: proporcionamos expresiones generales para los coeficientes de los operadores de dimensión seis en términos de los acoplamientos y masas de las nuevas partículas. Utilizando el Lagrangiano efectivo resultante, estudiamos las implicaciones de las nuevas contribuciones a los observables de precisión. Estas son calculadas usando una aproximación a nivel árbol, la cual da en general los efectos dominantes y está justificada por el hecho de que estos deben ser del orden de los errores experimentales, dado el buen acuerdo entre los datos y las predicciones del Modelo Estándar. Los resultados de todos estos cálculos son finalmente empleados para obtener las restricciones experimentales sobre el espacio de parámetros de la nueva física, confrontando las predicciones teóricas que incorporan las nuevas contribuciones, con los datos experimentales. Para ello realizamos un ajuste global de las extensiones propuestas a los datos electrodébiles de precisión existentes. Una discusión detallada de los datos empleados se incluye en un apéndice. Los resultados del ajuste son expresados en términos de límites sobre los valores de las masas y acoplamientos de las nuevas partículas. El objetivo principal de esta tesis es obtener dichos límites, así como identificar los posibles "huecos" en los datos que pudieran ser eventualmente cubiertos por algún tipo de nueva física. Los límites obtenidos son relevantes para la simulación de la producción y desintegración

de las partículas pesadas en grandes colisionadores. Ese tipo de análisis, sin embargo, va más allá del objetivo de esta tesis y como mucho nos restringiremos a una descripción cualitativa de las implicaciones de nuestro resultados en el LHC o futuros colisionadores de leptones.

El Lagrangiano efectivo utilizado durante la mayor parte de este trabajo está construido suponiendo nada más que las partículas y simetrías del Modelo Estándar. Extender el método a otros escenarios diferentes es sencillo: tan sólo necesitamos añadir nuevas partículas ligeras. Esto aumenta el número de operadores que podemos construir a cada orden en la expansión del Lagrangiano efectivo. Por otro lado, se pueden imponer simetrías de la teoría a altas energías, restringiendo los términos que pueden escribirse. Mientras que el segundo procedimiento no tiene limitación en principio, siempre que las simetrías del Modelo Estándar sean manifiestas a bajas energías, la ausencia de confirmación experimental sobre la existencia de partículas adicionales limita significativamente la libertad que tenemos para aumentar el espectro de partículas ligeras. Una extensión posible sería considerar la existencia de neutrinos singlete con quiralidad positiva, los cuales son necesarios para explicar las masas de los neutrinos si estas son de tipo Dirac. Estas partículas no tienen interacciones en una extensión minimal del Modelo Estándar, de forma que sólo pueden manifestarse a través de la masa de los neutrinos, y por lo tanto no son observables en los experimentos de laboratorio, donde las energías relevantes son mucho mayores. Podrían sin embargo venir acompañados de nuevas interacciones si surgen de extensiones más complicadas, como modelos con simetría gauge extendida. De este modo, la cuestión interesante es si estos nuevos neutrinos tienen interacciones observables aparte de sus masas, lo que motiva la extensión del Lagrangiano efectivo sugerida. Si tales interacciones son apreciables podrían dar lugar a efectos observables que nos guiáran en la búsqueda de estas partículas. Este tema es estudiado en la última parte de la tesis, la cual cierra además nuestro análisis de nuevos leptones.

En las siguientes lineas se detalla la estructura de esta tesis, resumiendo brevemente el contenido de cada capítulo:

En el Capítulo 1 se introduce el Modelo Estándar de física de partículas, explicando los problemas que sugieren la presencia de nueva física. Tras esto, se presenta el formalismo de la aproximación de Lagrangianos efectivos para el estudio de nueva física. Aquí se explica en detalle las hipótesis que utilizaremos a lo largo de este trabajo. Asimismo se establecen los operadores de dimensión seis relevantes para nuestros análisis.

El Capítulo 2 está dedicado a un estudio totalmente independiente de modelo de la fenomenología de la extensión del Modelo Estándar con los nuevos operadores introducidos. Estudiamos cuáles son los efectos de los mismos sobre las masas y acoplamientos de las partículas estándar una vez se rompe la simetría electrodébil, distinguiendo entre contribuciones directas e indirectas, donde las últimas se deducen de la influencia de los operadores en procesos físicos a partir de los cuales se derivan los parámetros de la teoría. Usando el Lagrangiano resultante calculamos las correcciones dominantes a los observables electrodébiles de precisión, proporcionando fórmulas explícitas para las nuevas contribuciones. Este análisis nos permite distinguir de entre todos los operadores considerados aquellos de los que podemos obtener información usando los datos experimentales actuales. Las principales restricciones de los datos electrodébiles de precisión sobre cada uno de dichos operadores son estudiadas. También discutimos el impacto de estos en la determinación indirecta de la masa del Higgs.

En el Capítulo 3 nos centramos en las implicaciones de la existencia de nuevos fermiones pesados no-quirales. Clasificamos todos los nuevos leptones y quarks que pueden mezclarse con los fermiones del Modelo Estándar, y calculamos el Lagrangiano efectivo resultante de su integración. Asimismo, realizamos un análisis fenomenológico de los efectos de los nuevos leptones sobre los datos electrodébiles de precisión, y obtenemos límites sobre la mezcla de estos con los leptones ligeros. También discutimos la correlación entre los efectos de dicha mezcla y los del Higgs, centrándonos

en los casos en los que dicha correlación nos permite relajar los límites sobre la masa del escalar.

De manera análoga al Capítulo 3, en el Capítulo 4 analizamos los efectos de nuevas partículas de tipo vectorial. Siguiendo una estructura similar, realizamos una clasificación de los nuevos vectores que puedan dar un efecto observable dentro de nuestras aproximaciones, y los integramos de la teoría obteniendo los coeficientes de los operadores de dimensión seis en el Lagrangiano efectivo. Realizando el correspondiente ajuste a los datos electrodébiles de precisión, obtenemos de nuevo los límites sobre los parámetros físicos de las nuevas partículas, discutiendo en particular la relevancia de los datos de LEP 2 en su obtención. El efecto sobre la asimetría angular del quark b, una de las pocas discrepancias con la predicción del Modelo Estándar, y aquellos casos en los que los nuevos vectores permiten acomodar un Higgs pesado con los datos experimentales son también estudiados en detalle.

El último capítulo de esta tesis se dedica a las modificaciones que deben aplicarse al Lagrangiano efectivo empleado en los capítulos anteriores de cara a extender el formalismo para poder describir la presencia en el espectro de neutrinos singlete con quiralidad positiva. Como una aplicación del método investigamos la posibilidad de encontrar evidencia de la existencia de estas partículas en factorías de neutrinos, si ciertas interacciones no estándar son lo suficientemente grandes. Como allí se discute, estas son permitidas por los datos aunque requieren una cancelación adecuada entre distintos efectos. En ese caso se espera un déficit en el número de eventos observados en un detector cercano, que puede ser tan grande como $\sim 10\,\%$. Una realización posible de este escenario también es presentada.

Finalmente, se encuentra un apéndice donde explicamos los datos experimentales incluidos en nuestros análisis así como la metodología utilizada. También se proporcionan detalles del ajuste del Modelo Estándar, los cuales son utilizados o mencionados a lo largo de la discusión en el texto principal.

El material contenido en esta tesis ha dado lugar a varias publicaciones. El análisis de las implicaciones de los nuevos leptones en el Capítulo 3 ha sido publicado en [1, 2, 3, 4]. Para los nuevos vectores discutidos en el Capítulo 4 nuestros estudios han dado lugar a otro trabajo [5]. Finalmente, la discusión principal del Capítulo 5 puede encontrarse en las referencias [6, 7].[2]

[2] Mis trabajos en colaboración con A. Falkowski, M. Pérez-Victoria y S. Pokorsky [8], y con P. Langacker, G. Paz y L-T. Wang [9] no están directamente relacionados con el tema central de esta tesis y por lo tanto no han sido incluidos aquí.

Chapter 1

Effective field theories: The Standard Model and beyond

In 1961 Sheldon Glashow [10] proposed a model combining the electromagnetic and weak interactions, which was completed in 1967 by Steven Weinberg [11] and (independently in 1968) Abdus Salam [12]. Together with Quantum Chromodinamics (QCD) for the description of the strong interactions, it gave rise during the early seventies to what today is accepted as the Standard Model (SM) of particle physics. With the exception of the sector responsible of the electroweak symmetry breaking (EWSB), all particles in the spectrum of the electroweak model have been discovered up to complete three families in subsequent years[1], whereas the electroweak precision tests performed at the Large Electron-Positron collider (LEP), at the Slac Linear Accelerator Center (SLAC) and at Tevatron have confirmed the validity of the description of their interactions to the level of radiative corrections. There are, however, some issues that are either not addressed or not satisfactorily explained by the model and nowadays it is believed that, though it is a very good description of nature at energies up to the electroweak scale, it cannot be considered as the ultimate theory and needs to be extended in order to describe the physics at higher energy scales, i.e., it must be thought of as an effective theory.

In this chapter, apart from the mandatory review of the SM, we introduce the formalism of effective field theories, for physics *beyond the Standard Model*, which will be used in our analysis in the subsequent chapters of this thesis. Some good reviews of the SM (and beyond) used as reference for this chapter are [13, 14, 15, 16, 17, 18]. For reviews on effective field theories see for instance [19, 20, 21, 22, 23, 24].

1.1 The Standard Model of particle physics

The interactions in the SM are described by a renormalizable gauge quantum field theory with gauge group $SU(3)_c \otimes SU(2)_L \otimes U(1)_Y$, whose quantum numbers are known as color, weak isospin and hypercharge, respectively. The corresponding gauge fields are denoted by G^A_μ, W^a_μ and B_μ, with gauge indices $A = 1, 2, \ldots, 8$ and $a = 1, 2, 3$ labeling directions in the $SU(3)_c$ and $SU(2)_L$ Lie

[1] In 1974 the charm quark was uncovered, in 1975 the first evidence of the τ lepton was found and in 1977 the bottom quark was seen. We had to wait until 1995 for the discovery of the top quark and until 2000 for the confirmation of the τ neutrino, both observed at Fermilab. Meanwhile, during the eighties, the mediators of the electroweak charged and neutral current interactions were discovered at CERN.

algebras, respectively. The covariant derivative of the model is then given by

$$D_\mu = \partial_\mu + ig_s G_\mu^A \mathrm{T}_A + igW_\mu^a T_a + ig' B_\mu Y, \tag{1.1}$$

where g_s, g and g' are the $SU(3)_c$, $SU(2)_L$ and $U(1)_Y$ gauge coupling constants and T_A, T_a and Y the corresponding generators. The same notation as for the gauge fields is used for the field strengths

$$\begin{aligned} G_{\mu\nu}^A &= \partial_\mu G_\nu^A - \partial_\nu G_\mu^A - g_s\ f_{BC}^A G_\mu^B G_\nu^C, \\ W_{\mu\nu}^a &= \partial_\mu W_\nu^a - \partial_\nu W_\mu^a - g\ \varepsilon^{abc} W_\mu^b W_\nu^c, \\ B_{\mu\nu} &= \partial_\mu B_\nu - \partial_\mu B_\mu, \end{aligned} \tag{1.2}$$

with f_{BC}^A and ε_{abc} the $SU(3)_c$ and $SU(2)_L$ structure constants:

$$[\mathrm{T}_A, \mathrm{T}_B] = i f_{BC}^A \mathrm{T}_C \quad \text{and} \quad [T_a, T_b] = i\varepsilon_{abc} T_c. \tag{1.3}$$

Matter is chiral respect to the electroweak gauge group, $SU(2)_L \otimes U(1)_Y$, and consists of three fermion generations (or families) with left-handed (LH) components transforming as weak iso-doublets and right-handed (RH) ones as weak iso-singlets. Within each generation, labelled by lower case latin indices $i, j = 1, 2, 3$, there are three color-triplet species describing quarks

$$q_L^i = \begin{pmatrix} u_L^i \\ d_L^i \end{pmatrix} \sim (3,2)_{\frac{1}{6}}, \qquad u_R^i \sim (3,1)_{\frac{2}{3}}, \qquad d_R^i \sim (3,1)_{-\frac{1}{3}}, \tag{1.4}$$

and two color-singlet species describing leptons

$$l_L^i = \begin{pmatrix} \nu_L^i \\ e_L^i \end{pmatrix} \sim (1,2)_{-\frac{1}{2}}, \qquad e_R^i \sim (1,1)_{-1}. \tag{1.5}$$

We have used the short notation $(d_c, d_L)_Y$ to specify the corresponding SM irreducible representations (irreps), where d_c and d_L stand for the dimensions of the $SU(3)_c$ and $SU(2)_L$ irreps while Y is the field hypercharge. The hypercharge assignment, chosen to reproduce the fermionic electric charges, ensures that this chiral structure is free of gauge anomalies. In the minimal SM there are no RH counterpart for neutrinos, which are massless. The electroweak symmetry is spontaneously broken at low energies to the electromagnetic $U(1)_{\mathrm{em}}$, describing Quantum Electrodynamics (QED) with electric charge defined by $Q \equiv T_3 + Y$ [25, 26, 27, 28]. The Higgs field transforms as an iso-doublet of hypercharge 1/2

$$\phi = \begin{pmatrix} \phi^+ \\ \phi^0 \end{pmatrix} \sim (1,2)_{-\frac{1}{2}}, \tag{1.6}$$

The SM Lagrangian is

$$\begin{aligned} \mathcal{L}_{\mathrm{SM}} = &-\frac{1}{4} G_{\mu\nu}^A G^{A\ \mu\nu} - \frac{1}{4} W_{\mu\nu}^a W^{a\ \mu\nu} - \frac{1}{4} B_{\mu\nu} B^{\mu\nu} + \\ &+ \overline{l_L^i}\, i\not{D}\, l_L^i + \overline{q_L^i}\, i\not{D}\, q_L^i + \overline{e_R^i}\, i\not{D}\, e_R^i + \overline{u_R^i}\, i\not{D}\, u_R^i + \overline{d_R^i}\, i\not{D}\, d_R^i + \\ &+ (D_\mu \phi)^\dagger D^\mu \phi - V(\phi) - \left(y_{ii}^e\ \overline{l_L^i} \phi e_R^i + y_{ii}^d\ \overline{q_L^i} \phi d_R^i + V_{ij}^\dagger y_{jj}^u\ \overline{q_L^i} \tilde{\phi} u_R^j + \mathrm{h.c.} \right), \end{aligned} \tag{1.7}$$

where we have introduced the hypercharge $-1/2$ scalar iso-doublet $\tilde{\phi} = i\sigma_2 \phi^*$ and the scalar potential

$$V(\phi) = -\mu_\phi^2 |\phi|^2 + \lambda_\phi |\phi|^4. \tag{1.8}$$

The Lagrangian is the most general renormalizable one with the given gauge symmetry and field content. For $\mu_\phi^2 < 0$ the minimum of the potential occurs for a non-zero *vacuum expectation value* (vev) of the neutral scalar field, $\langle \phi^0 \rangle = v/\sqrt{2}$, with $v = \sqrt{\mu_\phi^2/\lambda_\phi} \approx 246$ GeV, spontaneously breaking the electroweak symmetry $SU(2)_L \otimes U(1)_Y \to U(1)_{\rm em}$. In order to quantize around the classical vaccum we expand:

$$\phi = \frac{1}{\sqrt{2}} e^{i\xi^a T_a} \begin{pmatrix} 0 \\ v+H \end{pmatrix} \overset{\text{unitary gauge}}{\longrightarrow} \phi' = e^{-i\xi^a T_a}\phi = \frac{1}{\sqrt{2}} \begin{pmatrix} 0 \\ v+H \end{pmatrix}, \tag{1.9}$$

where ξ^a are the massless pseudoscalar Nambu-Goldstone bosons (NGB) [29, 30] associated to each broken generator and H is the Higgs boson. The Higgs is the only physical scalar degree of freedom as it is apparent going to the unitary gauge where the NGB are gauged away and become the longitudinal components of the corresponding massive gauge bosons. Replacing Eq. (1.9) into the scalar kinetic term results in masses for all the electroweak gauge bosons other than the combination coupled to the electric charge, which remains massless. We can classify the physical sector of spin-1 particles in the SM according to this conserved charge, distinguising between a charged sector with massive vector bosons

$$W_\mu^\pm = \frac{1}{\sqrt{2}} \left(W_\mu^1 \mp i W_\mu^2 \right), \qquad M_W = \frac{g}{2} v, \tag{1.10}$$

and a neutral sector containing both a massive vector and the massless combination corresponding to the unbroken gauge symmetry vector boson, the photon:

$$\begin{aligned} Z_\mu &= -\sin\theta_W B_\mu + \cos\theta_W W_\mu^3, \qquad & M_Z &= \frac{\sqrt{g^2+g'^2}}{2} v, \\ A_\mu &= \cos\theta_W B_\mu + \sin\theta_W W_\mu^3, & M_A &= 0. \end{aligned} \tag{1.11}$$

The mixing in this neutral sector is described by the weak angle, with $\tan\theta_W \equiv \frac{g'}{g}$. Comparing (1.10) and (1.11) we observe that at tree level the W and Z masses are related by $M_W = M_Z \cos\theta_W$. Radiative corrections change these parameters but, if $\rho \equiv M_W^2/M_Z^2 \cos\theta_W{}^2$, one still finds $\rho \approx 1$. This is implied by an approximate accidental global $SU(2)$ symmetry in the scalar sector of the Lagrangian, called *custodial symmetry* because it protects the tree-level relation $\rho = 1$. As we will see below there are other accidental global symmetries in the SM Lagrangian but they affect only to the fermionic sector.

The Higgs mechanism is also responsible of giving masses to fermions which, being chiral under the electroweak gauge group, do not admit any mass term in the Lagrangian (1.7). Under the unbroken gauge symmetry the two chiralities for each fermion transform in the same way, and are then paired by the Yukawa couplings in Eq. (1.7) into the mass term

$$\mathcal{L}_{\rm m}^f = -m_i^e \, \overline{l_L^i} \phi e_R^i - m_i^d \, \overline{q_L^i} \phi d_R^i - V_{ij}^\dagger m_j^u \, \overline{q_L^i} \tilde{\phi} u_R^j + \text{h.c.}, \tag{1.12}$$

with masses given by

$$m_i^f = \frac{v}{\sqrt{2}} y_{ii}^f. \tag{1.13}$$

Note that in writing the Yukawa terms we chose a fermion basis such that y^e and y^d are diagonal. Within the SM this can always be done without loss of generality. Had we started from an arbitrary basis

$$\mathcal{L}_{\rm Yuk} = -y_{ij}^e \, \overline{l_L^i} \phi e_R^j - y_{ij}^d \, \overline{q_L^i} \phi d_R^j - y_{ij}^u \, \overline{q_L^i} \tilde{\phi} u_R^j + \text{h.c.}, \tag{1.14}$$

the general Yukawa matrices, which do not have to be real nor hermitian, can be diagonalized by bi-unitary transformations

$$y^f_{ij} = \left(\mathcal{U}^f_L\right)_{ik} y^f_{kk} \left(\mathcal{U}^f_R\right)^\dagger_{kj} , \tag{1.15}$$

with y^f_{ii} the square root of the (real and positive) eigenvalues of the hermitian products $y^f \left(y^f\right)^\dagger$ and $\left(y^f\right)^\dagger y^f$, which are diagonalized by the unitary matrices $\mathcal{U}^f_L$ and $\mathcal{U}^f_R$, respectively. Note now that, if we exclude the Yukawa terms from the Lagrangian, each fermion type spans a global $U(3)$ symmetry allowing for arbitrary unitary redefinitions in family space. For quarks, one can use this freedom to diagonalize only one of the Yukawa matrices, since by $SU(2)_L$ gauge symmetry LH u and d quarks must be rotated by the same transformation. We choose as a convention to diagonalize the d Yukawa matrix. For the charged leptons, the absence of RH neutrinos guarantees that their Yukawas can always be rotated to diagonal form. Therefore, we have rotated (1.14) defining $l_L \to \mathcal{U}^e_L l_L$, $e_R \to \mathcal{U}^e_R e_R$, $q_L \to \mathcal{U}^d_L q_L$, $u_R \to \mathcal{U}^u_R u_R$ and $d_R \to \mathcal{U}^d_R d_R$ to obtain the Lagrangian in (1.7). With this convention $V \equiv \left(\mathcal{U}^u_R\right)^\dagger \mathcal{U}^d_L$ in Eq. (1.7).

Note that not all the $U(3)^5$ global symmetry is broken by the Yukawa terms. Actually there are four global accidental $U(1)$ symmetries left unbroken. Their charges are given by baryon number (B), which assigns $B = (-)1/3$ to (anti) quarks, and by the three lepton flavors ($L_i,\ i = e, \mu, \tau$), with $L_i = (-)1$ for (anti)leptons in the i-th generation. In consequence, total lepton number ($L = L_e + L_\mu + L_\tau$) is also preserved. It must be noted though, that B and L are exact symmetries only at the perturbative level, while the combination $B - L$ is exact.

In order to write Eq. (1.7) in the fermion mass eigenstate basis we only need to rotate the LH u quarks. In general, since generators corresponding to broken symmetries can mix different components of the fermion multiplets, going to the physical basis will imply that flavor mixing encoded in the mass matrices translates to the gauge currents. However, this mixing only appears in the quark charged currents through V, known as the *Cabbibo-Kobayashi-Maskawa* (CKM) matrix [31, 32], because of the particular SM algebraic structure with diagonal neutral couplings. Thus, the interactions between physical fermions and charged and neutral vector bosons are given by:

$$\begin{aligned}
\mathcal{L}_{\rm CC} =& -\frac{g}{\sqrt{2}} W^+_\mu \left(\overline{\nu^i_L}\gamma^\mu e^i_L + V_{ij}\overline{u^i_L}\gamma^\mu d^i_L\right) + \text{h.c.} , \\
\mathcal{L}_{\rm NC} =& -\frac{g}{\cos\theta_W} Z_\mu \sum_\psi \overline{\psi}\gamma^\mu \left(g^\psi_L P_L + g^\psi_R P_R\right)\psi , \\
\mathcal{L}_{\rm em} =& -e\, A_\mu \sum_\psi Q^\psi\, \overline{\psi}\gamma^\mu\psi ,
\end{aligned} \tag{1.16}$$

with the electric charge $e \equiv g'g/\sqrt{g^2 + g'^2} = g'\cos\theta_W = g\sin\theta_W$, the neutral current couplings $g^\psi_L \equiv T_3^{\psi_L} - \sin^2\theta_W\, Q^\psi$ and $g^\psi_R \equiv -\sin^2\theta_W\, Q^\psi$, and the chirality projectors $P_{L,R} \equiv (1 \mp \gamma^5)/2$.

Finally, the same Yukawa couplings generating masses for the fermions, couple them to the physical Higgs field. In the fermion mass eigenstate basis

$$\mathcal{L}_H = -\frac{1}{\sqrt{2}} H \left(y^e_{ii}\ \overline{e^i_L} e^i_R + y^u_{ii}\ \overline{u^i_L} u^i_R + y^d_{ii}\ \overline{d^i_L} d^i_R\right) + \text{h.c.} , \tag{1.17}$$

where interactions are diagonal, for they are proportional to fermion masses. In consequence, looking at (1.16) and (1.17), we observe that the SM is free from tree-level flavor-changing neutral currents (FCNC) and that all the flavor structure is contained in the charged currents and solely

described by the CKM matrix. This unitary matrix is also the only source of CP violation in the model. Morevoer, using the fact that all the other terms in the Lagrangian are invariant under rephasing of quark fields, it can be easily shown that all CP violation is governed by only one complex phase.

The current status of the Standard Model

The SM is in excellent agreement with available data. Besides the observation of all fermions as well as of the neutral and charged current mediators, precision measurements have probed the model including radiative corrections, and have found no significant deviation from the SM predictions. For instance, electroweak precision tests performed during the first run of LEP and at SLC have provided extremely accurate measurements of the properties of the neutral current sector. On the other hand, during the second run of LEP, LEP 2, the available center of mass energy allowed to pair produce the W and measure its mass, decay width and branching fractions. Moreover, since two of the three tree-level diagrams contributing to W pair production contain the triple gauge boson coupling, the non-abelian nature of the electroweak interactions has been also tested. Further measurements of the W parameters were also performed at Tevatron where in addition W's can be single produced with a large cross section. Up to now, and despite a few discrepancies that might be eventually interpreted as hints of the existence of new physics and will be discussed below, all experimental data are consistent with the SM, with the only exception of neutrino oscillations, which require the neutrinos to be massive particles and then to extend the SM. Putting neutrino masses aside, we can quantify the degree of agreement of the SM with experimental data by performing a global fit to the model. The detailed results of the SM global fit to the electroweak precision data (EWPD) as well as the methodology we used are described in Appendix A, where we also list all the data included in the fit. Here, the results are illustrated in Fig. 1.1, where the discrepancies between the experimental measurements and the theoretical predictions for the most relevant observables are given in terms of the *pulls*: the difference between measurement and prediction normalized to the experimental error. As can be seen the agreement is very good, even if a few measurements show discrepancies $\sim 2\text{-}3$ standard deviations (σ). It is important to note that when many different observables are included in the fit, the presence of a few of these discrepancies is expected as a consequence of statistical fluctuations and, therefore, they should not be necessarily taken as an indication of a problem in the model. They could also have an experimental origin, coming for instance from underestimated systematics. In any case, the quality of the fit can be globally evaluated attending to the value of the χ^2 over the number of degrees of freedom (d.o.f.) or, better, by reporting the p-value[2]. For the SM fit we get good overall results[3]

$$\frac{\chi^2}{\text{d.o.f.}} = 1.08,\ p = 0.34.$$

Now, the fact that a few discrepancies do not necessarily point to a problem of the model does not mean that they should not be analyzed as possible hints of new physics. Therefore, it is worth reviewing which are the major disagreements between the model and data, in order to determine whether they follow any pattern that may be predicted by some extension of the SM. The most significant discrepancy with the SM predictions comes from the anomalous magnetic moment for

[2]For a given χ^2, the p-value is the probability that the hypothesis would lead to a χ^2 value larger than the one obtained. This means that if one would repeat the experiments many times and with the obtained data in each iteration perform a new fit, the expected value for the χ^2 would be worse than the one obtained in $100 \cdot p$ % of the cases.

[3]This fit corresponds to the "standard" fit as described in Appendix A. More details such as the best fit values and errors for the SM parameters or the results of different fits are also given there.

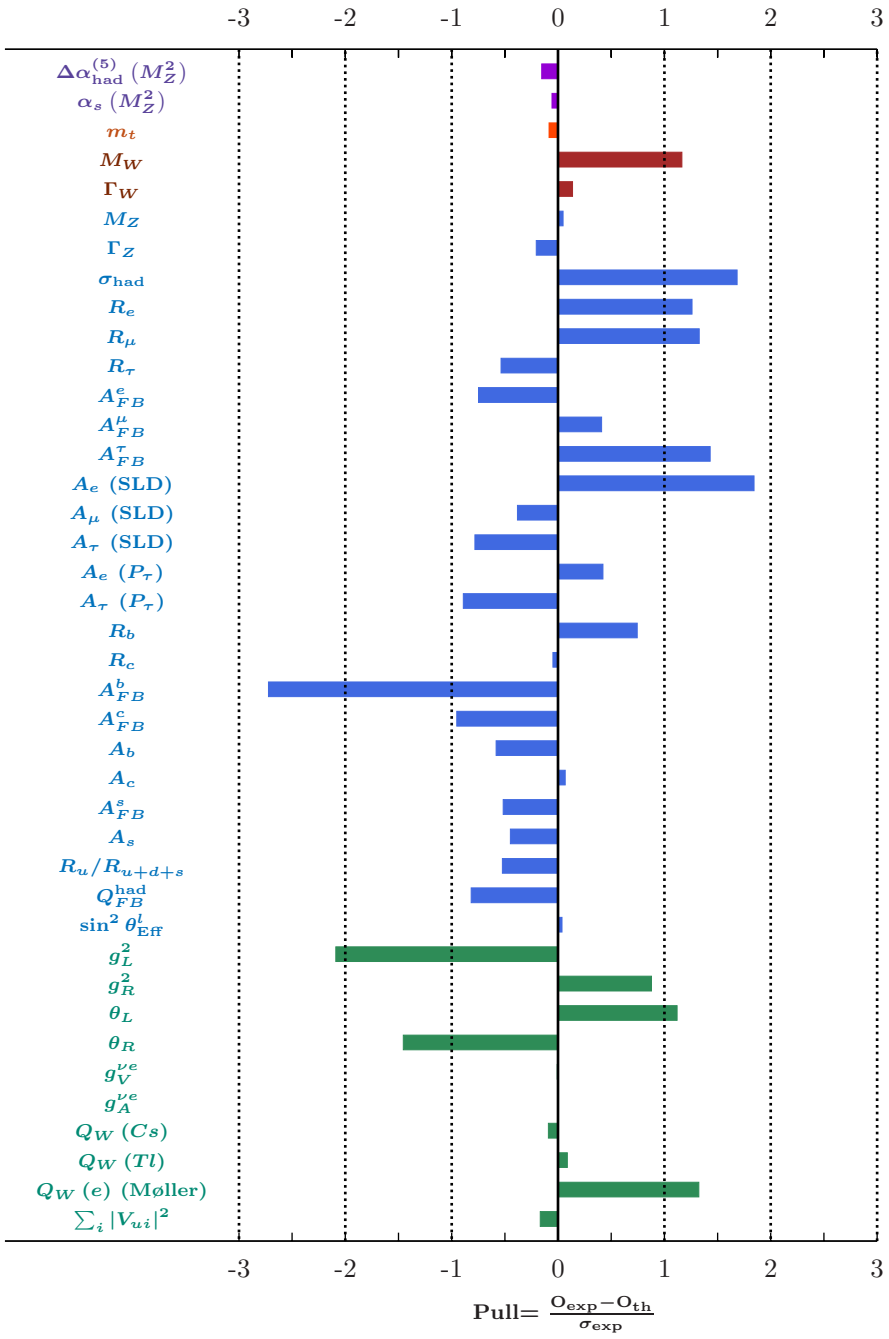

Figure 1.1: Pulls for the SM theoretical predictions for some of the most representative observables included in the fit.

the muon $a_\mu \equiv (g_\mu - 2)/2$. This has been computed within the SM including up to four loops and leading five-loop estimates for the QED contribution. For the electroweak part the full two-loop result is also known, as well as the leading logarithm three-loop contribution. Finally, there are hadronic vacuum polarization and light-by-light scattering corrections. These are the major sources of the theoretical uncertainty. In particular, the vacuum polarization piece is extracted from the $e^+e^- \to \gamma^* \to$ hadrons cross section making use of a dispersion relation. Combining the existing e^+e^- data for the hadronic corrections, including the latest ones from Babar [33], and adding the result to all the other contributions, one finds that the SM prediction departs by $\sim 3.2\ \sigma$ respect to the experimental value measured at BNL [34] by the E821 experiment[4]. The deviation could be accounted by contributions of new physics, such as supersymmetry with large $\tan\beta$. The main problem at the Z pole is with the value of $\sin^2\theta_{\rm eff}^{\rm lept}$, which is distinctively higher when derived from hadronic asymmetries than when derived from the leptonic ones. The statistical probability that the set of asymmetry data is consistent with the SM hypothesis is only 3.7 % [36]. This low probability is driven by the two most precise determinations of $\sin^2\theta_{\rm eff}^{\rm lept}$, obtained from the leptonic asymmetry parameter A_l by the SLD collaboration at SLAC and of the bottom forward-backward asymmetry $A_{\rm FB}^b$ at LEP, respectively. These measurements differ by 3.2 σ. The best-fit value gives a prediction for $A_{\rm FB}^b$ that is 2.7 σ above its experimental value, while the leptonic asymmetries differ by less than 1.8 σ [37]. For this reason, it is common to speak of an $A_{\rm FB}^b$ anomaly, and to implicitly consider that the leptonic data are in good agreement with the SM. This bottom anomaly could be interpreted as an indication of the presence of new physics strongly coupled to the third quark family. Finally, the measurement of the effective neutrino-quark couplings in deep inelastic neutrino-nucleon scattering by the NuTeV collaboration, which was at $\sim 3\ \sigma$ a few years ago, has also recently entered in the class of minor discrepancies, as it has been reduced to $\sim 2\ \sigma$ [38].

The only SM prediction not confirmed experimentally thus far is the existence of the Higgs boson, responsible of the spontaneous breaking of the electroweak symmetry. In consequence, its mass, M_H, is the only input parameter in the model that has not been measured. Direct searches at LEP 2 and Tevatron have put, however, constraints on the possible values that this parameter may have. Assuming a pure SM Higgs, LEP 2 searches put a direct lower bound $M_H \geq 114.4$ GeV at 95% C.L. [39] and Tevatron searches have recently excluded $163 \leq M_H \leq 166$ GeV at 95% C.L., window that is expected to be extended to $159 \leq M_H \leq 168$ GeV for the same confidence level [40] [5]. It is noteworthy that, as a result of some excess events seen by both collaborations, when the results of both direct searches are combined there is a significative preference for a Higgs mass of ~ 116 GeV. As can be seen in Figure 1.2 (Left), there is a relatively pronounced dip in the observed log-likelihood ratio of data probabilities comparing the hypothesis of SM background to background plus Higgs signal. This preference for a light Higgs is extended up to $M_H \lesssim 155$ GeV by Tevatron searches, sensitive to masses up to 200 GeV. On the other hand, since the SM predictions depend through quantum corrections on the unknown value of the Higgs boson mass, the global fit provides indirect information about the value of M_H. In particular, electroweak data tend to prefer a relatively light Higgs, $M_H = 101^{+32}_{-26}$ GeV, slightly below the direct LEP 2 lower bound. The upper bound at 95 % C.L. is $M_H < 159$ GeV. Note that this indirect determination of M_H does not seem compelling, as it arises from the combination of somewhat contradictory measurements if the SM gives a complete description of nature: M_W and the leptonic asymmetries at the Z pole point to a very light Higgs, whereas the hadronic asymmetries prefer a heavy one [42]. On the other hand, it has been argued that there is some tension between the indirect determination of the Higgs

[4] One could however use τ decay data instead of e^+e^-, reducing the discrepancy in such case to the 1 σ level [35].

[5] It has been noted recently however that these last exclusion limits should be reconsidered in the light of the large theoretical uncertainties affecting the production cross sections of the Higgs at Tevatron [41].

mass and the direct limit because the former is below of the latter [43]. However the direct bound is nowadays well within the 1 σ confidence interval of the indirect measurement. It is also important to note in this regard that the indirect determination of the Higgs mass is rather correlated with the assumed top quark mass, which matches its experimental value since it is measured with a good precision. This implies that a shift in the central value of m_t can ameliorate or worsen the tension between direct and indirect determinations. For instance, in these last years m_t has been changing between 170.9 ± 1.8 GeV and the current value of 173.1 ± 1.3 GeV. For the lowest value, $M_H = 86^{+30}_{-23}$ GeV while for $m_t \gtrsim 175$ GeV, with the current error, the best fit value is above the direct LEP 2 constraint. In any case, this mild tension will be meaningless if a ~ 120 - 140 GeV Higgs is eventually found at the LHC, and only in the case that it is significantly heavier the presence of extra physics would be necessary to explain the data. Having in mind these different preferences for the Higgs mass between different data sets, and the small tension between direct and indirect results, what one should in principle do is to include all the available information in the fit, and in particular the Higgs direct searches limits. This is what we will do in our analysis, giving a Higgs mass value centered in the dip of Figure 1.2 (Left) at $M_H \approx 116$ GeV. The results from direct searches also affect the upper limit which is reduced to $M_H < 138$ GeV at 95% C.L. . The χ^2 distribution as a function of the Higgs mass including direct searches and ignoring them is shown in Figure 1.2 (Right). Obviously, both profiles coincide in the region $M_H > 200$ GeV where there are no bounds from direct searches, but in the favored region around $M_H \sim 116$ GeV the fit including the Higgs searches data gives a deeper minimum. It is important to note that, although we will systematically include these direct searches limits in our fits, one needs to be careful as these are referred to a SM Higgs and may not necessarily apply in a generic SM extension.

Apart from these experimental constraints, there are also theoretical bounds on M_H. In particular, tree-level unitarity constraints in longitudinally polarized WW scattering imply that the Higgs mass should not be larger than 1 TeV [44]. Triviality limits are derived assuming the SM to be valid up to some energy scale and requiring that the quartic coupling λ_ϕ does not blow up in the running. For a value of the cut-off scale not much larger than M_H this implies that $M_H \lesssim 800$ GeV, while $M_H \lesssim 150$ GeV if we assume perturbativity up to the reduced Planck scale $\kappa_P \sim 10^{18}$ GeV [45]. Theoretical considerations about the stability of the scalar potential provide lower bounds on M_H, also depending on the scale until which we assume the SM to be valid. If, again, we assume it is valid up to the reduced Planck scale, vacuum stability requires $M_H \gtrsim 130$ GeV, and $M_H \gtrsim 115$ GeV if we simply require a sufficiently long-lived metastable vacuum [46].

At this point, despite a few experimental disagreements, there is no strong experimental reason to believe in the existence of new physics beyond the SM [6]. The main reasons why nowadays most physicist are convinced that the SM cannot be a fundamental theory come from theoretical and/or "aesthetic" considerations. The model has too much arbitrariness to begin with, with a total of 20 free parameters. Apart from that, there are several open questions such as why only the electroweak gauge group is chiral, why there are three fermion families and, more intriguing, why there is such a hierarchical pattern for their masses and mixings, ... It also suffers from several fine-tuning problems such as the strong CP problem [47], or the well known hierarchy problem. This directly affects to our understanding of the EWSB mechanism. As explained above, for the SM to be consistent with the data, the Higgs should not be very heavy and, in particular, from theoretical arguments we know that its mass should not be in any case larger than ∼TeV. Now, it is a fact that the Higgs mass is very sensitive to high energy scales through radiative corrections. This becomes apparent if one computes the one-loop corrections to the mass squared using a cut-off Λ to regulate the integrals. In such a case one finds that these corrections diverge quadratically

[6] Apart from providing a mechanism for neutrino masses.

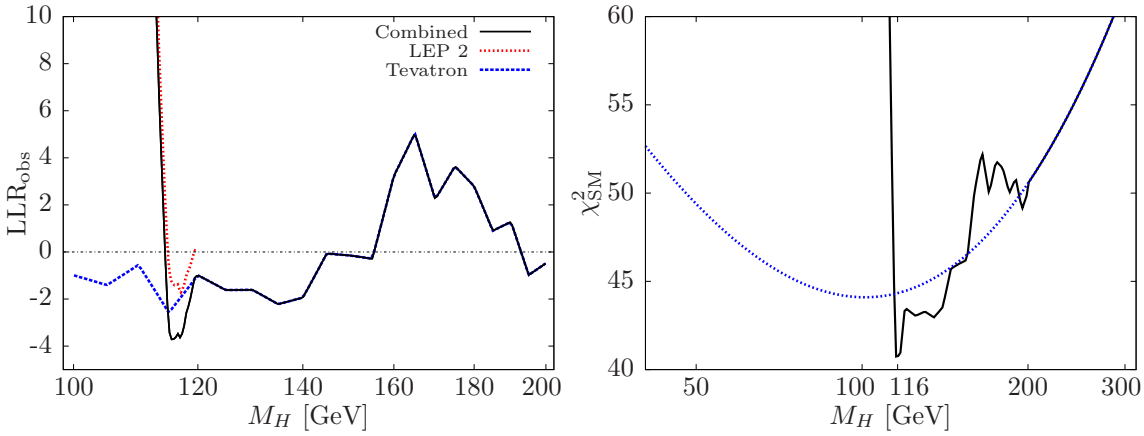

Figure 1.2: (Left) Higgs direct searches results from LEP 2 (red dotted line), Tevatron (blue dashed line), and the total combined contribution (black solid line) to the observed log-likelihood ($\mathrm{LLR}_{\mathrm{obs}}$). (Right) Minimum of the χ^2 in the SM as a function on the Higgs mass for the "standard" fit (blue dotted line) described in Appendix A and the fit including the Higgs direct searches results (black solid line). Note that the latter has been normalized to agree with the former for large M_H.

with the cut-off,

$$M_H^2 = M_H^{\mathrm{bare}\ 2} + \mathcal{O}\left(\lambda_\phi, g^2, y_f^2\right)\Lambda^2. \tag{1.18}$$

Note that this is not strictly a problem if the SM is valid at all scales, since only M_H and not M_H^{bare} is observable. Consider, however, the case where there is a real physical cut-off, i.e., an energy scale where new physics enters altering the high energy behaviour of the theory. In such a case, the SM Higgs mass receives physical corrections from threshold effects at that scale which, as in Eq. (1.18), depend quadratically on the cut-off [7]. We know that in the absence of any other new physics beyond the SM, the theory has at least one physical cut-off at the reduced Planck scale, where the gravitational effects start to be important. Then, one-loop threshold effects at κ_P imply that $M_H \sim \kappa_P$, well above the electroweak scale, unless some fine-tuning is at work between the bare parameters and loop corrections in order to cancel more than 30 figures in the mass square. Moreover, this cancellation must take place at every order in perturbation theory since, even assuming that the parameters have been tuned to cancel the one-loop quadratic divergence, another quadratic divergence appears at two loops and so on. This means that the fine-tuned values depend on all the parameters of the theory. Therefore, the origin of the hierarchy problem is, as its name suggests, the large spacing between the electroweak and the Planck scales, which is not stable in a natural way. This is why most physicists expect that new physics explaining the stability of the electroweak scale must cut-off the SM, and that it must do it not much beyond 1 TeV. Finally note that unlike for the Higgs mass, this hierarchy poses no problem for fermion masses or dimensionless couplings, for these are only logarithmically sensitive to the cut-off.

As we have tried to emphasize in this section, the SM explains very well the results of the experiments performed up to now, but our theoretical understanding suggest that the model must be completed when we go to higher energies. In other words, the SM can be considered just as

[7] These threshold effects arise from demanding the "continuity" of the low-energy correlation functions across the cut-off energy.

a low-energy approximation to a more fundamental theory. Theories of this kind are known as *effective theories*.

1.2 The effective Lagrangian approach for the description of new physics

There are many different scales in nature and it is a fact that the knowledge of the exact physical details at all of them is not necessary in order to describe phenomena that occur at a given one. In other words, one does not need the fundamental theory to describe physics, which is a good thing because nobody knows it. Actually, even in the case we knew it, a simpler description where the details of little relevance for the phenomena we are interested in are "ignored" could be a more convenient quantitative approach. Effective theories are a tool which allows us to simplify the study of physical systems with very different scales. In particle physics, where the mathematical formalism used to describe nature is quantum field theory (QFT), these techniques configure the framework known as *effective field theory*.

Consider a renormalizable QFT involving light and heavy fields denoted by ϕ and Φ, respectively. Such a theory would be described by a Lagrangian that can be splitted into three different pieces

$$\mathcal{L}\left[\phi,\Phi\right]=\mathcal{L}_{\ell}\left[\phi\right]+\mathcal{L}_{h}\left[\Phi\right]+\mathcal{L}_{\ell h}\left[\phi,\Phi\right], \tag{1.19}$$

where $\mathcal{L}_{\ell}\left[\phi\right]$ and $\mathcal{L}_{h}\left[\Phi\right]$ describe interactions involving only light and heavy fields, respectively, whereas the interactions between both are contained in $\mathcal{L}_{\ell h}\left[\phi,\Phi\right]$. If we are interested in describing physical processes involving only the light fields at energies $E\ll\Lambda$, with Λ the characteristic mass scale of the heavy fields, the Φ degrees of freedom can be integrated out of the theory to obtain an *effective Lagrangian* valid to describe the interactions of the light fields at low energies:

$$\exp\left(i\int\mathcal{L}_{\text{eff}}\left[\phi\right]d^{4}x\right)=\int\mathcal{D}\phi\left(x\right)\big|_{p>\Lambda}\,\mathcal{D}\Phi\left(x\right)\exp\left(i\int\mathcal{L}\left[\phi,\Phi\right]d^{4}x\right). \tag{1.20}$$

In general, the effective Lagrangian $\mathcal{L}_{\text{eff}}\left[\phi\right]$ can be expanded as

$$\mathcal{L}_{\text{eff}}\left[\phi\right]=\mathcal{L}_{\ell}\left[\phi\right]+\sum_{i}\,C_{i}\mathcal{O}_{i}\left(x\right), \tag{1.21}$$

with $\mathcal{O}_i$ being a set (in general infinite) of local operators built from the light modes ϕ. The coefficients C_i of such operators are known as *Wilson coefficients* and encode the effects of the high-energy physics at energies $E\ll\Lambda$. These coefficients scale according to the mass dimension of the operator $d_i=[\mathcal{O}_i]$

$$C_{i}=\frac{\alpha_{i}}{\Lambda^{d_{i}-4}}, \tag{1.22}$$

with α_i a dimensionless number. Thus, we have a finite number of operators with mass dimension $d_i\leq 4$ that renormalize the action of the light fields, and an infinite number of operators with $d_i>4$, whose effects become irrelevant as we go to lower energies, i.e., as Λ is taken to infinite. This particular structure of the effects of the high energy dynamics over the low-energy physics is known as *decoupling*. In field theory, decoupling was first made rigorous in the Appelquist-Carazzone theorem [48] which essentially states that, apart from coupling constant and field strength renormalization, the effects of the heavy degrees of freedom are suppressed by some inverse power of the cut-off Λ. This will be our first assumption about the nature of the physics beyond the SM:

□ **Hypothesis 1:** *The new physics satisfy the conditions of the Appelquist-Carazzone theorem and decouples in the limit $\Lambda \to \infty$, with Λ some characteristic scale of the new physics acting as a cut-off. This can be the mass of the heavy particles, for instance.*

It is important to note that, although decoupling is a rather general property, there are interesting physical cases where the decoupling theorem does not apply. For instance, the fermions in the electroweak theory cannot be decoupled by taking their masses to be large.

Although in the above discussion we have used an up-bottom approach, using the Lagrangian of the fundamental theory as a starting point from which the effective Lagrangian is derived, via the integration of the heavy degrees of freedom, it must be emphasized that we do not need to know what the theory at high energies is in order to build a useful effective theory for a given set of light states. In general, the methods of QFT allow us to use a bottom-up approach and construct a general effective Lagrangian, provided we know a few of its ingredients. This remark can be made precise in the form of a theorem [49] [8]:

Theorem. *For a given set of asymptotic states, perturbation theory with the most general Lagrangian containing all terms allowed by the assumed symmetries will yield the most general S-matrix elements consistent with analyticity, perturbative unitarity, cluster decomposition and the assumed symmetries.*

This is very convenient when we are interested in new physics studies, for in that case the high-energy theory is unknown. What we know is that at low energies (up to the electroweak scale at least) the SM is a good effective theory. Then, we can set it as our starting point and use the SM fields and symmetries to construct an effective Lagrangian which apart from the SM interactions contains an infinite set of operators of mass dimension $d > 4$. Such a theory provides a model-independent description of physics beyond the SM and, in particular, must include the "true" effective field theory if our understanding of the physics at low energies is correct. In this regard, as the Higgs has not been discovered yet, we will make an assumption about the content of the light scalar sector [9]. In general it suffices to consider the SM Higgs, since scalar singlets which can acquire a vev do not transform under the SM and scalar triplets or higher representations can only get very small vevs, v_R, as otherwise they would give sizable contributions to the ρ parameter, which are experimentally very constrained. Then, their effects are suppressed by v_R/v and can be neglected in most cases. Finally, there can be several scalar doublets but we can always identify the SM one as the combination getting the vev v. Therefore:

□ **Hypothesis 2:** *We parametrize new physics in terms of the most general effective Lagrangian that can be built from the minimal SM field content and symmetries. This implies, in particular, that we consider only the SM Higgs.*

According to the scaling behaviour (1.22), the effective Lagrangian can be ordered according to the mass dimensions of the operators as follows

$$\mathcal{L}_{\text{eff}} = \sum_{d=4}^{\infty} \frac{1}{\Lambda^{d-4}} \mathcal{L}_d = \mathcal{L}_4 + \frac{1}{\Lambda}\mathcal{L}_5 + \frac{1}{\Lambda^2}\mathcal{L}_6 + \dots , \tag{1.23}$$

where Λ is the (unknown) threshold energy scale up to which the effective Lagrangian description is valid, and each $\mathcal{L}_d$ contains all the local operators of canonical dimension d allowed by the

[8] The exact formulation presented here has been directly taken from Ref. [21].

[9] A chiral effective theory with a nonlinear realization of the SM symmetry, including the Goldstone bosons but no physical Higgs field, is also possible [50].

symmetry requirements:

$$\mathcal{L}_d = \sum_i \alpha_i^d \mathcal{O}_i^d, \quad [\mathcal{O}_i^d] = d. \tag{1.24}$$

Note that Eq. (1.23) contains an infinite tower of operators. This might seem to pose a problem for computational purposes. But, following the effective theory philosophy, we do not need to know the effects of all operators (otherwise the use of the fundamental theory would be simpler and then there would be no reason to use the effective description) but only of those that are relevant for the physical observables we are interested in and up to the required precision. Here is where the idea of ordering operators according to their mass dimension becomes meaningful, since it also classifies them according to the size of their corrections to the relevant observables. By power counting, the operators in $\mathcal{L}_d$ will give contributions $\sim (E/\Lambda)^{n \geq d-4} \ll 1$, with E the typical energy of the process. Thus, in practice, the presence of this infinite set of operators in the effective Lagrangian is not a problem because a given physical observable can only be determined experimentally with a finite experimental precision σ_{exp}. Therefore, among the whole set of operators in Eq. (1.23) we only need to consider operators of mass dimension $d \leq N + 4$, with N fixed by

$$\sigma_{\text{exp}} \sim \left(\frac{E}{\Lambda}\right)^N. \tag{1.25}$$

For new physics around the TeV scale, we expect terms of dimension $d > 6$ to give small corrections compared to the current experimental precision. This can be justified by the fact that most of the electroweak precision measurements are taken at the Z pole or at lower energies and $(M_Z/\text{TeV})^N < 0.8‰$ for $N \geq 3$, while for LEP 2 measurements, although there are data taken up to energies of 209 GeV, the precision is significantly lower. Therefore, we will consider the effects of operators up to dimension six in our analysis. This will be our third working assumption:

□ **Hypothesis 3:** *We assume that the precision of current electroweak precision data allows to test only operators up to dimension six in the effective Lagrangian.*

Once we have the operators entering in the effective Lagrangian and have established a way of truncating the infinite sum in Eq. (1.23), we still need to know the coefficients α_i^d. These encode the effects of the virtual exchange of the heavy degrees of freedom and can be obtained by comparing the exact and the effective Lagrangian results for a certain set of S-matrix elements involving only the light degrees of freedom around the threshold energy Λ, for the effective and the fundamental theories must provide the same results at that scale. This process is illustrated in Fig. 1.3 and it is known as *matching*. If perturbation theory can be applied to the high energy theory, performing the matching at the desired order provides the corresponding perturbative expansion for each coefficient. This is the way the Fermi theory can be derived from the SM, for instance.

There are situations where the above procedure cannot be applied either because the underlying theory is unknown, as in the case of the SM, or because it is non-perturbative, as for instance in Chiral perturbation theory where the high energy theory is known, QCD, but it is strongly coupled. In these cases one can still obtain the values for the higher dimensional operator coefficients by comparing the predictions for the S-matrix elements in the effective theory with the experimental measurements of the corresponding observables. Since a given operator can contribute in principle to several different observables this is best done by performing a global fit of the operator coefficients to data.

The comparison of a given theory beyond the SM with data requires evaluating its contributions to the corresponding observables, and this must be repeated for each theory. In contrast, the effective Lagrangian approach offers an unified framework for the computation of the corrections

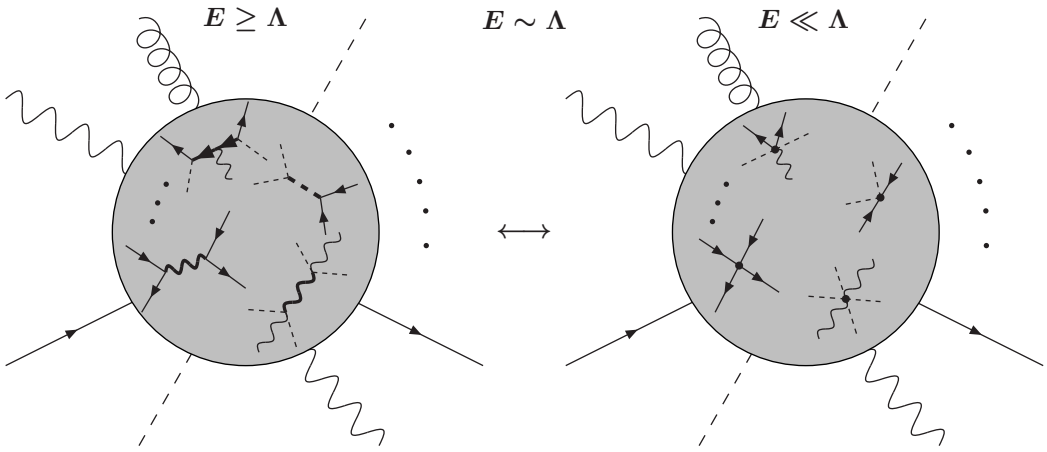

Figure 1.3: For an S-matrix element involving only light particles (thin lines) in the initial and final states, the effect of the exchange of the heavy ($M \sim \Lambda$) particles (thick lines) is mimicked in the effective theory by the presence of new interactions and/or corrections to the existing vertex and propagators. The exact correspondence between both theories is performed by matching their results at the threshold $E \sim \Lambda$.

to the different observables given the light fields and symmetries. Thus one only needs to compute them once in terms of the higher dimensional operator coefficients and then translate whatever model we may want to consider to the corresponding effective theory, instead of computing the corrections to all physical quantities again for any possible new physics scenario.

Completely model-independent studies of new physics using the effective Lagrangian set-up have been performed in the past, see for instance [51, 52, 53]. In practice, they are not very illuminating if one is interested in extracting some details of the structure of the high energy theory. This is so because model-independent results are given in terms of central values, errors and correlations of the operators coefficients, but there can be many different types of new physics contributing to the same operators and a careful comparison of the resulting correlations with definite models is necessary. Given the large number of possible operators, this is a highly non-trivial task. One should also be careful since these results may be not unique. In this thesis we will follow a slightly different approach. We will perform model-independent studies within a class of models,in the sense that we will assume some of the structure of the high-energy theory by introducing by hand different particles that may be present in the spectrum, but with completely general couplings and masses. They must be rather heavy -otherwise they would have been observed- and therefore the use of the effective Lagrangian description is justified. The advantage of this method is that, upon integration of the new fields, only some of the operator coefficients in the effective Lagrangian will be different from zero and they will also exhibit some degree of correlation. Then, the fit is directly sensitive to the assumed structure but the results can be still rather model independent as we are not assuming further details about the underlying theory where the new particles may be embedded. In general, if one is interested in which ingredients of a possible high energy theory are favored or excluded by data, this is a convenient approach.

As we will use matching in order to compute the effective Lagrangian for each kind of extra particles we need to require that the high energy physics is perturbative. Regarding perturbativity a second comment is in order: independently of whether the fundamental theory is known or

not, perturbativity guarantees that the term ordering according to their mass dimensions as in Eq. (1.23) is stable. This is so because under quantum corrections the scaling relations, Eq. (1.22), are modified to

$$C_i = \frac{\alpha_i}{\Lambda^{d_i-\gamma_i-4}}, \tag{1.26}$$

with γ_i the anomalous dimension of the operator $\mathcal{O}_i$. Thus, in order for the scaling behaviour of the Wilson coefficients to be unaltered the γ_i must be small, which is ensured if the new physics is weakly coupled. Therefore we will assume:

□ **Hypothesis 4:** *The new physics is weakly coupled. Thus, we can use perturbation theory to compute the operator coefficients and the classification of the relevance of the extra operators attending to their mass dimension is stable under quantum corrections.*

Finally, upon the integration of the heavy particles we will only consider the effects from those operators which receive non-vanishing contributions at tree level. More than an extra restriction, this can be actually thought as a consequence of the considerations we made on the effective Lagrangian expansion and the current experimental precision, together with the above assumption requiring that the new physics must be weakly coupled. Indeed, loop corrections to dimension-six operators are suppressed by additional $1/16\pi^2$ factors, so they are expected to be beyond the experimental sensitivity. In general, tree-level contributions provide the largest effects and therefore allow to derive the strongest constraints. On the other hand, and also related to the consistency of the truncation in the expansion (1.23), we must note that when computing new physics corrections to physical observables only the interference with the SM amplitudes needs to be taken into account, as quadratic effects are expected to be comparable with interference effects from higher order terms.

□ **Hypothesis 5:** *We limit our study to new physics with non-vanishing tree-level effects* [10]*. For the computation of physical observables, unless otherwise is stated, only the interference with the SM contributions will be taken into account, so the results are consistent at the order in the effective Lagrangian expansion we are working at.*

Performing the matching at tree level reduces to inserting in the high energy Lagrangian the classical solution for the heavy fields, obtained by solving their Euler-Lagrange equations. In this process a lot of many different operators arise, and therefore it is convenient to work in a definite operator basis. At a given dimension, one can always construct a complete basis of independent operators. Complete here is understood in the sense that it contains all the possible effects in S-matrix elements at that order. Independent means that each operator in the basis cannot be written in terms of the others using algebraic relations or perturbative field redefinitions[11]. One of such basis for the operators of dimension $d \leq 6$ was presented long ago by W. Buchmuller and D. Wyler in [57]. That was complete with the exception of one missing operator, to be added later by the authors of [58]. (In this last reference the operators were also classified according to whether they can be generated at tree level or at the loop level in SM extensions with an arbitrary number of extra fermions, vector bosons or scalars.) There is only one dimension-five operator, and this violates lepton number. At dimension six, a total of 81 operators (without taking into account flavor) were found if we impose independent conservation of baryon and lepton number. In what follows we review what will be relevant in this thesis. As we will see, actually not all the

[10] Scenarios where the leading corrections enter at the loop level are therefore not considered. This is the case of theories with a "parity", such as R-parity in supersymmetric theories, T-parity [54] in Little Higgs models or Kaluza-Klein parity [55] in universal extra dimensions.

[11] Being computed via the *Lehmann Symanzik and Zimmermann* (LSZ) reduction formula [56], a perturbative redefinition of fields has no effect on S-matrix elements at a given order.

operators in Ref. [57] are independent so the basis is somewhat smaller [59]. The main effect of each type of operator will be studied in more detail in the next chapter.

1.2.1 The dimension-six effective Lagrangian

As mentioned above there is only one dimension-five operator that can be made up of SM fields. This is the Weinberg operator [60] in the first line of Table 1.1 and its effect is to provide Majorana masses for the SM neutrinos. At dimension six we can find a large variety of operators that can be generated at tree level. Before introducing them, let us first point out that in this thesis we will find situations where the assumptions of baryon and lepton number conservation in Ref. [57] do not apply. Therefore we have also included operators that violate B and L, but preserve $B-L$. There is no dimension-six operator violating $B-L$ [61]. Extending the basis of Ref. [57] to one where B and L are not necessarily preserved is trivial. By Lorentz invariance fermions must come in pairs and by dimensional analysis we can have only operators with two or four fermions. Since quanta of B comes in units of $\pm 1/3$ while L comes in units of ± 1, it is impossible to construct a B and L violating but $B-L$ preserving quantity with just two fermions. Thus, the extension of the basis only requires to add extra four-fermion interactions. Now, in a L violating four-fermion operator we can compensate at most $\Delta L = 1$ for it is the largest ΔB we can get with three quarks. Hence the kind of operators we are considering are made up of the color antisymmetric combination of three quarks and one lepton. $U(1)_Y$ invariance then requires the quark combination to carry $Y = 1/2$ ($q_L q_L q_L$ and $q_L u_R d_R$) if coupled to l_L or $Y = 1$ ($u_R u_R d_R$ and $q_L q_L u_R$) if coupled to e_R. Finally, $SU(2)_L$ invariance fixes the final form of the operator.

The list of dimension-six operators we will deal with contains:

- Operators involving only fermionic fields with different chiralities. These appear in sets 2 to 5 in Table 1.1. We refer to them using the list of chiralities of the fermionic fields: *LLLL*, *RRRR*, *LRRL* and *LRLR*. Here we must note that some of the interactions listed in [57] as independent are actually redundant. This can be seen by direct application of several Fierz identities. For instance, the operator $\mathcal{O}_{ll}^{(3)} = \frac{1}{2}\left(\overline{l_L}\gamma^\mu\sigma_a l_L\right)\left(\overline{l_L}\gamma_\mu\sigma_a l_L\right)$ can be written in terms of $\mathcal{O}_{ll}^{(1)}$ by using $(\gamma^\mu P_L)_{12}\,(\gamma_\mu P_L)_{34} = -(\gamma^\mu P_L)_{14}\,(\gamma_\mu P_L)_{32}$ and the properties of the Pauli matrices[12]:
$$\left(\mathcal{O}_{ll}^{(3)}\right)_{ijkl} = 2\left(\mathcal{O}_{ll}^{(1)}\right)_{ilkj} - \left(\mathcal{O}_{ll}^{(1)}\right)_{ijkl}. \tag{1.27}$$
We can do the same for $\mathcal{O}_{uu}^{(8)}$ and $\mathcal{O}_{dd}^{(8)}$, using the analogous Fierz reordering for the Gell-Mann matrices[13]
$$\left(\mathcal{O}_{uu(dd)}^{(8)}\right)_{ijkl} = 2\left(\mathcal{O}_{uu(dd)}^{(1)}\right)_{ilkj} - \frac{2}{3}\left(\mathcal{O}_{uu(dd)}^{(1)}\right)_{ijkl}. \tag{1.28}$$
This cannot be done however to write $\mathcal{O}_{qq}^{(1,3)}$ nor $\mathcal{O}_{qq}^{(8,1)}$ only in terms of $\mathcal{O}_{qq}^{(1,1)}$ because they carry both isospin and color indices and the direct application of the corresponding Fierz identity over the Pauli or Gell-Mann matrices would lead to an operator where the other type of indices (color or isospin, respectively) are not paired as in $\mathcal{O}_{qq}^{(1,1)}$. The most we can do here is to get rid of one of the three operators. For instance,
$$\left(\mathcal{O}_{qq}^{(8,1)}\right)_{ijkl} = \left(\mathcal{O}_{qq}^{(1,1)}\right)_{ilkj} - \frac{2}{3}\left(\mathcal{O}_{qq}^{(1,1)}\right)_{ijkl} + \left(\mathcal{O}_{qq}^{(1,3)}\right)_{ilkj}. \tag{1.29}$$

[12] In particular, $\delta_{ij}\delta_{kl} = \frac{1}{2}\delta_{il}\delta_{kj} + \frac{1}{2}(\sigma_a)_{il}(\sigma_a)_{kj}$, where sum in $a = 1,2,3$ is implicit. For one of the relations below we will also need $(\sigma_a)_{ij}(\sigma_a)_{kl} = \frac{3}{2}\delta_{il}\delta_{kj} - \frac{1}{2}(\sigma_a)_{il}(\sigma_a)_{kj}$.

[13] In this case, $\delta_{ij}\delta_{kl} = \frac{1}{3}\delta_{il}\delta_{kj} + \frac{1}{2}(\lambda_A)_{il}(\lambda_A)_{kj}$.

The operator $\mathcal{O}_{qq}^{(8,3)}$ can also be rewritten in terms of $\mathcal{O}_{qq}^{(1,1)}$ and $\mathcal{O}_{qq}^{(1,3)}$:

$$\left(\mathcal{O}_{qq}^{(8,3)}\right)_{ijkl} = 3\left(\mathcal{O}_{qq}^{(1,1)}\right)_{ilkj} - \frac{2}{3}\left(\mathcal{O}_{qq}^{(1,3)}\right)_{ijkl} - \left(\mathcal{O}_{qq}^{(1,3)}\right)_{ilkj}. \tag{1.30}$$

Note that the LLLL operators $(\mathcal{O}_{ll}^{(1)})_{ijkl}$, $(\mathcal{O}_{qq}^{(1,1),(1,3)})_{ijkl}$ and the RRRR operators $(\mathcal{O}_{ee})_{ijkl}$ and $(\mathcal{O}_{uu(dd)}^{(1)})_{ijkl}$ are symmetric under the interchange $\{ij\} \leftrightarrow \{kl\}$ but only $(\mathcal{O}_{ee})_{ijkl}$ is also symmetric under $j \leftrightarrow l$ (or equivalently under $i \leftrightarrow k$) as can be seen by using another Fierz reordering. This symmetry does not apply for any of the others since, as mentioned above, they also carry $SU(2)_L$ and/or $SU(3)_c$ indices. Finally, the new B and L violating operators correspond to the last three rows of LRRL operators and the last one of the LRLR (note that $(\overline{q_L} i\sigma_2 q_L^c)$ is color anti-symmetric while $\left(\overline{u_R^c} u_R\right)$ and $\left(\overline{d_R^c} d_R\right)$ are color-symmetric but the latter can appear in the operators since there are also flavor indices that must be taken into account). Any other operator violating B and L can be rewritten in terms of the five operators presented here by using the properties of charge conjugation and suitable Fierz transformations.

- One operator built-up exclusively with scalar fields. This is the one named $\mathcal{O}_{\phi 6}$ in set 6 of Table 1.1. There we have also included for notational purposes the dimension-four operator $\left(\phi^\dagger \phi\right)^2$, as it will appear in some cases when we integrate the extra particles. These two operators correct the scalar potential.

- Operators made of scalars, fermions and gauge bosons appear in set 7 of Table 1.1. In short, we refer to these as *SVF operators*. Their main observable effect is to correct the fermionic gauge couplings.

- Operators made of scalars and fermions and therefore refered as *SF operators*. These appear in set 8 of Table 1.1 and their main effect is to correct the fermion masses and Yukawa interactions.

- Finally, in the last set of Table 1.1 we find what we will call *Oblique operators*. These do not involve any fermion. After EWSB they correct the gauge boson masses. The operator $\mathcal{O}_{WB}$ arises only at the loop level [58] and has been introduced here only because it allows to connect with the standard oblique corrections formalism [62], as it is directly related to the S parameter. The operator $\mathcal{O}_{\phi}^{(3)}$, on the other hand, is related to the T parameter, while there are no contributions to the U parameter at dimension six.

	Operator	Notation	Operator	Notation
	$\overline{l_L^c}\tilde{\phi}^*\tilde{\phi}^\dagger l_L$	$\mathcal{O}_5$		
LLLL	$\frac{1}{2}\left(\overline{l_L}\gamma_\mu l_L\right)\left(\overline{l_L}\gamma^\mu l_L\right)$	$\mathcal{O}_{ll}^{(1)}$	$\frac{1}{2}\left(\overline{l_L}\gamma_\mu\sigma_a l_L\right)\left(\overline{l_L}\gamma^\mu\sigma_a l_L\right)$	$\mathcal{O}_{ll}^{(3)}$
	$\frac{1}{2}\left(\overline{q_L}\gamma_\mu q_L\right)\left(\overline{q_L}\gamma^\mu q_L\right)$	$\mathcal{O}_{qq}^{(1,1)}$	$\frac{1}{2}\left(\overline{q_L}\gamma_\mu\sigma_a q_L\right)\left(\overline{q_L}\gamma^\mu\sigma_a q_L\right)$	$\mathcal{O}_{qq}^{(1,3)}$
	$\left(\overline{l_L}\gamma_\mu l_L\right)\left(\overline{q_L}\gamma^\mu q_L\right)$	$\mathcal{O}_{lq}^{(1)}$	$\left(\overline{l_L}\gamma_\mu\sigma_a l_L\right)\left(\overline{q_L}\gamma^\mu\sigma_a q_L\right)$	$\mathcal{O}_{lq}^{(3)}$
	$\frac{1}{2}\left(\overline{q_L}\gamma_\mu\lambda_A q_L\right)\left(\overline{q_L}\gamma^\mu\lambda_A q_L\right)$	$\mathcal{O}_{qq}^{(8,1)}$	$\frac{1}{2}\left(\overline{q_L}\gamma_\mu\sigma_a\lambda_A q_L\right)\left(\overline{q_L}\gamma^\mu\sigma_a\lambda_A q_L\right)$	$\mathcal{O}_{qq}^{(8,3)}$
RRRR			$\frac{1}{2}\left(\overline{e_R}\gamma_\mu e_R\right)\left(\overline{e_R}\gamma^\mu e_R\right)$	$\mathcal{O}_{ee}$
	$\frac{1}{2}\left(\overline{u_R}\gamma_\mu u_R\right)\left(\overline{u_R}\gamma^\mu u_R\right)$	$\mathcal{O}_{uu}^{(1)}$	$\frac{1}{2}\left(\overline{d_R}\gamma_\mu d_R\right)\left(\overline{d_R}\gamma^\mu d_R\right)$	$\mathcal{O}_{dd}^{(1)}$
	$\left(\overline{e_R}\gamma_\mu e_R\right)\left(\overline{u_R}\gamma^\mu u_R\right)$	$\mathcal{O}_{eu}$	$\left(\overline{e_R}\gamma_\mu e_R\right)\left(\overline{d_R}\gamma^\mu d_R\right)$	$\mathcal{O}_{ed}$
	$\left(\overline{u_R}\gamma_\mu u_R\right)\left(\overline{d_R}\gamma^\mu d_R\right)$	$\mathcal{O}_{ud}^{(1)}$		
	$\frac{1}{2}\left(\overline{u_R}\gamma_\mu\lambda_A u_R\right)\left(\overline{u_R}\gamma^\mu\lambda_A u_R\right)$	$\mathcal{O}_{uu}^{(8)}$	$\frac{1}{2}\left(\overline{d_R}\gamma_\mu\lambda_A d_R\right)\left(\overline{d_R}\gamma^\mu\lambda_A d_R\right)$	$\mathcal{O}_{dd}^{(8)}$
	$\left(\overline{u_R}\gamma_\mu\lambda_A u_R\right)\left(\overline{d_R}\gamma^\mu\lambda_A d_R\right)$	$\mathcal{O}_{ud}^{(8)}$		
LRRL	$\left(\overline{l_L}e_R\right)\left(\overline{e_R}l_L\right)$	$\mathcal{O}_{le}$	$\left(\overline{q_L}e_R\right)\left(\overline{e_R}q_L\right)$	$\mathcal{O}_{qe}$
	$\left(\overline{l_L}u_R\right)\left(\overline{u_R}l_L\right)$	$\mathcal{O}_{lu}$	$\left(\overline{l_L}d_R\right)\left(\overline{d_R}l_L\right)$	$\mathcal{O}_{ld}$
	$\left(\overline{q_L}u_R\right)\left(\overline{u_R}q_L\right)$	$\mathcal{O}_{qu}^{(1)}$	$\left(\overline{q_L}d_R\right)\left(\overline{d_R}q_L\right)$	$\mathcal{O}_{qd}^{(1)}$
	$\left(\overline{l_L}e_R\right)\left(\overline{d_R}q_L\right)$	$\mathcal{O}_{qde}$		
	$\left(\overline{q_L}\lambda_A u_R\right)\left(\overline{u_R}\lambda_A q_L\right)$	$\mathcal{O}_{qu}^{(8)}$	$\left(\overline{q_L}\lambda_A d_R\right)\left(\overline{d_R}\lambda_A q_L\right)$	$\mathcal{O}_{qd}^{(8)}$
	$\epsilon_{ABC}(\overline{l_L}i\sigma_2 q_L^{c\,A})(\overline{d_R^B}u_R^{c\,C})$	$\mathcal{O}_{lqdu}$	$\epsilon_{ABC}(\overline{q_L^B}i\sigma_2 q_L^{c\,C})(\overline{e_R}u_R^{c\,A})$	$\mathcal{O}_{qqeu}$
	$\epsilon_{ABC}(\overline{u_R^A}u_R^{c\,B})(\overline{d_R^C}e_R^c)$	$\mathcal{O}_{uude}$		
LRLR	$\left(\overline{q_L}u_R\right)i\sigma_2\left(\overline{q_L}d_R\right)$	$\mathcal{O}_{qq}^{(1)}$	$\left(\overline{q_L}\lambda_A u_R\right)i\sigma_2\left(\overline{q_L}\lambda_A d_R\right)$	$\mathcal{O}_{qq}^{(8)}$
	$\left(\overline{l_L}e_R\right)i\sigma_2\left(\overline{q_L}u_R\right)$	$\mathcal{O}_{lq}$	$\left(\overline{l_L}u_R\right)i\sigma_2\left(\overline{q_L}e_R\right)$	$\mathcal{O}_{lq'}$
	$\epsilon_{ABC}(\overline{l_L}i\sigma_2 q_L^{c\,A})(\overline{q_L^B}i\sigma_2 q_L^{c\,C})$	$\mathcal{O}_{qqql}$	$\epsilon_{ABC}(\overline{u_R^{c\,A}}d_R^B)(\overline{u_R^{c\,C}}e_R)$	$\mathcal{O}_{udue}$
	$\left(\phi^\dagger\phi\right)^2$	$\mathcal{O}_{\phi 4}$	$\frac{1}{3}\left(\phi^\dagger\phi\right)^3$	$\mathcal{O}_{\phi 6}$
SVF	$\left(\phi^\dagger iD_\mu\phi\right)\left(\overline{l_L}\gamma^\mu l_L\right)$	$\mathcal{O}_{\phi l}^{(1)}$	$\left(\phi^\dagger\sigma_a iD_\mu\phi\right)\left(\overline{l_L}\gamma^\mu\sigma_a l_L\right)$	$\mathcal{O}_{\phi l}^{(3)}$
	$\left(\phi^\dagger iD_\mu\phi\right)\left(\overline{e_R}\gamma^\mu e_R\right)$	$\mathcal{O}_{\phi e}^{(1)}$		
	$\left(\phi^\dagger iD_\mu\phi\right)\left(\overline{q_L}\gamma^\mu q_L\right)$	$\mathcal{O}_{\phi q}^{(1)}$	$\left(\phi^\dagger\sigma_a iD_\mu\phi\right)\left(\overline{q_L}\gamma^\mu\sigma_a q_L\right)$	$\mathcal{O}_{\phi q}^{(3)}$
	$\left(\phi^\dagger iD_\mu\phi\right)\left(\overline{u_R}\gamma^\mu u_R\right)$	$\mathcal{O}_{\phi u}^{(1)}$	$\left(\phi^\dagger iD_\mu\phi\right)\left(\overline{d_R}\gamma^\mu d_R\right)$	$\mathcal{O}_{\phi d}^{(1)}$
	$\left(\phi^T i\sigma_2 iD_\mu\phi\right)\left(\overline{u_R}\gamma^\mu d_R\right)$	$\mathcal{O}_{\phi ud}$		
SF	$\left(\phi^\dagger\phi\right)\left(\overline{l_L}\,\phi\,e_R\right)$	$\mathcal{O}_{e\phi}$		
	$\left(\phi^\dagger\phi\right)\left(\overline{q_L}\,\tilde{\phi}\,u_R\right)$	$\mathcal{O}_{u\phi}$	$\left(\phi^\dagger\phi\right)\left(\overline{q_L}\,\phi\,d_R\right)$	$\mathcal{O}_{d\phi}$
Oblique	$\phi^\dagger\phi\left(D^\mu\phi\right)^\dagger D_\mu\phi$	$\mathcal{O}_\phi^{(1)}$	$\left(\phi^\dagger D_\mu\phi\right)\left(\left(D^\mu\phi\right)^\dagger\phi\right)$	$\mathcal{O}_\phi^{(3)}$
	$\phi^\dagger\sigma_a\phi\,W_{\mu\nu}^a B^{\mu\nu}$	$\mathcal{O}_{WB}$		

Table 1.1: Dimension five and six operators arising from the integration of heavy scalars, vector bosons or fermions at tree level. We also include the dimension-four operator $\mathcal{O}_{\phi 4}$ and the loop-level generated dimension-six operator $\mathcal{O}_{WB}$ for notational purposes. Transposition of the second $SU(2)_L$ doublet is understood in the first four LRLR operators. σ_a and λ_A stand for the Pauli and Gell-Mann matrices, respectively, and ϵ_{ABC} is the totally antisymmetric tensor for color indices ($A, B, \cdots = 1, 2, 3$ in this case).

Chapter 2

Phenomenological implications of the dimension-six effective Lagrangian

In absence of any direct evidence of new physics, indirect searches become mandatory to unveil possible hints of physics beyond the SM and/or to constrain the parameter space of definite SM extensions. Thus, even if the new particles are so heavy that they cannot be directly produced, they can still be exchanged as virtual states, leading to corrections to physical observables, and eventually to a sizable departure from the SM. Then, more precise experiments should confirm such deviations or further constrain the parameters describing the new interactions. Their effects are encoded in the coefficients of the higher-dimensional operators in the effective Lagrangian approach, and the computation of the induced corrections to the electroweak precision observables is the ultimate goal of this chapter.

In order to study the impact of the new operators on physical observables it is reasonable, given the current experimental precision, to truncate the effective Lagrangian expansion keeping only terms up to dimension six,

$$\mathcal{L}_{\text{eff}} = \mathcal{L}_4 + \frac{1}{\Lambda}\mathcal{L}_5 + \frac{1}{\Lambda^2}\mathcal{L}_6,$$

as argued in the previous chapter. One important source of corrections comes from the dimension-six interactions involving the Higgs field, which after EWSB give rise to extra contributions to dimension-four operators

$$\frac{1}{\Lambda^2}\mathcal{L}_6 \supset \frac{1}{\Lambda^2}\mathcal{L}_6^{\phi} \overset{\text{EWSB}}{\longrightarrow} \frac{v^2}{\Lambda^2}\mathcal{L}_4',$$

and in particular to the neutral current (NC) and charged current (CC) couplings. Thus, prior to the computation of the corrections for the observables of interest, we will derive the pertinent effective Lagrangian after EWSB.

2.1 The effective Lagrangian after electroweak symmetry breaking

We review in this section the modifications of the SM interactions generated from higher-dimensional operators after EWSB. They result from terms in $\mathcal{L}_6$ [1] involving scalar fields and giving SM operators suppressed by a v^2/Λ^2 factor when the Higgs is replaced by its vev

$$\phi \to \langle \phi \rangle = \frac{1}{\sqrt{2}} \begin{pmatrix} 0 \\ v \end{pmatrix}. \tag{2.1}$$

A few comments are in order:

1. The vev in Eq. (2.1) is not necessarily related to the scalar potential parameters in the same way as in the SM, because the potential is in general also modified. Hence we should distinguish between the SM vev, which we call v_0, and the actual vev v. Their expressions only differ in terms of order $1/\Lambda^2$.

2. In principle when one replaces the Higgs by its vev one should use v. Note however that, as stressed in the previous chapter, we only consider new physics effects suppressed by inverse powers of Λ not larger than two. Therefore, when the replacement is done on the higher-dimensional operators, v and v_0 can be used indistinctly, since the difference will be of order $1/\Lambda^4$ and then negligible within our approximations. Obviously, this argument applies more generally: when two quantities differ only in terms of order $1/\Lambda^2$ they can be used indistinctly in any expression of order $1/\Lambda^2$. On the other hand, one should take all the corrections into account when working with order one expressions. For instance, in the SM expression for gauge boson masses we must use v and not v_0.

3. In practice, comparing to data, we assign a value to the vev, ~ 246 GeV. This figure does not correspond neither to v nor v_0. It is extracted from the Fermi constant G_F measured in muon decays, which in the SM equals $1/\sqrt{2}v_0^2$. In order to find the connection between v or v_0 and the above numerical value one must include the new physics correction to that process but, again, the difference will be of order $1/\Lambda^2$ so following the previous argument, in the higher-dimensional operators these are subleading effects, and we can simply insert v and replace it by the number 246 GeV.

Similar comments apply to all the relations and parameters derived within the SM. We discuss in what follows the corrections after EWSB on the different theory sectors due to the operators in Table 1.1.

2.1.1 Scalar potential

There are two operators in Table 1.1 which modify the structure of the scalar potential: $\mathcal{O}_{\phi 6}$ which adds a new piece to the original potential (1.8) and $\mathcal{O}_{\phi 4}$ which corrects the quartic coupling:

$$V(\phi) = -\mu_\phi^2 |\phi|^2 + \left(\lambda_\phi + \frac{\alpha_{\phi 4}}{\Lambda^2}\right) |\phi|^4 - \frac{1}{3}\alpha_{\phi 6} |\phi|^6 \frac{1}{\Lambda^2}. \tag{2.2}$$

Thus, these operators modify the expression for the Higgs vev, as emphasized above. Note first that the parameter $\alpha_{\phi 4}$ can be absorbed into the SM parameter λ_ϕ by redefining $\lambda_\phi \to \lambda_\phi - \alpha_{\phi 4}/\Lambda^2$.

[1] The unique operator in $\mathcal{L}_5$ does not modify the SM interactions but introduce additional ones besides Majorana neutrino masses, lepton flavor violating Yukawa interactions.

On the contrary, $\alpha_{\phi 6}$ does have an effect. The extremal points for the modified potential and the redefined λ_ϕ are

$$|\phi_\mp|^2 = \frac{\lambda_\phi \Lambda^2}{\alpha_{\phi 6}} \left(1 \mp \sqrt{1 - \frac{\alpha_{\phi 6}\mu_\phi^2}{\lambda_\phi^2 \Lambda^2}}\right), \tag{2.3}$$

where only the "$-$" solution deviates little from the SM relation for large Λ values. Actually, inserting (2.3) in the second derivative of $V(\phi)$

$$2\lambda_\phi - \frac{2\alpha_{\phi 6}}{\Lambda^2}|\phi|^2\Big|_{|\phi|^2=|\phi_\mp|^2} = \pm\sqrt{1 - \frac{\alpha_{\phi 6}\mu_\phi^2}{\lambda_\phi^2\Lambda^2}},$$

so if $\frac{\alpha_{\phi 6}}{\Lambda^2} < \frac{\lambda_\phi^2}{\mu_\phi^2}$ the "$-$" solution corresponds to a minimum whereas the "$+$" solution is a maximum (and goes to infinite when $\Lambda \to \infty$). Linearizing in $1/\Lambda^2$ the minimum solution we obtain for the scalar vev

$$v \equiv \sqrt{2}\,\langle|\phi|\rangle = \sqrt{\frac{\mu_\phi^2}{\lambda_\phi}}\left(1 + \frac{1}{8}\alpha_{\phi 6}\frac{\mu_\phi^2}{\lambda_\phi^2}\frac{1}{\Lambda^2}\right) = v_0\left(1 + \frac{1}{8}\frac{\alpha_{\phi 6}}{\lambda_\phi}\frac{v^2}{\Lambda^2}\right), \tag{2.4}$$

where we have used the SM expression $v_0 = \sqrt{\mu_\phi^2/\lambda_\phi}$ and replaced v_0 by v in the second term, which does not matter at the order we are working at.

2.1.2 Redefinition of gauge fields, coupling constants and vector boson masses.

There are no tree-level generated dimension-six operators in our basis correcting the gauge field kinetic term. Moreover, at the loop level there is only one operator that can have observable effects [2]. This is $\mathcal{O}_{WB}$, which can be identified with the S parameter, and introduces kinetic mixing between the neutral gauge fields: $\langle \mathcal{O}_{WB}\rangle = -v^2 \hat{W}^3_{\mu\nu}\hat{B}^{\mu\nu}/2$. We have placed a "hat" on the fields to indicate that they are not canonically normalized:

$$\mathcal{L}^{\text{Kin}}_{\text{Gauge}} = -\frac{1}{4}\hat{W}^a_{\mu\nu}\hat{W}^{a\ \mu\nu} - \frac{1}{4}\hat{B}_{\mu\nu}\hat{B}^{\mu\nu} - \frac{1}{2}\alpha_{WB}\frac{v^2}{\Lambda^2}\hat{W}^3_{\mu\nu}\hat{B}^{\mu\nu}. \tag{2.5}$$

In order to remove the kinetic mixing we can perform the field redefinition

$$\begin{aligned} W^3_\mu &= \hat{W}^3_\mu + \frac{\alpha_{WB}}{2}\frac{v^2}{\Lambda^2}\hat{B}_\mu, \\ B_\mu &= \hat{B}_\mu + \frac{\alpha_{WB}}{2}\frac{v^2}{\Lambda^2}\hat{W}^3_\mu, \end{aligned} \tag{2.6}$$

which diagonalizes the kinetic term at order v^2/Λ^2. This removes the kinetic mixing but modifies the gauge couplings and the covariant derivative, which reads in the canonical basis

$$D_\mu = \partial_\mu + ig_s G^A_\mu \mathrm{T}_A + ig\big(W^1_\mu T_1 + W^2_\mu T_2\big) + iW^3_\mu\left(gT_3 - g'\frac{\alpha_{WB}}{2}\frac{v^2}{\Lambda^2}Y\right) + iB_\mu\left(g'Y - g\frac{\alpha_{WB}}{2}\frac{v^2}{\Lambda^2}T_3\right). \tag{2.7}$$

[2] The others are of the form $\phi^\dagger\phi\ F_{\mu\nu}F^{\mu\nu}$ and their effect after EWSB can be removed by rescaling the gauge kinetic terms and coupling constants at the same time.

Thus, the neutral gauge boson mass matrix receives extra contributions:

$$\left\langle (D_\mu\phi)^\dagger D^\mu\phi \right\rangle = \frac{g^2v^2}{8}(W_\mu^1 - iW_\mu^2)(W_\mu^1 + iW_\mu^2) + \frac{v^2}{8}\left[-\left(g + g'\frac{\alpha_{WB}}{2}\frac{v^2}{\Lambda^2}\right)W_\mu^3 + \left(g' + g\frac{\alpha_{WB}}{2}\frac{v^2}{\Lambda^2}\right)B_\mu\right]^2. \tag{2.8}$$

Besides, gauge bosons masses also receive further corrections from the dimension-six operators $\mathcal{O}_\phi^{(1)}$ and $\mathcal{O}_\phi^{(3)}$

$$\begin{aligned}\left\langle \mathcal{O}_\phi^{(1)} \right\rangle &= \frac{v^2}{2}\left[\frac{g^2v^2}{8}\left(W_\mu^1 - iW_\mu^2\right)\left(W_\mu^1 + iW_\mu^2\right) + \frac{v^2}{8}\left(-gW_\mu^3 + g'B_\mu\right)^2\right], \\ \left\langle \mathcal{O}_\phi^{(3)} \right\rangle &= \frac{v^4}{16}\left(-gW_\mu^3 + g'B_\mu\right)^2,\end{aligned} \tag{2.9}$$

where we have neglected v^4/Λ^4 contributions. Hence, the physical charged vector boson mass now reads

$$M_W^2 = \left(M_W^0\right)^2\left(1 + \left(\frac{1}{2}\alpha_\phi^{(1)} + \frac{1}{4}\frac{\alpha_{\phi 6}}{\lambda_\phi}\right)\frac{v^2}{\Lambda^2}\right), \tag{2.10}$$

where $M_W^0 = \frac{gv_0}{2}$ is the SM mass and we use (2.4) to rewrite v as a function of v_0. In the neutral sector the combination that acquires a mass defines the physical Z boson

$$Z_\mu = \frac{1}{N}\left[\left(1 + \frac{g'}{g}\frac{\alpha_{WB}}{2}\frac{v^2}{\Lambda^2}\right)gW_\mu^3 - \left(1 + \frac{g}{g'}\frac{\alpha_{WB}}{2}\frac{v^2}{\Lambda^2}\right)g'B_\mu\right], \tag{2.11}$$

where the normalization constant

$$N = \sqrt{g^2 + g'^2}\left(1 + \frac{gg'}{g^2 + g'^2}\alpha_{WB}\frac{v^2}{\Lambda^2}\right). \tag{2.12}$$

Then, the massive neutral gauge boson coincides with the SM one $Z_\mu^{\rm SM}$ up to a field renormalization,

$$Z_\mu = \frac{Z_Z^{-\frac{1}{2}}}{\sqrt{g^2 + g'^2}}\left(g\hat{W}_\mu^3 - g'\hat{B}_\mu\right) = Z_Z^{-\frac{1}{2}}Z_\mu^{\rm SM}, \quad \text{with} \quad Z_Z = 1 + \frac{2gg'}{g^2 + g'^2}\alpha_{WB}\frac{v^2}{\Lambda^2}. \tag{2.13}$$

Whereas the renormalized mass

$$M_Z^2 = \left(M_Z^0\right)^2\left(1 + \left[\frac{2gg'}{g^2 + g'^2}\alpha_{WB} + \frac{1}{2}\alpha_\phi^{(1)} + \frac{1}{2}\alpha_\phi^{(3)} + \frac{1}{4}\frac{\alpha_{\phi 6}}{\lambda_\phi}\right]\frac{v^2}{\Lambda^2}\right), \tag{2.14}$$

where we have used the SM relation $M_Z^0 = \frac{\sqrt{g^2+g'^2}}{2}v_0$ and (2.4). On the other hand, the photon is defined as the orthonormal combination to (2.11), which is massless as required by $U(1)_{\rm em}$ gauge invariance. In this case, however, the photon cannot be expressed as a simple renormalization of the SM field, $A_\mu^{\rm SM}$. This is ultimately a consequence of the kinetic mixing:

$$A_\mu = \frac{Z_A^{-\frac{1}{2}}}{\sqrt{g^2 + g'^2}}\left(g'\hat{W}_\mu^3 + g\hat{B}_\mu\right) + \frac{Z_{ZA}^{-1}}{\sqrt{g^2 + g'^2}}\left(g\hat{W}_\mu^3 - g'\hat{B}_\mu\right) = Z_A^{-\frac{1}{2}}A_\mu^{\rm SM} + Z_{ZA}^{-1}Z_\mu^{\rm SM}, \tag{2.15}$$

with the field renormalizations given by

$$Z_A = 1 - \frac{2gg'}{g^2 + g'^2}\alpha_{WB}\frac{v^2}{\Lambda^2} \quad \text{and} \quad Z_{ZA}^{-1} = \alpha_{WB}\frac{g^2 - g'^2}{g^2 + g'^2}\frac{v^2}{\Lambda^2}. \tag{2.16}$$

Finally, it is straightforward to obtain the covariant derivative in the basis of physical vector fields using Eq. (2.13) and Eq. (2.15),

$$D_\mu = \partial_\mu + ig_s G_\mu^A \mathrm{T}_A + i\frac{e_0}{\sqrt{2}s_0}\left(W_\mu^+ T_+ + W_\mu^- T_-\right) + i\frac{e_0}{s_0 c_0} Z_Z^{\frac{1}{2}} Z_\mu \left(T_3 - s_0^2 Q - s_0 c_0 Z_A^{\frac{1}{2}} Z_{ZA}^{-1} Q\right) + ie_0 Z_A^{\frac{1}{2}} A_\mu Q, \tag{2.17}$$

where we have introduced for latter convenience the SM value for the electric charge e_0 and the weak mixing angle $s_0 \equiv \sin\theta_W^{\mathrm{SM}}$, $c_0 \equiv \cos\theta_W^{\mathrm{SM}}$, instead of the gauge couplings g and g'. This is the expression for the covariant derivative we will use in the following.

2.1.3 Fermion masses and rotation matrices

There are several operators in the effective Lagrangian that upon EWSB generate extra mass terms for the SM fermions but, as we will argue below, these will be of no relevance for our fits. Nevertheless, it is worth reviewing them for they may have interest for other studies. In particular, contributions to neutrino masses are of great phenomenological interest. Within our effective Lagrangian approach these can only arise at dimension five, being of Majorana type. On the other hand, dimension-six operators correct the Dirac masses for all the other SM fermions.

Majorana masses

Up to dimension six, neutrino masses can only arise from the famous lepton number violating dimension-five Weinberg operator, $\mathcal{O}_5 = \overline{l_L^c}\tilde{\phi}^*\tilde{\phi}^\dagger l_L$ [60]. After EWSB:

$$\langle \mathcal{O}_5 \rangle_{ij} = \frac{1}{2}\begin{pmatrix} \overline{\nu_L^{i\,c}} & \overline{e_L^{i\,c}} \end{pmatrix}\begin{pmatrix} v \\ 0 \end{pmatrix}\begin{pmatrix} v & 0 \end{pmatrix}\begin{pmatrix} \nu_L^j \\ e_L^j \end{pmatrix} = \frac{1}{2}v^2\overline{\nu_L^{i\,c}}\nu_L^j, \tag{2.18}$$

so the dimension-five Lagrangian gives a Majorana mass term for SM neutrinos:

$$\mathcal{L}_m^\nu = -\frac{1}{2}\left[m_{ij}^\nu\ \overline{\nu_L^{i\,c}}\nu_L^j + m_{ij}^{\nu\dagger}\ \overline{\nu_L^i}\nu_L^{j\,c}\right], \qquad m^\nu = -\frac{\alpha_5}{\Lambda}v^2. \tag{2.19}$$

Then, neutrino masses m_i^ν are obtained rotating to the mass eigenstate basis $\nu_L^i \to (\mathcal{U}_L^\nu)_{ij}\,\nu_L^j$,

$$m_i^\nu = -(\mathcal{U}_L^{\nu\ T})_{ik}\frac{(\alpha_5)_{kl}}{\Lambda}v^2(\mathcal{U}_L^\nu)_{li}. \tag{2.20}$$

This transformation introduces a mixing in the SM leptonic CC:

$$\mathcal{L}_{\mathrm{CC}} = -\frac{e_0}{\sqrt{2}s_0}U_{ij}W_\mu^-\overline{e_L^i}\gamma^\mu\nu_L^j + \mathrm{h.c.}, \tag{2.21}$$

with $U = \mathcal{U}_L^\nu$, when charged leptons are in the mass eigenstate basis. The matrix U is the analogous to the CKM matrix for quarks, and it is known as the *Pontecorvo-Maki-Nakagawa-Sakata* (PMNS) mixing matrix [63]. Contrary to the case of quarks it is conventional to assign U to the positive CC. It is important to note that, although the mixing matrix U is crucial for describing neutrino oscillations, it is irrelevant for all the EWPD analyses, and in general for describing any physical process where neutrino masses can be neglected. This is so because only the product $U^\dagger U = \mathbb{1}_3$ enters in all such processes. Therefore, we will ignore the leptonic mixing in what follows.

Dirac masses

Recall that after EWSB the Yukawa couplings in (1.7) give masses to fermions

$$\mathcal{L}_{\rm Yuk} \longrightarrow \mathcal{L}^f_{\rm m} = -m_i^{e\ \rm SM}\overline{e_L^i}e_R^i - m_i^{d\ \rm SM}\overline{d_L^i}d_R^i - V_{ij}^{0\ \dagger}m_j^{u\ \rm SM}\overline{u_L^i}u_R^j + \text{h.c.}, \tag{2.22}$$

where $m_i^{f\ \rm SM}$ are given by Eq. (1.13), and with our choice of fermion basis going to the mass eigenstate basis only requires rotating the LH u quarks, $u_L \to V^\dagger u_L$. However, dimension-six operators give further contributions to fermion masses

$$\langle \mathcal{O}_{e\phi}\rangle_{ij} = \frac{v^3}{2\sqrt{2}}\,\overline{e_L^i}e_R^j, \quad \langle \mathcal{O}_{u\phi}\rangle_{ij} = \frac{v^3}{2\sqrt{2}}\,\overline{u_L^i}u_R^j \quad \text{and} \quad \langle \mathcal{O}_{d\phi}\rangle_{ij} = \frac{v^3}{2\sqrt{2}}\,\overline{d_L^i}d_R^j, \tag{2.23}$$

implying extra, in general non-diagonal, corrections to Eq. (2.22). There are also extra diagonal contributions coming from the Higgs vev modification in Eq. (2.4). In summary

$$\begin{aligned}\mathcal{L}^f_{\rm m} =& -\left[m_i^{e\,\rm SM}\left(1+\frac{1}{8}\frac{\alpha_{\phi 6}}{\lambda_\phi}\frac{v^2}{\Lambda^2}\right)\delta_{ij} - \frac{(\alpha_{e\phi})_{ij}}{2\sqrt{2}}\frac{v^3}{\Lambda^2}\right]\overline{e_L^i}e_R^j - \left[m_i^{d\,\rm SM}\left(1+\frac{1}{8}\frac{\alpha_{\phi 6}}{\lambda_\phi}\frac{v^2}{\Lambda^2}\right)\delta_{ij} - \frac{(\alpha_{d\phi})_{ij}}{2\sqrt{2}}\frac{v^3}{\Lambda^2}\right]\overline{d_L^i}d_R^j - \\ &-\left[V_{ij}^{0\ \dagger}m_j^{u\ \rm SM}\left(1+\frac{1}{8}\frac{\alpha_{\phi 6}}{\lambda_\phi}\frac{v^2}{\Lambda^2}\right) - \frac{(\alpha_{u\phi})_{ij}}{2\sqrt{2}}\frac{v^3}{\Lambda^2}\right]\overline{u_L^i}u_R^j + \text{h.c.}\ .\end{aligned}$$

Therefore, in general not only the LH u quarks but all massive fermions must be rotated to go to the mass eigenstate basis. Thus,

$$m^f_{ij} \equiv \hat{m}^{f\ \rm SM}_{ij}\left(1+\frac{1}{8}\frac{\alpha_{\phi 6}}{\lambda_\phi}\frac{v^2}{\Lambda^2}\right) - \frac{v\,(\alpha_{f\phi})_{ij}}{2\sqrt{2}}\frac{v^2}{\Lambda^2} = \left(\mathcal{U}^f_L\right)_{ik} m^f_k \left(\mathcal{U}^f_R\right)^\dagger_{kj}, \tag{2.24}$$

where $m^f_i \geq 0$ are the fermion masses and $\mathcal{U}^f_{L,R}$ the corresponding diagonalizing unitary transformations. Note that we have defined $\hat{m}^{u\,\rm SM}_{ij} \equiv V^{0\ \dagger}_{ij} m^{u\ \rm SM}_j$, $\hat{m}^{e,d\,\rm SM}_{ij} \equiv m^{e,d\,\rm SM}_i \delta_{ij}$.

The matrices $\mathcal{U}^f_{L,R}$ can be expanded to order v^2/Λ^2,

$$\mathcal{U}^f_L \equiv \begin{cases} \mathbb{1}_3 + iA^f_L\frac{v^2}{\Lambda^2} & f=e,d \\ V^{0\ \dagger}\left(\mathbb{1}_3 + iA^u_L\frac{v^2}{\Lambda^2}\right) & f=u \end{cases}, \quad \mathcal{U}^f_R \equiv \mathbb{1}_3 + iA^f_R\frac{v^2}{\Lambda^2}, \quad f=e,d,u, \tag{2.25}$$

with $A^f_{L,R}$ hermitian to ensure the unitarity of $\mathcal{U}^f_{L,R}$. Fermion masses can be easily obtained from Eq. (2.24). They are given by the square root of the $m^f m^{f\ \dagger}$ or $m^{f\ \dagger}m^f$ eigenvalues and only depend on the SM masses, $\alpha_{\phi 6}$ and the diagonal $\alpha_{f\phi}$ entries:

$$m^f_i = m^{f\ \rm SM}_i\left(1+\frac{1}{8}\frac{\alpha_{\phi 6}}{\lambda_\phi}\frac{v^2}{\Lambda^2}\right) - \frac{v}{4\sqrt{2}}\left(\hat{\alpha}_{f\phi} + \hat{\alpha}^\dagger_{f\phi}\right)_{ii}\frac{v^2}{\Lambda^2}, \tag{2.26}$$

with $\hat{\alpha}_{u\phi} \equiv V\alpha_{u\phi}$, $\hat{\alpha}_{d\phi} \equiv \alpha_{d\phi}$ and $\hat{\alpha}_{e\phi} \equiv \alpha_{e\phi}$. The form of the hermitian matrices $A^f_{L,R}$ can be then derived from their definition, $\mathcal{U}^f_{L(R)}$ must diagonalize $m^f m^{f\ \dagger}$ ($m^{f\ \dagger}m^f$). Thus they read up to order v^2/Λ^2

$$\begin{aligned} i\left(A^f_L\right)_{ij} =& \frac{v}{2\sqrt{2}}\frac{(\hat{\alpha}^\dagger_{f\phi})_{ij}m^f_i + (\hat{\alpha}_{f\phi})_{ij}m^f_j}{\left(m^f_i\right)^2 - \left(m^f_j\right)^2}\left(1-\delta_{ij}\right), \\ i\left(A^f_R\right)_{ij} =& \frac{v}{2\sqrt{2}}\frac{(\hat{\alpha}_{f\phi})_{ij}m^f_i + (\hat{\alpha}^\dagger_{f\phi})_{ij}m^f_j}{\left(m^f_i\right)^2 - \left(m^f_j\right)^2}\left(1-\delta_{ij}\right), \end{aligned} \tag{2.27}$$

which are valid $\forall\ i,j$ [3].

In practice, the corrections just discussed will have no impact in the fits because the Yukawa couplings are arbitrary. Then, we can always redefine them from the beginning to absorb the corrections from the dimension-six operators $\mathcal{O}_{f\phi}$. This does not mean that the effects of these operators are unobservable because they do generate other interactions, as we will see. Nevertheless, they are not constrained by the electroweak precision observables included in our fits, though they do constribute to other physical processes.

2.1.4 Neutral and charged current couplings I: Direct corrections

The SM description of neutral and charged currents has been experimentally confirmed with high accuracy, thus constraining new physics predicting relatively large departures from the SM predictions. In this section we describe those operators that correct the SM neutral and charged gauge couplings to fermions. We must distinguish between two different types of corrections. Those that come from operators which, after the Higgs gets a vev, are trilinear receive the name of *direct corrections*. They are easily obtained and are discussed in the following. There is, however, a second source of corrections involving contributions from operators that indirectly influence the trilinear couplings, because they correct physical processes determining the input parameters. These are called *indirect corrections* and will be explained in next section.

Of all the dimension-six operators those of type $\mathcal{O}_{\phi\psi}^{(1,3)}$ give, after EWSB, the mentioned direct corrections to NC and CC couplings:

$$\left\langle \mathcal{O}_{\phi\psi}^{(1)} \right\rangle_{ij} = \frac{e_0 v^2}{4 s_0 c_0} Z_\mu \left(\overline{\psi^i} \gamma^\mu \psi^j \right), \tag{2.29}$$

$$\left\langle \mathcal{O}_{\phi F}^{(3)} \right\rangle_{ij} = -\frac{e_0 v^2}{\sqrt{2} s_0} W_\mu^+ \left(\overline{F^i} \gamma^\mu \sigma_+ F^j \right) - \frac{e_0 v^2}{4 s_0 c_0} Z_\mu \left(\overline{F^i} \gamma^\mu \sigma_3 F^j \right), \tag{2.30}$$

$$\left\langle \mathcal{O}_{\phi ud} \right\rangle_{ij} = \frac{e_0 v^2}{2\sqrt{2} s_0} W_\mu^+ \left(\overline{u_R^i} \gamma^\mu d_R^j \right), \tag{2.31}$$

with $\sigma_+ = (\sigma_1 + i\ \sigma_2)/2$. We generically write LH and RH fermion multiplets as $F = l_L, q_L$ and $f = e_R, u_R, d_R$, respectively, and use ψ to denote any SM fermion. Combining these vevs with those of the hermitian conjugate we can easily derive the shifts in the fermion couplings to $W^\pm$ and Z.

Neutral current couplings

The SM NC interactions are described by the following Lagrangian (see Eq. (1.16))

$$\mathcal{L}_{\rm NC}^{\rm SM} = -\frac{e_0}{s_0 c_0} Z_\mu \sum_\psi \overline{\psi} \gamma^\mu \left(g_L^\psi P_L + g_R^\psi P_R \right) \psi, \tag{2.32}$$

with $g_L^\psi = T_3^{\psi_L} - s_0^2 Q^\psi$ and $g_R^\psi = -s_0^2 Q^\psi$. As mentioned in Chapter 1, the SM NC are flavor blind, which is not necessarily true when we include the new corrections in Eqs. (2.29) and (2.30), as these involve arbitrary matrices and therefore in general introduce FCNC. After rotating to the mass eigenstate basis (this only requires to rotate the u_L quarks at first order), the direct contributions to NC couplings, $\delta^D g_{L,R}^\psi$, are given by:

[3] For $i = j$ the $1 - \delta_{ij}$ in the numerator is cancelled by the denominator and Eq. (2.27) reduces to

$$i\left(A_L^f\right)_{ii} = \frac{v}{4\sqrt{2}} \frac{\left(\hat{\alpha}_{f\phi}^\dagger - \hat{\alpha}_{f\phi}\right)_{ii}}{m_i^f}, \quad i\left(A_R^f\right)_{ii} = \frac{v}{4\sqrt{2}} \frac{\left(\hat{\alpha}_{f\phi} - \hat{\alpha}_{f\phi}^\dagger\right)_{ii}}{m_i^f}. \tag{2.28}$$

$$\begin{aligned}
\delta^D g_L^\nu &= -\tfrac{1}{4}\left(\alpha_{\phi l}^{(1)} - \alpha_{\phi l}^{(3)} + \text{h.c.}\right)\tfrac{v^2}{\Lambda^2}, \\
\delta^D g_L^e &= -\tfrac{1}{4}\left(\alpha_{\phi l}^{(1)} + \alpha_{\phi l}^{(3)} + \text{h.c.}\right)\tfrac{v^2}{\Lambda^2}, \qquad & \delta^D g_R^e &= -\tfrac{1}{4}\left(\alpha_{\phi e}^{(1)} + \text{h.c.}\right)\tfrac{v^2}{\Lambda^2}, \\
\delta^D g_L^u &= -\tfrac{1}{4} V\left(\alpha_{\phi q}^{(1)} - \alpha_{\phi q}^{(3)} + \text{h.c.}\right)V^\dagger\tfrac{v^2}{\Lambda^2}, & \delta^D g_R^u &= -\tfrac{1}{4}\left(\alpha_{\phi u}^{(1)} + \text{h.c.}\right)\tfrac{v^2}{\Lambda^2}, \\
\delta^D g_L^d &= -\tfrac{1}{4}\left(\alpha_{\phi q}^{(1)} + \alpha_{\phi q}^{(3)} + \text{h.c.}\right)\tfrac{v^2}{\Lambda^2}, \qquad & \delta^D g_R^d &= -\tfrac{1}{4}\left(\alpha_{\phi d}^{(1)} + \text{h.c.}\right)\tfrac{v^2}{\Lambda^2}.
\end{aligned} \tag{2.33}$$

As can be seen from the expression of the total covariant derivative in Eq. (2.17), there are two extra oblique corrections: one universal and coming from the renormalization of the Z boson, and a nonuniversal one from the Z-A mixing and proportional to the electric charge. We consider these two corrections separately from those coming from the operators in Eq. (2.29) and Eq. (2.30):

$$\delta^U g_{\text{NC}} \equiv Z_Z^{\frac{1}{2}} - 1 = s_0 c_0 \alpha_{WB}\frac{v^2}{\Lambda^2}, \tag{2.34}$$

$$\delta^Q g_{\text{NC}} \equiv -s_0 c_0 Z_A^{\frac{1}{2}} Z_{ZA}^{-1} Q = -\frac{1}{4}\sin 4\theta_W^{\text{SM}}\alpha_{WB}\frac{v^2}{\Lambda^2}. \tag{2.35}$$

Thus, the total direct contribution to $\mathcal{L}_{\text{NC}}$ is given by

$$\delta^D\mathcal{L}_{\text{NC}} = \delta^U g_{\text{NC}}\mathcal{L}_{\text{NC}}^{\text{SM}} - \frac{e_0}{s_0 c_0}Z_\mu \sum_\psi \overline{\psi^i}\gamma^\mu\left((\delta^D g_L^\psi)_{ij}P_L + (\delta^D g_R^\psi)_{ij}P_R + \delta^Q g_{\text{NC}}\delta_{ij}\right)\psi^j. \tag{2.36}$$

Charged current couplings

The SM CC interaction is described in the weak eigenstate basis by the Lagrangian

$$\mathcal{L}_{\text{CC}} = -\frac{e_0}{\sqrt{2}s_0}W_\mu^+ \sum_F \overline{F}\gamma^\mu\sigma_+ F + \text{h.c.}\,, \tag{2.37}$$

whose couplings receive extra contributions from (2.30) and its hermitian conjugate. In addition, (2.31) introduces $W^\pm$ couplings to RH quarks. The CC Lagrangian then reads

$$\mathcal{L}_{\text{CC}} = -\frac{e_0}{\sqrt{2}s_0}W_\mu^+\left[\sum_F\left(\delta_{ij} + \left(\alpha_{\phi F}^{(3)}\right)_{ij}\frac{v^2}{\Lambda^2}\right)\overline{F^i}\gamma^\mu\sigma_+F^j - \frac{(\alpha_{\phi ud})_{ij}}{2}\frac{v^2}{\Lambda^2}\,\overline{u_R^i}\gamma^\mu d_R^j\right] + \text{h.c.}\,, \tag{2.38}$$

which can be written in the physical fermion basis using (2.25). This leaves the RH quark CC invariant at order v^2/Λ^2 because they only appear at this order and RH quarks were assumed to be in the SM mass eigenstate basis. For the LH quark CC we need to take into account the rotations for both u_L and d_L, leading to

$$\frac{e_0}{\sqrt{2}s_0}\left(V_{ij}^0 + i\left(VA_L^d - A_L^u V\right)_{ij}\frac{v^2}{\Lambda^2} + \left(V\alpha_{\phi q}^{(3)}\right)_{ij}\frac{v^2}{\Lambda^2}\right). \tag{2.39}$$

Finally, for the leptonic CC we would also have to rotate the charged leptons:

$$\frac{e_0}{\sqrt{2}s_0}\left(\delta_{ij} + i\left(A_L^e\right)_{ij}\frac{v^2}{\Lambda^2} + \left(\alpha_{\phi l}^{(3)}\right)_{ij}\frac{v^2}{\Lambda^2}\right), \tag{2.40}$$

but the effect of such a rotation can be cancelled by rotating the neutrinos in the same way, $\nu_L \to \mathcal{U}_L^e \nu_L$, which is allowed, for neutrino masses are negligible.

Thus all the direct corrections to the CC Lagrangian are in principle nonuniversal and read

$$\delta^D \mathcal{L}_{\rm CC} = -\frac{e_0}{\sqrt{2}s_0} W_\mu^+ \left[\left(\delta^D U_L^\dagger\right)_{ij} \overline{\nu_L^i} \gamma^\mu e_L^j + \left(\delta^D V_L\right)_{ij} \overline{u_L^i} \gamma^\mu d_L^j + \left(\delta^D V_R\right)_{ij} \overline{u_R^i} \gamma^\mu d_R^j \right] + \text{h.c.} \,, \tag{2.41}$$

where we use the standard notation for lepton mixing matrix, U_L, and for quarks, $V_{L,R}$. Thus, conventionally, charged lepton currents are taken to be positive and quark CC negative, so the mixing definitions differ by a complex conjugation. The explicit form of the corrections to the SM couplings reads

$$\begin{aligned} \delta^D U_L &= \left(\alpha_{\phi l}^{(3)}\right)^\dagger \tfrac{v^2}{\Lambda^2}, \\ \delta^D V_L &= \left(V \alpha_{\phi q}^{(3)} + i \left(V A_L^d - A_L^u V\right)\right) \tfrac{v^2}{\Lambda^2}, \quad \delta^D V_R = -\tfrac{1}{2} \alpha_{\phi ud} \tfrac{v^2}{\Lambda^2}. \end{aligned} \tag{2.42}$$

As stressed in Section 2.1.3 the corrections to fermion masses can be always redefined away. In what follows we shall assume that this is the case so we can use

$$\delta^D V_L = V \alpha_{\phi q}^{(3)} \frac{v^2}{\Lambda^2}. \tag{2.43}$$

If one wants to recover the effect of the matrices A_L at some point (for instance, if one works within a model where the structure of Yukawa matrices are known), we only need to replace $V\alpha_{\phi q}^{(3)}$ by $V\alpha_{\phi q}^{(3)} + i\left(V A_L^d - A_L^u V\right)$.

2.1.5 Neutral and charged current couplings II: Indirect corrections

In order to make a quantitative use of the effective Lagrangian we first have to assign a definite value to each free parameter. In our case these are the electric charge, e_0, the weak mixing angle, s_0, the CKM matrix elements, V_{ij}^0, and the coefficients α_i encoding the new physics contributions. Our goal is determining the latter from the global fit to all experimental data. In practice, some of the SM parameters can be fixed, as they are very precisely measured. One must be careful though because the new physics will also in general contribute to the processes used to derive the values of the SM input parameters. Then, the values will also be modified because the expressions previously implemented to derive them no longer apply. In general a SM relation $a = a_0$, with a the experimental value and a_0 the SM expression, will be modified to include corrections depending on the operator coefficients which at the order we are working can be written

$$a = a_0 \left(1 + f\left(\alpha_i\right) \frac{v^2}{\Lambda^2}\right).$$

In this way, besides the direct corrections discussed above, the effect of dimension-six operators will indirectly influence the SM couplings derivation. We will therefore refer to these as *indirect corrections*. In the following we focus on the SM parameters and compute the new physics corrections for the processes used to determine them. We will then solve for a_0 and take the corresponding expression back to the neutral and charged couplings.

Electric charge e

The experimental value for the electric charge is extracted from the fine-structure constant, α. Its most accurate determination comes from the measurement of the $e^{\pm}$ anomalous magnetic moment [64]. In the SM we have

$$\alpha = \frac{e_0^2}{4\pi}. \tag{2.44}$$

The only new effect from the operators considered in Chapter 1 is the replacement of e_0 by $e_0 Z_A^{\frac{1}{2}}$. Hence,

$$e_0 = e\ Z_A^{-\frac{1}{2}} = e\left(1 + s_0 c_0 \alpha_{WB} \frac{v^2}{\Lambda^2}\right), \tag{2.45}$$

with e defined by Eq. (2.44), $e = \sqrt{4\pi\alpha}$.

Weak mixing angle $\sin^2\theta_W$

As it is well known, within the SM there are several definitions of the weak mixing angle which agree at lowest order but involve different radiative corrections. One possible definition, introduced in the on-shell renormalization scheme, is in terms of the W and Z masses, $\sin^2\theta_W = 1 - M_W^2/M_Z^2$, to any order in perturbation theory. Other definition is in terms of the Fermi coupling, the Z mass and the hyperfine structure constant, $\sin^2\theta_W \cos^2\theta_W = \pi\alpha/\sqrt{2}G_F M_Z^2$. Note that, as the presence of new physics modifies the previous relations, these definitions are no longer equal at tree level. We shall adopt the definition involving the more precisely measured inputs. This is the last one because the Fermi coupling constant is determined with a much better precision than the W mass. Therefore, let us focus on how the new physics alters the experimental determination of G_F. This is extracted from the muon lifetime, τ_μ, measured in muon decay experiments [65, 66]. In the SM the muon decay amplitude is given at tree level by

$$\mathcal{M}_{\rm SM} = -i\frac{g^2}{2\left(M_W^0\right)^2}(\overline{\nu_L^\mu}\gamma^\lambda\mu_L)(\overline{e_L}\gamma_\lambda\nu_L^e), \tag{2.46}$$

where the W has been integrated out, since $m_\mu \ll M_W$. The coefficient of such amplitude is directly related to the Fermi constant:

$$\frac{4G_F}{\sqrt{2}} = \frac{g^2}{2\left(M_W^0\right)^2} = \frac{e_0^2}{2s_0^2c_0^2\left(M_Z^0\right)^2} = \frac{2}{v_0^2}, \tag{2.47}$$

where the second and third identities come from SM tree-level relations. With the amplitude (2.46) one can compute the muon decay width, whose inverse gives the muon lifetime:

$$\frac{1}{\tau_\mu} \equiv \Gamma\left(\mu^- \to \nu e^- \bar{\nu}\right) = \frac{G_F^2\ m_\mu^5}{192\pi^3}. \tag{2.48}$$

When dimension-six effects are taken into account the previous expression is modified but, similarly as we did for the electric charge, we define the *muon decay constant*, G_μ, to be the quantity given by Eq. (2.48), $G_\mu^2 \equiv 192\pi^3/\tau_\mu m_\mu^5$. This differs from G_F by new dimension-six operator contributions.

Unlike in the SM (where only the decay into the $\nu^\mu\overline{\nu^e}$ pair is available), CC couplings do not have to be flavor diagonal in the presence of new physics, and channels with other $\nu\overline{\nu}$ neutrino flavors can be open. Since experiments are blind to the final neutrino flavor, except in neutrino oscillations, for they just see missing energy, all channels should be added when computing the total

width. However, as we only consider new physics effects resulting from the interference, we can still restrict ourselves to the analysis of the SM channel. Then, the amplitude (2.46) must also include the CC couplings and the W mass corrections in Eq. (2.42) and Eq. (2.10), respectively, as well as the four-fermion contributions from $\mathcal{O}_{ll}^{(1)}$ and $\mathcal{O}_{ll}^{(3)}$. There are six different index assignments giving the operator structure in Eq. (2.46), $(\mathcal{O}_{ll}^{(1)})_{2112}$, $(\mathcal{O}_{ll}^{(1)})_{1221}$, $(\mathcal{O}_{ll}^{(3)})_{1122}$, $(\mathcal{O}_{ll}^{(3)})_{2211}$, $(\mathcal{O}_{ll}^{(3)})_{2112}$ and $(\mathcal{O}_{ll}^{(3)})_{1221}$. Putting all the pieces together and expressing the result in terms of the Fermi constant, G_F, the total amplitude reads

$$\mathcal{M} = -i\frac{4G_F}{\sqrt{2}}\left(1+\left[\left(\alpha_{\phi l}^{(3)}\right)_{22}+\left(\alpha_{\phi l}^{(3)}\right)_{11}^{\dagger}-\frac{\alpha_\phi^{(1)}}{2}-\frac{1}{4}\frac{\alpha_{\phi 6}}{\lambda_\phi}-\frac{(\alpha_{ll})_{2211}}{\sqrt{2}G_F v^2}\right]\frac{v^2}{\Lambda^2}\right)(\overline{\nu_L^\mu}\gamma^\lambda\mu_L)\,(\overline{e_L}\gamma_\lambda\nu_L^e)\,. \tag{2.49}$$

We have used the symmetry $\{ij\}\leftrightarrow\{kl\}$ on the operator indices of $(\mathcal{O}_{ll}^{(1,3)})_{ijkl}$ to define the combination

$$(\alpha_{ll})_{2211} \equiv \left(\alpha_{ll}^{(3)}\right)_{2211}+\frac{1}{2}\left(\alpha_{ll}^{(1)}-\alpha_{ll}^{(3)}\right)_{1221}\,.$$

In the term suppressed by v^2/Λ^2 we can also replace v by v_0, and use the relation (2.47) between G_F and v_0. Eq. (2.49) allows us to directly read the corrections to the muon decay width[4], and obtain the relation between G_μ and G_F. At linear order in v^2/Λ^2

$$G_F = G_\mu\left(1-\left[\Delta_{G_F}-\frac{\alpha_\phi^{(1)}}{2}-\frac{1}{4}\frac{\alpha_{\phi 6}}{\lambda_\phi}\right]\frac{v^2}{\Lambda^2}\right), \tag{2.50}$$

where we have introduced

$$\Delta_{G_F} \equiv \mathrm{Re}\left[\left(\alpha_{\phi l}^{(3)}\right)_{22}+\left(\alpha_{\phi l}^{(3)}\right)_{11}\right]-(\alpha_{ll})_{2211} \tag{2.51}$$

for convenience for it will be the combination appearing in subsequent expressions involving the relation (2.50).

Let us finally express s_0 and c_0 in terms of the inputs and the operators coefficients. This can be done simply using the second identity in Eq. (2.47) and rewriting G_F, e_0 and M_Z^0 in terms of the inputs G_μ, α and M_Z (see Eq. (2.50), Eq. (2.45) and Eq. (2.14)). Thus, solving the corresponding quadratic equation

$$s_0^2 = s^2\left(1+\frac{4sc^3}{c^2-s^2}\alpha_{WB}\frac{v^2}{\Lambda^2}+\frac{c^2}{c^2-s^2}\left(\Delta_{G_F}+\frac{\alpha_\phi^{(3)}}{2}\right)\frac{v^2}{\Lambda^2}\right), \tag{2.52}$$

$$c_0^2 = c^2\left(1-\frac{4s^3c}{c^2-s^2}\alpha_{WB}\frac{v^2}{\Lambda^2}-\frac{s^2}{c^2-s^2}\left(\Delta_{G_F}+\frac{\alpha_\phi^{(3)}}{2}\right)\frac{v^2}{\Lambda^2}\right), \tag{2.53}$$

where s^2 and $c^2=1-s^2$ are defined by

$$s^2c^2 \equiv \frac{\pi\alpha}{\sqrt{2}G_\mu M_Z^2}. \tag{2.54}$$

To conclude, just recall that the muon decay constant also allows to derive the input value for the Higgs vev using the SM relation $v_0^2=(\sqrt{2}\,G_F)^{-1}$. This, together with Eqs. (2.4) and (2.51), give the relation between the actual vev v and the input G_μ:

$$v^2 = \frac{1}{\sqrt{2}G_\mu}\left(1+\left[\Delta_{G_F}-\frac{\alpha_\phi^{(1)}}{2}\right]\frac{v^2}{\Lambda^2}\right). \tag{2.55}$$

[4]There are no corrections from the muon mass, for it is the physical mass which is an input.

Cabibbo-Kobayashi-Maskawa matrix elements V_{ij}

There is no general expression for the SM CKM matrix in terms of experimental inputs and dimension-six operator coefficients, since each element is experimentally determined from different processes. Here we derive the expressions for the magnitudes of V_{ud} and V_{us}, which we will use when discussing the measurements of the unitarity of the first row of the CKM matrix. We do not work out the corresponding expression for V_{ub} as its contribution to that sum is negligible compared to the other two terms.

V_{ud}

$|V_{ud}|$ is extracted from $0^+ \to 0^+$ superallowed nuclear β-decays by measuring the corresponding decay rate $\Gamma^{\frac{1}{2}} \propto G_\mu |V_{ud}|$ [67]. Computing the corrections to the SM decay rate one then can find the relation between V_{ud} and V_{ud}^0 in the same way as we did for the Fermi constant. Note that a transition between two $J^P = 0^+$ states is parity conserving, and therefore only the vector part of the quark CC $\overline{u}\gamma^\mu d$ is involved. As in the case of muon decay the new contributions to the decay width come from replacing the SM CC couplings and W mass in the $d \to u + e^- + \bar{\nu}$ amplitude by the corrected ones, as well as from adding the contributions from four-fermion operators. In this case the only four-fermion operator that contributes to the process is $\mathcal{O}_{lq}^{(3)}$. As we also did before, only the standard channel with an outgoing $\overline{\nu^e}$ is considered. Besides, in this case there can be also contributions from the CC couplings with RH quarks (see Eq. (2.42)). After computing the decay width from the resulting amplitude and rewriting it in terms of the Fermi constant, we can use Eq. (2.50) to obtain:

$$\left|V_{ud}^0\right| = |V_{ud}| \left(1 + \Delta V_{ud} \frac{v^2}{\Lambda^2}\right), \tag{2.56}$$

with

$$\Delta V_{ud} \equiv -\mathrm{Re}\left[\frac{\left(V\alpha_{\phi q}^{(3)} - \frac{1}{2}\alpha_{\phi ud}\right)_{11} - \sum_i V_{ui}\left(\alpha_{lq}^{(3)}\right)_{11i1}}{V_{ud}} - \left(\alpha_{\phi l}^{(3)}\right)_{22} + (\alpha_{ll})_{2211}\right]. \tag{2.57}$$

V_{us}

Until recently, semileptonic kaon decays, $K \to \pi\ell\nu$ with $\ell = e$ or μ, have provided the best determination of the V_{us} matrix element through the measurement of the transition $s \to u + \ell^- + \nu$. The derivation of the relation between V_{us} and V_{us}^0 matches the previous one between V_{ud} and V_{ud}^0 [5], but now the charged lepton in the final state can be either an electron or a muon. Since both decays are used to obtain an averaged value for V_{us} [68], the relation is in this case

$$\left|V_{us}^0\right| = |V_{us}| \left(1 + \Delta V_{us}^{K\ell 3} \frac{v^2}{\Lambda^2}\right), \tag{2.58}$$

$$\begin{aligned}\Delta V_{us}^{K\ell 3} \equiv &- \mathrm{Re}\left[\frac{\left(V\alpha_{\phi q}^{(3)} - \frac{1}{2}\alpha_{\phi ud}\right)_{12} - \sum_i V_{ui}\left[\omega_e\left(\alpha_{lq}^{(3)}\right)_{11i2} + \omega_\mu\left(\alpha_{lq}^{(3)}\right)_{22i2}\right]}{V_{us}}\right] - \\ &- \mathrm{Re}\left[-\omega_\mu\left(\alpha_{\phi l}^{(3)}\right)_{11} - \omega_e\left(\alpha_{\phi l}^{(3)}\right)_{22} + (\alpha_{ll})_{2211}\right],\end{aligned} \tag{2.59}$$

[5] Although this time it is a $0^- \to 0^-$, the vector part of the quark current is still the only one involved.

where the numerical coefficients $\omega_e,\ \omega_\mu$ are the weights in the average of $K\to\pi e\nu$ and $K\to\pi\mu\nu$ data, respectively. We will use the K_Le3, $K_L\mu3$, K_Se3, $K^\pm e3$ and $K^\pm\mu3$ decay modes [68], resulting in $\omega_e\approx 0.6$ and $\omega_\mu\approx 0.3$.

Another determination of V_{us} with similar precision can be obtained by comparing the decay rates $K\to\mu\nu(\gamma)$ and $\pi\to\mu\nu(\gamma)$. Including the different corrections to the ratio $|V_{us}|^2/|V_{ud}|^2\propto\Gamma\left(K\to\mu\nu(\gamma)\right)/\Gamma\left(\pi\to\mu\nu(\gamma)\right)$, we find[6]

$$\frac{|V_{us}|}{|V_{ud}|}=\frac{\left|V_{us}^0\right|}{|V_{ud}^0|}\left(1+\mathrm{Re}\left[\frac{\left(V\alpha_{\phi q}^{(3)}\right)_{12}-\sum_i V_{ui}\left(\alpha_{lq}^{(3)}\right)_{22i2}}{V_{us}}-\frac{\left(V\alpha_{\phi q}^{(3)}\right)_{11}-\sum_i V_{ui}\left(\alpha_{lq}^{(3)}\right)_{22i1}}{V_{ud}}\right]\frac{v^2}{\Lambda^2}\right). \tag{2.60}$$

Using the relation between V_{ud} and V_{ud}^0 derived above we can obtain a second one between V_{us} and V_{us}^0:

$$\left|V_{us}^0\right|=|V_{us}|\left(1+\Delta V_{us}^{K/\pi}\frac{v^2}{\Lambda^2}\right), \tag{2.61}$$

$$\begin{aligned}\Delta V_{us}^{K/\pi}\equiv&-\mathrm{Re}\left[\frac{\left(V\alpha_{\phi q}^{(3)}\right)_{12}-\sum_i V_{ui}\left(\alpha_{lq}^{(3)}\right)_{22i2}}{V_{us}}-\frac{\frac{1}{2}\left(\alpha_{\phi ud}\right)_{11}+\sum_i V_{ui}\left[\left(\alpha_{lq}^{(3)}\right)_{11i1}-\left(\alpha_{lq}^{(3)}\right)_{22i1}\right]}{V_{ud}}\right]-\\&-\mathrm{Re}\left[-\left(\alpha_{\phi l}^{(3)}\right)_{22}+\left(\alpha_{ll}\right)_{2211}\right].\end{aligned} \tag{2.62}$$

Thus, taking the weighted average between the two determinations, $\left|V_{us}^{Kl3}\right|=0.2246\pm0.0012$ and $\left|V_{us}^{K/\pi}\right|=0.2259\pm0.0014$ [68], we finally get

$$\left|V_{us}^0\right|=|V_{us}|\left(1+\omega_{K\ell3}\ \Delta V_{us}^{K\ell3}\ \frac{v^2}{\Lambda^2}+\omega_{K/\pi}\ \Delta V_{us}^{K/\pi}\ \frac{v^2}{\Lambda^2}\right), \tag{2.63}$$

with $\omega_{K\ell3}\approx 0.57$, $\omega_{K/\pi}\approx 0.43$.

Once we have reviewed how the different parameters entering the neutral and charged current lagrangrians are derived from experiment, including new physics effects, we can come back to the computation of the corrections to the Z and W couplings to fermions.

Neutral current couplings

As we have done previously, we can replace the parameters $e_0,\ s_0$ and c_0 by their counterparts $e,\ s$ and c in the new physics corrections for no extra dimension-six contribution arises from such a replacement. On the other hand, using (2.45), (2.52) and (2.53) to correct the SM coupling $\frac{e_0}{s_0c_0}\left(T_3-s_0^2Q\right)$, we get extra contributions to $\delta^U g_{\rm NC}$ and $\delta^Q g_{\rm NC}$. These add to those in (2.34) and (2.35) to give

$$\delta^U g_{\rm NC}=-\frac{1}{2}\left[\Delta_{G_F}+\frac{\alpha_\phi^{(3)}}{2}\right]\frac{v^2}{\Lambda^2} \tag{2.64}$$

and

$$\delta^Q g_{\rm NC}=-Q\left(\frac{sc}{c^2-s^2}\alpha_{WB}+\frac{s^2c^2}{c^2-s^2}\left[\Delta_{G_F}+\frac{\alpha_\phi^{(3)}}{2}\right]\right)\frac{v^2}{\Lambda^2}. \tag{2.65}$$

[6] This time there are no corrections from the RH quark CC for these do not interfere with the SM amplitude. Besides, there are no corrections from the leptonic CC transition, as they cancel because both decays are into muon flavor.

Therefore, the final NC Lagrangian is given by

$$\mathcal{L}_{\rm NC}=-\frac{e}{sc}\left(1+\delta^U g_{\rm NC}\right)Z_\mu\sum_\psi \overline{\psi^i}\gamma^\mu\Big[\Big(g_L^\psi\delta_{ij}+(\delta^D g_L^\psi)_{ij}\Big)P_L+\Big(g_R^\psi\delta_{ij}+(\delta^D g_R^\psi)_{ij}\Big)P_R+\delta^Q g_{\rm NC}\delta_{ij}\Big]\psi^j, \tag{2.66}$$

where from now on $g^\psi_{L,R}$ denote the SM couplings evaluated for s^2, $g^\psi_{L,R}\equiv g^\psi_{L,R}\left(s^2\right)=T_3^{\psi_L}-s^2Q^\psi$.

Charged current couplings

Now, using (2.45) and (2.52) in the global CC factor, we obtain the universal correction

$$\delta^U g_{\rm CC}=\left[\frac{sc}{s^2-c^2}\alpha_{WB}-\frac{c^2}{2\left(c^2-s^2\right)}\left(\Delta_{G_F}+\frac{\alpha_\phi^{(3)}}{2}\right)\right]\frac{v^2}{\Lambda^2}. \tag{2.67}$$

Additional indirect corrections to LH quark couplings take the form $V_{ij}^0=V_{ij}\left(1+\delta^I V_{ij}\right)$. The complete CC Lagrangian reads

$$\begin{aligned}\mathcal{L}_{\rm CC}=-\frac{e}{\sqrt{2}s}\left(1+\delta^U g_{\rm CC}\right)W_\mu^+\ &\Big[\Big(\delta_{ij}+\left(\delta^D U_L^\dagger\right)_{ij}\Big)\overline{\nu_L^i}\gamma^\mu e_L^j+\left(\delta^D V_R\right)_{ij}\overline{u_R^i}\gamma^\mu d_R^j+\\ &+\Big(V_{ij}+\left(\delta^D V_L\right)_{ij}+V_{ij}\delta^I V_{ij}\Big)\overline{u_L^i}\gamma^\mu d_L^j\Big]+\text{h.c.}\,.\end{aligned} \tag{2.68}$$

2.1.6 Yukawa interactions

Obviously, the operators $\mathcal{O}_{f\phi}$ in Eq. (2.23) also correct Yukawa interactions coupling the physical Higgs boson to fermions. Expanding the scalar field around its vev we obtain

$$\left(\mathcal{O}_{f\phi}\right)_{ij}=\left\langle\mathcal{O}_{f\phi}\right\rangle_{ij}+\frac{3v^2}{2\sqrt{2}}\,H\overline{f_L^i}f_R^j+\ldots,\quad f=e,u,d. \tag{2.69}$$

So when writing the interactions in the fermion mass eigenstate basis using the matrices $\mathcal{U}^f_{L,R}$, they in general are no longer diagonal. Similarly, the operator $\mathcal{O}_5$ generates lepton number violating neutrino-Higgs interactions:

$$\left(\mathcal{O}_5\right)_{ij}=\left\langle\mathcal{O}_5\right\rangle_{ij}+vH\overline{\nu_L^{i\,c}}\nu_L^j+\ldots, \tag{2.70}$$

though these are very suppressed by the tiny neutrino masses.

Note that in expanding the operators $\mathcal{O}^{(1)}_{\phi\psi}$ and $\mathcal{O}^{(3)}_{\phi F}$ around the scalar vev, derivative Higgs couplings are generated as well[7]

$$\begin{aligned}\left(\mathcal{O}^{(1)}_{\phi\psi}\right)_{ij}&=\left\langle\mathcal{O}^{(1)}_{\phi\psi}\right\rangle_{ij}+\frac{v^2}{2}i\partial_\mu H\left(\overline{\psi^i}\gamma^\mu\psi^j\right),\\ \left(\mathcal{O}^{(3)}_{\phi F}\right)_{ij}&=\left\langle\mathcal{O}^{(3)}_{\phi F}\right\rangle_{ij}+\frac{v^2}{2}i\partial_\mu H\left(\overline{F^i}\gamma^\mu\sigma_3F^j\right).\end{aligned} \tag{2.71}$$

[7]Note that these can be written as further Yukawa interactions integrating by parts and using perturbative field redefinitions [69].

Finally, there are further corrections from the operators $\mathcal{O}_\phi^{(1)}$ and $\mathcal{O}_\phi^{(3)}$, that contribute to the Higgs kinetic term,

$$\mathcal{L}_H^{\text{Kin}} = \frac{1}{2}\left(1+\frac{1}{2}\left(\alpha_\phi^{(1)}+\alpha_\phi^{(3)}\right)\frac{v^2}{\Lambda^2}\right)\partial_\mu H \partial^\mu H, \tag{2.72}$$

entering in the Yukawa interactions after writing the Lagrangian in the canonical basis.

Therefore, the final form of the scalar coupling to fermions reads

$$\mathcal{L}_H = -\frac{1}{\sqrt{2}} H\left(1+\delta^U y\right)\left[\sum_f \left(y_{ii}^f \delta_{ij} + \delta y_{ij}^f\right)\overline{f_L^i} f_R^j + \delta y_{ij}^{\nu^c}\overline{\nu_L^{i\,c}}\nu_L^j + \text{h.c.}\right] + i\partial_\mu H \sum_f h_{ij}^f\ \overline{f^i}\gamma^\mu f^j, \tag{2.73}$$

with

$$\delta^U y = -\frac{1}{4}\left(\alpha_\phi^{(1)}+\alpha_\phi^{(3)}\right)\frac{v^2}{\Lambda^2} \tag{2.74}$$

and

$$\begin{aligned}
\delta y_{ij}^{\nu^c} &= -\sqrt{2}\,(\alpha_5)_{ij}\,\tfrac{v}{\Lambda}, & h_{ij}^{\nu_L} &= \tfrac{1}{2}\left(\alpha_{\phi l}^{(1)} - \alpha_{\phi l}^{(3)} - \text{h.c.}\right)_{ij}\tfrac{v}{\Lambda^2},\\
\delta y_{ij}^{e} &= -\left((\alpha_{e\phi})_{ij} + \tfrac{1}{4}\left(\alpha_{e\phi}+\text{h.c.}\right)_{ii}\delta_{ij}\right)\tfrac{v^2}{\Lambda^2}, & h_{ij}^{e_L} &= \tfrac{1}{2}\left(\alpha_{\phi l}^{(1)} + \alpha_{\phi l}^{(3)} - \text{h.c.}\right)_{ij}\tfrac{v}{\Lambda^2},\\
& & h_{ij}^{e_R} &= \tfrac{1}{2}\left(\alpha_{\phi e}^{(1)} - \text{h.c.}\right)_{ij}\tfrac{v}{\Lambda^2},\\
\delta y_{ij}^{u} &= -\left((V\alpha_{u\phi})_{ij} + \tfrac{1}{4}\left(V\alpha_{u\phi}+\text{h.c.}\right)_{ii}\delta_{ij}\right)\tfrac{v^2}{\Lambda^2}, & h_{ij}^{u_L} &= \tfrac{1}{2}V_{ik}\left(\alpha_{\phi q}^{(1)} - \alpha_{\phi q}^{(3)} - \text{h.c.}\right)_{kl}V_{lj}^\dagger\tfrac{v}{\Lambda^2},\\
& & h_{ij}^{u_R} &= \tfrac{1}{2}\left(\alpha_{\phi u}^{(1)} - \text{h.c.}\right)_{ij}\tfrac{v}{\Lambda^2},\\
\delta y_{ij}^{d} &= -\left((\alpha_{d\phi})_{ij} + \tfrac{1}{4}\left(\alpha_{d\phi}+\text{h.c.}\right)_{ii}\delta_{ij}\right)\tfrac{v^2}{\Lambda^2}, & h_{ij}^{d_L} &= \tfrac{1}{2}\left(\alpha_{\phi q}^{(1)} + \alpha_{\phi q}^{(3)} - \text{h.c.}\right)_{ij}\tfrac{v}{\Lambda^2},\\
& & h_{ij}^{d_R} &= \tfrac{1}{2}\left(\alpha_{\phi d}^{(1)} - \text{h.c.}\right)_{ij}\tfrac{v}{\Lambda^2}.
\end{aligned} \tag{2.75}$$

As we will see, these Higgs interactions will have no direct impact in the precision observables used in our fits, which will be then completely blind to the $\mathcal{O}_{f\phi}$ operators. Nevertheless the contributions of these can not be ignored, since in general they can yield contributions to FCNC processes. Although such rare processes receive only quadratic contributions from the dimension-six operators, the stringent bounds on FCNC can result in quite restrictive limits on the $\alpha_{f\phi}$ coefficients, and then on the new physics flavor-violating parameters. The corresponding limits provide important information, complementary to that derived from EWPD, where only flavor-conserving neutral current processes are considered. Obviously, the same remark applies to the non-diagonal entries of $\mathcal{O}_{\phi\psi}^{(1)}$ and $\mathcal{O}_{\phi F}^{(3)}$, which generate vector-exchange flavor-changing contributions, as pointed out in Section 2.1.4.

2.2 Corrections to electroweak precision observables

Let us now translate the corrections to the SM Lagrangian just derived and the genuine new four-fermion interactions into extra contributions to precision observables [8] entering in our fits. We consider several different types of observables:

- Measurements of Z properties at the pole. These include partial decay widths as well as left-right and forward-backward asymmetries.
- The W mass and decay widths, as well as the leptonic branching ratios, which are useful to test lepton universality, for instance.
- Low-energy effective ν-q and ν^μ-e couplings entering in the description of neutrino-nucleon deep-inelastic scattering (DIS) and neutrino-electron scattering, respectively.
- Low-energy effective couplings describing parity violation in atoms and in Møller scattering: the atomic and the electron weak charges.
- Unitarity constraints on the CKM matrix (first row).
- $e^+e^- \to \overline{f}f$ cross sections and asymmetries off the Z pole measured at LEP 2.

As already emphasized new physics corrections will be evaluated at tree level, and only the interference with the SM amplitudes will be considered. For the SM predictions, on the other hand, we include the state-of-the-art of radiative corrections (see Appendix A for details).

The computation of the observables is straightforward: we only have to take the SM tree-level amplitudes, replace the SM couplings and masses by the corrected ones, and whenever they can interfere add the new amplitudes involving the four-fermion operators. Once all corrections are included, the SM-new physics interference can be obtained linearizing the resulting expression in $\frac{v^2}{\Lambda^2}$. In this way we get a tree-level prediction for any observable O

$$O^{\rm tree} = O^{\rm tree}_{\rm SM} + \delta O^{\rm tree}_{\rm New}\frac{v^2}{\Lambda^2}, \quad \delta O^{\rm tree}_{\rm New} \equiv \frac{\partial O^{\rm tree}}{\partial(v^2/\Lambda^2)}, \tag{2.76}$$

that must be improved to include the higher-order corrections in perturbation theory for the SM part. The final expression for the observable is then of the form

$$O^{\rm New-tree}_{\rm SM-loop} = O^{\rm tree}_{\rm SM} + O^{\rm loop}_{\rm SM} + \delta O^{\rm tree}_{\rm New}\frac{v^2}{\Lambda^2}. \tag{2.77}$$

2.2.1 Z lineshape observables

The LEP and SLC measurements of $e^+e^- \to \bar{f}f$ cross sections near the Z pole [70] provide the most precise determination of the properties of the Z boson, and have been crucial in determining the validity of the SM description of NC. Around the Z pole the process is dominated by the Z-exchange diagram and the differential cross section for $f \neq e$ is given by[9]

$$\frac{d\sigma_{e^+e^-\to Z\to\bar{f}f}}{d\Omega} = \frac{9}{4}\frac{s\Gamma_e\Gamma_f}{\left(s-M_Z^2\right)^2 + s^2\Gamma_Z^2/M_Z^2}\left[\left(1+\cos^2\theta\right)\left(1-P_eA_e\right) + 2\cos\theta A_f\left(-P_e+A_e\right)\right], \tag{2.78}$$

[8] We could distinguish between *observables* and *pseudo-observables*. The former refer to cross sections and asymmetries directly measured in experiments, while the latter are derived quantities and are usually definition dependent. For simplicity we will use the term *observable* to refer to both of them.

[9] For $f = e^-$ there is also a t-channel diagram contributing to the cross section.

where P_e is the polarization of the electron in the beam, and Γ_f and A_f are the partial decay width of the Z into $\bar{f}f$ and the left-right asymmetries, respectively, whose expressions will be given below. Roughly speaking, once we know the beam polarization, these quantities as well as the Z boson mass can be determined from experiment by scanning in the center of mass energy and fitting the above expression to the total cross section as well as the angular distribution of the outgoing particles.

Here we review the expression for the corrections to the different Z boson partial decay widths and asymmetries, where the former provide information on the overall strength of the coupling to fermions while the latter tell us about the chirality of such interactions. Therefore, among the different types of new physics, these observables are especially sensitive to those correcting trilinear couplings. On the other hand, they are rather insensitive to other types of extra interactions, in particular to the effects of four-fermion operators. Within our approximation this is clear since at the Z pole there is no interference between four-fermion and Z-exchange amplitudes, as the former are purely imaginary and the latter real. Therefore, when computing the corrections to Z-pole observables we simply have to replace the SM couplings by the corrected ones in the SM tree-level expression

$$g_{L(R)} \longrightarrow g_{L(R)} + \delta g_{L(R)},$$

keeping only the linear terms in $\delta g_{L(R)}$. Then, we have to express these shifts as a function of the coefficients α_i, as previously computed. In order to maintain the expressions as short as possible we will omit here this last step, and write everything in terms of the $\delta g_{L(R)}$.

Z Decay widths

The tree-level Z-boson partial width into a given fermion-antifermion pair reads at the Z pole

$$\Gamma_f = \frac{\alpha\, M_Z}{6 s^2 c^2} \left(|g_L^f|^2 + |g_R^f|^2 \right) N_f, \tag{2.79}$$

with N_f the f fermion effective number of colors:

$$\begin{array}{ll} N_l = 1, & l = \nu, e, \\ N_q = 3\left(1 + \frac{\alpha_s}{\pi} + 1.409\frac{\alpha_s^2}{\pi^2} - 12.77\frac{\alpha_s^3}{\pi^3} + \dots\right), & q = u, d, \end{array} \tag{2.80}$$

where N_q includes the universal QCD corrections for massless quarks [38].

The above formula is the basis for the determination of several observables. These are:

- The total Z decay width: $\Gamma_Z = \sum_{f \neq t} \Gamma_f$.
- The ratio of the total hadronic width, $\Gamma_{\rm had} = \sum_{q \neq t} \Gamma_q$, and the width into a definite charged lepton flavor: $R_l = \frac{\Gamma_{\rm had}}{\Gamma_l}$.
- For heavy quark flavors ($q = b, c$) the quantity usually reported by the experimental groups at LEP is the corresponding (inverted) ratio: $R_q = \frac{\Gamma_q}{\Gamma_{\rm had}}$, while for light flavors the given ratio is R_u/R_{u+d+s}.
- The total Z-pole $e^+e^- \to$ hadrons cross section, which can be written in terms of the Z decay widths as $\sigma_{\rm had} = 12\pi \frac{\Gamma_e \Gamma_{\rm had}}{M_Z^2 \Gamma_Z^2}$.

Let us compute the deviations from the SM predictions, starting with Γ_f. First note that the Z-boson mass appearing in Eq. (2.79) is the physical mass as it appears in the phase space integral.

Then, since M_Z is one of the inputs, there are no corrections related to the Z-boson mass. Hence, as indicated above, we just have to replace $g^f_{L,R} \to g^f_{L(R)} + \delta g^f_{L(R)}$ to obtain the corrected partial width

$$\Gamma_f = \Gamma_f^{\rm SM}\left(1 + 2\frac{g_L^f \delta g_L^f + g_R^f \delta g_R^f}{|g_L^f|^2 + |g_R^f|^2}\right). \tag{2.81}$$

The width into hadrons and the total Z decay width read

$$\Gamma_{\rm had} = \Gamma_{\rm had}^{\rm SM}\left(1 + 2\frac{\sum_{q\neq t}\left[g_L^q \delta g_L^q + g_R^q \delta g_R^q\right]}{\sum_{q\neq t}\left[|g_L^q|^2 + |g_R^q|^2\right]}\right), \quad \Gamma_Z = \Gamma_Z^{\rm SM}\left(1 + 2\frac{\sum_{f\neq t}\left[g_L^f \delta g_L^f + g_R^f \delta g_R^f\right] N_f}{\sum_{f\neq t}\left[|g_L^f|^2 + |g_R^f|^2\right] N_f}\right). \tag{2.82}$$

The ratios R_l, R_q and R_u/R_{u+d+s}, are given by (see (2.81) and (2.82))

$$R_l = R_l^{\rm SM}\left(1 - 2\frac{g_L^l \delta g_L^l + g_R^l \delta g_R^l}{|g_L^l|^2 + |g_R^l|^2} + 2\frac{\sum_{q\neq t}\left[g_L^q \delta g_L^q + g_R^q \delta g_R^q\right]}{\sum_{q\neq t}\left[|g_L^q|^2 + |g_R^q|^2\right]}\right), \tag{2.83}$$

$$R_q = R_q^{\rm SM}\left(1 + 2\frac{g_L^q \delta g_L^q + g_R^q \delta g_R^q}{|g_L^q|^2 + |g_R^q|^2} - 2\frac{\sum_{\tilde q\neq t}\left[g_L^{\tilde q} \delta g_L^{\tilde q} + g_R^{\tilde q} \delta g_R^{\tilde q}\right]}{\sum_{\tilde q\neq t}\left[|g_L^{\tilde q}|^2 + |g_R^{\tilde q}|^2\right]}\right), \tag{2.84}$$

$$\frac{R_q}{R_{u+d+s}} = \frac{R_q^{\rm SM}}{R_{u+d+s}^{\rm SM}}\left(1 + 2\frac{g_L^q \delta g_L^q + g_R^q \delta g_R^q}{|g_L^q|^2 + |g_R^q|^2} - 2\frac{\sum_{\tilde q=u,d,s}\left[g_L^{\tilde q} \delta g_L^{\tilde q} + g_R^{\tilde q} \delta g_R^{\tilde q}\right]}{\sum_{\tilde q=u,d,s}\left[|g_L^{\tilde q}|^2 + |g_R^{\tilde q}|^2\right]}\right). \tag{2.85}$$

Finally, the total Z-pole hadronic cross section is

$$\sigma_{\rm had} = \sigma_{\rm had}^{\rm SM}\left(1 + 2\frac{g_L^e \delta g_L^e + g_R^e \delta g_R^e}{|g_L^e|^2 + |g_R^e|^2} + 2\frac{\sum_{q\neq t}\left[g_L^q \delta g_L^q + g_R^q \delta g_R^q\right]}{\sum_{q\neq t}\left[|g_L^q|^2 + |g_R^q|^2\right]} - 4\frac{\sum_{f\neq t}\left[g_L^f \delta g_L^f + g_R^f \delta g_R^f\right] N_f}{\sum_{f\neq t}\left[|g_L^f|^2 + |g_R^f|^2\right] N_f}\right). \tag{2.86}$$

Asymmetries

The forward-backward asymmetry for a given fermion f is defined as the difference between the cross sections for forward σ_F and backward σ_B scattering ($\cos\theta_{e^-f} > 0$ and $\cos\theta_{e^-f} < 0$, respectively), normalized to the total cross section: $A_{FB}^f = (\sigma_F - \sigma_B)/(\sigma_F + \sigma_B)$. Using (2.78) we obtain the tree-level expression for the asymmetry at LEP ($P_e = 0$):

$$A_{FB}^f = \frac{3}{4} A_e A_f, \tag{2.87}$$

where A_f are the fermionic left-right asymmetries

$$A_f = \frac{|g_L^f|^2 - |g_R^f|^2}{|g_L^f|^2 + |g_R^f|^2}. \tag{2.88}$$

Again, replacing $g^f_{L(R)} \to g^f_{L(R)} + \delta g^f_{L(R)}$ we get the corrected expressions

$$A_f = A_f^{\rm SM}\left(1 + \frac{4 g_L^f g_R^f}{|g_L^f|^4 - |g_R^f|^4}\left[g_R^f \delta g_L^f - g_L^f \delta g_R^f\right]\right), \tag{2.89}$$

$$A_{FB}^{f} = A_{FB}^{f\ \mathrm{SM}} \left(1 + \frac{4 g_L^e g_R^e}{|g_L^e|^4 - |g_R^e|^4} \left[g_R^e \delta g_L^e - g_L^e \delta g_R^e \right] + \frac{4 g_L^f g_R^f}{|g_L^f|^4 - |g_R^f|^4} \left[g_R^f \delta g_L^f - g_L^f \delta g_R^f \right] \right). \quad (2.90)$$

Effective fermionic weak angle $\sin^2\theta_{\mathrm{eff}}^f$

In the SM one can define effective Z-pole couplings, $\mathcal{G}_L^f = \sqrt{\rho_f}\left(T_3^{f_L} - Q^f \sin^2\theta_{\mathrm{eff}}^f\right)$ and $\mathcal{G}_R^f = -\sqrt{\rho_f} Q^f \sin^2\theta_{\mathrm{eff}}^f$, where the effective quantities ρ_f and $\sin^2\theta_{\mathrm{eff}}^f$ absorb the bulk of the electroweak radiative corrections for each fermion species. Since new physics can also correct fermionic couplings the definition of the effective weak angles can be also applied to tree level. Including the corrections to the SM relation

$$\sin^2\theta_{\mathrm{eff}}^f = \frac{1}{4\,|Q_f|}\left(1 - \frac{\mathcal{G}_L^f + \mathcal{G}_R^f}{\mathcal{G}_L^f - \mathcal{G}_R^f}\right), \quad (2.91)$$

where now the couplings $\mathcal{G}_{L(R)}^f$ are $g_{L(R)}^f + \delta g_{L(R)}^f$, we obtain

$$\sin^2\theta_{\mathrm{eff}}^f = \sin^2\theta_{\mathrm{eff}}^f\Big|_{\mathrm{SM}} \left(1 + \frac{g_L^f}{g_L^f - g_R^f}\left(\frac{\delta g_R^f}{g_R^f} - \frac{\delta g_L^f}{g_L^f}\right)\right). \quad (2.92)$$

Of particular interest is the effective leptonic weak mixing angle, which can be derived from many different measurements. At LEP one of the determinations is provided by the measurement of the hadronic forward-backward charge asymmetry. This can be written in terms of the quark branching ratios and forward-backward asymmetries

$$Q_{FB} = \sum_{q=d,s,b} R_q A_{FB}^q - \sum_{q=u,c} R_q A_{FB}^q. \quad (2.93)$$

The corrections to the above formula are immediate to compute from those for the R_q's and A_{FB}^q's (see Eqs. (2.84) and (2.90)). In our fits we will include directly this observable instead of the value of the leptonic effective angle derived from it, since this makes clearer the kind of new physics that each quantity is sensitive to.

2.2.2 W mass and width

Being one of the most sensitive observables to the Higgs mass, a precise measurement of the W mass is of great importance. This was performed at LEP 2 and Tevatron [71], where also the total W decay width and branching fractions were determined. To obtain the expression for the corrections to the W mass, we use the SM relation $M_W^0 = c_0 M_Z^0$ and equations (2.10), (2.14) and (2.53) to express everything in terms of the SM inputs and the dimension-six operator coefficients,

$$M_W^2 = M_Z^2 c^2 \left(1 - \frac{c^2}{c^2 - s^2}\left(\frac{\alpha_\phi^{(3)}}{2} + \frac{2s}{c}\alpha_{WB} + \frac{s^2}{c^2}\Delta_{G_F}\right)\frac{v^2}{\Lambda^2}\right) \equiv M_Z^2 c^2 \left(1 + 2\Delta_{M_W}\right). \quad (2.94)$$

For the W partial decay widths into a pair of fermions we proceed as in the Z case. At tree level and within the SM

$$\Gamma\left(W^- \to \bar{\nu}^i e^j\right) = \frac{\alpha\, M_W}{12 s^2}\delta_{ij}, \qquad \Gamma\left(W^- \to \bar{u}^i d^j\right) = \frac{\alpha\, M_W}{12 s^2}\,|V_{ij}|^2\, N_f. \quad (2.95)$$

These decays only involve LH couplings within the SM, so we would have first to generalize these expressions to include RH couplings in the quark case, $|V_{ij}|^2 \to |V_{Lij}|^2 + |V_{Rij}|^2$. However, as LH and RH interactions do not interfere the latter enter quadratically, and then at order v^4/Λ^4, so we can neglect them. Lepton couplings stay purely LH at any rate because we have not included RH neutrinos in the light sector of the theory. Hence, we simply replace $\delta_{ij} \to |U_{Lij}|^2$. Regarding the W mass in the above equations, note that although the M_W value corresponds to the physical mass coming from the phase space integration, now and unlike in the Z case, it is not an input but a model-dependent prediction. Then, as we have to use the same set of inputs for all observables, we also need to rewrite M_W as a function of them making use of Eq. (2.94). Rewritting the result in terms of G_μ in Eq. (2.54) we finally obtain

$$\Gamma\left(W^- \to \bar{\nu}^i e^j\right) = \frac{G_\mu M_Z^3 c^3}{6\sqrt{2}\pi}\left(1+\Delta_{M_W}\right)|U_{Lij}|^2 = \Gamma_{\nu e}^{\rm SM}\left(1+\Delta_{M_W}+2\delta_{ij}{\rm Re}\left[(\delta U_L)_{ii}\right]\right),$$

$$\Gamma\left(W^- \to \bar{u}^i d^j\right) = \frac{G_\mu M_Z^3 c^3}{6\sqrt{2}\pi}\left(1+\Delta_{M_W}\right)|V_{Lij}|^2 N_q = \Gamma_{ud}^{\rm SM}\left(1+\Delta_{M_W}+2\frac{{\rm Re}\left[V_{Lij}\left(\delta V_L^*\right)_{ij}\right]}{|V_{Lij}|^2}\right). \tag{2.96}$$

From which one can easily derive the expression for the leptonic, hadronic and total W widths and branching ratios. These can be read from the equations given for the Z boson replacing g_L^f by the corresponding CC couplings, setting g_R^f to zero and adding the correction from the W mass Δ_{M_W}.

2.2.3 Low-energy observables

As the previous observables are in general insensitive to four-fermion interactions, data off the Z peak become compulsory in order to constrain them. In particular, low-energy observables measured with a remarkable precision provide stringent constraints on these four-fermion interactions. Some of those observables are:

- Effective couplings describing deep-inelastic neutrino-nucleon scattering.
- The corresponding NC effective couplings for muon neutrino-electron scattering.
- The weak charges of atoms, derived from experimental measurements of atomic parity violation.
- The weak charge of the electron, determined from the parity violating asymmetry in Møller scattering.

In the SM these are all NC mediated processes. Since they are measured at energies $E \ll M_W$, they are well described by the four-fermion effective Lagrangian obtained by integrating out the massive SM vector bosons, as well as whatever new physics we may consider. The pieces of the

low-energy effective Lagrangian relevant to our analysis are:

$$-\mathcal{L}^{\nu q} = \frac{4G_\mu}{\sqrt{2}}\overline{\nu_L}\gamma^\alpha\nu_L\sum_q\left[\epsilon_L\left(q\right)\overline{q_L}\gamma_\alpha q_L+\epsilon_R\left(q\right)\overline{q_R}\gamma_\alpha q_R\right], \tag{2.97}$$

$$-\mathcal{L}^{\nu^\mu e} = \frac{2G_\mu}{\sqrt{2}}\left(\overline{\nu_L^\mu}\gamma^\alpha\nu_L^\mu\right)\left(\overline{e}\gamma_\alpha\left(g_V^{\nu e}-g_A^{\nu e}\gamma_5\right)e\right), \tag{2.98}$$

$$-\mathcal{L}_{\not P}^{eq} = -\frac{G_\mu}{\sqrt{2}}\sum_q\left[C_{1q}\left(\overline{e}\gamma^\alpha\gamma_5 e\right)\left(\overline{q}\gamma_\alpha q\right)+C_{2q}\left(\overline{e}\gamma^\alpha e\right)\left(\overline{q}\gamma_\alpha\gamma_5 q\right)\right], \tag{2.99}$$

$$-\mathcal{L}_{\not P}^{ee} = -\frac{G_\mu}{\sqrt{2}}C_e\ \left(\overline{e}\gamma^\alpha e\right)\left(\overline{e}\gamma_\alpha\gamma_5 e\right), \tag{2.100}$$

where in the last two equalities $\not P$ means the parity-violating part. Note that none of the above processes can receive contributions from Higgs boson exchange, since there are no neutrino Yukawa interactions and these result in parity-conserving contributions for other fermions. The SM expressions of the effective parameters just introduced are

$$\epsilon_L\left(q\right)=2g_L^\nu g_L^q, \qquad \epsilon_R\left(q\right)=2g_L^\nu g_R^q, \tag{2.101}$$

$$g_V^{\nu e}=2g_L^{\nu_\mu}\left(g_L^e+g_R^e\right), \qquad g_A^{\nu e}=2g_L^{\nu_\mu}\left(g_L^e-g_R^e\right), \tag{2.102}$$

$$C_{1q}=2\left(g_L^e-g_R^e\right)\left(g_L^q+g_R^q\right), \qquad C_{2q}=2\left(g_L^e+g_R^e\right)\left(g_L^q-g_R^q\right), \tag{2.103}$$

$$C_e=2\left(g_L^e-g_R^e\right)\left(g_L^e+g_R^e\right). \tag{2.104}$$

In the following we focus on the different processes reviewing the corrections to the Lagrangian parameters in (2.97) to (2.100), and paying special attention to which of new four-fermion interactions are relevant.

Deep-inelastic neutrino-nucleon scattering

The NC deep-inelastic scattering of neutrinos on nucleons is described by the ratios

$$R_\nu=\frac{\sigma\left(\nu N\to\nu X\right)}{\sigma\left(\nu N\to\mu^- X\right)}\equiv\frac{\sigma_{\nu N}^{\mathrm{NC}}}{\sigma_{\nu N}^{\mathrm{CC}}}, \qquad R_{\bar\nu}=\frac{\sigma\left(\bar\nu N\to\bar\nu X\right)}{\sigma\left(\bar\nu N\to\mu^+ X\right)}\equiv\frac{\sigma_{\bar\nu N}^{\mathrm{NC}}}{\sigma_{\bar\nu N}^{\mathrm{CC}}}, \qquad R^-=\frac{\sigma_{\nu N}^{\mathrm{NC}}-\sigma_{\bar\nu N}^{\mathrm{NC}}}{\sigma_{\nu N}^{\mathrm{CC}}-\sigma_{\bar\nu N}^{\mathrm{CC}}}. \tag{2.105}$$

where the first two are measured by the CDHS [72], CHARM [73] and CCFR [74] collaborations, and the third one by the NuTeV collaboration [75]. Although these can be easily computed from the effective couplings in Eq. (2.97), for a fit it is more convenient to use a different parametrization, because the coefficients $\epsilon_{L,R}\left(q\right)$ are strongly correlated and non-Gaussian [38]. We will instead use the parameters $g_{L,R}^2$ and $\theta_{L,R}$ defined as follows

$$\begin{aligned} g_{L,R}^2 &\equiv \epsilon_{L,R}\left(u\right)^2+\epsilon_{L,R}\left(d\right)^2, \\ \theta_{L,R} &\equiv \arctan\frac{\epsilon_{L,R}\left(u\right)}{\epsilon_{L,R}\left(d\right)}. \end{aligned} \tag{2.106}$$

The ratios in Eq. (2.105) only depend on $g_{L,R}^2$

$$R_\nu=g_L^2+rg_R^2, \qquad R_{\bar\nu}=g_L^2+\frac{g_R^2}{r}, \qquad R^-=g_L^2-g_R^2, \tag{2.107}$$

where r is the ratio of anti-neutrino to neutrino CC cross sections, which can be directly measured. In the presence of new physics Eq. (2.107) still holds if we adjust the definition of $g_{L,R}^2$ to accommodate the corrections to the CC cross section in the former ratios. This can be done defining them with a correcting factor $F_{\rm CC} = \frac{\sigma_{\rm CC}}{\sigma_{\rm CC}^{\rm SM}}$,

$$g_{L,R}^2 \equiv \frac{\epsilon_{L,R}\left(u\right)^2 + \epsilon_{L,R}\left(d\right)^2}{F_{\rm CC}}. \tag{2.108}$$

As for all the previous observables, we now have to replace the SM couplings by the corrected ones in the effective parameters $\epsilon_{L,R}$. We must also include the new contributions to (2.97) from the four-fermion operators $\mathcal{O}_{lq}^{(1)}$, $\mathcal{O}_{lq}^{(3)}$, $\mathcal{O}_{lu}$ and $\mathcal{O}_{ld}$. However, in order to determine which entries affect this process, we need to know the nature of the incident neutrino. The former ratios have been measured by several experiments, but in all cases the neutrino beam originates from pion and kaon decays. Then, it is dominantly composed by muon neutrinos ($\mathrm{Br}\left(\pi^+ \to \mu^+\nu^\mu\right) \approx 100\%$ and $\mathrm{Br}\left(K^+ \to \mu^+\nu^\mu \text{ anything}\right) \approx 67\%$ [18]). We neglect the effects resulting from the small electron neutrino contamination ($\mathrm{Br}\left(K^+ \to e^+\nu^e \text{ anything}\right) \approx 5\%$ [18]). Therefore,

$$\begin{aligned}
\epsilon_L\left(u\right) =& \epsilon_L^{\rm SM}\left(u\right)\left(1 + \frac{\delta g_L^{\nu_\mu}}{g_L^{\nu_\mu}} + \frac{\delta g_L^u}{g_L^u}\right) - \frac{\sqrt{2}}{4G_\mu\Lambda^2}\sum_{i,j} V_{1i}\left(\alpha_{lq}^{(1)} + \alpha_{lq}^{(3)}\right)_{22ij} V_{j1}^\dagger, \\
\epsilon_R\left(u\right) =& \epsilon_R^{\rm SM}\left(u\right)\left(1 + \frac{\delta g_L^{\nu_\mu}}{g_L^{\nu_\mu}} + \frac{\delta g_R^u}{g_R^u}\right) + \frac{\sqrt{2}}{8G_\mu\Lambda^2}\left(\alpha_{lu}\right)_{2112}, \\
\epsilon_L\left(d\right) =& \epsilon_L^{\rm SM}\left(d\right)\left(1 + \frac{\delta g_L^{\nu_\mu}}{g_L^{\nu_\mu}} + \frac{\delta g_L^d}{g_L^d}\right) - \frac{\sqrt{2}}{4G_\mu\Lambda^2}\left(\alpha_{lq}^{(1)} - \alpha_{lq}^{(3)}\right)_{2211}, \\
\epsilon_R\left(d\right) =& \epsilon_R^{\rm SM}\left(d\right)\left(1 + \frac{\delta g_L^{\nu_\mu}}{g_L^{\nu_\mu}} + \frac{\delta g_R^d}{g_R^d}\right) + \frac{\sqrt{2}}{8G_\mu\Lambda^2}\left(\alpha_{ld}\right)_{2112},
\end{aligned} \tag{2.109}$$

where the RH corrections from contact interactions are obtained rewritting the corresponding operators in the form they appear in the Lagrangian (2.97), using the Fierz identity $\left(\gamma^\mu P_L\right)_{12}\left(\gamma_\mu P_R\right)_{34} = 2\left(P_R\right)_{14}\left(P_L\right)_{32}$. This explains the extra $-1/2$ compared to the LH corrections. Instead of keeping the factor $1/G_\mu$ in front of the four-fermion coefficients (which comes from factorizing the global G_μ to compare with Eq. (2.97)), we will rewrite it in terms of the Higgs vev, $1/G_\mu = \sqrt{2}v^2$, so we have corrections ordered in powers of v/Λ. We will do also the same for the other low-energy observables when considering new four-fermion interactions.

Finally, for the computation of the correction factor $F_{\rm CC}$ we neglect the contribution from sea quarks. On the other hand, we only consider $d \leftrightarrow u$ transitions. Therefore, $\sigma_{\rm CC}^{\rm SM} \approx \sigma_{\rm CC}^{\rm SM}\left(d \leftrightarrow u\right) \propto G_\mu^2\left|V_{ud}\right|^2$, and gets corrections from the extra CC couplings as well as from the four-fermion interaction $\mathcal{O}_{lq}^{(3)}$. Contributions from the LRRL operator $\mathcal{O}_{qde}^\dagger$ and from the LRLR operators $\mathcal{O}_{lq}^\dagger$ and $\mathcal{O}_{lq'}^\dagger$ do not interfere with the SM amplitude and can be ignored at order v^2/Λ^2. The same applies for RH quark CC, though these also enter through the definition of V_{ud}^0 in terms of V_{ud}, and give a new contribution to the cross section at leading order. With all these changes the correction factor $F_{\rm CC}$ reads

$$F_{\rm CC} = 1 + 2\ \mathrm{Re}\left[\frac{\frac{1}{2}\left(\alpha_{\phi ud}\right)_{11} + \sum_i V_{ui}\left[\left(\alpha_{lq}^{(3)}\right)_{11i1} - \left(\alpha_{lq}^{(3)}\right)_{22i1}\right]}{V_{ud}} + \left(\alpha_{\phi l}^{(3)}\right)_{22} - \left(\alpha_{\phi l}^{(3)}\right)_{11}\right]\frac{v^2}{\Lambda^2}. \tag{2.110}$$

Taking (2.109) and (2.110) back to (2.108) we finally obtain the correction to $g^2_{L,R}$,

$$g_L^2 = \left(g_L^2\right)^{\rm SM}\Bigg(1+2\frac{\delta g_L^{\nu_\mu}}{g_L^{\nu_\mu}}+2\frac{g_L^u\delta g_L^u+g_L^d\delta g_L^d}{{g_L^u}^2+{g_L^d}^2}-\frac{g_L^u\sum_{ij}V_{1i}\left(\alpha_{lq}^{(1)}+\alpha_{lq}^{(3)}\right)_{22ij}V^\dagger_{j1}+g_L^d\left(\alpha_{lq}^{(1)}-\alpha_{lq}^{(3)}\right)_{2211}}{2g_L^{\nu^\mu}\left({g_L^u}^2+{g_L^d}^2\right)}\frac{v^2}{\Lambda^2}-$$
$$-2\ {\rm Re}\left[\frac{\frac{1}{2}\left(\alpha_{\phi ud}\right)_{11}+\sum_i V_{ui}\left[\left(\alpha_{lq}^{(3)}\right)_{11i1}-\left(\alpha_{lq}^{(3)}\right)_{22i1}\right]}{V_{ud}}+\left(\alpha_{\phi l}^{(3)}\right)_{22}-\left(\alpha_{\phi l}^{(3)}\right)_{11}\right]\frac{v^2}{\Lambda^2}\Bigg),$$

$$g_R^2 = \left(g_R^2\right)^{\rm SM}\Bigg(1+2\frac{\delta g_L^{\nu_\mu}}{g_L^{\nu_\mu}}+2\frac{g_R^u\delta g_R^u+g_R^d\delta g_R^d}{{g_R^u}^2+{g_R^d}^2}+\frac{1}{4g_L^{\nu^\mu}}\frac{g_R^u\left(\alpha_{lu}\right)_{2112}+g_R^d\left(\alpha_{ld}\right)_{2112}}{{g_R^u}^2+{g_R^d}^2}\frac{v^2}{\Lambda^2}-$$
$$-2\ {\rm Re}\left[\frac{\frac{1}{2}\left(\alpha_{\phi ud}\right)_{11}+\sum_i V_{ui}\left[\left(\alpha_{lq}^{(3)}\right)_{11i1}-\left(\alpha_{lq}^{(3)}\right)_{22i1}\right]}{V_{ud}}+\left(\alpha_{\phi l}^{(3)}\right)_{22}-\left(\alpha_{\phi l}^{(3)}\right)_{11}\right]\frac{v^2}{\Lambda^2}\Bigg). \tag{2.111}$$

For $\theta_{L,R}$, from (2.106) and (2.109),

$$\theta_L = \theta_L^{\rm SM}+\frac{1}{{g_L^u}^2+{g_L^d}^2}\left[g_L^d\delta g_L^u-g_L^u\delta g_L^d+\frac{v^2}{4g_L^{\nu_\mu}\Lambda^2}\left(g_L^u\sum_{ij}V_{1i}\left(\alpha_{lq}^{(1)}-\alpha_{lq}^{(3)}\right)_{22ij}V^\dagger_{j1}-g_L^d\left(\alpha_{lq}^{(1)}+\alpha_{lq}^{(3)}\right)_{2211}\right)\right],$$

$$\theta_R = \theta_R^{\rm SM}+\frac{1}{{g_R^u}^2+{g_R^d}^2}\left[g_R^d\delta g_R^u-g_R^u\delta g_R^d+\frac{v^2}{8g_L^{\nu_\mu}\Lambda^2}\left(g_R^d\,\alpha_{lu}-g_R^u\,\alpha_{ld}\right)_{2112}\right]. \tag{2.112}$$

Neutrino-electron scattering

Let us now consider the process $\nu^\mu e^- \longrightarrow \nu^\mu e^-$. In the SM this receives contributions only from NC and is described by the low-energy Lagrangian (2.98). The vector and axial ν-e effective couplings introduced there are directly related to the measured cross sections, which for $E_\nu \gg m_e$ can be written

$$\begin{aligned}\sigma\left(\nu^\mu e^- \to \nu^\mu e^-\right) &= \frac{G_\mu^2 m_e E_\nu}{2\pi}\left[\left(g_V^{\nu e}+g_A^{\nu e}\right)^2+\frac{1}{3}\left(g_V^{\nu e}-g_A^{\nu e}\right)^2\right],\\ \sigma\left(\overline{\nu^\mu} e^- \to \overline{\nu^\mu} e^-\right) &= \frac{G_\mu^2 m_e E_\nu}{2\pi}\left[\left(g_V^{\nu e}-g_A^{\nu e}\right)^2+\frac{1}{3}\left(g_V^{\nu e}+g_A^{\nu e}\right)^2\right].\end{aligned} \tag{2.113}$$

These were measured by the CHARM II collaboration [76], which determined the values for the effective couplings $g_V^{\nu e}$ and $g_A^{\nu e}$. The new physics corrections to the effective parameters are computed as in the previous case. Among our list of contact interactions the relevant ones for these processes are only $\mathcal{O}_{ll}^{(1)}$, $\mathcal{O}_{ll}^{(3)}$ and $\mathcal{O}_{le}$. Including them, as well as the modifications of the SM

couplings, we find

$$g_V^{\nu e} = (g_V^{\nu e})^{\rm SM}\left(1+\frac{\delta g_L^{\nu_\mu}}{g_L^{\nu_\mu}}+\frac{\delta g_L^e+\delta g_R^e}{g_L^e+g_R^e}\right)-\frac{v^2}{2\Lambda^2}\left[\left(\alpha_{ll}^{(1)}-\alpha_{ll}^{(3)}\right)_{2211}+\left(2\alpha_{ll}^{(3)}-\frac{1}{2}\alpha_{le}\right)_{2112}\right],$$

$$g_A^{\nu e} = (g_A^{\nu e})^{\rm SM}\left(1+\frac{\delta g_L^{\nu_\mu}}{g_L^{\nu_\mu}}+\frac{\delta g_L^e-\delta g_R^e}{g_L^e-g_R^e}\right)-\frac{v^2}{2\Lambda^2}\left[\left(\alpha_{ll}^{(1)}-\alpha_{ll}^{(3)}\right)_{2211}+\left(2\alpha_{ll}^{(3)}+\frac{1}{2}\alpha_{le}\right)_{2112}\right], \tag{2.114}$$

where we have used the permutation symmetry $\{ij\}\leftrightarrow\{kl\}$ of $\alpha_{ll}^{(1)}$ and $\alpha_{ll}^{(3)}$ indices and the adequate Fierz reordering to rewrite the operators as in Eq. (2.98).

Atomic parity violation

The results from atomic parity violation (APV) experiments are given in terms of the atomic weak charges, which can be computed as a function of the parameters in the effective Lagrangian (2.99). For an atomic nucleus with N neutrons and Z protons the weak charge, Q_W, is defined by

$$Q_W(Z,N) = -2\left[C_{1u}(2Z+N)+C_{1d}(Z+2N)\right]. \tag{2.115}$$

We include the measurements for Cesium [77, 78] (the most precise one, with an error at the per mille level) and Thallium [79] in our fit.

As for previous low-energy effective parameters, apart from the corrections from trilinear couplings we have to consider those from four-fermion contact interactions. The Lagrangian (2.99) receives contributions from the parity-violating part of the operators $\mathcal{O}_{lq}^{(1)}$, $\mathcal{O}_{lq}^{(3)}$, $\mathcal{O}_{eu}$, $\mathcal{O}_{ed}$, $\mathcal{O}_{lu}$, $\mathcal{O}_{ld}$ and $\mathcal{O}_{qe}$. The corrections to C_{1q} and C_{2q} are then given by

$$\begin{aligned}
C_{1u} &= C_{1u}^{\rm SM}\left(1+\frac{\delta g_L^e-\delta g_R^e}{g_L^e-g_R^e}+\frac{\delta g_L^u+\delta g_R^u}{g_L^u+g_R^u}\right)-\frac{v^2}{2\Lambda^2}\left[\sum_{ij}V_{1i}\left[\left(\alpha_{lq}^{(1)}-\alpha_{lq}^{(3)}\right)_{11ij}+\frac{(\alpha_{qe})_{i11j}}{2}\right]V_{j1}^\dagger-\left(\alpha_{eu}+\frac{\alpha_{lu}}{2}\right)_{1111}\right],\\
C_{1d} &= C_{1d}^{\rm SM}\left(1+\frac{\delta g_L^e-\delta g_R^e}{g_L^e-g_R^e}+\frac{\delta g_L^d+\delta g_R^d}{g_L^d+g_R^d}\right)+\frac{v^2}{2\Lambda^2}\left(-\alpha_{lq}^{(1)}-\alpha_{lq}^{(3)}+\alpha_{ed}-\frac{\alpha_{qe}}{2}+\frac{\alpha_{ld}}{2}\right)_{1111},\\
C_{2u} &= C_{2u}^{\rm SM}\left(1+\frac{\delta g_L^e+\delta g_R^e}{g_L^e+g_R^e}+\frac{\delta g_L^u-\delta g_R^u}{g_L^u-g_R^u}\right)-\frac{v^2}{2\Lambda^2}\left[\sum_{ij}V_{1i}\left[\left(\alpha_{lq}^{(1)}-\alpha_{lq}^{(3)}\right)_{11ij}-\frac{(\alpha_{qe})_{i11j}}{2}\right]V_{j1}^\dagger-\left(\alpha_{eu}-\frac{\alpha_{lu}}{2}\right)_{1111}\right],\\
C_{2d} &= C_{2d}^{\rm SM}\left(1+\frac{\delta g_L^e+\delta g_R^e}{g_L^e+g_R^e}+\frac{\delta g_L^d-\delta g_R^d}{g_L^d-g_R^d}\right)+\frac{v^2}{2\Lambda^2}\left(-\alpha_{lq}^{(1)}-\alpha_{lq}^{(3)}+\alpha_{ed}+\frac{\alpha_{qe}}{2}-\frac{\alpha_{ld}}{2}\right)_{1111}.
\end{aligned} \tag{2.116}$$

Using these expressions for C_{1q} we can compute the corresponding modification for the atomic

weak charges

$$Q_W(Z,N) = Q_W^{\rm SM}(Z,N)\left(1+\frac{\delta g_L^e-\delta g_R^e}{g_L^e-g_R^e}+\frac{(2Z+N)\left(\delta g_L^u+\delta g_R^u\right)+(Z+2N)\left(\delta g_L^d+\delta g_R^d\right)}{(2Z+N)\left(g_L^u+g_R^u\right)+(Z+2N)\left(g_L^d+g_R^d\right)}\right)+$$
$$+(2Z+N)\left(\sum_{ij}V_{1i}\left[\left(\alpha_{lq}^{(1)}-\alpha_{lq}^{(3)}\right)_{11ij}+\frac{(\alpha_{qe})_{i11j}}{2}\right]V_{j1}^\dagger-\left(\alpha_{eu}+\frac{\alpha_{lu}}{2}\right)_{1111}\right)\frac{v^2}{\Lambda^2}+$$
$$+(Z+2N)\left(\alpha_{lq}^{(1)}+\alpha_{lq}^{(3)}-\alpha_{ed}+\frac{\alpha_{qe}}{2}-\frac{\alpha_{ld}}{2}\right)_{1111}\frac{v^2}{\Lambda^2}. \tag{2.117}$$

Parity violation in Møller scattering

Parity violation can be also measured in Møller scattering $e^-e^-\to e^-e^-$ at low Q^2 by scattering longitudinally polarized electrons on an unpolarized target and determining the parity-violating or left-right asymmetry [80]

$$A_{\rm PV}=\frac{\sigma_L-\sigma_R}{\sigma_L+\sigma_R}, \tag{2.118}$$

where $\sigma_{L(R)}$ is the cross section for incident LH (RH) electrons. The above asymmetry can be expressed in terms of the electron NC couplings

$$A_{\rm PV}=\frac{G_\mu Q^2}{\sqrt{2}\pi\alpha}\frac{1-y}{1+y^4+(1-y)^4}Q_W(e), \quad y\equiv\frac{Q^2}{E_{\rm CM}^2}, \tag{2.119}$$

with the weak charge $Q_W(e)=-2C_e$ and C_e the effective coupling in Eq. (2.100). Only the new LLLL and RRRR four-fermion operators $\mathcal{O}_{ll}^{(1)}$, $\mathcal{O}_{ll}^{(3)}$ and $\mathcal{O}_{ee}$ contribute to the electron weak charge[10],

$$Q_W(e)=Q_W^{\rm SM}(e)\left(1+\frac{\delta g_L^e-\delta g_R^e}{g_L^e-g_R^e}+\frac{\delta g_L^e+\delta g_R^e}{g_L^e+g_R^e}\right)+\frac{v^2}{\Lambda^2}\left(\alpha_{ll}^{(1)}+\alpha_{ll}^{(3)}-\alpha_{ee}\right)_{1111}, \tag{2.120}$$

where we have also included the corrections to the NC couplings.

2.2.4 Unitarity of the Cabibbo-Kobayashi-Maskawa matrix

The unitarity condition on the CKM matrix elements provides very stringent constraints on new CC interactions. The most precise measurement comes from the first row $|V_{ud}|^2+|V_{us}|^2+|V_{ub}|^2=0.9999\pm0.0006$ [68]. New physics in general contributes to these mixing parameters correcting the SM matrix elements V_{ij}^0, that satisfy the unitarity condition by construction. Using the expressions collected in Section 2.1.5 together with $\sum_i\left|V_{ui}^0\right|^2=1$, one can derive the corrected expression at order v^2/Λ^2:

$$\sum_i|V_{ui}|^2=1-2\left[|V_{ud}|^2\Delta V_{ud}+|V_{us}|^2\left(\omega_{K\ell3}\ \Delta V_{us}^{K\ell3}+\omega_{K/\pi}\ \Delta V_{us}^{K/\pi}\right)-|V_{ub}|^2\,{\rm Re}\left[\frac{\left(V\alpha_{\phi q}^{(3)}\right)_{13}}{V_{ub}}\right]\right]\frac{v^2}{\Lambda^2}, \tag{2.121}$$

[10] The corresponding piece in the LRRL operator $\mathcal{O}_{le}$ is parity conserving.

where ΔV_{ud}, $\omega_{K\ell 3}$, $\Delta V_{us}^{K\ell 3}$, $\omega_{K/\pi}$ and $\Delta V_{us}^{K/\pi}$ are defined in Section 2.1.5. Note that this relation is mainly dominated by V_{ud} and V_{us}. Actually, $|V_{ub}|^2 \approx 10^{-5}$ is almost two orders of magnitude below the experimental uncertainty so one can in principle neglect the contributions from this matrix element. We have only included the direct corrections in this case.

2.2.5 Fermion pair production at LEP 2

During the second stage of LEP operation (LEP 2) the center of mass energy was increased above the Z pole, providing measurements of $e^+e^- \longrightarrow \bar{f}f$ from 130 GeV to 209 GeV [81]. As in the case of the low-energy observables discussed above, the data taken during this second run is sensitive to new physics resulting in four-fermion interactions. Although the precision of these measurements is in general poor, compared to those obtained at the Z pole or below, this is compensated by the relatively large number of data points allowing to reconstruct the energy dependence of the cross sections and forward-backward asymmetries for different final states. This makes LEP 2 data decisive when trying to constrain four-fermion interactions, and quite complementary to low-energy data. On the other hand, when new physics does not generate any of these contact interactions but only corrects trilinear couplings, LEP 2 $e^+e^- \longrightarrow \bar{f}f$ observables can be safely ignored in the fits. In this case new interactions are more stringently constrained by the Z-pole measurements, where rather precise data is also available.

Let us focus then on the process $e^+e^- \longrightarrow \bar{f}f$ at energies above the Z mass. As for the low-energy observables, besides the shift of the SM couplings we must also consider the contributions from the contact interactions to this process. Although in principle we should also consider corrections from Higgs exchange as well as to Yukawa interactions, these are negligibly small for they are proportional to the electron mass. Then, we can also neglect contributions from the operators $\mathcal{O}_{qde}$, $\mathcal{O}_{lq}$ and $\mathcal{O}_{lq'}$, that can only interfere with those amplitudes. The four-fermion Lagrangian contributing to this process is thus

$$\begin{aligned}\mathcal{L}_{4F}^{ef} =& \bar{e}_L\gamma^\mu e_L\,(1+\delta_{ef})^{-1}\left[\mathcal{A}_{LL}^f \bar{f}_L\gamma_\mu f_L + \mathcal{A}_{LR}^f \bar{f}_R\gamma_\mu f_R\right]\frac{1}{\Lambda^2} + \\ &+\bar{e}_R\gamma^\mu e_R\,(1+\delta_{ef})^{-1}\left[\mathcal{A}_{RR}^f \bar{f}_R\gamma_\mu f_R + \mathcal{A}_{RL}^f \bar{f}_L\gamma_\mu f_L\right]\frac{1}{\Lambda^2},\end{aligned} \tag{2.122}$$

where the different coupling matrices are defined in terms of the four-fermion operator coefficients:

$$\begin{aligned}
&\mathcal{A}_{LL}^\ell = \frac{\left(\alpha_{ll}^{(1)}+\alpha_{ll}^{(3)}\right)_{11ii}+\left(\alpha_{ll}^{(1)}+\alpha_{ll}^{(3)}\right)_{1ii1}}{1+\delta_{e\ell}}, && \mathcal{A}_{LR}^\ell = -\tfrac{1}{2}\,(\alpha_{le})_{1ii1}\,,\\
&\mathcal{A}_{LL}^u = \textstyle\sum_{k,l} V_{ik}\left(\alpha_{lq}^{(1)}-\alpha_{lq}^{(3)}\right)_{11kl} V_{li}^\dagger, && \mathcal{A}_{LR}^u = -\tfrac{1}{2}\,(\alpha_{lu})_{1ii1}\,,\\
&\mathcal{A}_{LL}^d = \left(\alpha_{lq}^{(1)}+\alpha_{lq}^{(3)}\right)_{11ii}, && \mathcal{A}_{LR}^d = -\tfrac{1}{2}\,(\alpha_{ld})_{1ii1}\,,\\
&\mathcal{A}_{RR}^\ell = \tfrac{2(\alpha_{ee})_{11ii}}{1+\delta_{e\ell}}, && \mathcal{A}_{RL}^\ell = -\tfrac{1}{2}\,(\alpha_{le})_{i11i}\,,\\
&\mathcal{A}_{RR}^u = (\alpha_{eu})_{11ii}\,, && \text{and} \quad \mathcal{A}_{RL}^u = -\tfrac{1}{2}\textstyle\sum_{kl} V_{ik}\,(\alpha_{qe})_{k11l}\,V_{li}^\dagger,\\
&\mathcal{A}_{RR}^d = (\alpha_{ed})_{11ii}\,, && \mathcal{A}_{RL}^d = -\tfrac{1}{2}\,(\alpha_{qe})_{i11i}\,,
\end{aligned}$$

where i stands for any given flavor. The factors $1+\delta_{ef}$ have been introduced for convenience in order to take into account the different contributions to the Lagrangian for $e^+e^- \to \ell^+\ell^-$, depending on whether ℓ is or not an electron. We must remember that the coefficients $\alpha_{ll}^{(1)}$ and $\alpha_{ll}^{(3)}$ are symmetric under the interchange of the first and last two indices, so we have two contributions to the LL couplings with the same coefficient if $\ell \neq e$, $\frac{1}{2}(\alpha_{ll}^{(1)}+\alpha_{ll}^{(3)})_{11ii}$. Moreover, we also have another two contributions proportional to $\frac{1}{2}(\alpha_{ll}^{(1)}+\alpha_{ll}^{(3)})_{1ii1}$ (the corresponding operators can be

rewritten as above by Fierz reordering after EWSB). In contrast, for $\ell = e$ we only have one contribution proportional to $\frac{1}{2}(\alpha_{ll}^{(1)} + \alpha_{ll}^{(3)})_{1111}$. For RR, contributions arise only from $(\mathcal{O}_{ee})_{ijkl}$. This is not only symmetric under $\{ij\} \leftrightarrow \{kl\}$ but also under $j \leftrightarrow l$. In summary, for $\ell \neq e$ there are four contributions proportional to $\frac{1}{2}(\alpha_{ee})_{11ii}$, while for $\ell = e$ there is only one proportional to $\frac{1}{2}(\alpha_{ee})_{1111}$. Finally note that $\mathcal{A}^e_{LR} = \mathcal{A}^e_{RL}$, so the global factor $(1-\delta_{ef})^{-1}$ allows to use a common $\mathcal{A}^\ell_{LR,RL}$ expression for all leptons.

The differential cross section for $e^+e^- \to \bar{f}f$, including the contributions from the four-fermion Lagrangian (2.122), can be written [82]

$$\begin{aligned}\frac{1}{N_f}\frac{4s}{\alpha^2}\frac{d\sigma}{d\Omega}\left(e^+e^- \to \bar{f}f\right) = &\left[\left|\mathcal{M}^{ee}_{LR}(t)\right|^2 + \left|\mathcal{M}^{ee}_{RL}(t)\right|^2\right]\frac{s^2}{t^2}\delta_{ef} + \\ &+\left[\left|\mathcal{M}^{ef}_{LR}(s)\right|^2 + \left|\mathcal{M}^{ef}_{RL}(s)\right|^2\right]\frac{t^2}{s^2} + \\ &+\left[\left|\mathcal{M}^{ef}_{LL}(s)\right|^2 + \left|\mathcal{M}^{ef}_{RR}(s)\right|^2\right]\frac{u^2}{s^2}.\end{aligned} \tag{2.123}$$

with $s = 4E^2_{\text{beam}}$, $t = -\frac{1}{2}s(1-\cos\theta)$ and $s+t+u = 0$. Whereas the helicity amplitudes read

$$\begin{aligned}\mathcal{M}^{ee}_{\alpha\beta}(t) =& 1 + \frac{g^e_\alpha g^e_\beta}{\sin^2\theta_W\cos^2\theta_W}\frac{t}{t-M_Z^2} + \frac{t}{4\pi\alpha}\frac{\mathcal{A}^f_{\alpha\beta}}{\Lambda^2}, \quad (\alpha \neq \beta)\,, \\ \mathcal{M}^{ef}_{\alpha\beta}(s) =& -Q_f + \frac{g^e_\alpha g^f_\beta}{\sin^2\theta_W\cos^2\theta_W}\frac{s}{s-M_Z^2+iM_Z\Gamma_Z} + \frac{s}{4\pi\alpha}\frac{\mathcal{A}^f_{\alpha\beta}}{\Lambda^2}, \quad (\alpha \neq \beta)\,, \\ \mathcal{M}^{ef}_{\alpha\alpha}(s) =& -Q_f + \frac{g^e_\alpha g^f_\alpha}{\sin^2\theta_W\cos^2\theta_W}\left[\frac{s}{s-M_Z^2+iM_Z\Gamma_Z} + \frac{s}{t-M_Z^2}\delta_{ef}\right] + \frac{s}{t}\delta_{ef} + (1+\delta_{ef})\frac{s}{4\pi\alpha}\frac{\mathcal{A}^f_{\alpha\alpha}}{\Lambda^2},\end{aligned}$$

with $\alpha, \beta = L, R$. Now that the effects of four-fermion interactions have been included, we only have to replace $g_{L(R)} \to g_{L(R)} + \delta g_{L(R)}$ to take into account the new physics contributions to the couplings. Note that these shifts must be also introduced in the Z decay width, although for LEP 2 energies this effect is negligible and it can be safely neglected. Finally, integrating Eq. (2.123) we obtain the total cross sections as well as the corresponding forward-backward asymmetries. Given the length of the resulting expressions we do not write them here.

2.3 Electroweak precision constraints on dimension-six operators

Let us summarize the implications in the analysis of the EWPD of the dimension-six interactions included in our fits. Here we classify the operators according to whether they can be actually constrained by current data and to which observables are most relevant in deriving these constraints. First, in Table 4.3 we identify the operators contributing to the observables discussed in this chapter. They are a total of 21 operators of the 52 in Table 1.1. Then, in order to illustrate the relevance of each data set to constrain a given operator, we show in Table 2.2 the fits for each case considering only one operator at a time [11]. We provide the 95% C.L. limits for the corresponding operator coefficient. In all fits we include bounds from direct Higgs searches to constrain the value

[11] The names of all data sets are self-explanatory, and we only remark that in the one named W data we include apart from the W mass and width, and the leptonic branching ratios, the measurement of the unitarity of the first row of the CKM matrix.

of the Higgs mass, which is the only SM parameter we allow to vary. All the other SM parameters are fixed at their best fit value. The inclusion of these direct searches data, however, screens the possible correlations between the operator coefficients and M_H. For this reason we have performed another fit excluding these data for the sole purpose of identifying such correlations. These will be commented at the end of this section in those cases where they are significant. Finally, for simplicity, we assume a family universal structure for the four-fermion and SVF operators. This implies that the operators $(\mathcal{O}_{\phi\psi}^{(1,3)})_{ij}$ and $(\mathcal{O}_{\phi ud})_{ij}$ are diagonal and with all the non-zero entries fixed to the same value, whereas LLLL and RRRR four-fermion operators $\mathcal{O}_{ijkl}$ are proportional to $\delta_{ij}\delta_{kl}$ and the LRRL $\mathcal{O}_{ijkl}$ to $\delta_{il}\delta_{kj}$, with the same values for all non-zero entries. It must be emphasized that for a definite type of new physics several operators may be generated upon integration of the extra particles, and the resulting limits may significantly differ from those obtained here due to cancellations. Let us discuss the implications of the different sets of operators introduced at the end of Chapter 1:

	Operators	Z pole $e^+e^-\to\bar{f}f$	M_W	ν-N DIS	NC $\nu e\to\nu e$	APV	PV in $e^-e^-\to e^-e^-$	CKM	LEP 2 $e^+e^-\to\bar{f}f$
LLLL	$\mathcal{O}_{ll}^{(1)}, \mathcal{O}_{ll}^{(3)}$	✓	✓	✓	✓	✓	✓	✓	✓
	$\mathcal{O}_{lq}^{(1)}$			✓		✓			✓
	$\mathcal{O}_{lq}^{(3)}$			✓		✓		✓	✓
RRRR	$\mathcal{O}_{ee}$						✓		✓
	$\mathcal{O}_{eu}, \mathcal{O}_{ed}$					✓			✓
LRRL	$\mathcal{O}_{le}$				✓				✓
	$\mathcal{O}_{lu}, \mathcal{O}_{ld}$			✓		✓			✓
	$\mathcal{O}_{qe}$					✓			✓
SVF	$\mathcal{O}_{\phi\psi}^{(1)}$	✓		✓	✓	✓	✓		✓
	$\mathcal{O}_{\phi l}^{(3)}$	✓	✓	✓	✓	✓	✓	✓	✓
	$\mathcal{O}_{\phi q}^{(3)}$	✓		✓		✓		✓	✓
	$\mathcal{O}_{\phi ud}$			✓				✓	
Oblique	$\mathcal{O}_{\phi}^{(3)}, \mathcal{O}_{WB}$	✓	✓	✓	✓	✓	✓		✓

Table 2.1: Dimension-six operators contributing (directly or indirectly) to the different observables included in the fits.

- **Four-fermion interactions:** As argued in Section 2.2.1, the contributions of four-fermion operators to the observables at the Z peak are negligible. Therefore, these can only be constrained by low-energy data as well as by cross sections and asymmetries measured at LEP 2. There are two exceptions: the operators $\mathcal{O}_{ll}^{(1)}$ and $\mathcal{O}_{ll}^{(3)}$, which correct the theoretical prediction for the muon decay constant and, since we consider this as an input, have a

	Operator coefficient	Z pole	W data	Low Energy	LEP 2	Global fit
		95% C.L. limits [TeV^{-2}]				
LLLL	$\frac{\alpha_{ll}^{(1)}}{\Lambda^2}$	-	-	$[-0.033, 0.245]$	$[-0.089, 0.024]$	$[-0.065, 0.040]$
	$\frac{\alpha_{ll}^{(3)}}{\Lambda^2}$	$[-0.010, 0.012]$	$[-0.007, 0.009]$	$[-0.088, -0.007]$	$[-0.046, 0.041]$	$[-0.007, 0.006]$
	$\frac{\alpha_{lq}^{(1)}}{\Lambda^2}$	-	-	$[-0.027, 0.020]$	$[-0.007, 0.433]$	$[-0.024, 0.022]$
	$\frac{\alpha_{lq}^{(3)}}{\Lambda^2}$	-	$[-0.007, 0.009]$	$[-0.003, 0.090]$	$[-6{\cdot}10^{-4}, 0.056]$	$[-0.003, 0.012]$
RRRR	$\frac{\alpha_{ee}}{\Lambda^2}$	-	-	$[-0.257, 0.031]$	$[-0.057, 0.011]$	$[-0.060, 0.006]$
	$\frac{\alpha_{eu}}{\Lambda^2}$	-	-	$[-0.040, 0.057]$	$[-0.195, 0.001]$	$[-0.057, 0.030]$
	$\frac{\alpha_{ed}}{\Lambda^2}$	-	-	$[-0.041, 0.048]$	$[-0.002, 0.260]$	$[-0.025, 0.059]$
LRRL	$\frac{\alpha_{le}}{\Lambda^2}$	-	-	$[-1.146, 1.132]$	$[-0.059, 0.101]$	$[-0.059, 0.101]$
	$\frac{\alpha_{lu}}{\Lambda^2}$	-	-	$[-0.090, 0.100]$	$[-0.005, 0.947]$	$[-0.070, 0.116]$
	$\frac{\alpha_{ld}}{\Lambda^2}$	-	-	$[-0.078, 0.098]$	$[-1.263, 0.007]$	$[-0.089, 0.085]$
	$\frac{\alpha_{qe}}{\Lambda^2}$	-	-	$[-0.052, 0.041]$	$[-0.006, 0.561]$	$[-0.044, 0.048]$
SVF	$\frac{\alpha_{\phi l}^{(1)}}{\Lambda^2}$	$[-0.004, 0.009]$	-	$[-0.023, 0.072]$	$[-0.037, 0.170]$	$[-0.003, 0.010]$
	$\frac{\alpha_{\phi q}^{(1)}}{\Lambda^2}$	$[-0.021, 0.033]$	-	$[-0.025, 0.023]$	$[-0.014, 1.149]$	$[-0.013, 0.022]$
	$\frac{\alpha_{\phi e}^{(1)}}{\Lambda^2}$	$[-0.011, 0.006]$	-	$[-0.147, 0.053]$	$[-0.233, 0.103]$	$[-0.012, 0.006]$
	$\frac{\alpha_{\phi u}^{(1)}}{\Lambda^2}$	$[-0.054, 0.066]$	-	$[-0.035, 0.060]$	$[-0.076, 2.796]$	$[-0.026, 0.048]$
	$\frac{\alpha_{\phi d}^{(1)}}{\Lambda^2}$	$[-0.130, 0.032]$	-	$[-0.060, 0.046]$	$[-3.727, 0.101]$	$[-0.049, 0.028]$
	$\frac{\alpha_{\phi l}^{(3)}}{\Lambda^2}$	$[-0.007, 0.006]$	$[-0.009, 0.006]$	$[\ 0.010, 0.068]$	$[-0.151, 0.008]$	$[-0.005, 0.004]$
	$\frac{\alpha_{\phi q}^{(3)}}{\Lambda^2}$	$[-0.008, 0.011]$	$[-0.009, 0.007]$	$[-0.090, -0.003]$	$[-0.002, 0.305]$	$[-0.007, 0.006]$
	$\frac{\alpha_{\phi ud}}{\Lambda^2}$	-	$[-0.015, 0.018]$	$[-0.006, 0.208]$	-	$[-0.012, 0.020]$
Oblique	$\frac{\alpha_{\phi}^{(3)}}{\Lambda^2}$	$[-0.031, 0.019]$	$[-0.041, 0.003]$	$[0.024, 0.174]$	$[-0.344, 0.033]$	$[-0.031, 0.008]$
	$\frac{\alpha_{WB}}{\Lambda^2}$	$[-0.006, 0.006]$	$[-0.019, 0.001]$	$[0.007, 0.068]$	$[-0.155, 0.017]$	$[-0.006, 0.004]$

Table 2.2: 95% C.L. limits on (90% central confidence interval of) the operator coefficients in Table 4.3, considering only one operator at a time and for each data set. Limits are in units of TeV^{-2}. The different columns show the results for different fits depending on the observables included.

propagating effect contributing in particular to NC and CC couplings. Hence, these two operators can be also constrained by precise measurements at the Z pole [12]. On the other hand, none of the operators involving four quark fields can be constrained since data come from processes with initial and/or final leptonic states. Note also that none of the LRLR operators has any $1/\Lambda^2$ effect in the observables considered. Only the two operators involving leptons, $\mathcal{O}_{lq}$ and $\mathcal{O}_{lq'}$, may give corrections, and only to neutrino-nucleon scattering or to LEP 2 cross sections. The same happens for the LRRL operator $\mathcal{O}_{qde}$. As explained before, these operators either have no interference with the SM amplitude or, in the case of LEP 2 observables, do interfere with the Higgs exchange but this is proportional to the electron Yukawa coupling and then negligible.

When comparing the results obtained from both low-energy and LEP 2 data in Table 2.2 we find they are highly complementary. We also observe that, although these two data sets are quite effective in constraining $\alpha_{ll}^{(3)}$, the main restriction comes indirectly from the measurement of the unitarity of the first row of the CKM matrix. Indirect constraints from Z-pole data are also significant. Finally, the upper bound for $\mathcal{O}_{lq}^{(3)}$ is also indirectly fixed from the precise determination of the CKM unitarity.

- **Scalar-Vector-Fermion interactions:** These dimension-six operators correcting trilinear couplings are in general constrained by all data sets. In particular, the operator $\mathcal{O}_{\phi l}^{(3)}$ contributes to all observables through indirect corrections. Let us first note in view of the results in Table 2.2 that although these trilinear corrections also enter in the LEP 2 observables, these play no rôle at the end because they imply bounds in general much weaker than those derived from other measurements, in particular at the Z pole. Therefore, as advanced in Section 2.2.5, when performing a fit to new physics only correcting trilinear couplings, like for instance extra vector-like heavy fermions, we can safely neglect LEP 2 constraints. Low-energy data, however, still provide competitive limits for several operators, and should not be ignored. Finally, the operator $\mathcal{O}_{\phi ud}$ correcting RH quark CC lacks precise direct restrictions, and enters in our fits only through corrections for the extraction of the CKM matrix elements. When considering this operator alone, the fit yields bounds similar to those for the other SVF operators, due to the high precision of the CKM unitarity determination.

- **Scalar-Fermion interactions:** SF interactions correct fermion masses and Yukawa interactions. As explained in the corresponding sections the effect of these operators on fermion masses can be always removed by redefining the original Yukawa couplings. On the other hand, the corrections to Yukawa interactions only enter some of the observables through the interference with Higgs exchange amplitudes that are proportional to the electron Yukawa couplings and thus negligible.

- **Scalar operators:** As discussed at the beginning of the Section 2.1.1, the contributions from the operator $\mathcal{O}_{\phi 4}$ are unobservable since this is nothing but a renormalization of the SM scalar quartic coupling. The operator $\mathcal{O}_{\phi 6}$ on the other hand is a genuine dimension-six contribution but it does not appear in the corrections to any of the observables. This is so because we can absorb it inside the Higgs vev or, more precisely, within the value of G_μ, which is the input we use for the determination of v (see Eq. (2.55)).

- **Oblique operators:** Since they directly correct gauge boson masses ($\mathcal{O}_\phi^{(1)}$, $\mathcal{O}_\phi^{(3)}$ and $\mathcal{O}_{WB}$) and couplings ($\mathcal{O}_{WB}$), oblique operators should in principle affect to most observables. While

[12] Note that in the fits of Table 2.2 the corresponding entries of $\mathcal{O}_{ll}^{(1)}$ are fixed to zero, and then only direct effects from this operator are constrained.

this is true for $\mathcal{O}_\phi^{(3)}$ and $\mathcal{O}_{WB}$, all observables are completely blind to $\mathcal{O}_\phi^{(1)}$. The reason, as in the case of $\mathcal{O}_{\phi 6}$, is that we can also absorb its effects in one of the inputs, in M_Z, because this operator contributes exclusively and in the same way to the W and Z masses. The operator $\mathcal{O}_\phi^{(3)}$ only corrects M_Z and then is observable through indirect effects. While the lower bound for this operator in Table 2.2 is essentially determined by Z data, the upper bound is mostly dominated by M_W which is below the SM prediction. On the other hand, $\mathcal{O}_{WB}$ which also enters indirectly in all observables, directly corrects all NC couplings and therefore the Z-pole observables determine the corresponding bound, though also in collaboration with M_W for the upper limit.

Finally, let us discuss the implications of these operators for the determination of the Higgs mass. There are only a few operator coefficients that exhibit a significant correlation with M_H at the minimum. These are $\alpha_{ll}^{(3)}$, $\alpha_{\phi l}^{(3)}$, $\alpha_\phi^{(3)}$ and α_{WB}, as can be seen in Table 2.3 where we gather such correlations as well as the corresponding bounds from the global fit without Higgs direct searches data. The effect on M_H is also show in Fig. 2.1 left, where we plot the χ^2 distribution as a function of the Higgs mass for the different fits. To show the correlations between the last two operators, in Fig. 2.1 right we draw the 95% C.L. regions from a fit to (only) the $\alpha_\phi^{(3)}$ and α_{WB} coefficients for a Higgs mass equal to 116, 300 and 1000 GeV. This analysis can be put in a more familiar form identifying these coefficients with the oblique parameters T and S [62][13]:

$$T = -\frac{1}{2\alpha}\alpha_\phi^{(3)}\frac{v^2}{\Lambda^2} \ , \qquad S = \frac{4sc}{\alpha}\alpha_{WB}\frac{v^2}{\Lambda^2} \ , \tag{2.124}$$

The leading Higgs corrections for a heavy Higgs ($M_H \gg M_Z$) are logarithmic and oblique, and to a good approximation can be encoded in the following contributions to the oblique parameters [62]

$$\Delta T \approx -\frac{3}{8\pi c^2}\log\frac{M_H}{M_H^{\rm ref}} \ , \qquad \Delta S \approx \frac{1}{6\pi}\log\frac{M_H}{M_H^{\rm ref}} \ , \qquad \Delta U \approx 0 \ , \tag{2.125}$$

with $M_H^{\rm ref}$ a given reference value for the Higgs mass from which S and T are defined. Then, the effect of a heavy Higgs can be compensated by a positive (negative) contribution to the T (S) parameter. When interpreted in terms of operator coefficients, a heavy Higgs is then favored by negative contributions to both $\alpha_\phi^{(3)}$ and α_{WB}, which explains the anti-correlations in Fig. 2.1 right. When only one of the operators is included, the effect of a heavy Higgs can be only partially cancelled out. But, as we can also observe from both plots in Fig. 2.1, we can still compensate a 1 TeV Higgs without increasing significantly the value of the χ^2 (less than 1 σ) including just the operator $\mathcal{O}_\phi^{(3)}$.

The strong correlation of the other two coefficients $\alpha_{ll}^{(3)}$ and $\alpha_{\phi l}^{(3)}$ in Table 2.3 with the Higgs mass might seem puzzling at first sight for they are not of oblique type. After inspection one realizes that both contribute to muon decay and then correct the relation between G_μ and G_F. This is the key to understand why these coefficients exhibit also a remarkable correlation [83, 84]. These new contributions can be understood as tree-level additions to the Sirlin's parameter Δr [85],

$$G_\mu = \frac{\alpha\pi}{\sqrt{2}M_Z^2 s^2 c^2(1-\Delta r)} \ , \tag{2.126}$$

which within the SM parametrizes the radiative corrections to the Fermi constant extracted from muon decay. Hence, a shift in Δr can be compensated by a shift in the T parameter in Z-pole

[13] There are no dimension-six contributions to the U parameter.

		$\frac{\alpha_{ll}^{(3)}}{\Lambda^2}$	$\frac{\alpha_{\phi l}^{(3)}}{\Lambda^2}$	$\frac{\alpha_{\phi}^{(3)}}{\Lambda^2}$	$\frac{\alpha_{WB}}{\Lambda^2}$
	$\rho_{\log M_H, \frac{\alpha_i}{\Lambda^2}}$	0.53	-0.62	-0.98	-0.96
95% C.L.	$\frac{\alpha_i}{\Lambda^2}$ [TeV^{-2}] $\in$	$[-0.010, 0.005]$	$[-0.005, 0.007]$	$[-0.117, 0.022]$	$[-0.011, 0.018]$
	M_H [GeV]$<$	149	158	> 1000	245

Table 2.3: Correlation (ρ_{ij}) between the operator coefficients and $\log M_H$ at the global minimum, and without Higgs direct searches data. The corresponding 95% C.L. limits for the coefficients and M_H are also given.

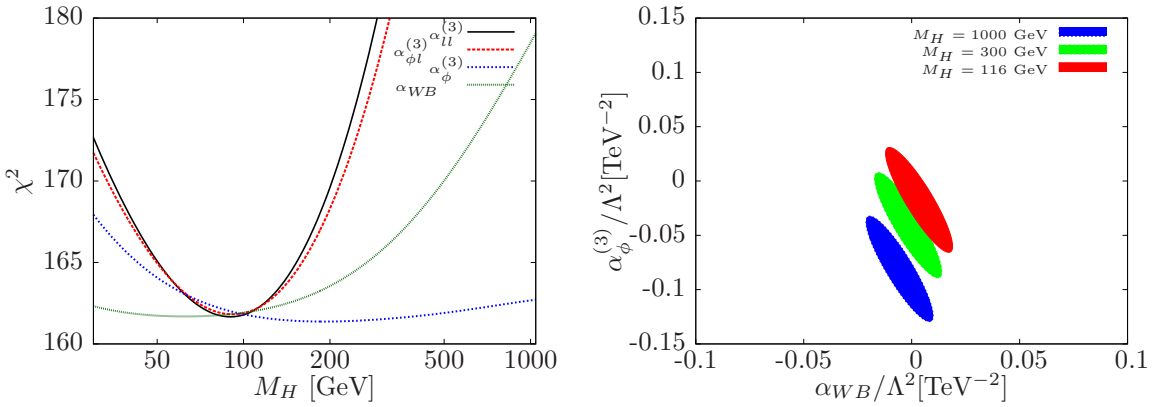

Figure 2.1: (Left) χ^2 profile as a function of M_H from the global fit excluding Higgs direct searches for the operator coefficients $\alpha_{ll}^{(3)}$, $\alpha_{\phi l}^{(3)}$, $\alpha_{\phi}^{(3)}$ and α_{WB}. (Right) 95% C.L. regions in the $\alpha_{\phi}^{(3)}$- α_{WB} plane for $M_H = 116, 300$ and 1000 GeV.

observables. Indeed, taking $\Delta r = \Delta_{G_F} \frac{v^2}{\Lambda^2}$ and using Eqs. (2.64) and (2.65) we see that Δr and T always appear in NC couplings in the combination $\Delta r - \alpha T$. Then, for Z-pole observables a negative Δr plays the rôle of a positive T, and we can in principle cancel the corresponding contribution from a heavy Higgs. This is not the case, however, for all observables and, in particular, for the W mass which is crucial in determining the preferred M_H value. In this case (2.94) implies $\Delta_{M_W} \propto \alpha T - \frac{s^2}{c^2}\Delta r$, and there is no cancellation between the Higgs and the G_μ contribution for M_W once the relation between both of them from Z-pole observables has been implemented. As a consequence, in the global fit the corresponding contribution to Δr can be adjusted to cancel only a small part of of the heavy Higgs effect, explaining why the M_H correlations with $\alpha_{ll}^{(3)}$ and $\alpha_{\phi l}^{(3)}$ are weaker. The signs of the correlations simply reflects how each quantity enters in Δr (see Eq. (2.51)). At any rate, the possibility of compensating a large M_H is in this way rather mild, for the possible cancellation in M_W, which prefers a light Higgs, is in any case small. Besides, the allowed values for $\alpha_{ll}^{(3)}$ and $\alpha_{\phi l}^{(3)}$ are also quite restricted by other observables they contribute to, and not only through G_μ, and then their contributions become negligible in the cases we consider. Indeed, $\mathcal{O}_{\phi l}^{(3)}$ contributes to all NC processes involving LH trilinear lepton couplings and then is

directly constrained by Z-pole data. The strongest constraint on $\alpha_{ll}^{(3)}$ follows indirectly from the measurement of the unitarity of the first row of the CKM matrix, which is also sensitive to $\alpha_{\phi l}^{(3)}$. Nevertheless, it is important to have these correlations in mind when there are contributions from new physics to several operators at the same time, because it may be possible that the former constraints do not held, and the corresponding contributions to G_μ do help in accounting for a relatively heavy Higgs. (Actually, we will comment on one of such case in the next chapter.) Obviously, this scenario would be further favoured if the new physics also contributed to the W mass positively. Finally, let us point out that a non-vanishing $(\alpha_{ll}^{(1)})_{1221}$ and $(\alpha_{ll}^{(3)})_{1221}$, which are not considered in the fits in this section as explained above, can also play the same rôle for they contribute to muon decay too.

Chapter 3

New matter fields: Extra spin-1/2 particles

Extra fermionic particles are common in many scenarios of physics beyond the SM. These are required for instance in Grand Unification Theories (GUT) [86, 87] when we complete the multiplets where we embed the SM fermions, or in scenarios with extra chiral symmetries in order to cancel gauge quantum anomalies. They also appear in Little Higgs models [88] where they play a crucial role in canceling the quadratically divergent contributions to the Higgs mass from the SM top quark. In theories with extra dimensions [89], on the other hand, these are not required in principle but arise naturally if the SM fermions propagate along the bulk of the extra dimension. In this case we actually have a infinite tower of replicas with increasing masses for each SM fermion multiplet. In all the previous examples extra fermions are vector-like respect to the SM, i.e. both chiralities transform in the same way under the SM gauge group. This guarantees that they do not introduce gauge quantum anomalies. By vector-like, we refer also to Majorana fermions, for which both chiralities are not independent but related by charge conjugation. Scenarios with extra chiral fermions can also be considered if the corresponding gauge anomalies are canceled. This is possible, for instance, if they complete an additional SM family. This *fourth generation* of fermions has regained interest recently. There are, however, problems when one considers new chiral fermions. Fermion masses in this case can only be generated upon EWSB so, since experiments require that they be heavy, the corresponding Yukawa couplings are large and may destabilize the Higgs potential. Furthermore, if large enough, the running Yukawa coupling may blow up leading to Landau poles before the Planck scale. On the other hand, an additional generation is known to have problems with electroweak precision tests, for it gives a too large contribution to the S parameter, excluded at the 6 σ level [38]. This can be relaxed by considering non-degenerate new families or allowing the T parameter to vary as well. However, a very recent analysis including the current status of EWPD and these considerations reveals that, though electroweak precision constraints have relaxed, the presence of an extra generation of chiral fermions is still disfavored [90].

In this chapter we analyze the low-energy effects of heavy vector-like fermions. Since they must be relatively heavy the effective Lagrangian approach should be a good approximation. We consider all possible new vector-like fermions that, after EWSB, mix with the SM ones, and hence contribute to precision observables. Then, we compute the corresponding effective Lagrangian describing their low-energy interactions. With the aid of the computations in the previous chapter, this can be used to obtain the limits that EWPD imposes on the couplings and masses of these extra particles. In this regard we focus on the analysis of extra vector-like leptons. The case of extra vector-like

quarks has been actively considered in the literature [87, 91, 92, 93, 94, 95, 96], including recent analysis of their implications on EWPD [94, 95, 96]. Most of the analysis, however, focus in the effects of extra SM-like singlets or doublets and mainly in the case of couplings with the third family. Exotic quark doublets has been also considered. On the other hand, there is no detailed analysis of the effects that quark triplets would have on data. The corresponding general analysis will be presented in a future publication [97].

Since these hypothetical new leptons modify leptonic observables, it looks plausible, a priori, that they may improve the electroweak fit and/or change the prediction for the Higgs mass. We observe that the quality of the global fit (including high- and low-Q^2 data) hardly improves when the new leptons are included. The case of neutrino singlets has the interesting feature of raising the preferred Higgs mass above the direct LEP limit $M_H = 114.4$ GeV. Due to the values of M_W measured at LEP 2 and Tevatron, however, the Higgs cannot be very heavy. For other kinds of new leptons, the SM prediction for M_H is mostly unchanged.

We shall derive limits on the mixing of the SM leptons with the different possible new vector-like additions. (Previous fits for specific additions [98, 99, 100] are improved.) The upper bounds range from 0.01 to 0.08 at 95 % C.L., depending on the quantum numbers of the new lepton and the SM family it mixes with. If the new leptons are weakly coupled, the largest allowed mixing requires that their masses are near the TeV scale. We will give results in the case of one extra multiplet at a time because the global fit does not improve when several of them are considered.

It is important to note that new leptons with significant mixing are generically ruled out when they mediate FCNC [101, 102, 103, 104], generate masses for the SM neutrinos [2], or contribute to neutrinoless double β decay [105]. To avoid these constraints, we must assume that each new lepton mixes mostly with just one family, and that their contributions to the light Majorana masses and neutrinoless double β decay, when possible, are very suppressed [106]. This scenario with new Majorana particles at the TeV scale that have sizable mixings with the SM leptons can be made natural with the help of extra symmetries. In general, these include lepton number conservation [107] and must be very slightly broken, if at all. At any rate, we find that new leptons with the quantum numbers of the see-saw messengers of type I [108] and III [109] can have sizable mixings. The neutrino singlets are also relevant to models of resonant leptogenesis [110]. All our limits apply independently of the Majorana or Dirac character of the heavy leptons, but in the Majorana case the restrictions mentioned above must be taken into account.

Finally, let us emphasize that our results are relevant to LHC, since the production and decay of these new leptons can be constrained by the limits on their mixings derived here. This is decisive for neutrino singlets, as they can be only produced through such a mixing [111]. All the other extra leptons can, in addition, be pair produced. Even if their decays are proportional to their mixing, this is still large enough for the new leptons to decay within the detector [112]. On the other hand, new leptons with masses of the order of 1 TeV and relatively large mixing with the SM leptons may be observable at future $e^+ e^-$ colliders [113]. They can also give deviations in neutrino couplings, which could be measured at future neutrino experiments (see for instance [114]).

In the next section we enumerate the different possibilities of vector-like fermions and write down their couplings to the SM fields. In Section 3.2 we derive the effective Lagrangian describing the effect of new fermions below threshold. We also describe the constraints from FCNC and neutrino masses. The resulting EWPD constraints are given in Section 3.3. Limits on the mixings are derived in general and assuming universality. Section 3.4 is devoted to a detailed discussion of the interplay between heavy lepton singlets and the Higgs mass. Section 3.5 contains the conclusions of this chapter, including the implications of our fits for the observation of heavy leptons at large colliders.

3.1 Extending the Standard Model with vector-like fermions

As emphasized, many models of new physics beyond the SM include extra fermions, and these are usually vector-like to avoid the problems inherent to the addition of new chiral matter. It is, therefore, interesting to study the impact of new vector-like fermions at the TeV scale on low-energy observables, and the limits implied on their couplings and masses. To give sizable contributions to EWPD, the new fermions must mix at tree level with the SM ones. This condition together with renormalizability and the fact that the theory must be invariant under the SM gauge group restrict the new particles quantum numbers. The different possible additions are gathered in Tables 3.1 and 3.2, which also settles our notation for the extra multiplets.

Leptons	N	E	$\begin{pmatrix} N \\ E^- \end{pmatrix}$	$\begin{pmatrix} E^- \\ E^{--} \end{pmatrix}$	$\begin{pmatrix} E^+ \\ N \\ E^- \end{pmatrix}$	$\begin{pmatrix} N \\ E^- \\ E^{--} \end{pmatrix}$
Notation			Δ_1	Δ_3	Σ_0	Σ_1
$SU(3)_c \otimes SU(2)_L \otimes U(1)_Y$	$(3,1)_0$	$(3,1)_{-1}$	$(3,2)_{-\frac{1}{2}}$	$(3,2)_{-\frac{3}{2}}$	$(3,3)_0$	$(3,3)_{-1}$
Spinor	Dirac or Majorana	Dirac	Dirac	Dirac	Dirac or Majorana	Dirac

Table 3.1: Lepton multiplets mixing with the SM leptons through Yukawa couplings to the SM Higgs.

Quarks	U	D	$\begin{pmatrix} U \\ D \end{pmatrix}$	$\begin{pmatrix} X \\ U \end{pmatrix}$	$\begin{pmatrix} D \\ Y \end{pmatrix}$	$\begin{pmatrix} X \\ U \\ D \end{pmatrix}$	$\begin{pmatrix} U \\ D \\ Y \end{pmatrix}$
Notation			Ξ_1	Ξ_7	Ξ_5	Ω_2	Ω_1
$SU(3)_c \otimes SU(2)_L \otimes U(1)_Y$	$(3,1)_{\frac{2}{3}}$	$(3,1)_{-\frac{1}{3}}$	$(3,2)_{\frac{1}{6}}$	$(3,2)_{\frac{7}{6}}$	$(3,2)_{-\frac{5}{6}}$	$(3,3)_{\frac{2}{3}}$	$(3,3)_{-\frac{1}{3}}$

Table 3.2: Quark multiplets mixing with the SM leptons through Yukawa couplings to the SM Higgs. In this case the spinor field describing the fermions can be only of Dirac type.

We consider a generic renormalizable extension of the SM including these vector-like fermions. After diagonalizing the fermionic kinetic terms and the corresponding mass matrices before EWSB, the Lagrangian of the theory can be split into three pieces:

$$\mathcal{L} = \mathcal{L}_\ell + \mathcal{L}_h + \mathcal{L}_{\ell h}. \tag{3.1}$$

$\mathcal{L}_\ell$ is the SM Lagrangian and contains only light fields (with no RH neutrinos). As stated in Chapter 1, we choose to work in the basis in which the leptonic and d quark Yukawa terms are diagonal. Then, the fermionic sector is given by

$$\begin{aligned} \mathcal{L}_\ell \supset\ & \overline{l_L^i}\, i\not{D} l_L^i + \overline{q_L^i}\, i\not{D} q_L^i + \overline{e_R^i}\, i\not{D} e_R^i + \overline{u_R^i}\, i\not{D} u_R^i + \overline{d_R^i}\, i\not{D} d_R^i - \\ & - \left(y^e_{ii}\ \overline{l_L^i}\phi e_R^i + y^d_{ii}\ \overline{q_L^i}\phi d_R^i + V^\dagger_{ij} y^u_{jj}\ \overline{q_L^i}\tilde{\phi} u_R^j + \text{h.c.} \right). \end{aligned} \tag{3.2}$$

$\overline{[\psi_1]}\,[\psi_2]$	$\overline{2_Y}1_{Y+\frac{1}{2}}$	$\overline{2_Y}1_{Y-\frac{1}{2}}$	$\overline{3_Y}2_{Y-\frac{1}{2}}$	$\overline{3_Y}2_{Y+\frac{1}{2}}$
$\Phi_{\psi_1\psi_2}$	$\tilde{\phi}$	ϕ	$\tilde{\phi}^\dagger\frac{\sigma_a}{2}$	$\phi^\dagger\frac{\sigma_a}{2}$

Table 3.3: Form of the scalar doublet required to make the operators $\overline{\Psi_L}\Phi\Psi'_R$, $\overline{\Psi_R}\Phi\psi_L$ and $\overline{\Psi_L}\Phi\psi_R$ gauge invariant, in terms of the quantum numbers of the fermions appearing in the operator.

$\mathcal{L}_h$ contains the terms involving heavy vector-like fermions:

$$\mathcal{L}_h = \sum_\Psi \eta_\Psi \left(\overline{\Psi^I}\, i\not{D}\Psi^I - M_I\overline{\Psi^I}\Psi^I\right) - \sum_{\Psi<\Psi'}\left((y_{\Psi\Psi'})_{IJ}\,\overline{\Psi^I}\Phi_{\Psi\Psi'}\Psi'^J + \text{h.c.}\right), \tag{3.3}$$

where Ψ stands for the Dirac spinor of any of the multiplets in Tables 3.1 and 3.2, with $\Psi_{L,R}$ its two chiral components. In particular, we will use $\Psi = L$ to refer to the extra leptons, and $\Psi = Q$ for the new quarks. In our basis, the mass matrices M are real and diagonal. We also allow for the possibility that L is Majorana when $L = N$ or $L = \Sigma_0$, adjusting the normalization constants η_L to reproduce the standard values 1 and $\frac{1}{2}$ for Dirac and Majorana spinors, respectively. For new quarks $\eta_Q = 1$ for they are Dirac fermions. The capital latin superindices I, J refer to the different exotic species with the same quantum numbers. Finally, $\Phi_{\Psi\Psi'}$ represents the form of the SM scalar doublet needed for the Yukawa terms to be gauge invariant, which can be read from Table 3.3.

The last piece, $\mathcal{L}_{\ell h}$, contains all the Yukawa couplings between light and heavy fermions:

$$\begin{aligned}\mathcal{L}_{\ell h} = &-(y_{Le})_{Ij}\,\overline{L_L^I}\Phi_{Le}e_R^j - (y_{Ll})_{Ij}\,\overline{L_R^I}\Phi_{Ll}l_L^j - \\ &-(y_{Qu})_{Ij}\,\overline{Q_L^I}\Phi_{Qu}u_R^j - (y_{Qd})_{Ij}\,\overline{Q_L^I}\Phi_{Qd}d_R^j - (y_{Qq})_{Ij}\,\overline{Q_R^I}\Phi_{Qq}q_L^j + \text{h.c.}.\end{aligned} \tag{3.4}$$

After EWSB there are mass terms mixing SM and extra fermions. Within our fermion basis convention, if each SM flavor mixes at most with one extra fermion, as we shall eventually assume, the diagonalizing matrices for charged leptons and d quarks are 2×2. These unitary matrices are thus fixed by one mixing angle $s = \sin\theta$, up to phases. For u quarks this is still approximately true for the top because it mainly couples to the bottom. Let us focus on the case of extra leptons, whose implications on EWPD will be discussed later, in order to introduce some notation and further conventions. We shall take the mixing s to be non-negative, except for Σ_1, where we keep a convenient relative minus sign between the mixing of ν_L and e_L. At first order, these mixings are given by the ratio of the Yukawa coupling, y, to a heavy mass M (times v). The precise expressions for the different possible extra leptons are collected in Table 3.4. After diagonalization, the charged and neutral currents for light and heavy mass eigenstates are written as a function of the lepton mixing s. The strength of the interactions involving only light leptons are modified with respect to the SM ones, correcting electroweak precision observables. On the other hand, the very same mixings appear in the charged and neutral currents with one light and one heavy lepton, which are relevant for the production and decay of these heavy particles at large colliders. We present our results in terms of the complete subset of independent charged current couplings with one light and one heavy lepton gathered in Table 3.5. As shown in this table, they turn out to be directly related to the lepton mixings. For this reason we shall generically use the term "mixing" for both U and s.

	N	E	Δ_1	Δ_3	Σ_0	Σ_1
s_L^ν	$\left\lvert\frac{y_{Nl}v}{\sqrt{2}M_N}\right\rvert$	–	–	–	$\left\lvert\frac{y_{\Sigma_0 l}v}{2\sqrt{2}M_{\Sigma_0}}\right\rvert$	$-\sqrt{2}s_L^e$
s_L^e	–	$\left\lvert\frac{y_{El}v}{\sqrt{2}M_E}\right\rvert$	negligible	negligible	$\sqrt{2}s_L^\nu$	$\left\lvert\frac{y_{\Sigma_1 l}v}{2\sqrt{2}M_{\Sigma_1}}\right\rvert$
s_R^e	–	negligible	$\left\lvert\frac{y_{\Delta_1 e}v}{\sqrt{2}M_{\Delta_1}}\right\rvert$	$\left\lvert\frac{y_{\Delta_3 e}v}{\sqrt{2}M_{\Delta_3}}\right\rvert$	negligible	negligible

Table 3.4: First order expressions in $\frac{yv}{M}$ of the mixing between one SM lepton of a given flavor and one extra lepton. Family indices are implicit and "negligible" stands for higher order contributions.

	N	E	Δ_1	Δ_3	Σ_0	Σ_1
$\overline{f_\alpha}\gamma^\mu f'_\alpha$	$\overline{e_L^-}\gamma^\mu N_L$	$\overline{E_L^-}\gamma^\mu \nu_L$	$\overline{e_R^-}\gamma^\mu N_R$	$\overline{E_R^{--}}\gamma^\mu e_R^-$	$\overline{e_L^-}\gamma^\mu N_L$	$\overline{E_L^-}\gamma^\mu \nu_L$
$\left\lvert U_\alpha^{ff'}\right\rvert$	s_L^ν	s_L^e	s_R^e	s_R^e	s_L^ν	s_L^e

Table 3.5: Resulting first order expressions of a complete subset of independent charged current couplings $-\frac{g}{\sqrt{2}}U_\alpha^{ff'}W_\mu^-\overline{f_\alpha}\gamma^\mu f'_\alpha$, $\alpha = L, R$, as a function of the lepton mixing.

3.2 The effective Lagrangian for new fermions

As we are interested in the effects of heavy particles at energies much smaller than their masses, we can integrate them out and use the resulting effective Lagrangian. This is completely equivalent, for our purposes, to diagonalizing the mass matrices to first order and using the resulting charged and neutral couplings for light fields. Nevertheless, following the general method in this thesis, we write down the completely-gauge-invariant induced operators and their coefficients before electroweak symmetry breakdown. In particular, this may be useful to compare with other new physics effects on EWPD. Because the heavy fermions are vector-like, they decouple in the limit when their mass goes to infinity. If they have masses of the order of TeV, we expect that the terms of dimension $d > 6$ give small corrections compared to the current experimental precision, as argued in Chapter 1. Therefore we do not take them into account in our fits. Our results will be consistent within this approximation.

Let us derive the effective Lagrangian after integrating out the heavy vector-like fermions. As interactions between two heavy species may contribute to the dimension-six effective Lagrangian, performing the integration of heavy fermions in general requires the integration of two different species at the same time. Note also that only one of them can be of Majorana type for the hypercharge of Φ can only be $\pm 1/2$. Suppose then that we have two generic fermionic species Ψ and Ψ', with masses M and M', and with the possibility of Ψ being Majorana. This last possibility is accounted by the parameter η_ψ as in Eq. (3.3). The Euler-Lagrange equations for each chirality read

$$\begin{aligned} i\not{D}\Psi_L^I - M_I\Psi_R^I &= (y_{\Psi\Psi'})_{IJ}\,\Phi_{\Psi\Psi'}\Psi_R^{'J} + (y_{\Psi f})_{Ij}\,\Phi_{\Psi f}f^j + (y^*_{\Psi F})_{Ij}\,\Phi^*_{\Psi F}F^{c\ j}\delta_{\eta_\Psi \frac{1}{2}}, \\ i\not{D}\Psi_R^I - M_I\Psi_L^I &= (y_{\Psi\Psi'})_{IJ}\,\Phi_{\Psi\Psi'}\Psi_L^{'J} + (y_{\Psi F})_{Ij}\,\Phi_{\Psi F}F^j + \left(y^*_{\Psi f}\right)_{Ij}\,\Phi^*_{\Psi f}f^{c\ j}\delta_{\eta_\Psi \frac{1}{2}}, \end{aligned} \tag{3.5}$$

and similarly for Ψ' (replacing $y_{\Psi\Psi'}$, $\Phi_{\Psi\Psi'}$ by $y^\dagger_{\Psi\Psi'}$, $\Phi^\dagger_{\Psi\Psi'}$, respectively, and taking $\eta_{\Psi'} = 1$). So, they can be solved iteratively. For SM fermions we have used the notation introduced previously: $F = q_L, l_L,\ f = e_R, u_R, d_R$. The last terms in the equations above come from the hermitian

conjugate in Eq. (3.4) for Majorana fermions, because in such case $\Psi_{L,(R)} = \Psi^c_{R,(L)}$. In order to keep up to dimension-six operator effects in the effective Lagrangian, we expand the solutions up to order $1/M^2$

$$\begin{aligned}\Psi^I_R =& -\frac{(y_{\Psi f})_{Ij}}{M_I}\Phi_{\Psi f} f^j - \frac{(y_{\Psi F})_{Ij}}{M_I^2}\, i\not{D}\big(\Phi_{\Psi F} F^j\big) + \frac{(y_{\Psi\Psi'})_{IJ}\,(y_{\Psi' f})_{Jj}}{M_I M'_J}\Phi_{\Psi\Psi'}\Phi_{\Psi' f} f^j - \\ &- \left(\frac{(y^*_{\Psi F})_{Ij}}{M_I}\Phi^*_{\Psi F} F^{c\ j} + \frac{(y^*_{\Psi f})_{Ij}}{M_I^2}\, i\not{D}\big(\Phi^*_{\Psi f} f^{c\ j}\big) - \frac{(y_{\Psi\Psi'})_{IJ}\,(y^*_{\Psi' F})_{Jj}}{M_I M'_J}\Phi_{\Psi\Psi'}\Phi^*_{\Psi' F} F^{c\ j}\right)\delta_{\eta_\Psi \frac{1}{2}}\end{aligned}$$

$$\begin{aligned}\Psi^I_L =& -\frac{(y_{\Psi F})_{Ij}}{M_I}\Phi_{\Psi F} F^j - \frac{(y_{\Psi f})_{Ij}}{M_I^2}\, i\not{D}\big(\Phi_{\Psi f} f^j\big) + \frac{(y_{\Psi\Psi'})_{IJ}\,(y_{\Psi' F})_{Jj}}{M_I M'_J}\Phi_{\Psi\Psi'}\Phi_{\Psi' F} F^j - \\ &- \left(\frac{(y^*_{\Psi f})_{Ij}}{M_I}\Phi^*_{\Psi f} f^{c\ j} + \frac{(y^*_{\Psi F})_{Ij}}{M_I^2}\, i\not{D}\big(\Phi^*_{\Psi F} F^{c\ j}\big) - \frac{(y_{\Psi\Psi'})_{IJ}\,(y^*_{\Psi' f})_{Jj}}{M_I M'_J}\Phi_{\Psi\Psi'}\Phi^*_{\Psi' f} f^{c\ j}\right)\delta_{\eta_\Psi \frac{1}{2}},\end{aligned} \tag{3.6}$$

and take them (these and those for Ψ') back to the Lagrangian $\mathcal{L}_h + \mathcal{L}_{\ell h}$, where again terms of order $1/M^3$ or higher are discarded. Note that with the exception of Majorana fermions, none of the multiplets in Tables 3.1 and 3.2 allows for Yukawa couplings with SM fields for both (positive and negative) chiralities. Thus, unless there are Majorana terms in Eq. (3.3) which are only possible for extra singlets and triplets of zero hypercharge, the order $1/M$ term will be absent for one of the chiralities in the above expansion and no dimension-five effects do arise upon the integration. In that specific case the lepton number violating Weinberg operator [60], the unique operator in $\mathcal{L}_5$, is generated,

$$\mathcal{L}_5 = (\alpha_5)_{ij}\overline{l^{c\,i}_L}\tilde{\phi}^*\tilde{\phi}^\dagger l^j_L + \text{h.c.}. \tag{3.7}$$

After EWSB it gives masses to light neutrinos, $m_\nu = -v^2\alpha_5/\Lambda$, with $(\alpha_5)_{ee}$ also contributing to neutrinoless double β decay. The corresponding values for the coefficient α_5 are given in Table 3.6. The fact that neutrino masses are tiny, and the strict bounds on neutrino double β decay, are usually explained by the large scale Λ. However, we want to keep the scale Λ near the TeV range to have non-negligible effects from $\mathcal{L}_6$. Then we need to assume that some mechanism in the high energy model keeps the coefficient $(\alpha_5)_{ij}$ very small. As we will illustrate below, a natural way to achieve this in any model is to implement lepton number conservation, up to possible breaking terms with adimensional coefficients α_5 smaller than 10^{-11} [2]. This scenario is stable under quantum corrections and is realized in models in which the heavy fermions are of Dirac type [107]. Unnatural cancellations are also possible [106].

At order $1/\Lambda^2$ there are essentially [1] two types of operators:

- Operators with two fermions, two scalars and a covariant derivative: $(\overline{\psi}\ \Phi^\dagger_{\Psi\psi}) i\not{D}(\Phi_{\Psi\psi}\ \psi)$. The only case where the two fermions can be different multiplets is for quark doublets with the SM hypercharge.
- Operators with two fermions and three scalars: $\overline{F}\,\Phi^\dagger_{\Psi' F}\Phi^\dagger_{\Psi\Psi'}\Phi_{\Psi f} f$.

While the former is always generated, the latter requires two different multiplets types and the adequate Yukawa coupling mixing them. None of the above operators is in the basis introduced in Chapter 1. In the first case, we can use the Leibniz rule to act with the covariant derivative separately on the scalar and fermion fields. Then, after applying the SM equations of motion

[1] Up to the use of charge conjugation properties and integration by parts in the case of Majorana fermions.

(EOM) (which are equivalent to perform an order $1/\Lambda^2$ field redefinition) on the operator with $\not{D}\psi$ and performing the adequate Fierz reordering, we can rewrite the first operator in terms of $\mathcal{O}^{(1)}_{\phi\psi}$, $\mathcal{O}^{(3)}_{\phi\psi}$ and $\mathcal{O}_{\psi\phi}$. For the second one we only need Fierz reordering to relate it with an operator of type $\mathcal{O}_{\psi\phi}$. The dimension-six effective Lagrangian resulting from integrating out the heavy leptons then contains

$$\begin{aligned}\mathcal{L}_6^L = &\left(\alpha^{(1)}_{\phi l}\right)_{ij}\left(\phi^\dagger i D_\mu \phi\right)\left(\overline{l^i_L}\gamma^\mu l^j_L\right) + \left(\alpha^{(3)}_{\phi l}\right)_{ij}\left(\phi^\dagger i\sigma_a D_\mu \phi\right)\left(\overline{l^i_L}\sigma_a\gamma^\mu l^j_L\right) + \\ &+ \left(\alpha^{(1)}_{\phi e}\right)_{ij}\left(\phi^\dagger i D_\mu \phi\right)\left(\overline{e^i_R}\gamma^\mu e^j_R\right) + \left(\alpha_{e\phi}\right)_{ij}\left(\phi^\dagger\phi\right)\overline{l^i_L}\phi\, e^j_R + \text{h.c.},\end{aligned} \tag{3.8}$$

while from extra vector-like quarks

$$\begin{aligned}\mathcal{L}_6^Q = &\left(\alpha^{(1)}_{\phi q}\right)_{ij}\left(\phi^\dagger i D_\mu \phi\right)\left(\overline{q^i_L}\gamma^\mu q^j_L\right) + \left(\alpha^{(3)}_{\phi q}\right)_{ij}\left(\phi^\dagger i\sigma_a D_\mu \phi\right)\left(\overline{q^i_L}\sigma_a\gamma^\mu q^j_L\right) + \\ &+ \left(\alpha^{(1)}_{\phi u}\right)_{ij}\left(\phi^\dagger i D_\mu \phi\right)\left(\overline{u^i_R}\gamma^\mu u^j_R\right) + \left(\alpha^{(1)}_{\phi d}\right)_{ij}\left(\phi^\dagger i D_\mu \phi\right)\left(\overline{d^i_R}\gamma^\mu d^j_R\right) + \\ &+ \left(\alpha_{\phi ud}\right)_{ij}\left(\phi^T i\sigma_2 i D_\mu \phi\right)\left(\overline{u^i_R}\gamma^\mu d^j_R\right) + \left(\alpha_{u\phi}\right)_{ij}\left(\phi^\dagger\phi\right)\overline{q^i_L}\tilde{\phi}\, u^j_R + \left(\alpha_{d\phi}\right)_{ij}\left(\phi^\dagger\phi\right)\overline{q^i_L}\phi\, e^j_R + \text{h.c.}.\end{aligned} \tag{3.9}$$

The values of the coefficients for extra leptons are given in Tables 3.6 and 3.8, while those for extra quarks are given in Tables 3.7 and 3.9. The latter were first obtained in Ref. [115] [2].

After EWSB $\alpha^{(1)}_{\phi\psi}$ and $\alpha^{(3)}_{\phi\psi}$ modify the NC and CC fermion couplings, as explained in Chapter 2 (see Eqs. (2.33) and (2.42)). In particular, in the case of extra SM-like quark doublets they introduce RH quark CC, not present in the SM. Though fermion masses are also modified, those changes can be absorbed into the mass definition. On the other hand, neglecting tiny irrelevant contributions from neutrino masses, we can re-diagonalize the charged lepton mass matrix by bi-unitary transformations without introducing further corrections in neutral and charged currents to order $1/\Lambda^2$. Note also (see Table 3.6) that the combination of Yukawa couplings entering $\alpha^{(1,3)}_{\phi l,e}$ is different from that in α_5, so it is possible to have sizable $\alpha^{(1,3)}_{\phi l,e}$ and vanishing α_5 simultaneously, even for N and Σ_0 multiplets [2]. Indeed, in both cases the coefficient of the dimension-five operator is proportional to $y^T M^{-1} y$, thus it only depends (quadratically) on y, while the coefficients of the dimension-six operators involve $y^\dagger M^{-2} y$, and then y and $y^\dagger$. Thus it is possible that there are cancellations in the former which do not hold in the latter. This is what happens for quasi-Dirac neutrinos. Consider, for instance, the addition of a heavy Dirac neutrino singlet N coupled to only one family. The generic mass matrix is given by

$$\begin{array}{c} \\ \nu_L \\ N_L \\ N^c_R \end{array}\!\!\begin{array}{c} \begin{array}{ccc} \nu_L & N_L & N^c_R \end{array} \\ \begin{pmatrix} 0 & 0 & \frac{y_N\, v}{\sqrt{2}} \\ 0 & 0 & M_N \\ \frac{y_N\, v}{\sqrt{2}} & M_N & 0 \end{pmatrix} \end{array}, \tag{3.10}$$

where lepton number can be broken by a small entry μ instead of some of the zeroes in the above matrix, giving a Majorana mass proportional to it for the light neutrino. This is true even if the nonzero entry is in the $(3,3)$ position because one-loop radiative corrections also generate a non-zero mass for ν_L proportional to μ. (A similar behaviour is found in Little Higgs models [116].)

[2] Unlike there, we do not include V in the definition of any of the Yukawa couplings mixing light and heavy quarks.

If the lepton number violating parameter μ is in the (2,2) position, the SM neutrino acquires a Majorana mass m_ν [3]

$$-y_N^T M_N^{-1} y_N \frac{v^2}{2} \approx -\frac{y_N^2}{2}\left[\frac{(1-\frac{\mu}{4M_N})^2}{M_N+\frac{\mu}{2}} - \frac{(1+\frac{\mu}{4M_N})^2}{M_N-\frac{\mu}{2}}\right]\frac{v^2}{2} \approx \frac{\mu y_N^2}{M_N^2}\frac{v^2}{2}, \tag{3.11}$$

where we only keep the dominant terms in μ/M_N. Hence, while m_ν is proportional to μ, the coefficients of the dimension-six operators are not,

$$y_N^\dagger M_N^{-2} y_N \approx \frac{|y_N|^2}{2}\left[\frac{(1-\frac{\mu}{4M_N})^2}{(M_N+\frac{\mu}{2})^2} + \frac{(1+\frac{\mu}{4M_N})^2}{(M_N-\frac{\mu}{2})^2}\right] \approx \frac{|y_N|^2}{M_N^2}\,. \tag{3.12}$$

Then, new fermions can exist near the TeV scale with observable effects beyond the SM, and the SM neutrinos be still light enough.

L	$\frac{\alpha_5}{\Lambda}$	$\frac{\alpha_{\phi l}^{(1)}}{\Lambda^2}$	$\frac{\alpha_{\phi l}^{(3)}}{\Lambda^2}$	$\frac{\alpha_{\phi e}^{(1)}}{\Lambda^2}$	$\frac{\alpha_{e\phi}}{\Lambda^2}$
N	$\frac{1}{2}y_{Nl}^T M_N^{-1} y_{Nl}$	$\frac{1}{4}y_{Nl}^\dagger M_N^{-2} y_{Nl}$	$-\frac{\alpha_{\phi l}^{(1)}}{\Lambda^2}$	–	–
E	–	$-\frac{1}{4}y_{El}^\dagger M_E^{-2} y_{El}$	$\frac{\alpha_{\phi l}^{(1)}}{\Lambda^2}$	–	$-2\frac{\alpha_{\phi l}^{(1)}}{\Lambda^2}y_e$
Δ_1	–	–	–	$\frac{1}{2}y_{\Delta_1 e}^\dagger M_{\Delta_1}^{-2} y_{\Delta_1 e}$	$y_e\frac{\alpha_{\phi e}^{(1)}}{\Lambda^2}$
Δ_3	–	–	–	$-\frac{1}{2}y_{\Delta_3 e}^\dagger M_{\Delta_3}^{-2} y_{\Delta_3 e}$	$-y_e\frac{\alpha_{\phi e}^{(1)}}{\Lambda^2}$
Σ_0	$\frac{1}{8}y_{\Sigma_0 l}^T M_{\Sigma_0}^{-1} y_{\Sigma_0 l}$	$\frac{3}{16}y_{\Sigma_0 l}^\dagger M_{\Sigma_0}^{-2} y_{\Sigma_0 l}$	$\frac{1}{3}\frac{\alpha_{\phi l}^{(1)}}{\Lambda^2}$	–	$\frac{4}{3}\frac{\alpha_{\phi l}^{(1)}}{\Lambda^2}y_e$
Σ_1	–	$-\frac{3}{16}y_{\Sigma_1 l}^\dagger M_{\Sigma_1}^{-2} y_{\Sigma_1 l}$	$-\frac{1}{3}\frac{\alpha_{\phi l}^{(1)}}{\Lambda^2}$	–	$-\frac{2}{3}\frac{\alpha_{\phi l}^{(1)}}{\Lambda^2}y_e$

Table 3.6: Coefficients of the operators arising from the integration of heavy leptons. The dimension-five operator entry, $\frac{\alpha_5}{\Lambda}$, only appears when the singlet N and/or the triplet Σ_0 are Majorana fermions.

On the other hand, the off-diagonal elements of the matrices $\alpha_{\psi\phi}$ and $\alpha_{\phi\psi}^{(1,3)}$ induce FCNC through the corresponding contributions to Yukawa interactions and NC couplings, respectively. For the case of extra leptons discussed below, the current experimental limits on rare processes like $\mu \to e\gamma$ and $\mu \to eee$ imply that these off-diagonal coefficients are small [102, 103]. As can be seen from Table 3.6, this requires that each new lepton multiplet mixes mostly with only one of the known lepton flavors. This pattern of mixings is automatic with the extra assumption of an (approximate) conservation of individual lepton number. In that case, we do not have any other constraints than those from EWPD, where the operator $\left(\phi^\dagger\phi\right)\overline{l_L^i}\phi e_R^j$ and the corresponding coefficients $\alpha_{e\phi}$ in Tables 3.6 and 3.8 do not contribute. Finally note that there are no contributions to

[3] The 2×2 bottom-right submatrix must be diagonalised before applying the seesaw formula in order to make the cancellation apparent. The masses of the two Majorana eigenstates are taken to be positive, $M_{N_1} \approx M_N + \mu/2$, $M_{N_2} \approx M_N - \mu/2$.

Q	$\frac{\alpha^{(1)}_{\phi q}}{\Lambda^2}$	$\frac{\alpha^{(3)}_{\phi q}}{\Lambda^2}$	$\frac{\alpha^{(1)}_{\phi u}}{\Lambda^2}$	$\frac{\alpha^{(1)}_{\phi d}}{\Lambda^2}$	$\frac{\alpha_{\phi u d}}{\Lambda^2}$	$\frac{\alpha_{u\phi}}{\Lambda^2}$	$\frac{\alpha_{d\phi}}{\Lambda^2}$
U	$\frac{1}{4}y^\dagger_{Uq}M_U^{-2}y_{Uq}$	$-\frac{\alpha^{(1)}_{\phi q}}{\Lambda^2}$	–	–	–	$2\frac{\alpha^{(1)}_{\phi q}}{\Lambda^2}V^\dagger y_u$	–
D	$-\frac{1}{4}y^\dagger_{Dq}M_D^{-2}y_{Dq}$	$\frac{\alpha^{(1)}_{\phi q}}{\Lambda^2}$	–	–	–	–	$-2\frac{\alpha^{(1)}_{\phi q}}{\Lambda^2}y_d$
Ξ_1	–	–	$-\frac{1}{2}y^\dagger_{\Xi_1 u}M_{\Xi_1}^{-2}y_{\Xi_1 u}$	$\frac{1}{2}y^\dagger_{\Xi_1 d}M_{\Xi_1}^{-2}y_{\Xi_1 d}$	$-y^\dagger_{\Xi_1 u}M_{\Xi_1}^{-2}y_{\Xi_1 d}$	$-V^\dagger y_u\frac{\alpha^{(1)}_{\phi u}}{\Lambda^2}$	$y_d\frac{\alpha^{(1)}_{\phi d}}{\Lambda^2}$
Ξ_7	–	–	$\frac{1}{2}y^\dagger_{\Xi_7 u}M_{\Xi_7}^{-2}y_{\Xi_7 u}$	–	–	$V^\dagger y_u\frac{\alpha^{(1)}_{\phi u}}{\Lambda^2}$	–
Ξ_5	–	–	–	$-\frac{1}{2}y^\dagger_{\Xi_5 d}M_{\Xi_5}^{-2}y_{\Xi_5 d}$	–	–	$-y_d\frac{\alpha^{(1)}_{\phi d}}{\Lambda^2}$
Ω_2	$\frac{3}{16}y^\dagger_{\Omega_2 q}M_{\Omega_2}^{-2}y_{\Omega_2 q}$	$\frac{1}{3}\frac{\alpha^{(1)}_{\phi q}}{\Lambda^2}$	–	–	–	$\frac{2}{3}\frac{\alpha^{(1)}_{\phi q}}{\Lambda^2}V^\dagger y_u$	$\frac{4}{3}\frac{\alpha^{(1)}_{\phi q}}{\Lambda^2}y_d$
Ω_1	$-\frac{3}{16}y^\dagger_{\Omega_1 q}M_{\Omega_1}^{-2}y_{\Omega_1 q}$	$-\frac{1}{3}\frac{\alpha^{(1)}_{\phi q}}{\Lambda^2}$	–	–	–	$-\frac{4}{3}\frac{\alpha^{(1)}_{\phi q}}{\Lambda^2}V^\dagger y_u$	$-\frac{2}{3}\frac{\alpha^{(1)}_{\phi q}}{\Lambda^2}y_d$

Table 3.7: Coefficients of the operators arising from the integration of heavy quarks.

L_1, L_2	$\frac{\alpha_{e\phi}}{\Lambda^2}$
E, Δ_1	$y^\dagger_{El} M_E^{-1} y_{E\Delta_1} M^{-1}_{\Delta_1} y_{\Delta_1 e}$
E, Δ_3	$y^\dagger_{El} M_E^{-1} y_{E\Delta_3} M^{-1}_{\Delta_3} y_{\Delta_3 e}$
Δ_1, Σ_0	$\frac{1}{2} y^\dagger_{\Sigma_0 l} M^{-1}_{\Sigma_0} y_{\Sigma_0\Delta_1} M^{-1}_{\Delta_1} y_{\Delta_1 e}$
Δ_1, Σ_1	$\frac{1}{4} y^\dagger_{\Sigma_1 l} M^{-1}_{\Sigma_1} y_{\Sigma_1\Delta_1} M^{-1}_{\Delta_1} y_{\Delta_1 e}$
Δ_3, Σ_1	$-\frac{1}{4} y^\dagger_{\Sigma_1 l} M^{-1}_{\Sigma_1} y_{\Sigma_1\Delta_3} M^{-1}_{\Delta_3} y_{\Delta_3 e}$

Table 3.8: Combined contribution to $\alpha_{e\phi}$ from the simultaneous integration of different mixed lepton multiplets. Even if the corresponding operator does not affect our fits, we include the values of the coefficient for completeness.

derivative couplings of the SM fermions to the Higgs (which would redefine the Yukawa couplings) because the coefficients $\alpha^{(1,3)}_{\phi\psi}$ are hermitian.

In what follows we focus on the phenomenological implications on EWPD of the effective Lagrangian resulting from the addition of the new vector-like leptons in Table 3.1. We leave the corresponding analysis for heavy vector-like quarks to a future publication [97].

3.3 The global fit for extra leptons

We have performed global fits to EWPD, confronting the SM extensions with extra leptons and constraining the possible lepton mixings. The observables entering in our fits are shown in Appendix A, Tables A.1 and A.2, together with their current experimental values and the corresponding SM predictions. We do not include the $e^+e^- \to \overline{f}f$ data at higher energies from LEP 2 because they do not change significantly the fits. The reason is that the Z-pole observables have better precision and constrain strongly all the new parameters in the model, i.e. no independent parameters enter in the LEP 2 observables. This can be understood because new leptons change only the trilinear fermionic couplings, but do not generate four-fermion operators. This justifies ignoring LEP 2 data.

On the other hand, we have updated Ref. [1], with the current values of the top mass [117], the strong coupling constant [118], the five-flavor hadronic contribution to the α running [119, 120], the W mass [71], the low-energy effective coupling g_L^2 [38] and the weak charge for Cesium [78]. We have also included additional light flavor data at the Z pole [70], the Tevatron determination of the effective weak mixing angle [121], the unitarity constraints on the first row of the CKM matrix [68] and further low energy observables such as the weak charges for Thalium [79], and for the electron [80]. Finally, the sharp cut on $M_H = 114.4$ GeV imposed in Ref. [1] to implement the LEP 2 limit has been replaced by the direct inclusion of the results from Higgs direct searches at LEP 2 and Tevatron. See Appendix A for more details. The most significant change, as we will see, is that the unitarity of the CKM matrix further constrains the mixing of a heavy neutrino singlet with the muon, significantly strengthening the corresponding bound.

As explained in Appendix A, we minimize the χ^2 function constructed with the available data. The new free parameters always enter as ratios of Yukawa couplings to heavy masses, giving the mixing between light and heavy particles as explained above and gathered in Table 3.4. We present

Q_1, Q_2	$\frac{\alpha_{u\phi}}{\Lambda^2}$	$\frac{\alpha_{d\phi}}{\Lambda^2}$
U, Ξ_1	$y^\dagger_{Uq} M_U^{-1} y_{U\Xi_1} M_{\Xi_1}^{-1} y_{\Xi_1 u}$	–
U, Ξ_7	$y^\dagger_{Uq} M_U^{-1} y_{U\Xi_7} M_{\Xi_7}^{-1} y_{\Xi_7 u}$	–
D, Ξ_1	–	$y^\dagger_{Dq} M_D^{-1} y_{D\Xi_1} M_{\Xi_1}^{-1} y_{\Xi_1 d}$
D, Ξ_5	–	$y^\dagger_{Dq} M_D^{-1} y_{D\Xi_5} M_{\Xi_5}^{-1} y_{\Xi_5 d}$
Ξ_1, Ω_2	$\frac{1}{4} y^\dagger_{\Omega_2 q} M_{\Omega_2}^{-1} y_{\Omega_2\Xi_1} M_{\Xi_1}^{-1} y_{\Xi_1 u}$	$\frac{1}{2} y^\dagger_{\Omega_2 q} M_{\Omega_2}^{-1} y_{\Omega_2\Xi_1} M_{\Xi_1}^{-1} y_{\Xi_1 d}$
Ξ_1, Ω_1	$\frac{1}{2} y^\dagger_{\Omega_1 q} M_{\Omega_1}^{-1} y_{\Omega_1\Xi_1} M_{\Xi_1}^{-1} y_{\Xi_1 u}$	$\frac{1}{4} y^\dagger_{\Omega_1 q} M_{\Omega_1}^{-1} y_{\Omega_1\Xi_1} M_{\Xi_1}^{-1} y_{\Xi_1 d}$
Ξ_7, Ω_2	$-\frac{1}{4} y^\dagger_{\Omega_2 q} M_{\Omega_2}^{-1} y_{\Omega_2\Xi_7} M_{\Xi_7}^{-1} y_{\Xi_7 u}$	–
Ξ_5, Ω_1	–	$-\frac{1}{4} y^\dagger_{\Omega_1 q} M_{\Omega_1}^{-1} y_{\Omega_1\Xi_5} M_{\Xi_5}^{-1} y_{\Xi_5 d}$

Table 3.9: Combined contribution to $\alpha_{u\phi}$ and $\alpha_{d\phi}$ from the simultaneous integration of different mixed quark multiplets.

the results as a function of the corresponding CC coupling U in Table 3.5. The fits constrain only their magnitud $|U|$. The new leptons can modify the observables in two ways. First, they can give direct contributions to the processes determining a given observable. Alternatively, they can contribute to processes constraining the input parameters. In this case, the relation between the measured values and the SM parameters is modified, resulting in indirect corrections to all observables. The free parameters used in our fits are $\Delta\alpha^{(5)}_{\rm had}\left(M_Z^2\right)$, $\alpha_s\left(M_Z^2\right)$, M_Z, m_t, M_H and the mixing of the new leptons. Note that the first four parameters are to a great extent determined by the corresponding experimental measurements[4]. The Higgs mass on the other hand is only partially constrained by direct searches. In particular, $M_H \geq 114.4$ GeV, but it stays (directly) unconstrained above 200 GeV. Therefore, only M_H and the lepton mixing can vary significantly, so we will give our results in terms of these two parameters.

The minimization of χ^2 and the calculation of the confidence regions are performed by scanning over the parameter space[5], accepting or rejecting points according to their probability. The plots are obtained from the actual set of points keeping only the those within the 95% probability region, from which we extrapolate the corresponding contour.

3.3.1 Numerical results

In Table 3.10 we show the improvements $-\Delta\chi^2_{\rm min}$ with respect to the SM minimum, when we add independently one new lepton kind at a time. We have also performed a general fit including all possible heavy leptons, but there is no further significant improvement in $\chi^2_{\rm min}$ and we do not show the result here. We distinguish different scenarios depending on how we choose the couplings of the new leptons to the SM fields. We have considered the following cases:

- A single new lepton coupled only to one of the three SM families ("Only with e, μ or τ").

[4] We can neglect the effect of the heavy leptons on these measurements.

[5] In practice, we restrict the parameters $\Delta\alpha^{(5)}_{\rm had}\left(M_Z^2\right)$, $\alpha_s\left(M_Z^2\right)$, M_Z and m_t to $1\,\sigma$ intervals around their SM value for the reasons just discussed.

Coupling	$n_{\rm par}^{\rm new}$	$-\Delta\chi^2_{\rm min}$ $(\chi^2_{\rm min}/\text{d.o.f.})$					
		N	E	Δ_1	Δ_3	Σ_0	Σ_1
General	3	1.2 (1.11)	0.2 (1.13)	1.7 (1.09)	1.7 (1.09)	1.1 (1.11)	0 (1.14)
Universal	1	0.2 (0.94)	0 (0.94)	0 (0.94)	0.4 (0.93)	0.5 (0.93)	0 (0.94)
Only with e	1	0.4 (1.07)	0 (1.08)	0 (1.08)	0.9 (1.06)	0.8 (1.06)	0 (1.08)
Only with μ	1	0.1 (1.08)	0.2 (1.08)	1.7 (1.04)	0 (1.08)	0 (1.08)	0 (1.08)
Only with τ	1	1 (1.06)	0 (1.08)	0 (1.08)	0.5 (1.07)	0.4 (1.07)	0 (1.08)

Table 3.10: Decrease in $\chi^2_{\rm min}$ with respect to the SM minimum, $\chi^2_{\rm SM} = 44.32$ ($\chi^2_{\rm SM} = 30.23$ with lepton universality), obtained by adding to the SM the different leptons. The number of degrees of freedom is obtained as $\mathcal{N} - 5 - n_{\rm par}^{\rm new}$, where n_{par}^{new} is the number of independent lepton mixings and $\mathcal{N} = 47$ is the number of observables ($\mathcal{N} = 38$ for the universal case). In parenthesis we write the value of $\chi^2_{\rm min}$/d.o.f., which for the SM is 1.06 (0.92 with lepton universality).

- Three leptons, each coupled to one (different) SM family with independent couplings ("General").
- Three leptons, each coupled to one (different) SM family with the same coupling ("Universal").

The universal case requires an extra assumption. When we do the fit with universal couplings, we use this assumption of universality also for data. This means that the set of data is different and hence the comparison with the other fits is not straightforward. The observables included in the fit for this case, with their current experimental values and the SM predictions, are collected in Table A.2 in Appendix A.

We see that there are mild improvements with respect to the SM χ^2 for singlets N_τ, doublets $(\Delta_1)_\mu$ and $(\Delta_3)_e$, and triplets $(\Sigma_0)_e$. In all the other cases the χ^2 is lowered by less than half unit. The only fit with χ^2/d.o.f. smaller than in the SM is obtained for the SM-like doublet coupled to the second family, $(\Delta_1)_\mu$. Even if the improvements are marginal at best, it is interesting that in some cases the minima occur for significant values of the mixings, as can be seen in Table 3.11. Let us also mention the biggest changes in individual observables at the global minima. First, $\sigma_{\rm had}$ (with a 1.7 pull in the SM) is improved in several cases, up to a pull of 0.8 for the singlet N_τ. The pull in the SLD asymmetry A_e is lowered from 2.0 to 1.8 for the singlets N_e, but at the price of increasing the A_{FB}^b anomaly from 2.6 to 2.8. Conversely, $(\Delta_3)_e$ reduces the bottom anomaly to 2.3 but increases the discrepancy in A_e up to 2.3. This multiplet is another example where we improve the prediction for $\sigma_{\rm had}$, leaving the pull at 0.9. Finally, $(\Delta_1)_\mu$, reduces the pull in R_μ^0 from 1.4 to 0.1. From the fits, we can also extract limits on the values of the mixings U and s in Tables 3.4 and 3.5, respectively. We give the 95% C.L. upper bounds on the absolute value of U in Table 3.11. We stress again that these limits incorporate the information from the direct Higgs searches.

In Figs 3.1 to 3.6 we show the 95% C.L. regions in the $|U| - M_H$ parameter space. In these plots we display the contour of the 95% probability region of the fit without any restriction on M_H, and the 95% confidence region when we include the direct M_H limits (the solid region). The effect of these limits has a dramatic impact reducing the allowed regions. This is not only because of the LEP 2 lower bound but also because in almost all cases the contours are bounded below

Coupling		N	E	Δ_1	Δ_3	Σ_0	Σ_1
Only with e	$\lvert U\rvert <$	0.051	0.020	0.020	0.028	0.020	0.016
	$\lvert U_{\rm min}\rvert =$	0.023	0	0	0.019	0.012	0
Only with μ	$\lvert U\rvert <$	0.031	0.029	0.048	0.028	0.018	0.024
	$\lvert U_{\rm min}\rvert =$	0.012	0.014	0.033	0	0	0.005
Only with τ	$\lvert U\rvert <$	0.087	0.033	0.035	0.045	0.030	0.029
	$\lvert U_{\rm min}\rvert =$	0.056	0	0	0.027	0.016	0
Universal	$\lvert U\rvert <$	0.028	0.019	0.020	0.025	0.017	0.013
	$\lvert U_{\rm min}\rvert =$	0.013	0	0	0.014	0.010	0

Table 3.11: Upper limit at 95 % C.L. on the absolute value of the mixings in Table 3.5 and their value at the minimum. The first three rows are obtained by coupling each new lepton with only one SM family. The last one corresponds to the case of lepton universality. All numbers are computed including the M_H constraints from Higgs direct searches at LEP 2 and Tevatron.

$M_H = 200$ GeV and then only the small window allowed by LEP 2 and Tevatron survives in the region obtained from all data.

As it is apparent in the plots, in some cases there is a correlation between the mixing and M_H. In particular, we can see in Fig. 3.1 a strong positive correlation for the singlet N, as long as it mixes with the first family of SM leptons. As a result, the preferred Higgs mass is larger than in the SM[6]. This is in fact responsible for part of the (small) improvement in the χ^2 in this case. We analyze the interplay between the Higgs mass and the mixing of neutrino singlets in more detail in next section. In Table 3.12 we give the 95% C.L. upper limits that we find in the different scenarios. These limits take into account the bounds from direct searches. The limits with some of the extra singlets are significantly weaker than in the SM, $M_H \leq 228$ GeV at 95% C.L. for N_e.

3.3.2 Large neutrino mixing and the Higgs mass

From Table 3.11, we see that the less constrained extra leptons are the neutrino singlets. These fields can play the role of see-saw messengers, although as we have mentioned their contribution to α_5 must be suppressed or cancelled by another contribution. In this section we analize this case in detail, emphasizing the role of the Higgs boson.

The mixing of new leptons with the light neutrinos modifies the invisible width of the Z, $\Gamma_{\rm inv}$. This shifts the prediction for $\sigma_{\rm had}$ in the opposite direction, since

$$\sigma_{\rm had} = 12\pi \frac{\Gamma_e \Gamma_{\rm had}}{M_Z^2 \Gamma_Z^2}, \tag{3.13}$$

and $\Gamma_Z = \Gamma_l + \Gamma_{\rm had} + \Gamma_{\rm inv}$ (with the leptonic width $\Gamma_l = 3\Gamma_e$ in the universal case). For the singlets N, the invisible width is smaller and the shift in $\sigma_{\rm had}$ is positive, so the pull in this quantity is

[6]This effect has been discussed before by Loinaz et al. in [84]. In that reference, a much heavier Higgs is allowed because the constraint from M_W is not enforced (or it is compensated by unknown new physics). We discuss the differences between our analysis and the one in [84] below.

Couplings		N	E	Δ_1	Δ_3	Σ_0	Σ_1
Only with e	M_H [GeV] <	228	150	151	148	151	149
Only with μ	M_H [GeV] <	155	154	151	150	149	149
Only with τ	M_H [GeV] <	149	150	150	149	150	150
Universal	M_H [GeV] <	187	152	152	149	150	149

Table 3.12: Upper limit at 95 % C.L. on the Higgs mass (in GeV). The first three rows are obtained by coupling each new lepton with only one SM family. The last one correspond to the case of lepton universality. All numbers are computed taking into account the M_H constraints from Higgs direct searches at LEP 2 and Tevatron.

reduced. These are the only effects on Z-pole observables when the new singlet mixes only with the third family. On the other hand, the independence of these couplings for different families is limited in the fit by the decays of the $W^{\pm}$, which do not allow for big departures from universality in the neutrino couplings. For this reason, the pull decreases only from 1.7 in the SM to 0.8.

A more interesting feature appears as the result of the coupling of N to the first two families. These couplings generate the operators $(\mathcal{O}^{(3)}_{\phi l})_{11,22}$, which contribute to muon decay and affect the extraction of the Fermi constant G_F from the muon lifetime. As argued in Chapter 2, because G_F is an input parameter, this effect propagates to all observables, giving indirect corrections that mimic the ones of the Peskin and Takeuchi oblique parameter T [62]. In particular, as follows from the discussion presented there we can define

$$\alpha T_{\text{eff}} = -\text{Re}\left[\left(\alpha^{(3)}_{\phi l}\right)_{11} + \left(\alpha^{(3)}_{\phi l}\right)_{22}\right]\frac{v^2}{\Lambda^2}\,, \tag{3.14}$$

which applies to all NC observables. The parameter T_{eff} is directly related to Δr, as explained in Chapter 2. As the dominant effects of the Higgs boson are oblique as well, some cancellations can take place. Indeed, the corrections to the oblique parameter T including the leading contribution of the Higgs mass[7], Eq. (2.125), and the shift in G_F, are given by

$$T = -\frac{3}{8\pi c^2}\log\frac{M_H}{M_Z} + T_{\text{eff}}. \tag{3.15}$$

Hence, we see that the effect on T of a heavy Higgs mass can be compensated by a positive value of T_{eff}. In fact, as we observed in Fig. 2.1 a heavy Higgs can be made consistent with EWPD by new oblique physics that gives a positive T parameter, even if the positive contributions of the Higgs to S are not cancelled by an additional negative ΔS. For the neutrino singlets, the sign of T_{eff} is actually positive. This, combined with the improvement in the hadronic width, explains that the fit allows relatively large values of M_H, as can be seen in Table 3.12. In Fig. 3.1 we observe clearly how a non-vanishing mixing of new singlets with electron neutrinos allows for larger values of M_H, thus eliminating the (mild) tension between the global electroweak fit and the direct LEP lower bound on M_H. In particular, if we remove Higgs direct searches from the fit, which forces M_H to ~ 116 GeV, we find that for N_e the preferred value for the Higgs mass is 118 GeV, above

[7] We take M_Z as the reference mass from which we define T.

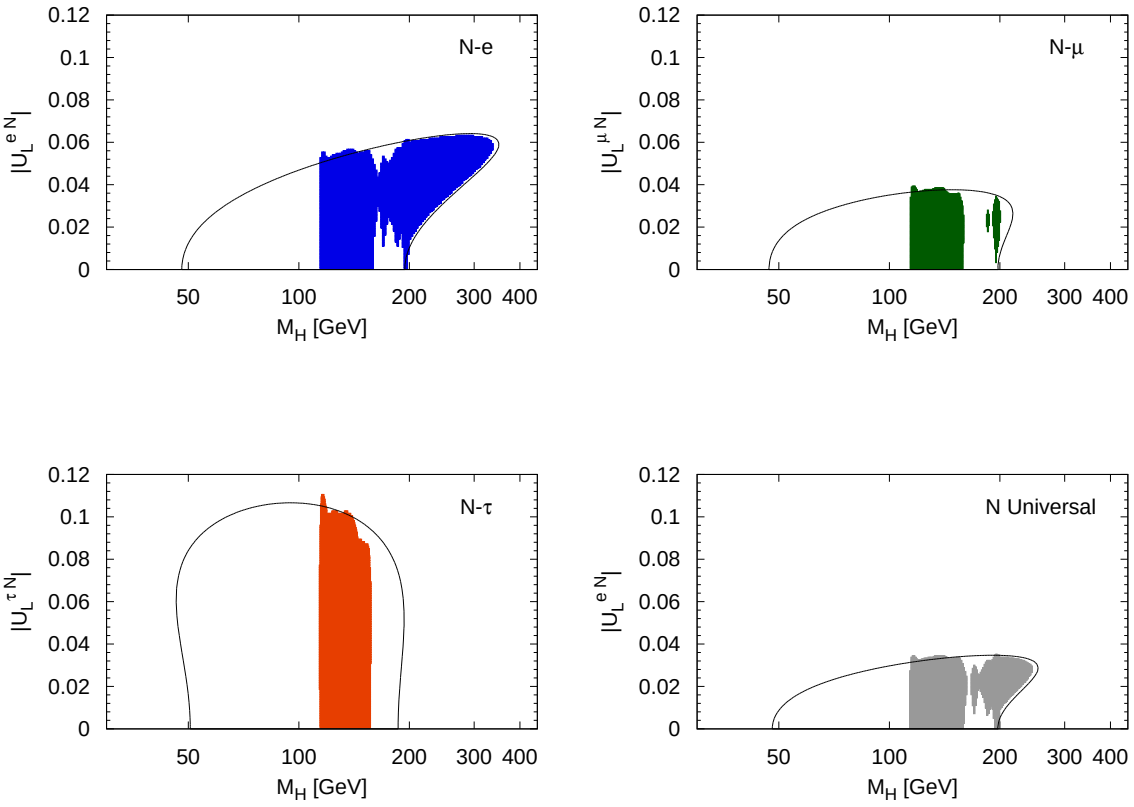

Figure 3.1: 95% confidence region in the $\left|U_L^{eN}\right| - M_H$ parameter space for the N singlet coupled to the first, second and third family (blue, green and orange solid regions, respectively). The last plot corresponds to the universal case (gray solid region). In all cases the corresponding 95% confidence region excluding Higgs direct searches from the fit is delimited by the solid line.

the direct limit and compatible with the event excess observed by LEP 2 and Tevatron. From Eq. (3.14) one would expect the same for mixing with muon neutrinos but these are stringently constrained by the good agreement of data with unitarity of the first row of the CKM matrix. This explains the different limits compared to the case of mixing with electron flavor, for which the CKM constraints are much weaker. We must emphasize that Eqs. (3.14) and (3.15) do not extend to all observables and, in particular, to M_W. Indeed, unlike the shift in G_F, a genuine T parameter from new oblique physics would give additional direct contributions to M_W (for fixed M_Z). These are not included in our T_{eff}, and in general cannot be generated by any kind of new leptons at tree level. A heavy Higgs gives the complete T-like contributions (in addition to S-like and suppressed U-like contributions). Therefore, singlet mixing can only cancel a part of the T-like Higgs effects. This prevents the Higgs from being too heavy, and the lepton mixings from being too large.

Let us also note that the net contribution of the new singlets to neutrino–nucleon deep inelastic

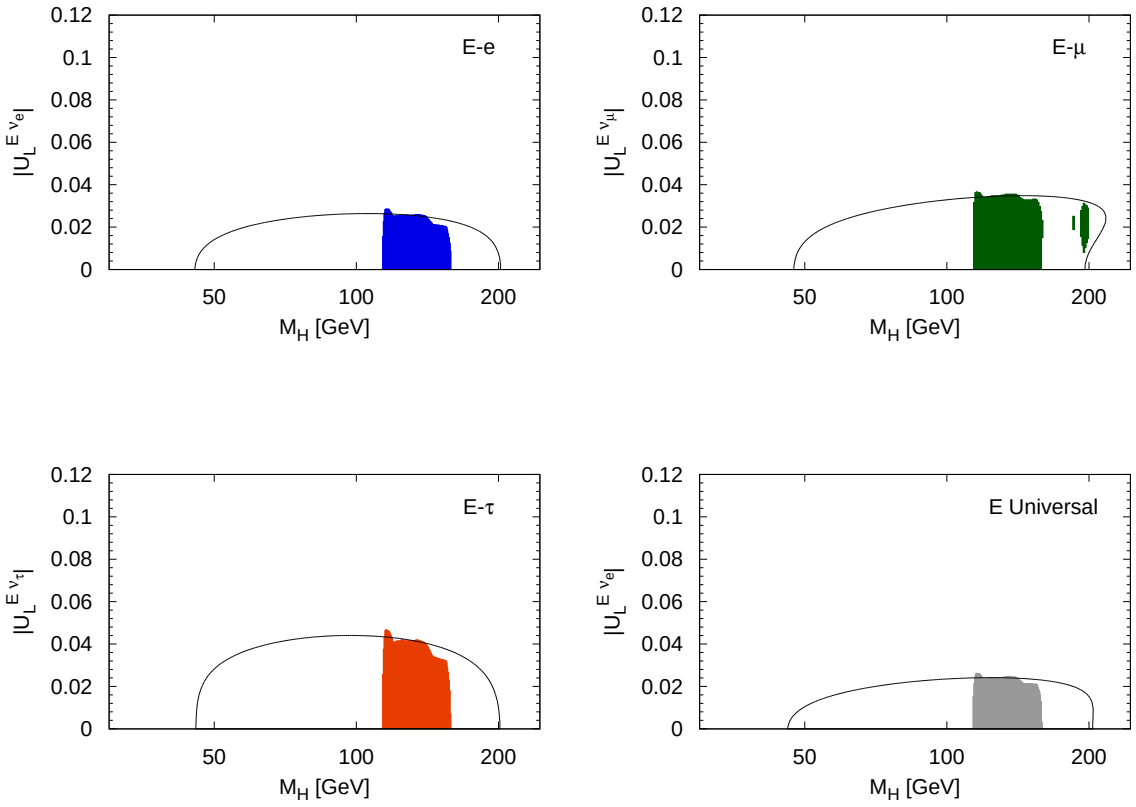

Figure 3.2: 95% confidence region in the $\left|U_L^{E\nu}\right| - M_H$ parameter space for the E singlet coupled to the first, second and third family (blue, green and orange solid regions, respectively). The last plot corresponds to the universal case (gray solid region). In all cases the corresponding 95% confidence region excluding Higgs direct searches from the fit is delimited by the solid line.

scattering is suppressed, due to an approximate cancellation between their indirect and direct effecs. Therefore, the dominant effect is the oblique Higgs boson contribution, which is negative when M_H is increased with respect to the reference value[8]. This would explain the NuTeV discrepancy if the Higgs were allowed to be very heavy. But as we have discussed above, M_W prefers a light Higgs, and in the best fit to all observables there is no improvement in g_L^2.

Our conclusions are not at odds with the one of Loinaz *et al.* in [84][9]. They claim that mixing of light and heavy neutrinos can account for the NuTeV discrepancy and, together with a heavy

[8] Alternatively, the Z-pole observables impose an approximate cancellation between the M_H and $T_{\rm eff}$ contributions. This leaves the negative direct contribution of the new singlets.

[9] As a technical point, let us mention that our formulas for g_L^2 and g_R^2 in neutrino deep inelastic scattering differ from the ones in this reference, because we include the heavy-lepton contributions to the determination of V_{ud} from β decay, just as we did for G_F and muon decay. These contributions reverse the sign of the singlet contributions to g_L, which then play against the improvement of the NuTeV anomaly. However, in both cases the singlet contributions are subleading with respect to the Higgs ones and do not alter the qualitative conclusions.

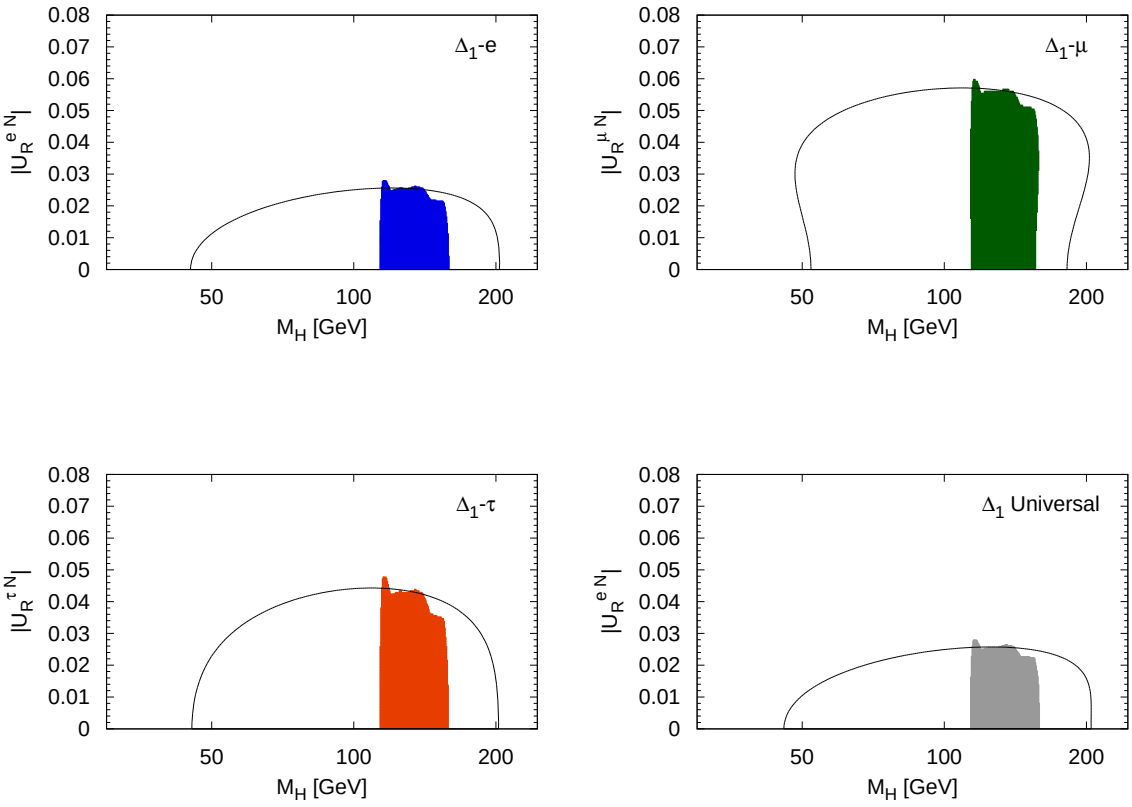

Figure 3.3: 95% confidence region in the $\left|U_R^{eN}\right| - M_H$ parameter space for the Δ_1 doublet coupled to the first, second and third family (blue, green and orange solid regions, respectively). The last plot corresponds to the universal case (gray solid region). In all cases the corresponding 95% confidence region excluding Higgs direct searches from the fit is delimited by the solid line.

Higgs, give an excelent fit *as long as* M_W is not included in the fit or additional new physics supplies a big U parameter. We have preferred, instead, to include M_W in our fits, as this observable is well measured nowadays. Moreover, dimensional and symmetry arguments suggest that, in the absence of fine tuning, U is smaller than T for any new physics coming in at a scale larger than M_W [62, 122]. This is indeed found in known calculable models. So, it seems difficult that any new physics can yield the values $U \gg T$ required in the fit of [84][10]. When M_W is included in the global fit and no *ad hoc* U parameter is introduced to eliminate its influence, the results are not that spectacular. We find that the Higgs cannot be very heavy and that the NuTeV discrepancy is not explained. Nevertheless, as we have discussed, there is an improvement in $\sigma_{\rm had}$ (through the invisible width) and a Higgs heavier than in the SM is allowed.

Finally, let us comment that in general the SM can "adapt" to relatively large values of M_H by

[10]We do not claim that this possibility is logically excluded. The authors of [84] propose the possibility that threshold effects in a strongly coupled sector might give rise to the necessary enhancement of U.

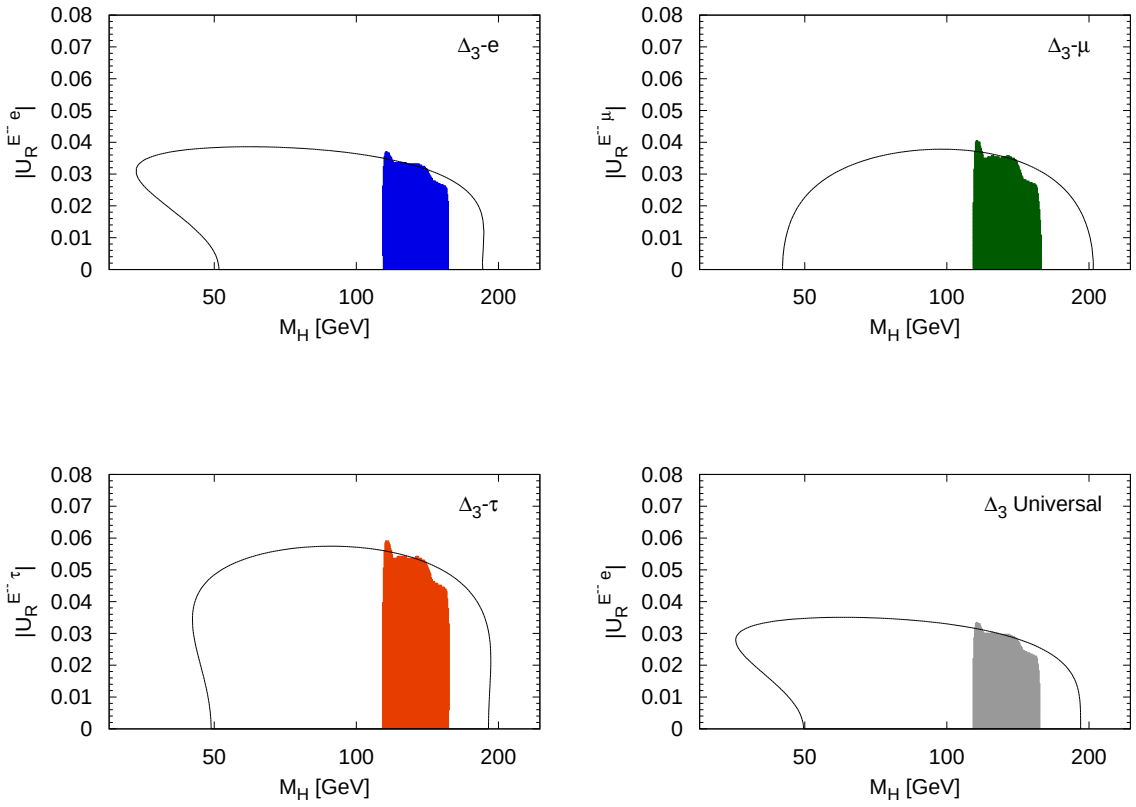

Figure 3.4: 95% confidence region in the $\left|U_R^{E^{--}e}\right| - M_H$ parameter space for the Δ_3 doublet coupled to the first, second and third family (blue, green and orange solid regions, respectively). The last plot corresponds to the universal case (gray solid region). In all cases the corresponding 95% confidence region excluding Higgs direct searches from the fit is delimited by the solid line.

lowering and increasing a bit the values of $\Delta\alpha^{(5)}_{\rm had}$ and m_t, respectively. This is not necessary with extra neutrino singlets coupled to the first family. In this regard, let us note that $g_\mu - 2$ prefers higher values of $\Delta\alpha^{(5)}_{\rm had}$, so that including it in the fits would favour the extension with singlets with respect to the SM [123].

3.4 Conclusions

In this chapter we have provided the dimension-six effective Lagrangian derived from the integration of any vector-like fermion that can give an observable effect at tree-level. This has been used to perform a global fit to existing EWPD for extensions of the SM with new vector-like leptons. The smallness of the mixings we find justifies the validity of the approximation. Our main results are displayed in Tables 3.11 and 3.12, and illustrated in the different plots. In the cases that had been

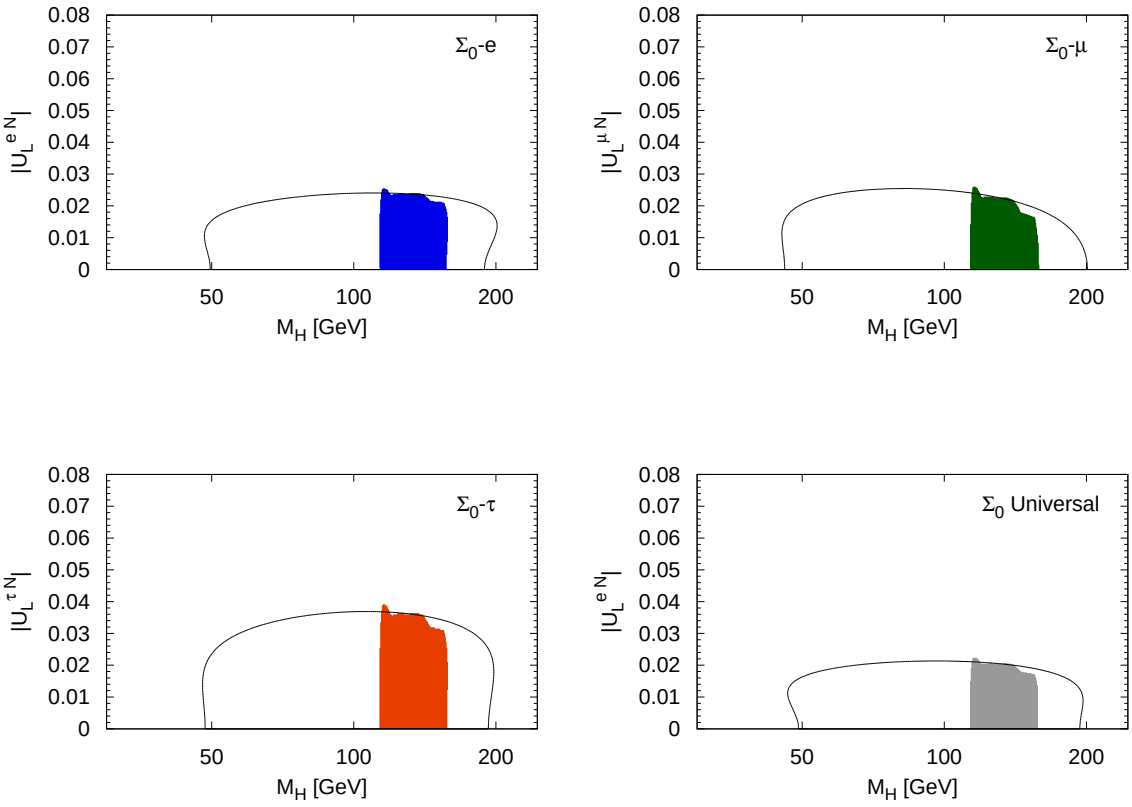

Figure 3.5: 95% confidence region in the $\left|U_L^{eN}\right| - M_H$ parameter space for the Σ_0 triplet coupled to the first, second and third family (blue, green and orange solid regions, respectively). The last plot corresponds to the universal case (gray solid region). In all cases the corresponding 95% confidence region excluding Higgs direct searches from the fit is delimited by the solid line.

analyzed before [98, 99, 100], we find more stringent limits (at the few per cent level). This reflects the better agreement of the SM predictions with the present data.

In Table 3.10, we give the improvements in the χ^2 of the global fit when the SM is supplemented by new leptons. The addition of more than one type of extra lepton multiplet at a time does not improve the quality of the fit. The χ^2/d.o.f. is (slightly) reduced with respect to the one in the SM for $(\Delta_1)_\mu$ only. Even if we do not find any significant improvement of the SM global fit, it is interesting to observe that TeV-scale vector-like leptons with sizable mixings are consistent with EWPD. An interesting feature of the fits is that the presence of extra singlets mixing with the electron neutrino favours higher value of the Higgs mass, which lies in the region allowed by direct searches of the Higgs at LEP. This accounts for part of the mild improvement in the χ^2 in this case, and implies significantly weaker upper bounds on the Higgs mass. In such case, $M_H < 228\,\text{GeV}$ (95% C.L.), with the best-fit value $M_H = 118\,\text{GeV}$ in the region favoured by Higgs direct searches. Conversely, such extra lepton singlets would be favoured with respect to the SM if the Higgs were

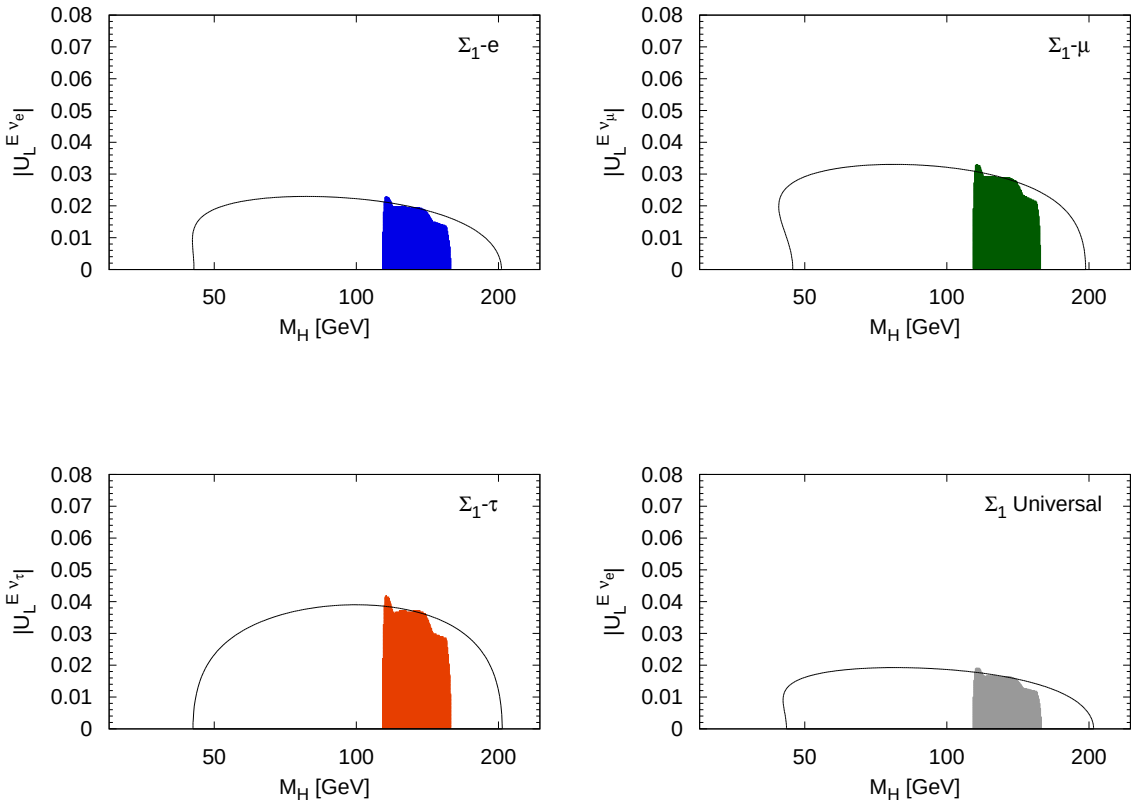

Figure 3.6: 95% confidence region in the $\left|U_L^{E\nu}\right| - M_H$ parameter space for the Σ_1 triplet coupled to the first, second and third family (blue, green and orange solid regions, respectively). The last plot corresponds to the universal case (gray solid region). In all cases the corresponding 95% confidence region excluding Higgs direct searches from the fit is delimited by the solid line.

eventually found to be heavy. We have also seen that an explanation of the NuTeV discrepancy by the mixing of the SM neutrinos with extra neutrinos is precluded, in the absence of additional new physics, by the constraints imposed by other electroweak observables.

In Table 3.11, we collect the 95 % C.L. bounds and the corresponding best values for the mixings between the different possible heavy vector-like leptons and the SM fermions. The mixing with the SM leptons can be as large as $|U_L^{\tau N}| \sim 0.087$ at 95 % C.L. for heavy neutrino singlets mixing only with the third family. Other mixings are bounded to be less than ~ 0.05 at 95 % C.L.. They are independent of the Dirac or Majorana character of the new leptons.

These limits have consequences for heavy lepton production and decay at large colliders. At LHC, they are in general more efficiently produced in pairs [112], except for heavy neutrino singlets, which have to be single produced in association with SM leptons through their mixing, as they have no other SM interactions. In this case the new limits $|U_L^{eN}| < 0.051$ and $|U_L^{\mu N}| < 0.031$ (at 95% C.L.) are better than those found previously, $|U_L^{eN}| < 0.074$ and $|U_L^{\mu N}| < 0.098$ (at 90% C.L.)

[100]. Therefore, the small parameter space accessible to the LHC [111] is further reduced. For instance, heavy Majorana neutrino singlets coupling only to muons may be difficult to observe at LHC even for masses below 200 GeV. This limit can be much higher, however, in the presence of other interactions, up to 2 TeV for new right-handed gauge bosons of a similar mass and with a standard gauge coupling strength [124] (see for a review [4, 7, 125]). Dirac neutrino singlets are expected to be beyond the LHC reach. All other lepton additions can be pair produced, and then their discovery limit does not depend on the mixings, which only enter in the decay rates and are still large enough to allow the heavy leptons decay inside the detector. Hence, their rough discovery limit is near the TeV scale [112]. On the other hand, at $e^+ e^-$ colliders the main production mechanism is through mixing with the first family. For instance, a neutrino singlet mixing with the electron neutrino with $|U_L^{eN}| > 0.01$ is allowed by our bounds and would be observed at ILC for masses $M_N < 400\,\text{GeV}$, and at CLIC for $M_N < 2\,\text{TeV}$ [113]. On the other hand, these stringent limits also makes more difficult the observation of possible deviations from unitarity in neutrino oscillations [126].

Vector-like leptons at the TeV scale appear naturally in many models, for example those with extra dimensions or larger gauge symmetries at low energy. As already emphasized, the new singlets and triplets of zero hypercharge can be Majorana and act as see-saw messengers of type I and III, respectively. If these fields exist with large mixings and relatively light masses, their contributions to neutrino masses and neutrinoless double β decay must be in general suppressed by extra, almost exact symmetries, typically lepton number [2, 107]. Thus, in general new leptons at the TeV scale and with relatively large mixings with the SM fermions must be (quasi)Dirac. If they are Majorana, the model must include a very efficient cancellation mechanism with an extended field content highly tuned [106].

The theory must also incorporate a rather precise alignment of the SM charged leptons and the new mass eigenstate leptons: each heavy lepton must mix mostly with only one light charged lepton to fulfill the limits on FCNC [101, 102, 103, 104]. The corresponding limits are a factor 3 to 60 times more stringent than the flavor conserving ones, derived here. This justifies neglecting FCNC effects in our analysis, but also implies a strong constraint on definite models.

Finally, it is interesting to study how our conclusions would change in the presence of other new particles, which are actually present in many of the models mentioned above. They may contribute constructively in many cases. We have checked, for instance, that the new leptons can further improve the global fit of the extra-quark solution to the A_{FB}^b anomaly proposed in [93]. The effective formalism we used here is particularly convenient to perform fits involving many different kinds of new particles [127].

Chapter 4

New interactions: Extra spin-1 particles

New vector bosons are also a common occurrence in theories beyond the SM. They appear whenever the gauge group of the SM is extended, as the gauge bosons of the extra (broken) symmetries. Thus, they are inherent to GUT [86], including string constructions, or Little Higgs models [88]. As in the case of fermions, they also occur in theories in extra dimensions [89], when the gauge bosons propagate through the bulk [128]. Strongly-interacting theories, such as technicolor [129], often give rise to spin-1 resonances. This can be related to the previous possibilities via hidden gauge symmetry [130] or holography [131, 132].

It is possible to classify vector bosons according to their electric charge: neutral vector bosons, called Z', charge ± 1 vector bosons, called W' and vectors with other integer or fractional charges. On the other hand, the complete theory including the new vectors must be invariant under the full $SU(3)_c \otimes SU(2)_L \otimes U(1)_Y$ gauge group. This imposes additional restrictions on the allowed couplings to the SM fields, and also implies that certain vectors must appear simultaneously and have similar masses. In order to make use of this information in a model-independent approach, we classify in this work the new vectors into irreducible representations of the full SM gauge group, and we impose the corresponding gauge invariance on the Lagrangian. We further restrict the possible couplings by the phenomenological requirement that the effects of the new vectors should be visible at available energies.

As a straightforward example of the implications of the complete SM gauge invariance, as opposed to simple conservation of electric charge, consider the case of a sequential Z' boson, with couplings proportional to the ones of the SM Z boson. Such a neutral vector boson is often included in electroweak fits and direct searches. In fact, this vector has different couplings to the two components of the $SU(2)_L$ doublets, and it cannot be a singlet under the SM group. Nevertheless, it can arise after EWSB as a mixture of a singlet vector and the third component of a vector in the adjoint of $SU(2)_L$. This is the case of models with a replica of the SM gauge group, or in extra dimensions. Thus, gauge invariance implies that the sequential Z' boson necessarily comes together with two charged vectors and another neutral vector, the γ'. All these new fields have similar masses, with splittings of the order of the Higgs vev. Similarly, the results in this chapter imply that a new charged vector boson with sizable couplings to both leptons and quarks must be accompanied by at least one neutral vector, with mass of the same order.

The extra vector bosons that have been most extensively studied are neutral singlets, usually associated to an extra abelian gauge symmetry (see, for instance, the review [133]). Here we

give general model-independent[1] limits on these Z's. We go far beyond this particular case, and study all the representations that could in principle give observable effects. We study the case of universal couplings to all families of quarks and leptons, and also cases with nonuniversal couplings. Furthermore, we consider a few examples with more than one type of vectors, which is the actual situation in most explicit models. We will show that the cooperation of several extra vectors allows, in some cases, to extend the allowed regions in parameter space.

In order to analyze the implications of the new vectors at energies below their mass, we first integrate them out and obtain the corresponding effective theory, including only operators of dimension six. This is useful to isolate the important effects, and also to exhibit more clearly which combinations of parameters are constrained by the data. The accuracy of this approximation is high for masses around the TeV. The effective Lagrangian is also helpful to study the interplay of the extra vector bosons with other new particles of different spin, but we will not perform that sort of analysis here.

It is well known that Z' bosons contribute with a positive sign to the ρ parameter (or, equivalently, to the Peskin-Takeuchi T parameter), and can be used to improve considerably the SM fit when the Higgs boson is heavy. We will see that the same rôle can be played by a hypercharged triplet. We analyze this effect quantitatively and show that, in extensions with these two kinds of vector bosons, a Higgs heavier than ~ 300 GeV is allowed by EWPD. On the other hand, it turns out that charged singlets give a negative contribution to ρ. This opens the door to cancellations of the different contributions to this parameter.

We classify in the next section the different types of extra vector bosons, and write their interactions with SM fields. In Section 4.2, we integrate the new vectors out, and obtain the coefficients of the dimension-six gauge-invariant operators in the effective Lagrangian. In Section 4.3 we perform fits to EWPD and find the limits on each type of vector boson. In Section 4.4 we discuss the effect on EWPD of including several types of extra vectors simultaneously. We give some phenomenologically interesting examples with nonuniversal couplings, including vector-boson explanations of the observed forward-backward asymmetry of the b quark. Section 4.5 is devoted to an analysis of the implications for the Higgs mass. Finally, we present our conclusions in Section 4.6. For the sake of clarity, given the large number of tables gathering the results of the integration of the extra vectors, we collect them at the end of the chapter in order to avoid disrupting the flow of the discussion.

4.1 General extra vector bosons

We want to study general vector bosons beyond the ones in the SM, with the only restrictions that they be heavier than LEP 2 energies, have perturbative couplings, and be potentially observable by their indirect effects on precision data or as resonances in colliders. The leading effects in EWPD arise from tree-level exchanges of just one heavy vector boson contributing to processes with four fermions in the external legs. This requires interactions that couple SM operators to the extra vector fields and are linear in the latter. Clearly, the interactions should be renormalizable to avoid further suppressions. From the point of view of the low-energy effective theory to be discussed below, these couplings produce dimension-six operators, while interactions with more than one new vector field in the same operator—and nonrenormalizable interactions—give rise to operators of higher scaling dimension. Moreover, vectors with linear interactions can be singly produced, and have the best chances of being observed at colliders.

The requirement of linear renormalizable couplings, together with Lorentz symmetry and invariance under the full SM gauge group, constrain the possible quantum numbers of the new vectors.

[1] We also give limits on some popular models to illustrate how the analyses of particular models fit in our general framework.

Vector	$\mathcal{B}_\mu$	$\mathcal{B}^1_\mu$	$\mathcal{W}_\mu$	$\mathcal{W}^1_\mu$	$\mathcal{G}_\mu$	$\mathcal{G}^1_\mu$	$\mathcal{H}_\mu$	$\mathcal{L}_\mu$
Irrep	$(1,1)_0$	$(1,1)_1$	$(1,\mathrm{Adj})_0$	$(1,\mathrm{Adj})_1$	$(\mathrm{Adj},1)_0$	$(\mathrm{Adj},1)_1$	$(\mathrm{Adj},\mathrm{Adj})_0$	$(1,2)_{-\frac{3}{2}}$

Vector	$\mathcal{U}^2_\mu$	$\mathcal{U}^5_\mu$	$\mathcal{Q}^1_\mu$	$\mathcal{Q}^5_\mu$	$\mathcal{X}_\mu$	$\mathcal{Y}^1_\mu$	$\mathcal{Y}^5_\mu$
Irrep	$(3,1)_{\frac{2}{3}}$	$(3,1)_{\frac{5}{3}}$	$(3,2)_{\frac{1}{6}}$	$(3,2)_{-\frac{5}{6}}$	$(3,\mathrm{Adj})_{\frac{2}{3}}$	$(\bar{6},2)_{\frac{1}{6}}$	$(\bar{6},2)_{-\frac{5}{6}}$

Table 4.1: Vector bosons contributing to the dimension-six effective Lagrangian.

In Table 4.1, we give the quantum numbers for the 15 irreducible representations of vector fields that can have linear and renormalizable interactions. This table also introduces our notation for each class of vector boson, which is partly inspired by the usual notation for SM fields. Note that the representations with nonvanishing hypercharge are complex.

For our purposes, it is not important whether the new vector bosons are the gauge bosons of a broken extended gauge group or not. Nevertheless, it is interesting to note that all the types of vector bosons in Table 4.1 can in principle be obtained as the gauge bosons of an extended gauge group broken down to the SM. We give explicit examples of the corresponding symmetry breaking patterns in Table 4.2. Models with bigger gauge groups usually incorporate new fermions, which in particular are necessary to cancel anomalies. Here, we will assume that these exotic fermions, if they exist at all, do not contribute to EWPD. At any rate, in our general low-energy formulation, we only impose the SM gauge invariance, and the absence of anomalies does not impose any restriction on the couplings of the new vectors to the SM fermions. As indicated in Table 4.2, some of these vector bosons—an infinite number of each type, actually—also appear in extra-dimensional theories when the gauge bosons of the corresponding SM group factor propagate in the bulk. In fact, the pattern of symmetry breaking in these cases is essentially a generalization of the one shown in the table, as can be best understood by dimensional deconstruction [135]. Other kinds of vectors can also appear in this context as well, when the higher-dimensional gauge group is bigger. We should also point out that the representations $\mathcal{U}^{2,5}$, $\mathcal{Q}^{1,5}$ and $\mathcal{X}$ correspond to the vector leptoquarks classified by Buchmüller, Rückl and Wyler in [136].

Once the field content of the theory has been established, we proceed to construct the most general renormalizable theory invariant under $SU(3)_c \otimes SU(2)_L \otimes U(1)_Y$. The Lagrangian has the form

$$\mathcal{L} = \mathcal{L}_{\mathrm{SM}} + \mathcal{L}_V + \mathcal{L}_{V-\mathrm{SM}} + \text{ nonlinear}, \tag{4.1}$$

where $\mathcal{L}_{\mathrm{SM}}$ is the SM Lagrangian, $\mathcal{L}_V$ contains the quadratic terms for the heavy vector bosons (with kinetic terms covariantized with respect to the SM group) and $\mathcal{L}_{V-\mathrm{SM}}$ contains the possible interaction or kinetic terms formed as products of SM fields and a single vector field. Mass mixing terms of SM and new vectors are forbidden by gauge invariance[2]. "Nonlinear" in Eq. (4.1) refers to interaction terms that are nonlinear in the heavy vector fields. As we have argued above, those terms can be safely neglected.

Before writing the different pieces in Eq. (4.1), let us introduce some notation. The gauge bosons of the SM are generically called A, i.e $A = B, W, G$. The new vectors are represented by the specific symbols in Table 4.1 or generically by V. The calligraphic letter $\mathcal{A}$ denotes any of the three extra vectors in the same representation as the SM gauge bosons, namely $\mathcal{B}$, $\mathcal{W}$ and $\mathcal{G}$. Covariant derivatives are always covariant with respect to the SM gauge group, and are defined

[2]There are, nevertheless, interactions with the Higgs doublet that give rise to mass mixing of the Z and W bosons with the new vectors when the electroweak symmetry is broken. This effect is in fact crucial for Z-pole observables.

Vector	Model
$\mathcal{B}_\mu$	$U(1)'$, Extra Dimensions
$\mathcal{B}^1_\mu$	$SU(2)_R \otimes U(1)_X \to U(1)_Y$
$\mathcal{W}_\mu$	$SU(2)_1 \otimes SU(2)_2 \to SU(2)_D \equiv SU(2)_L$, Extra Dimensions
$\mathcal{W}^1_\mu$	$SU(4) \to U(1) \otimes (SU(3) \to SU(2))$
$\mathcal{G}_\mu$	$SU(3)_1 \otimes SU(3)_2 \to SU(3)_D \equiv SU(3)_c$, Extra Dimensions
$\mathcal{G}^1_\mu$	$SO(12) \to (SO(8) \to SU(3)) \otimes (SU(2) \otimes SU(2) \to SU(2)_D \to U(1)_Y)$
$\mathcal{H}_\mu$	$SU(6) \to SU(3) \otimes SU(2)$
$\mathcal{L}_\mu$	$G_2 \to SU(2) \otimes (SU(2) \to U(1)_Y)$
$\mathcal{U}^2_\mu,\ \mathcal{U}^5_\mu$	$SU(4) \to SU(3) \otimes U(1)$
$\mathcal{Q}^1_\mu,\ \mathcal{Q}^5_\mu$	$SU(5) \to SU(3)_c \otimes SU(2)_L \otimes U(1)_Y$
$\mathcal{X}_\mu$	$SU(6) \to U(1) \otimes SU(3) \otimes (SU(3) \to SU(2))$
$\mathcal{Y}^1_\mu,\ \mathcal{Y}^5_\mu$	$F_4 \to SU(3) \otimes (SU(3) \to SU(2) \otimes U(1))$

Table 4.2: Examples of symmetry breaking patterns giving rise to each type of vectors bosons in Table 4.1 [134]. Generating the right Weinberg angle and accommodating the matter fields requires, in some cases, an extension of the gauge groups in this table and a more involved pattern of symmetry breaking.

as in Eq. (1.1). We use matrix notation to write the singlet product of two objects in a given representation and its complex conjugate: in the product $A^\dagger B$, $A^\dagger$ and B are row and column vectors, respectively, made out of the components of $A^\dagger$ and B in some orthonormal basis of the vector space for their representation. Finally, $[.]_R$ denotes a projection into the irreducible representation R. When we give the currents coupled to each of the vector bosons we shall be more explicit and use color and isospin indices.

The SM part of the Lagrangian can be read from Eq. (1.7). We have assumed a minimal Higgs sector, as we are not considering extra scalars here[3].

The quadratic terms for the new vector bosons are given by[4]

$$\mathcal{L}_V = -\sum_V \eta_V \left(\frac{1}{2} D_\mu V^\dagger_\nu D^\mu V^\nu - \frac{1}{2} D_\mu V^\dagger_\nu D^\nu V^\mu + \frac{1}{2} M_V^2 V^\dagger_\mu V^\mu \right), \tag{4.2}$$

The sum is over all new vectors V, which can be classified into the different irreducible representations of Table 4.1. We set $\eta_V = 1$ (2) when V is in a real (complex) representation, in order to use the usual normalization. Even though the kinetic terms of the extra vectors incorporate SM covariant derivatives to keep manifest gauge invariance, the corresponding interactions among SM gauge bosons and two new vectors could be moved to the "nonlinear" terms of Eq. (4.1). On

[3] Only the vev of the scalar is relevant for the new couplings that enter precision tests. Therefore, all our equations but Eq. (1.7) are valid for a completely general symmetry breaking sector. However, we have used the assumption of a single elementary scalar doublet in the SM loop corrections that enter our fits.

[4] Note that the most general kinetic term is $D_\mu V^\dagger_\nu D^\mu V^\nu + \beta D_\mu V^\dagger_\nu D^\nu V^\mu$, with β an arbitrary parameter. However, in this chapter we restrict ourselves to spin-1 degrees of freedom. Then we must take $\beta = -1$, for otherwise $\partial_\mu V^\mu$ would propagate as an independent scalar field.

the other hand, we have written explicit mass terms for the new vectors. The masses can arise, in particular, from vacuum expectation values of extra scalar fields, but this is not necessary. In writing Eq. (4.2), we have chosen a basis with diagonal, canonically normalized kinetic terms and diagonal masses. Mass terms often appear in nondiagonal form in explicit models. In these cases, it is necessary to diagonalize them before using our formulas. Finally, the couplings of the new vectors to the SM are given by

$$\mathcal{L}_{V-\mathrm{SM}} = -\sum_V \frac{\eta_V}{2}\left(V^{\mu\dagger} J_\mu^V + \mathrm{h.c.}\right). \tag{4.3}$$

The vector currents J_μ^V have the form

$$J_\mu^V = \sum_k g_V^k j_\mu^{Vk}, \tag{4.4}$$

where $g_V^k$is a coupling constant and j_μ^{Vk} is a vector operator of scaling dimension 3 in the same representation as V. Actually, the different currents that can be built with the SM fields determine the possible representations of the extra vectors. We can distinguish three kinds of SM currents:

- *With two fermions*. Schematically, $j_\mu^{V\psi_1\psi_2} = [\overline{\psi_1} \otimes \gamma_\mu \psi_2]_{R_V}$, with ψ_1, ψ_2 (different in principle) fermion multiplets, R_V the representation of V and $\otimes$ a product of representations.

- *With two scalars and a covariant derivative*: $j_\mu^{V\phi} = [\Phi^\dagger \otimes D_\mu \phi]_{R_V}$, where Φ denotes either ϕ or $\tilde{\phi}$.

- *With a gauge boson and two covariant derivatives*: $j_\mu^{\mathcal{A}} = D^\nu A_{\nu\mu}$.

The couplings to currents of the third type induce a kinetic mixing of the SM gauge bosons A with the heavy vectors $\mathcal{A}$ [137]. It turns out that the corresponding terms in $\mathcal{L}_{\mathrm{V-SM}}$ are redundant. In the case of only one extra vector multiplet, they can be eliminated by the field redefinition

$$\begin{aligned} A_\mu &\to A_\mu + g_{\mathcal{A}}^A \mathcal{A}_\mu, \\ \mathcal{A}_\mu &\to \left(1 + g_{\mathcal{A}}^{A\ 2}\right)^{-\frac{1}{2}} \mathcal{A}_\mu. \end{aligned} \tag{4.5}$$

This redefines the mass $M_{\mathcal{A}}$ and currents $J^{\mathcal{A}}$ in the following way:

$$\begin{aligned} M_{\mathcal{A}} &\to \left(1 + g_{\mathcal{A}}^{A\ 2}\right)^{-\frac{1}{2}} M_{\mathcal{A}}, \\ J_\mu^{\mathcal{A}} &\to \left(1 + g_{\mathcal{A}}^{A\ 2}\right)^{-\frac{1}{2}} \left(J_\mu^{\mathcal{A}} + g_{\mathcal{A}}^A J_\mu^A\right). \end{aligned} \tag{4.6}$$

In addition, new "nonlinear" terms are generated. In the following we shall work in the basis without kinetic A-$\mathcal{A}$ mixing (hence, with redefined couplings). This is a consistent choice that simplifies a lot many of the expressions below. At any rate, when kinetic mixing with just one extra vector is found in any particular model, it is possible to use our formulas as they stand, and simply perform the substitution in Eq. (4.6) (or Eq. (4.16) in Section 4.7) at the end.

The explicit expression of all the possible currents are given in the tables at the end of the chapter.

4.2 Effective description of new vector bosons

The theory in Eq. (4.1) belongs to a decoupling scenario, in which the conditions for the Appelquist-Carazone theorem are satisfied [48], so we can use the effective Lagrangian expansion in Eq. (1.23). In this section, we integrate out the new heavy vectors in Table 4.1 and obtain an effective Lagrangian at leading order, which can be used at energies smaller than the masses of the extra vectors. Starting with the theory Eq. (4.1), we will write the result in the operator basis introduced in Chapter 1, and obtain the contribution to the coefficients of each operator from the new vector bosons. These coefficients will depend on the masses M_V and the couplings g_V^k.

At the classical level, the integration can be carried out by computing the tree-level Feynman diagrams in Fig. 4.1 and matching to the corresponding amplitudes in the effective theory. Equivalently, we can solve the classical equations of motion for the heavy vectors and substitute

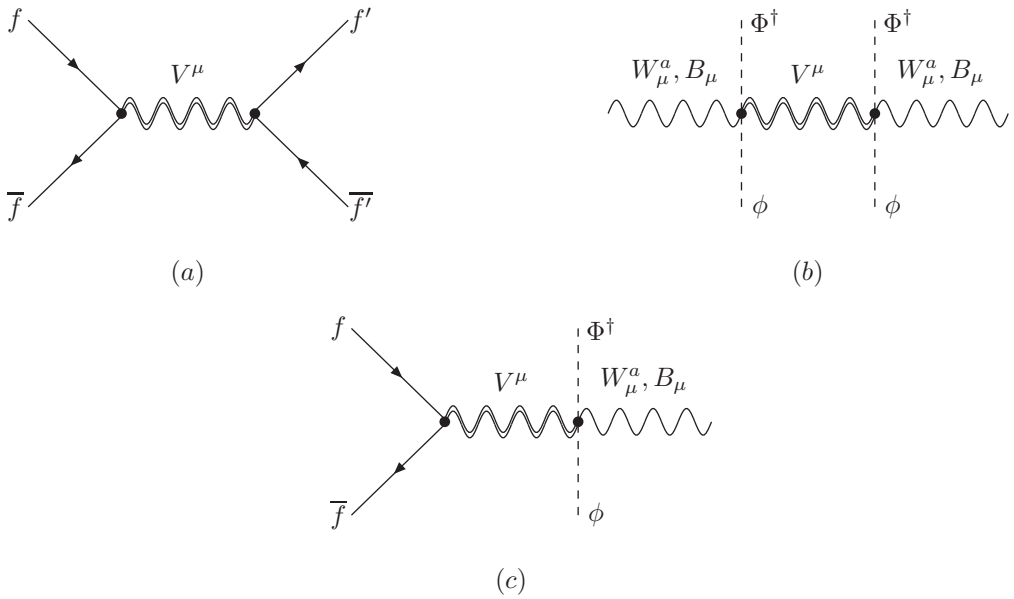

Figure 4.1: Feynman diagrams relevant for the dimension-six effective Lagrangian.

the solutions into the Lagrangian. Proceeding in this algebraic manner, we readily find from $\mathcal{L}_V + \mathcal{L}_{V-\mathrm{SM}}$ the on-shell vector fields

$$V_\mu = \frac{1}{p^2 - M_V^2}\left[\frac{p_\mu p_\nu}{M_V^2} - \eta_{\mu\nu}\right]\left(J^{V\,\nu} + O(V^\nu)\right). \tag{4.7}$$

The $O(V_\mu)$ terms arise from the "nonlinear" terms in $\mathcal{L}_{V-\mathrm{SM}}$. The next step is to expand this equation in powers of p^2/M_V^2 and solve for V_μ. At the leading order we simply have

$$V_\mu = \frac{1}{M_V^2} J_\mu^V + O\left(\frac{1}{M_V^4}\right), \tag{4.8}$$

where the order $1/M_V^4$ terms follow from both the $O(V_\mu)$ terms in (4.7) and the higher-order terms in the inverse propagator expansion. Then, we substitute Eq. (4.8) into the Lagrangian $\mathcal{L}$ and find

$$\mathcal{L}_{\mathrm{eff}} = \mathcal{L}_{\mathrm{SM}} - \frac{\eta_V}{2M_V^2}\,(J_\mu^V)^\dagger J^{V\,\mu} + O\left(\frac{1}{M_V^4}\right) \tag{4.9}$$

The terms of order $1/M_V^4$ contribute to operators of dimension eight and higher, and will be neglected in the following. In particular, we see that, as promised, the "nonlinear" terms in $\mathcal{L}_{V-\mathrm{SM}}$ do not contribute to the effective Lagrangian up to dimension six, and can be ignored. The result Eq. (4.9) includes a few operators that are not in the basis introduced in Table 1.1. In order to compare with previous work, it is convenient to express the result in our basis, performing some Fierz reorderings and field redefinitions (equivalent to the use of the SM EOM on the dimension-six operators). The final result can then be written as

$$\mathcal{L}_6^V = -\frac{\eta_V}{2M_V^2}\,(J_\mu^V)^\dagger J^{V\,\mu} = \sum_i \frac{\alpha_i}{M_V^2}\mathcal{O}_i, \tag{4.10}$$

where $\mathcal{O}_i$ are the operators collected in Table 1.1, and α_i their dimensionless numerical coefficients. It is clear from the general expression Eq. (4.9), and also from the Feynman diagrams in Fig. 4.1, that the terms in the effective Lagrangian can be of three basic forms:

1. *Four fermions*: $\frac{g_V^{\psi_1\psi_2} g_V^{\psi_3\psi_4}}{M_V^2}[\overline{\psi_1}\otimes\gamma_\mu\psi_2]_{R_V}[\overline{\psi_3}\otimes\gamma^\mu\psi_4]_{R_V}$.

2. *Oblique*: $\frac{g_V^\phi g_V^\phi}{M_V^2}[\Phi^\dagger\otimes D_\mu\phi]_{R_V}[D^\mu\phi^\dagger\otimes\Phi]_{R_V}$.

3. *Scalars, vectors and fermions*: $\frac{g_V^\phi g_V^{\psi_1\psi_2}}{M_V^2}[\Phi^\dagger\otimes D^\mu\phi]_{R_V}[\overline{\psi_1}\otimes\gamma_\mu\psi_2]_{R_V}$.

In addition there are operators that arise from the field redefinitions, which just redefine the fermion masses and Yukawa interactions, and the Higgs potential. The four-fermion terms are relevant for LEP 2 and low-energy observables. Upon EWSB, the oblique terms modify the gauge boson propagators[5] and those of the third type change the fermion-gauge trilinear couplings. Hence, the last two kinds of operators contribute mainly to observables at the Z pole (and the W mass, for the oblique operators). On the other hand, note that the coefficients of all the operators are given by the sum of the contributions of the different vector bosons, and the contribution of each vector is the product of two of its couplings divided by its mass squared.

As already mentioned, the explicit result of the integration of the new vector bosons is given in Tables 4.7 to 4.21 at the end of the chapter. There we collect the contributions of each kind of extra vector boson to the coefficients α_i of the dimension-six operators $\mathcal{O}_i$.

4.3 Limits on new vector bosons

We can now use the effective Lagrangian to perform fits to EWPD, and extract limits on the new vector bosons in Table 4.1. To start with, we assume that only one new vector gives sizable contributions. We will see in Section 4.4 that such "one-at-a-time" analysis is often justified (but not always).

The observables that enter the fits and the details of our fitting procedure are described in Appendix A [6]. In particular, LEP 2 cross sections and asymmetries are important to lift some flat directions that would remain in the fits to the other observables. In Table 4.3, we summarize

[5] The only observable oblique operator in our approximation is $\mathcal{O}_\phi^{(3)}$. Removing the kinetic mixing between SM and new vectors, as discussed in the previous section, prevents the operator $\mathcal{O}_{WB}$, related to the Peskin-Takeuchi S parameter [62], from being generated at tree level. The same formulas would follow had we left the kinetic mixing terms and performed a perturbative field redefinition in the effective Lagrangian to eliminate $\mathcal{O}_{WB}$.

[6] In general, in the fits in this chapter we keep M_H, m_t and $\alpha_s(M_Z^2)$ as floating parameters, while for simplicity M_Z and $\Delta\alpha^{(5)}_{\mathrm{had}}(M_Z^2)$ are kept fixed at their SM best-fit values.

Vector	Z pole $e^+e^- \to \bar{f}f$	M_W	CKM	ν-N DIS	NC $\nu e \to \nu e$	APV	PV in $e^-e^- \to e^-e^-$	LEP 2 $e^+e^- \to \bar{f}f$
$\mathcal{B}_\mu$	✓	✓	✓	✓	✓	✓	✓	✓
$\mathcal{W}_\mu$	✓	✓	✓	✓	✓	✓	✓	✓
$\mathcal{G}_\mu$								
$\mathcal{H}_\mu$								
$\mathcal{B}^1_\mu$	✓	✓	✓	✓	✓	✓	✓	✓
$\mathcal{W}^1_\mu$	✓	✓		✓	✓	✓	✓	✓
$\mathcal{G}^1_\mu$								
$\mathcal{L}_\mu$					✓			✓
$\mathcal{U}^2_\mu$			✓	✓		✓		✓
$\mathcal{U}^5_\mu$						✓		✓
$\mathcal{Q}^1_\mu$				✓		✓		✓
$\mathcal{Q}^5_\mu$				✓		✓		✓
$\mathcal{X}_\mu$			✓	✓		✓		✓
$\mathcal{Y}^1_\mu$								
$\mathcal{Y}^5_\mu$								

Table 4.3: Experimental data constraining (directly or indirectly) the couplings of the vector bosons.

which sets of data can constrain each kind of vector boson. We see that five types of vectors, $\mathcal{G}$, $\mathcal{H}$, $\mathcal{G}^1$, $\mathcal{Y}^1$ and $\mathcal{Y}^5$, are invisible to all the precision observables, as they couple to quarks only. These vectors could in principle be produced at hadron colliders, and the non-observation of the corresponding resonances at Tevatron places limits on their masses. In the following we focus on EWPD, so we restrict our attention to the cases that can modify these data.

All parameters are assumed to be real, as is the case in known models. On the other hand, for general coupling matrices, FCNC are induced (except for $\mathcal{W}^1$, which does not couple to fermions). These give, generally, bounds much stronger than the ones derived from EWPD. Avoiding these bounds requires fine tuning, or some mechanism that imposes a certain structure on the coupling matrices.

The hypothesis of diagonal and universal couplings is sufficient to avoid all FCNC for the vector fields that connect each fermion multiplet with its adjoint, i.e. $\mathcal{B}$ and $\mathcal{W}$. For the other types of vectors with couplings to fermions, universality does not guarantee the absence of FCNC. Another possibility is that the new vectors couple to just one family of fermions, in the fermion basis with maximally diagonal Yukawas (before electroweak breaking). In this case, there are still FCNC if the vector leptoquarks couple to LH quarks (in the up sector, for our choice of q_L basis), but they are suppressed by CKM off-diagonal entries. In particular, the FCNC are under control if the vectors couple to the third family of quarks only, as in the examples of Section 4.4.1. This particular structure of couplings is fine-tuned, since it breaks the $U(3)^5$ flavor symmetry of the SM, which allowed us to choose freely the fermion basis. Nevertheless, it can be explained by some mechanism in the complete theory. For instance, warped extra dimensions with bulk fermions incorporate a GIM-like mechanism in a natural manner [138].

In the fits of this section, we assume diagonal, universal couplings for $\mathcal{B}$, $\mathcal{W}$ and $\mathcal{B}^1$. For the representations in which this flavor structure would generate dangerous FCNC, we assume

couplings to just one family, as explained above, and explore all possibilities. The basic results are given in Table 4.4. The fits depend on the quadratic products of the different ratios $G_V^k \equiv g_V^k/M_V$. Therefore, relative signs among the different couplings are relevant, but the results are invariant under a global change of sign. The limits[7] on the parameters in Table 4.4, unlike the best values, do not depend on the signs of these ratios, as the other parameters are integrated. In the rest of this section, we discuss these results and give additional details. Nonuniversal couplings for $\mathcal{B}$, $\mathcal{B}^1$ and $\mathcal{W}$ are studied in Section 4.4.1.

4.3.1 Neutral singlet $\mathcal{B}$

Extra neutral vector bosons, known as Z' bosons, have been extensively studied in the past (see [133] for a review). In our gauge-invariant formalism, the only way neutral vectors can arise alone, without charged partners, is from the SM vector singlets $\mathcal{B}$. EWSB can then mix these fields with the SM Z boson, with a mixing angle proportional to the coupling of the $\mathcal{B}$ to the Higgs doublet. We reserve the name Z' to denote the corresponding heavy mass eigenstates. The physical Z' mass and the Z-Z' mixing, $\sin\theta_{ZZ'}$, are related to the mass parameter $M_{\mathcal{B}}$ and the Higgs coupling $g_{\mathcal{B}}^{\phi}$ by

$$M_{Z'}^2 \approx M_{\mathcal{B}}^2 \left[1 + (g_{\mathcal{B}}^{\phi})^2 \frac{v^2}{M_{\mathcal{B}}^2}\right] \quad \text{and} \quad \sin\theta_{ZZ'} \approx \frac{g_{\mathcal{B}}^{\phi}\sqrt{g^2+g'^2}}{2}\frac{v^2}{M_{\mathcal{B}}^2}, \tag{4.11}$$

where we are assuming $M_{\mathcal{B}} \gg gv, g_{\mathcal{B}}^{\phi}v$. These singlets appear in many extensions of the SM. They are usually associated with an extra abelian factor in the gauge group, which is broken down at a scale higher than electroweak (but hopefully small enough to allow for their eventual observation). This is the case of GUT/string and Little Higgs models, when the rank of the gauge group is higher than 4, and of theories with gauge fields in extra dimensions.

In our model-independent analysis, with the assumption of universality, the $\mathcal{B}$ scenario has six new free parameters: the couplings to each matter multiplet divided by the mass of the $\mathcal{B}$. The result of the fit, displayed in Table 4.4, can be understood as follows. First, the W mass and the Z-pole data constrain the Higgs coupling to be small. The direct Tevatron Higgs limits also contribute in the same direction, as discussed in Section 4.5.

Second, the low-energy data and the measurements of cross sections and asymmetries at LEP 2 impose significant constraints on the leptonic couplings, mostly independent of the Higgs coupling. This effect is apparent in Figs. 4.2 and 4.3, where for simplity we consider hadrophobic vectors. We display several confidence regions for fits with and without LEP 2 data, in planes parametrized by different couplings. In the left-hand plot of Fig. 4.2, we see that the regions with relatively large couplings along the diagonals, with equal absolute value of LH and RH couplings, are allowed by EWPD without LEP 2 data. In particular, this nonchiral combination avoids the constraints from parity violation in Møller scattering. However, the right-hand plot in this figure shows that these regions get excluded when the LEP 2 data are taken into account. In Fig. 4.3, we see how the LEP 2 data help in constraining the lepton couplings, but not the couplings to the Higgs. As a matter of fact, a small nonvanishing Higgs coupling is favored by LEP 2 data, as a modification of trilinear couplings of the Z boson can soften a bit the effect of four-fermion operators. Anyway, this effect is erased by Z-pole data.

Finally, for very small Higgs and lepton couplings, the fit is approximately flat along the directions of the quark couplings, due to the fact that no electroweak observable depends on their square. This implies the absence of limits on quark couplings in Table 4.4.

[7] Our 95% confidence limits are defined by requiring a change of 3.84 in χ^2 with respect to the minimal value.

Vector V_μ	$-\Delta\chi^2_{\rm min}$ ($\chi^2_{\rm min}$/d.o.f)	Parameter $G_V^k \equiv g_V^k/M_V$	Best Fit [TeV^{-1}]	Bounds [TeV^{-1}]	C.L.
$\mathcal{B}_\mu$	7.35 (0.77)	$G^\phi_{\mathcal{B}}$	-0.045	$[-0.098,\ 0.098]$	95%
		$G^l_{\mathcal{B}}$	0.021	$[-0.210,\ 0.210]$	95%
		$G^q_{\mathcal{B}}$	-0.89	-	-
		$G^e_{\mathcal{B}}$	0.048	$[-0.300,\ 0.300]$	95%
		$G^u_{\mathcal{B}}$	-2.6	-	-
		$G^d_{\mathcal{B}}$	-6.0	-	-
$\mathcal{W}_\mu$	1.51 (0.79)	$G^\phi_{\mathcal{W}}$	0.002	$[-0.12,\ 0.12]$	$1\ \sigma$
		$G^l_{\mathcal{W}}$	0.004	$[-0.26,\ 0.26]$	95%
		$G^q_{\mathcal{W}}$	-9.6	-	-
$\mathcal{B}^1_\mu$	0.16 (0.79)	$G^\phi_{\mathcal{B}^1}$	$6\cdot10^{-4}$	$[-0.11,\ 0.11]$	95%
		$G^{du}_{\mathcal{B}^1}$	6.6	-	-
$\mathcal{W}^1_\mu$	0.65 (0.78)	$\lvert G^\phi_{\mathcal{W}^1}\rvert$	0.18	< 0.50	95%
$\mathcal{L}_\mu$	0 (0.79)	$\lvert G^{el}_{\mathcal{L}}\rvert$	0	$< \begin{pmatrix} 0.29 & 0.33 & 0.39 \\ 0.34 & - & - \\ 0.39 & - & - \end{pmatrix}$	95%
$\mathcal{U}^2_\mu$	0 (0.79)	$\lvert G^{ed}_{\mathcal{U}^2}\rvert$	0	$< \begin{pmatrix} 0.21 & 0.49 & 0.49 \\ - & - & - \\ - & - & - \end{pmatrix}$	95%
		$\lvert G^{lq}_{\mathcal{U}^2}\rvert$	0	$< \begin{pmatrix} 0.12 & 0.29 & 0.29 \\ 0.56 & 0.65 & - \\ - & - & - \end{pmatrix}$	95%
$\mathcal{U}^5_\mu$	≤ 2.77 (0.77)	$\lvert G^{eu}_{\mathcal{U}^5}\rvert$	0.43 [1, 2]	$< \begin{pmatrix} 0.25 & 0.62 & - \\ - & - & - \\ - & - & - \end{pmatrix}$	95%
$\mathcal{Q}^1_\mu$	≤ 0.45 (0.79)	$\lvert G^{ul}_{\mathcal{Q}^1}\rvert$	0.27 [1, 2]	$< \begin{pmatrix} 0.22 & 0.54 & - \\ 0.57 & - & - \\ - & - & - \end{pmatrix}$	95%
$\mathcal{Q}^5_\mu$	≤ 3.36 (0.78)	$\lvert G^{dl}_{\mathcal{Q}^5}\rvert$	0.87 [1, 1]	$< \begin{pmatrix} 1.06 & 0.58 & - \\ 1.07 & - & - \\ 1.07 & - & - \end{pmatrix}$	95%
		$\lvert G^{eq}_{\mathcal{Q}^5}\rvert$	0.64 [1, 1]	$< \begin{pmatrix} 0.78 & 1.0 & 1.2 \\ - & - & - \\ - & - & - \end{pmatrix}$	95%
$\mathcal{X}_\mu$	≤ 2.86 (0.77)	$\lvert G^{lq}_{\mathcal{X}}\rvert$	0.65 [1, 2]	$< \begin{pmatrix} 0.27 & 0.93 & 0.57 \\ 1.04 & 1.40 & - \\ - & - & - \end{pmatrix}$	95%

Table 4.4: Results of the fit to EWPD for the extra vector bosons. We give $\Delta\chi^2_{\rm min} = \chi^2_{\rm min} - \chi^2_{\rm SM}$ values, together with the best fit values and bounds on the interactions of the new vectors. The results for the last six representations are obtained from a fit to each of the entries of the coupling matrices at a time. $[i, j]$ refers to the entries in the family matrices that give the best fit. See text for more details.

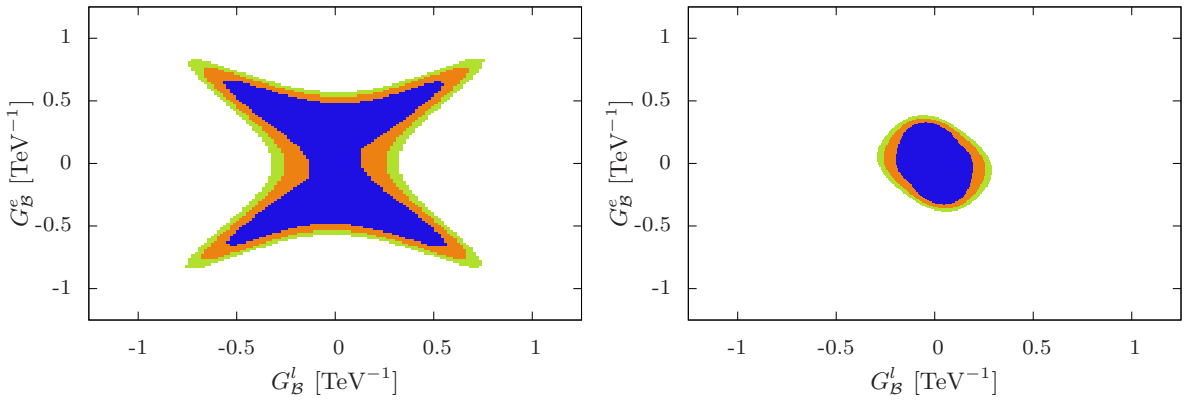

Figure 4.2: From darker to lighter, confidence regions with $\Delta\chi^2 \leq 2$ (blue), 4 (orange) and 6 (95% C.L.) (green), respectively, for the $\mathcal{B}$ couplings to leptons assuming no couplings to quarks. The region in the left plot results from the fit to EWPD without LEP 2 data. This is further constrained into the smaller region in the right plot by adding the LEP 2 cross sections and asymmetries to the fit.

It is also worth noting that, at the minimum, the RH quark couplings are pretty large [8]. The reason is that these couplings raise the prediction for the hadronic cross section measured at LEP 2, which in many energy bins is around 1 σ above the SM prediction. This results in a global 1.7 σ discrepancy when correlations are taken into account. The LH counterparts, on the other hand, are more tightly constrained by the Z-pole observables, and stay smaller. This preference for large RH couplings is stronger in the case of d quarks, due to the SM discrepancy in the bottom forward-backward asymmetry. Indeed, at the minimum we find $A^b_{FB} = 0.1016$, and the pull in this observable is reduced to 1.5 σ. We should stress, nevertheless, that such large couplings could drive the theory into a nonperturbative regime. We shall come back to this point in Section 4.4.

There is a lot of work on the electroweak limits for particular Z' models [139], so it may be useful to discuss at this point the relation between model-dependent and model-independent fits. Each particular model imposes correlations among the couplings, and corresponds to some lower-dimensional manifold in the complete model-independent fit. Therefore, the latter contains all the necessary information. However, for obvious reasons, here we are just showing partial information, in terms of one or two coupling-to-mass ratios at a time. In general, these will not be the free parameters in a particular model, so the translation of our results is not direct. Nevertheless, the one-dimensional limits and two-dimensional plots we have shown above provide basic guidelines to understand the constraints on explicit models. For instance, the allowed regions in the "minimal" class of Z' models considered in Ref. [140, 141], when given in terms of coupling-to-mass ratios, agree with those of Fig. 4.3 above.

To be more explicit, we show in Table 4.5, as an example, the limits on Z' masses and mixings that we find for some popular models usually considered in the literature [133, 142] [9]. As it is

[8] When we find large couplings we also include quadratic corrections in the new physics for LEP 2 observables.

[9] Leptophobic neutral gauge bosons derived, for example, from E_6 [143] are not constrained by EWPD, except

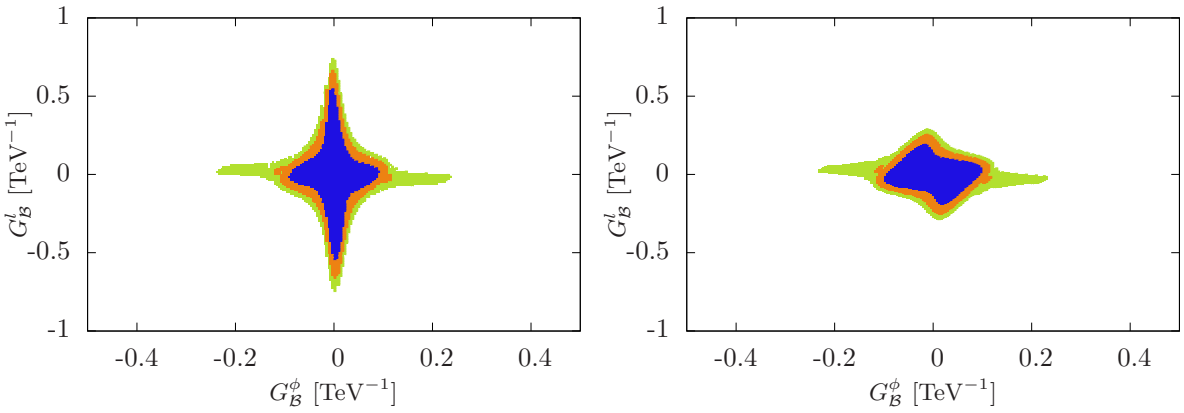

Figure 4.3: From darker to lighter, confidence regions with $\Delta\chi^2 \leq 2$(blue), 4 (orange) and 6 (95% C.L.) (green), respectively, for the $\mathcal{B}$ couplings to the Higgs and LH leptons assuming no couplings to quarks. The regions in the plot on the left are obtained from a fit to EWPD without LEP 2 data. They are reduced to smaller regions when the LEP 2 cross sections and asymmetries are added to the fit, as shown in the plot on the right.

customary, we leave the mixing as a free parameter, even though it would be fixed in a definite model [145]. We give limits from three data sets: i) EWPD excluding LEP 2 cross sections and asymmetries; ii) LEP 2 cross sections and asymmetries[10]; iii) all data. Our results for the first data set agree with the ones in the recent update [144], except for some differences in the limits for the mixing, which arise from our inclusion of Tevatron Higgs searches in the fit.

For most models, EWPD without LEP 2 are sufficient to constrain significantly both the mixing and the mass of the new vectors. The two exceptions are the ψ and R models, for which LEP 2 data are decisive to raise the limit on the mass. The correlations between the mixing and mass in these two models are illustrated in Fig. 4.4. For the ψ model, this behaviour can be inferred from Fig. 4.2, observing that the leptonic couplings are axial and lie along one diagonal of the plots in that figure.

4.3.2 Left-handed triplet: $\mathcal{W}$

This $SU(2)_L$ triplet decomposes after electroweak breaking into a neutral vector boson and a charge ± 1 complex vector boson. This representation appears, for instance, in theories with extra dimensions and in some Little Higgs models. The most general case has three new parameters: the couplings to the Higgs and to the lepton and quark doublets. As in the previous case, the parameter space has a flat direction along the quark coupling direction when the interactions with the Higgs and leptons vanish. On the other hand, the coupling of this vector to the Higgs does not appear quadratically, since the $\mathcal{W}$ field preserves custodial symmetry, which forbids the operator

for their possible mixing with the Z boson. If their coupling to the Higgs is nonvanishing, the Z-pole data can provide lower limits on $M_{Z'_L}$ around 1 TeV [144].

[10] Unlike [81], where the Z-Z' mixing is fixed to zero, we let $\sin\theta_{ZZ'}$ vary in the fit to LEP 2 data.

Model	95% C.L. Electroweak Limits on $\sin\theta_{ZZ'}$ $[\times 10^{-4}]$			95% C.L. Electroweak Limits on $M_{Z'}$ [TeV]		
	EWPD (no LEP 2)	LEP 2	All Data	EWPD (no LEP 2)	LEP 2	All Data
Z'_χ	$[-10,\ 7]$	$[-\ 80, 118]$	$[-11,\ 7]$	1.123	0.772	1.022
Z'_ψ	$[-19,\ 7]$	$[-196, 262]$	$[-19,\ 7]$	0.151	0.455	0.476
Z'_η	$[-22, 25]$	$[-150, 164]$	$[-23, 27]$	0.422	0.460	0.488
Z'_I	$[-\ 5,\ 9]$	$[-144,\ 96]$	$[-\ 5, 10]$	1.207	0.652	1.105
Z'_N	$[-14,\ 6]$	$[-165, 223]$	$[-14,\ 6]$	0.635	0.421	0.699
Z'_S	$[-\ 9,\ 5]$	$[-\ 85, 129]$	$[-10,\ 5]$	1.249	0.728	1.130
Z'_R	$[-17,\ 7]$	$[-166, 177]$	$[-15,\ 5]$	0.439	0.724	1.130
Z'_{LR}	$[-13,\ 5]$	$[-147, 189]$	$[-12,\ 4]$	0.999	0.667	1.162

Table 4.5: Comparison of 95% C.L. limits on $\sin\theta_{ZZ'}$ and $M_{Z'}$ obtained for several popular Z' models from a fit to standard EWPD without LEP 2, to LEP 2 cross sections and asymmetries, and to all data. The gauge coupling constants are taken equal to the GUT-inspired value, $\sqrt{5/3}\, g' \approx 0.46$.

$\mathcal{O}_\phi^{(3)}$. Therefore, there is an extra flat direction in the Higgs coupling for vanishing couplings to the fermions. This is illustrated in Figure 4.5, where we plot several confidence regions in the plane spanned by the lepton and Higgs couplings.

Note also that the χ^2 at the minimum, which is placed over both flat directions, is less than 2 units smaller than for the SM. Thus, any value of the Higgs and quark couplings is allowed by EWPD at that confidence level. For $G_{\mathcal{W}}^{\phi}$, the 1 σ interval is finite, as reported in Table 4.4, whereas there are no limits on $G_{\mathcal{W}}^{q}$. As in the case of the singlet $\mathcal{B}$, there is a preference for large values of the quark coupling.

4.3.3 Charged singlet: $\mathcal{B}^1$

This complex isosinglet vector has electric charge ± 1. After EWSB, it mixes with the SM charged bosons, with the mixing proportional to the Higgs coupling. With our assumption that the new vector is heavier than the W boson, this mixing decreases M_W, and gives a negative contribution to the ρ parameter. In the effective formalism, this effect is clear from the positive sign of the contribution of this vector to the operator $\mathcal{O}_\phi^{(3)}$. Therefore, the presence of this vector with a nonvanishing scalar coupling favors a value for the Higgs mass yet lower than in the SM, in contrast with the case of singlets of zero hypercharge, $\mathcal{B}$. The LEP 2 lower bound on the Higgs mass then forces the Higgs coupling to be very small. The other parameter in this scenario is the coupling of the $\mathcal{B}^1$ to the RH quarks. This coupling induces RH CC, via the operator $\mathcal{O}_{\phi ud}$. Unfortunately, there are no direct experimental constraints on these quark currents (our fits do not incorporate the possible hints from kaon physics described in Ref. [146]). At any rate, taking into account the preference for small Higgs coupling, the electroweak data are blind to these RH quark couplings.

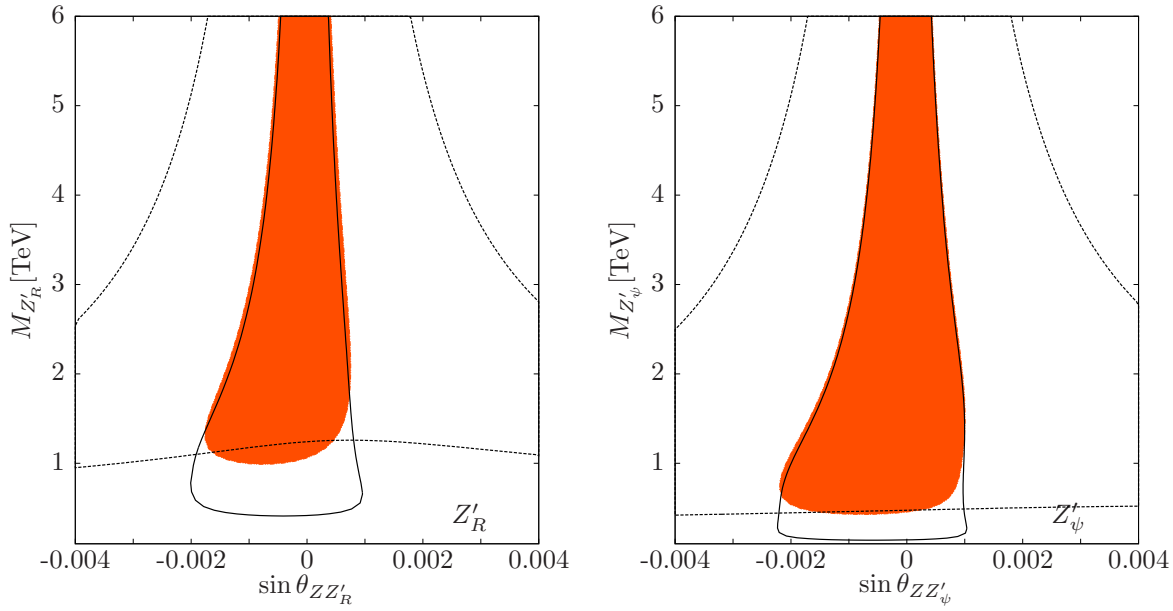

Figure 4.4: 95% C.L. contour in the $M_{Z'}$ - $\sin\theta_{ZZ'}$ plane for the Z'_R model (left) and Z'_ψ (right). The different contours correspond to the fit to EWPD without LEP 2 cross sections and asymmetries (solid line), to LEP 2 cross sections and asymmetries (dashed line), and to all data (solid region).

4.3.4 Fermiophobic triplet: $\mathcal{W}^1$

The triplet with hypercharge 1 contains two real neutral vectors, which mix with the Z boson upon EWSB, a complex vector of charge ±1, which mixes with the W, and a complex vector of charge ±2, which gives no observable effect. The characteristic feature of this representation is that it cannot couple to any SM fermions. Hence, its only visible effects are oblique. Moreover, the net contribution to the ρ parameter is positive, which makes EWPD consistent with a heavy Higgs. Therefore, the fit prefers a nonzero value of the coupling, in order to compensate the effect on EWPD of the direct LEP lower bound on the Higgs mass. The interplay with the Higgs mass is further discussed in Section 4.5.

4.3.5 Leptophilic vector: $\mathcal{L}$

This representation contains complex vectors of charges ±1 and ±2. Since it does not couple to the Higgs, the charge ±1 components do not mix with the W boson at tree level. The vector field is coupled to a $\Delta L = 2$ current mixing the LH and RH lepton multiplets. Despite this, no trace of lepton number violation remains in the effective Lagrangian, thanks to the absence of any other couplings. This fact allows to recover this symmetry by assigning lepton number $L = 2$ to the field $\mathcal{L}$. There can be, however, lepton flavor violation, even for diagonal couplings, as these create (destroy) two same-flavor anti-leptons (leptons), allowing for processes like $e^-e^- \to \mu^-\mu^-$. The only operator in the effective Lagrangian for this vector is the four-lepton interaction $\mathcal{O}_{le}$. This can contribute to $\nu^\mu e$ scattering as well as to $e^+e^- \to \ell^+\ell^-$ data at LEP 2. There are no restrictions from parity violating observables measured in Møller scattering, since $\mathcal{O}_{le}$ does not contribute to V-A couplings. In the case of couplings to only one flavor per SM multiplet, the

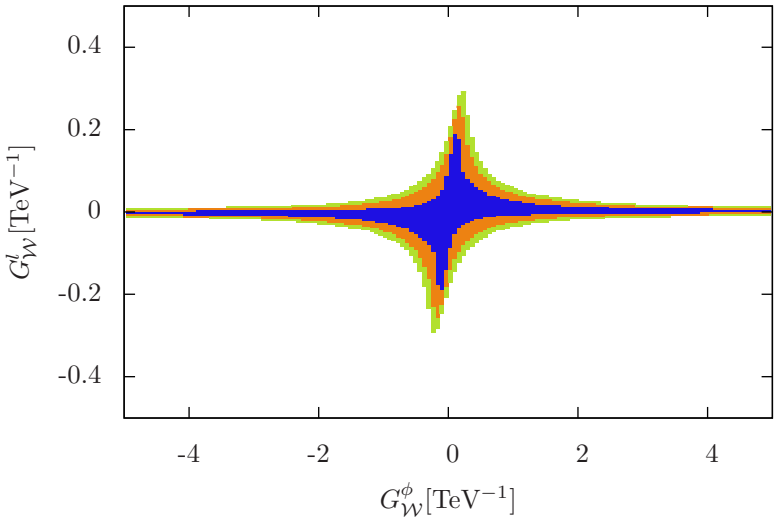

Figure 4.5: From darker to lighter, confidence regions with $\Delta\chi^2 \leq 2$ (blue), 4 (orange) and 6 (95% C.L.) (green), respectively, for the $\mathcal{W}$ couplings to LH leptons and to the Higgs boson. Notice the flat direction along the Higgs coupling axis when the lepton charge vanishes.

weakest constraint shown in Table 4.4 occurs for couplings between electrons and taus. Similar bounds apply to couplings to electrons and muons.

4.3.6 Singlet vector leptoquarks: $\mathcal{U}^2$ and $\mathcal{U}^5$

The two colored $SU(2)_L$ singlets $\mathcal{U}^2$ and $\mathcal{U}^5$ decompose into complex vectors of fractional charges $\pm 2/3$ and $\pm 5/3$, respectively. The associated currents carry nonvanishing L, B and $B-L$ numbers. But again, these global symmetries are preserved in the effective Lagrangian. For $\mathcal{U}^2$, this is so because the two terms in the current have the same B and L charges. The integration of $\mathcal{U}^2$ generates the operators $\mathcal{O}_{ed}$, $\mathcal{O}_{lq}^{(1,3)}$ and $\mathcal{O}_{qde}$, while for $\mathcal{U}^5$, only $\mathcal{O}_{eu}$ is generated. With the exception of $\mathcal{O}_{qde}$, which does not interfere with any of the SM amplitudes, these operators contribute to APV and to the inclusive hadronic cross section at LEP 2. $\mathcal{O}_{lq}^{(1,3)}$ can also contribute to neutrino-nucleon scattering if $\mathcal{U}^2$ couples to muons and first family quarks. Finally, $\mathcal{O}_{lq}^{(3)}$ can modify the unitarity relation of the CKM matrix. In particular, this is the only constraint when $\mathcal{U}^2$ couples to the second family. The precise determination of the weak charge for Cesium and its good agreement with the SM prediction is the strongest constraint when these operators are coupled to the first family (together with the CKM unitarity for $G_{\mathcal{U}^2}^{lq}$). It is worth noting that the negative contribution to $\mathcal{O}_{eu}$ is favored by LEP 2 data, as it increases the total hadronic cross section above the Z pole. For this reason, the fit with $\mathcal{U}^5$ gives some improvement in χ^2, with just one extra free parameter.

4.3.7 Doublet vector leptoquarks: $\mathcal{Q}^1$ and $\mathcal{Q}^5$

The $SU(2)_L$ doublet $\mathcal{Q}^1$ contains two complex vectors, of charges $\pm 1/3$ and $\pm 2/3$, whereas the doublet $\mathcal{Q}^5$ is made of complex vectors of charges $\pm 1/3$ and $\pm 4/3$. Again, the corresponding currents carry nontrivial B, L and $B-L$ numbers. Of these, $B-L$ is actually conserved, since all the terms in the current have the same charge, $\Delta(B-L) = -2/3$. On the other hand, there are dangerous contributions to baryon and lepton number violating operators. In order to avoid proton decay while allowing for contributions to EWPD, we consider here the case without the B violating couplings $g_{\mathcal{Q}^1}^{dq}$ and $g_{\mathcal{Q}^5}^{uq}$. Then, the vector $\mathcal{Q}^1$ generates only the operator $\mathcal{O}_{lu}$, while $\mathcal{Q}^5$ induces three operators: $\mathcal{O}_{ld}$, $\mathcal{O}_{qe}$ and $\mathcal{O}_{qde}$.

For $\mathcal{Q}^1$, the dominant constraint comes again from APV. Weaker bounds are obtained when we couple the new vector to electrons and c quarks, or to muons and u quarks, so that they affect LEP 2 data and the low-energy effective coupling g_R^2 in deep-inelastic neutrino-nucleon scattering, respectively. In the later case there is a small improvement in χ^2.

In the case of the vector $\mathcal{Q}^5$, the bounds from APV are mild for couplings $g_{\mathcal{Q}^5}^{dl}$ and $g_{\mathcal{Q}^5}^{eq}$ to the first family. This is so because the independent contributions to the atomic weak charges from $\mathcal{O}_{ld}$ and $\mathcal{O}_{qe}$ can be adjusted to approximately cancel. The strongest bound on $G_{\mathcal{Q}^5}^{dl}$ comes again from g_R^2, when $\mathcal{Q}^5$ couples to muons and down quarks. When it couples to electrons and s or b quarks, only the LEP 2 constraints apply. These are weaker, as a sizable value for these couplings is again favored. For $G_{\mathcal{Q}^5}^{eq}$, LEP 2 data give stronger constraints, which can be relaxed by the interplay with the other coupling, when the latter is not tied by other data.

The best minimum occurs for couplings to the first family. Besides the better agreement with LEP 2 hadronic data, there is an improvement in the combinations of the parity-violating eq effective parameters C_{1u} and C_{1d} that appear in Table A.1 in Appendix A. As a result, the χ^2 of the global fit is decreased by 3.4, with two extra parameters.

4.3.8 Triplet vector leptoquark: $\mathcal{X}$

Finally, this $SU(2)_L$ triplet decomposes into complex vectors of charges $\pm 1/3$, $\pm 2/3$ and $\pm 5/3$. It connects LH quarks with LH leptons. Even though the current carries lepton and baryon numbers, the B and L symmetries are preserved in the effective Lagrangian. $\mathcal{X}$ only generates the operators $\mathcal{O}_{lq}^{(1)}$ and $\mathcal{O}_{lq}^{(3)}$, whose effects are described in the $\mathcal{U}^2$ subsection. The coefficients are different, however, and so are the constraints.

The strongest bound in Table 4.4 is also provided by APV, in the case with couplings to electrons and first family quarks. The weakest nontrivial bound corresponds to the assumption that this vector only couples to the second family and, as in the case of $\mathcal{U}^2$, it comes from the CKM constraints. On the other hand, a $\mathcal{X}$ coupling muons to the LH u and d quarks allows to reduce to 1 σ the SM 2 σ discrepancy in the g_L^2 coupling extracted from deep-inelastic neutrino-nucleon scattering. A further reduction is prevented again by the precise measurement of unitarity in the first row of the CKM matrix. The global decrease in the χ^2 is, however, marginal: $\Delta\chi^2_{\text{min}} \approx -1.4$. In fact, a better improvement is found by choosing couplings between electrons and the second quark family, even if this does not modify g_L^2. It may seem surprising that, for this vector, the limits on couplings of electrons to the third family of quarks are significantly stronger than the corresponding ones for the second family. The explanation is that, for this representation, the contributions to the hadronic cross section at LEP 2 from the up (down) quarks are favored (disfavored), and in the case of the third family only the b quark contributes.

4.4 Several extra vectors

In this section we discuss scenarios with several new vector bosons, both in the same and in different SM representations.

It seems quite natural that an extra vector boson around the TeV scale will come accompanied by other new particles, in particular additional new vectors. This occurs in many explicit models beyond the SM. At the dimension-six order, the coefficients of the operators are just given by the sum of the contributions of each new vector, as we have shown explicitly before. Moreover, because the leading new effects come from the interference of SM amplitudes and diagrams with insertions of dimension-six operators, the interference between the contributions of different vectors to observables is negligible. On the other hand, opposite signs may occur in the sums. Hence, some (partial) cancellations are possible, both between contributions of different new vectors to a given operator, and between the contributions of different gauge-invariant operators to an observable.

One consequence of having more than one vector simultaneously is that some restrictions on the operator coefficients, which hold necessarily for just one vector, are removed. For example, for just one extra singlet $\mathcal{B}$ with arbitrary couplings, the following relations are always satisfied:

$$\left(\alpha_{\phi\psi}^{(1)}\right)^2 = \frac{1}{2}\alpha_{\phi}^{(3)}\alpha_{\psi\psi}, \tag{4.12}$$

$$\left(\alpha_{\psi\psi'}\right)^2 = \alpha_{\psi\psi}\alpha_{\psi'\psi'}, \tag{4.13}$$

where ψ and ψ' stand for any SM fermion multiplet. These relations do not hold any longer if there are two singlets $\mathcal{B}$. For instance, two vectors with the same couplings to the lepton doublet and opposite Higgs couplings,

$$\begin{aligned} g_{V_1}^{l} &= \quad g_{V_2}^{l}, \\ g_{V_1}^{\phi} &= -g_{V_2}^{\phi}, \end{aligned} \tag{4.14}$$

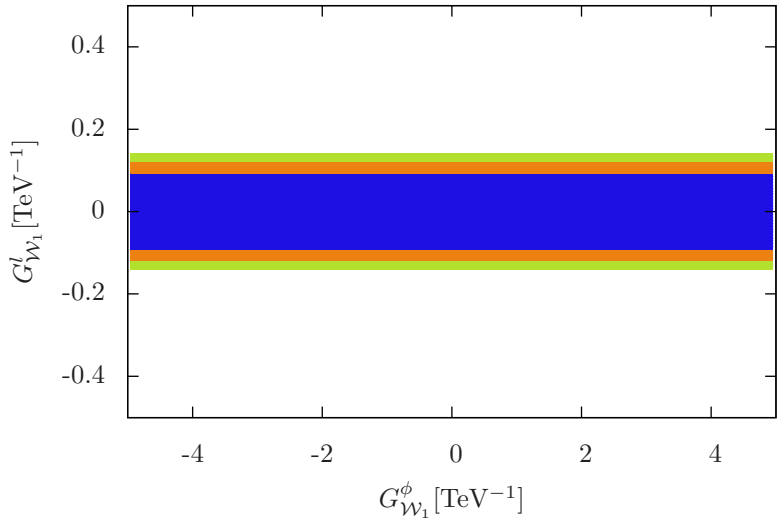

Figure 4.6: From darker to lighter, confidence regions with $\Delta\chi^2 \leq 2$ (blue), 4 (orange) and 6 (95% C.L.) (green), respectively, in the $G^l_{\mathcal{W}_1}$ - $G^\phi_{\mathcal{W}_1}$ plane of an extension with two mirror left-handed triplets, $\mathcal{W}_1$ and $\mathcal{W}_2$.

will have a vanishing coefficient $\alpha^{(1)}_{\phi l}$, but nonvanishing $\alpha^{(3)}_{\phi}$ and $\alpha^{(1)}_{ll}$. This would be impossible with only one extra vector, and it is an example of a cancellation of the effects of several vectors. The point is that models with more than one extra vector may have observable effects that cannot be reproduced by any model with just one.

An interesting possibility is that cancellations of this sort give rise to weaker bounds from EWPD on each vector. For the leptonic couplings, it turns out that there is little room for this effect, at least in the universal case. The reason is that the coefficients of the four-lepton operators $(\mathcal{O}^{(1)}_{ll})_{iiii}$ and $(\mathcal{O}_{ee})_{iiii}$ induced by any extra vector are negative definite, since they are given by minus sums of squares. Hence, no cancellations are possible here. For i=1 (first family), these coefficients are constrained to be very small by the differential cross sections in Bhabha scattering measured at LEP 2[11]. Furthermore, the operators modifying the trilinear couplings, which could counteract the action of the four-fermion operators, are independently constrained to be small by the Z-pole data.

Therefore, in universal scenarios with combinations of several vector bosons, the limits on the ratios of leptonic couplings to masses of each new vector are at least as stringent as the corresponding "one-at-a-time" limits in Table 4.4 [147]. In other words, new vector bosons must be, to a certain degree, leptophobic (or more precisely, electrophobic [141])[12].

Despite these limitations, the cooperation of several extra vectors can open new regions in the

[11] Cancellations between the contributions of a $\mathcal{B}$ and a $\mathcal{L}$ are possible in the four-lepton operator with mixed chiralities, $\mathcal{O}_{le}$, but the angular distributions allow to isolate the effects of each individual operator on the cross sections.

[12] Remember that we are always working with the assumption that no other kind of new physics modifies EWPD.

parameter space of couplings and masses. A simple example is the case of two left-handed triplets $\mathcal{W}$, with universal couplings as in Eq. (4.14). We show in Fig. 4.6 several confidence regions in the $G^l_{\mathcal{W}_1}$ - $G^\phi_{\mathcal{W}_1}$ plane. We see that the combination of these two "mirror" vectors make the EWPD blind to the coupling $g^\phi_{\mathcal{W}}$. This figure is to be compared with the corresponding plot for just one $\mathcal{W}$ in Fig. 4.5. A similar outcome is found in a model with "mirror" neutral singlets $\mathcal{B}$, when we also add a $\mathcal{B}^1$ vector boson to cancel the effect of the $\mathcal{B}$ bosons on the ρ parameter. In the next subsection, we give some examples of cancellations between the contributions of different types of vector bosons.

4.4.1 Nonuniversal couplings and the bottom forward-backward asymmetry

In some classes of models, the extra vector bosons couple in a nonuniversal way to the different families. Large couplings to the third family are expected, for instance, in models of dynamical EWSB. In extra-dimensional theories, nonuniversal couplings appear when the fermions are separated in the extra dimension, with heavier fermions having naturally bigger couplings to the new vectors. For the most common types of vector bosons, $\mathcal{B}$, $\mathcal{W}$ and $\mathcal{B}^1$, we have assumed so far family universal couplings. In this section, we explore the impact of dropping this assumption, both for a unique singlet vector and for a few interesting combinations. As we will see, the extra freedom allows to better reproduce the experimental data and even improve the SM fits. For simplicity, we assume in the following that all the new couplings are small, except the ones to the third family of quarks and to the Higgs doublet. This has the advantage of making FCNC innocuous, due to CKM suppression. Tuning the couplings of an extra singlet $\mathcal{B}$ to the RH bottom, it is possible to correct the deviation in the bottom forward-backward asymmetry at the Z pole (no other vector boson can play this role). We have actually seen some improvement in the prediction for this observable with universal singlets, but the nonuniversal scenario works better and allows to completely remove the discrepancy without modifying the observables that agree with the SM. This produces a significant decrease in the χ^2 of the global fits, as shown in the first column of Table 4.6 [13].

This "solution" to the A^b_{FB} anomaly puzzle suffers, however, from an important deficiency. In order to shift the asymmetry without modifying the $Z \to \overline{b}b$ partial decay width, we need a large correction to the $Z\overline{b}_R b_R$ vertex and a small nonvanishing correction to the $Z\overline{b}_L b_L$ vertex. These corrections are produced by the 3-3 entries of the operators $\mathcal{O}^{(1)}_{\phi d}$ and $\mathcal{O}^{(1)}_{\phi q}$, with coefficients proportional to the couplings of the extra vector to the Higgs, $g^\phi_{\mathcal{B}}$, and to the RH bottom and the LH top-bottom doublet, respectively. As we can see in Table 4.6, the ratio $G^b_{\mathcal{B}} = g^b_{\mathcal{B}}/M_{\mathcal{B}}$ is rather big at the minimum. Unless $M_{\mathcal{B}} \lesssim 1$ TeV, this can spoil perturbation theory in the complete theory, rendering the whole calculation meaningless[14]. In the second column of Table 4.6, we have forced $G^b_{\mathcal{B}}$ to be smaller than 1, and we see that the anomaly is then recovered.

The reason for the large coupling of the singlet to b_R, apart from the requisite of a big effect, is that it needs to compensate the smallness of the coupling to the Higgs. This is enforced by the data just as in the universal case. So, it is clear that we can alleviate this problem if we allow the Higgs coupling to become larger. This can be achieved in two ways. First, as we discuss in the next section in more detail, the coupling to the Higgs prefers to be larger when the Higgs mass increases. Therefore, if the Higgs were found to be heavy, smaller b_R couplings would be required.

[13] Even if we are focussing on the couplings to b quarks, we do not include LEP 2 b data in the fits we present here because, as explained in Appendix A, the reported values are derived with a strong SM dependence [81]. At any rate, we have checked that these data have little impact in the results of the fits.

[14] Remember also that we cannot trust our approximations for very light vectors, which in addition are subject to Tevatron bounds.

We show this in the third and fourth columns of Table 4.6. We see that the coupling-to-mass ratio $G^b_{\mathcal{B}}$ is still greater than 1 for $M_H \leq 500$ GeV.

	$\mathcal{B}$				$\mathcal{B}+\mathcal{B}^1$	
	Free	$G^b_{\mathcal{B}} \equiv 1$	$M_H = 200\,\text{GeV}$	$M_H = 500\,\text{GeV}$	Free	$G^b_{\mathcal{B}} \equiv 1$
$-\Delta\chi^2_{\text{min}}$	8.2	2.7	14.1	47.7	8.2	8.2
Pull$[A^b_{FB}]$	-0.5	-2.5	-0.4	-0.4	-0.5	-0.5
$G^b_{\mathcal{B}}$ [TeV^{-1}]	6.4	1	3.8	2.4	3.2	1
$G^\phi_{\mathcal{B}}$ [TeV^{-1}]	0.082	0.078	0.13	0.19	0.16	0.53
$G^\phi_{\mathcal{B}^1}$[TeV^{-1}]	-	-	-	-	0.20	0.73

Table 4.6: Effect of the SM singlets on the forward-backward asymmetry for the b quark from the nonuniveral fit. The improvement in the χ^2 for the cases of $M_H = 200, 500$ GeV is given with respect to the SM with the same values of the Higgs mass. The last two columns correspond to different points along a flat direction.

A more efficient way of reproducing the experimental asymmetry without too large couplings is to combine different new vectors. The only operator where the Higgs coupling enters quadratically is $\mathcal{O}^{(3)}_\phi$. While the coefficient of this operator is always positive when induced by a singlet neutral vector $\mathcal{B}$, the hypercharged vector $\mathcal{B}^1$ gives a negative contribution to it. Hence, if the theory contains a $\mathcal{B}$ and a $\mathcal{B}^1$, both contributions may cancel out[15]. Furthermore, the extra vector $\mathcal{B}^1$ gives no other observable effect in the fits if coupled only to the third family. In the last two columns of Table 4.6, we display the result of a global fit to a scenario with a neutral singlet $\mathcal{B}$ and a charged singlet $\mathcal{B}^1$, both coupled to the Higgs and to the third family of quarks only. We see that in this case the coupling to b_R can be made smaller than 1 at no cost in χ^2. In fact, there is an almost flat direction for fixed values of the product $G^b_{\mathcal{B}} G^\phi_{\mathcal{B}}$ (and the correct $G^\phi_{\mathcal{B}^1}$ to counteract the effect of $G^\phi_{\mathcal{B}}$). The impact of including the second vector boson is also manifest in Fig. 4.7, where we plot the allowed values for the Higgs and b_R couplings to the $\mathcal{B}$ singlet, with and without an additional $\mathcal{B}^1$ boson. We observe that introducing the charged singlet opens a new favored region in which $G^b_{\mathcal{B}}$ is smaller and $G^\phi_{\mathcal{B}}$ is larger. This very same mechanism is at work in the explicit extra-dimensional model in [148].

In definite models, having small couplings of the new vectors to b_L can be troublesome from a model building perspective, especially if the couplings to b_R are large. This issue can be addressed by adding another type of extra vector that balances the effect of the singlet. One possibility is a triplet $\mathcal{W}$. This vector boson generates the operator $\mathcal{O}^{(3)}_{\phi q}$. Because the correction to the $Z\overline{b}_L b_L$ vertex is proportional to $\alpha^{(1)}_{\phi q} + \alpha^{(3)}_{\phi q}$ and these coefficients do not have a definite sign, a cancellation is again possible. This mechanism is shown in Fig. 4.8. It can be made natural if the $\mathcal{B}$ and $\mathcal{W}$ couplings are related by some symmetry [149], as in the custodial protection proposed in [150]. Note that this protection requires new fermions, which might modify the electroweak fits [151]. We also point out that the correction to the $Z\overline{t}_L t_L$ vertex is proportional to $\alpha^{(1)}_{\phi q} - \alpha^{(3)}_{\phi q}$, so it can never be cancelled at the same time [149]. This has consequences for top physics at LHC [152].

[15] They cancel out automatically if the extension of the SM preserves custodial symmetry.

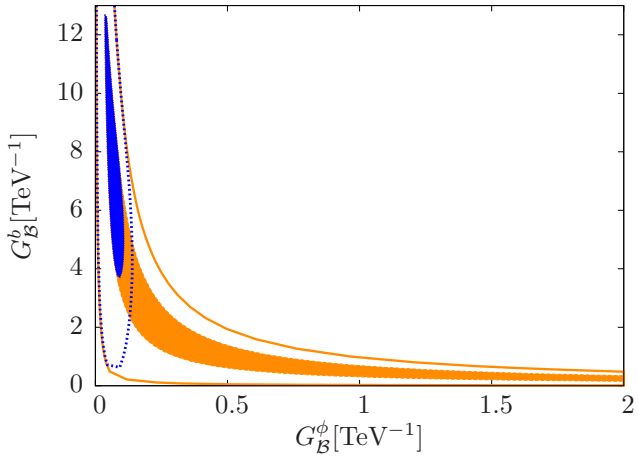

Figure 4.7: Allowed regions of the $\mathcal{B}$ couplings to the RH bottom and to the Higgs at 1 σ (solid regions) and at 95% C.L. (regions between lines) from the nonuniversal $\mathcal{B}$ fit (blue, dotted) and the $\mathcal{B} + \mathcal{B}^1$ fit (orange, solid).

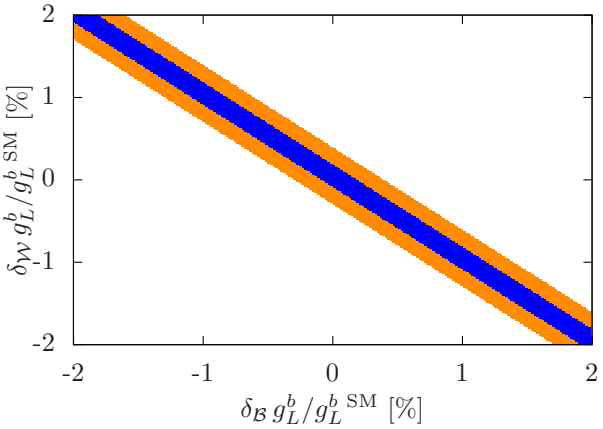

Figure 4.8: Confidence regions at 1 σ (blue, dark) and 95% C.L. (orange, light) on the plane determined by the corrections to the $Z\bar{b}_L b_L$ coming from a singlet $\mathcal{B}$ and a triplet $\mathcal{W}$.

4.5 New vector bosons and the Higgs mass

In this section we focus on the implications of new vector bosons on the Higgs mass. As in all the other fits in this thesis, we have considered the mass of the Higgs boson as a free parameter, and we have imposed the direct constraints from Higgs searches at LEP 2 and Tevatron, which in particular discard a light Higgs in a quite robust manner, with $M_H > 114.4$ GeV at 95% C.L. [39]. On the other hand, the global electroweak fit of the SM shows a preference for a light Higgs, $M_H = 101^{+32}_{-26}$ GeV. This would be strengthened if the $\sim 3\ \sigma$ deviation in A^b_{FB} were due to a systematic error. In that case it should be removed from the fit, and the minimum would have a Higgs mass lower than the LEP lower bound, $M_H = 73^{+28}_{-22}$ GeV. In this sense, there is a mild tension between indirect and direct limits [43].

As we have seen before, $\mathcal{B}$ vector bosons generate the oblique operator $\mathcal{O}^{(3)}_\phi$ with a negative coefficient, and since

$$\Delta\rho = -\frac{\alpha^{(3)}_\phi}{2}\frac{v^2}{\Lambda^2}, \tag{4.15}$$

they give a positive contribution to the ρ parameter. This has the right sign to neutralize the effect of increasing M_H on ρ. In fact, Z' bosons have been used in the past to render a heavy Higgs consistent with EWPD [153], and to release the tension with the LEP lower bound [154]. The other extra vectors that contribute to $\mathcal{O}^{(3)}_\phi$ are $\mathcal{B}^1$ and $\mathcal{W}^1$. The first one gives a contribution of opposite sign, so it favours smaller values of M_H. The contribution of the hypercharged triplet $\mathcal{W}^1$ has the same sign as for $\mathcal{B}$, and can be used to raise the allowed values M_H. It also has the virtue of not generating any other observable operator, which could worsen the quality of the fit. However, the appearance of this representation seems to require a rather contrived model building.

In Fig. 4.9 left, we plot the minimum of χ^2 as a function of the Higgs mass in three cases: SM, one extra $\mathcal{B}$ and one extra $\mathcal{W}^1$. In all cases, we have used the information from direct searches. The couplings are family universal. The effect of the $\mathcal{B}$ and the $\mathcal{W}^1$ vector bosons is apparent: they flatten the distribution when we go beyond the region disfavoured by the Tevatron searches. This allows to reach large values of M_H with a low cost in χ^2, as compared to the SM case. We also observe that, in the case of $\mathcal{B}$, the larger number of free parameters is used to lower the χ^2 with respect to the $\mathcal{W}^1$ case. This effect persists in the flat region, thanks to an improvement in the prediction for LEP 2 hadronic cross sections and for A^b_{FB} at the Z pole, which we have already discussed in Section 4.3.

The coefficient $\alpha^{(3)}_\phi$ is proportional to the square of the coupling of the vector bosons to the scalar doublet. Therefore, this coupling must increase when the Higgs mass gets larger. This correlation is shown, for the $\mathcal{W}^1$ boson, in Fig. 4.9 right, where we display several confidence regions in the M_H - $G^\phi_{\mathcal{W}^1}$ plane.

4.6 Conclusions

In this chapter, we have studied general extra particles of spin 1, concentrating on their effects in EWPD. Our results are relevant for model-independent searches and also for explicit models. We have classified all the possibilities that may produce observable effects, and have written the most general couplings consistent with the SM gauge symmetry that are linear in the new fields. We have then derived, to dimension six, the effective Lagrangian that describes the effect of the new vector bosons at energies smaller than their masses. The result is displayed in Tables 4.7 to 4.21 (see the addendum in next section). Our analysis includes the cases of Z' and W' particles, vector leptoquarks and a few vector particles that, to the best of our knowledge, had not been considered

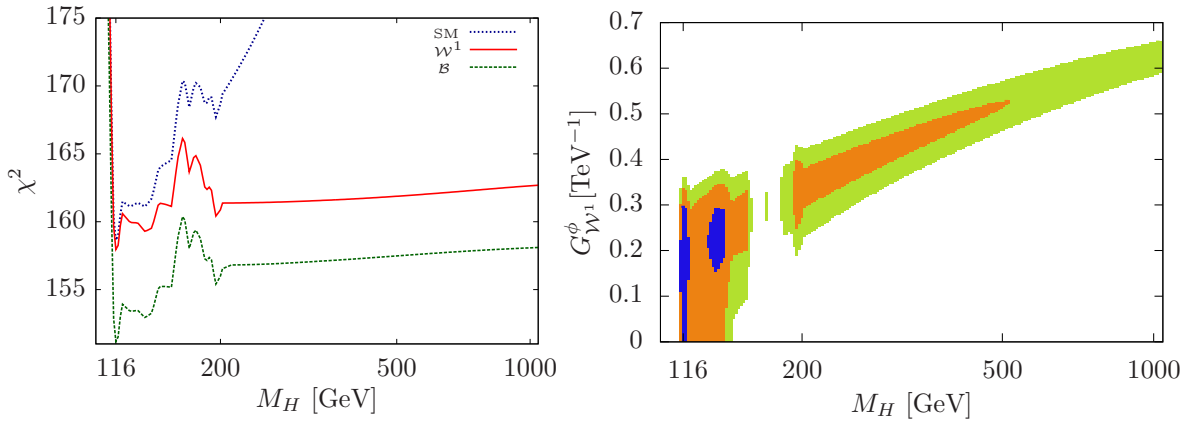

Figure 4.9: *Left:* Minimum of the χ^2 as a function of the Higgs mass for the SM fit, the $\mathcal{W}^1$ fit and the $\mathcal{B}$ fit. Higgs direct searches data are available up to $M_H = 200$ GeV. Above that value the effect of neutral-boson mixing flattens the curve. *Right:* From darker to lighter, confidence regions with $\Delta\chi^2 \leq 2$ (blue), 4 (orange) and 6 (95% C.L.) (green), in the plane parametrized by the Higgs mass and the $\mathcal{W}^1$ coupling to the Higgs.

previously in the literature. Some of the vector bosons we have studied couple to quarks only, so they are not constrained by EWPD. However, they may in principle be single-produced and seen as resonances at Tevatron and LHC [155, 156].

We have performed model-independent electroweak fits of the different types of new vectors, keeping the new couplings and masses as free parameters. We have studied scenarios with both family universal and nonuniversal couplings. The main results are collected in Table 4.4. In the fits, low-energy and LEP 2 data are crucial to constrain the different four-fermion interactions that appear upon the integration of the new particles. This translates into limits on the couplings to fermions that, unlike the ones from the Z-pole observables, cannot be avoided by making the couplings to the Higgs very small.

In a rough way, we observe that for all vector multiplets the purely leptonic couplings of the extra vectors are constrained to be pretty small, while the limits on quark and leptoquark couplings are weaker. Moreover, in some cases the data show a preference for pretty large quark couplings, driven by the SM discrepancies with the bottom forward-backward asymmetry at the Z-pole and with the hadronic cross sections at LEP 2. Finally, small Higgs couplings are also preferred, at least in the fits with just one type of extra vector.

We have also examined the implications of including several of these extra vector bosons at once, and looked for possible cancellations that may relax the electroweak limits. In particular, we have shown that a vector-boson solution to the bottom forward-backward anomaly is possible in a nonuniversal scenario with extra neutral and charged singlets. In this case, the charged vectors are needed to keep the couplings to the RH bottom in the perturbative regime.

An important variable in all the electroweak fits is the mass of the Higgs boson, which enters logarithmically through radiative corrections. We have kept it as a free parameter, and imposed the constraints from direct Higgs searches at LEP and Tevatron. As in the SM, the fits with new

vector bosons favor a light Higgs, close to the lower bound of 114 GeV. Nevertheless, there are two types of vector bosons (the neutral singlet and the fermiophobic triplet) that can make the electroweak data consistent with a heavy Higgs, as shown in Fig. 4.9.

The limits we have obtained are somewhat complementary to the ones from Tevatron. Both restrict the discovery potential of LHC. To simplify the following discussion, all limits on the masses of the heavy vector bosons are given with the assumption that the nonvanishing couplings to SM fields have the same strength as the massive gauge bosons in the SM (~ 0.2 for leptonic NC). At hadron colliders, the new vector bosons can be seen as resonances, if kinematically allowed, when the cross section is high enough to distinguish a bump above the SM backgrounds. The most efficient process is Drell-Yan, which requires trilinear couplings of an extra neutral vector (Z') with quarks and with leptons. These two kinds of couplings exist only for the singlet $\mathcal{B}$ and for the neutral component of the triplet $\mathcal{W}$. The lower limits from Tevatron on the mass of neutral vector bosons, coupled to leptons and quarks, are around 1 TeV [157], and the LHC discovery reach is near 5 TeV, assuming 14 TeV operation and an integrated luminosity of 100 fb^{-1} [158]. For $\sqrt{s} = 7$ TeV and an integrated luminosity of 100 pb^{-1} it should be possible to put bounds above 1 TeV. The limits from precision tests are in general around this value (see Table 4.4 and 4.5). On the other hand, charged vectors (W') are best seen as resonances produced by quark interactions and decaying into a charged lepton and a neutrino. This is only possible for the representation $\mathcal{W}$ and, if there were sufficiently light RH neutrinos, $\mathcal{B}^1$ [159]. Tevatron puts limits around 1 TeV [160], while LHC could discover a W' with mass up to 4 TeV for $\sqrt{s}$ =14 TeV and a few fb^{-1} of integrated luminosity [161]. The EWPD (for $\mathcal{W}$, with leptonic coupling $g \approx 0.66$) give a bound around 2.5 TeV.

It is also possible that the new vectors be leptophobic. This is automatic for many of the representations considered here. In this case, the most relevant decay mode is $V \to jj$. The Tevatron limits [162] and the LHC reach [163] are somewhat smaller than when the vectors couple to leptons. Since the quark couplings and the masses of the extra vectors are unconstrained by EWPD, the available parameter space for LHC discovery is pretty large in this case.

Some of the representations we have studied couple leptons to quarks. If there is enough available phase space, these vector leptoquarks can be double produced at hadron colliders via renormalizable coupling to gluons in the covariant kinetic term, Eq. (4.2). This interaction does not contribute to the dimension-six effective Lagrangian, so it is not seen, in our approximation, by EWPD. Single production through trilinear couplings, which are constrained by EWPD, is also possible [164]. The lower limits on leptoquark masses from Tevatron are around 250 GeV [165]. On the other hand, leptoquarks coupled to the first family could be single produced at HERA via trilinear couplings, and their nonobservation puts a lower bound of 290 GeV on their mass [166]. The limits on trilinear couplings that we have derived here, making use of low-energy and LEP 2 data, depend a lot on the particular representation of the vector leptoquark, and on the flavor structure of the couplings. They range from ~ 70 GeV to 830 GeV at 95% C.L. assuming a generic coupling $g_V^{\psi_1\psi_2} = 0.1$ (see Table 4.4).

The vectors bosons $\mathcal{L}$ only have leptonic couplings and cannot be seen at hadron colliders. At the ILC or muon colliders, they would only appear in the t channel, since they carry two lepton-number units. On the other hand, the vectors $\mathcal{W}^1$ only interact with fermions through their mixing with the SM gauge bosons. Even if this mixing can be relatively large for a heavy Higgs, this vector boson is basically invisible to hadron colliders. We should finally mention that, in principle, other exotic vector bosons in representations not considered here could exist. They cannot be single produced at colliders, nor contribute significantly to EWPD. However, if they were light enough, they could be pair produced. These exotic vector bosons, if coupled to gluons, would be seen as jets generated by their radiation.

4.7 Addendum: Operator coefficients in the effective Lagrangian

Here, we collect the results from the integration of each of the extra vector fields in Table 4.1. We give in Tables 4.7 to 4.21 the corresponding contributions to the dimension-six operator coefficients in the effective Lagrangian. The explicit expressions for the currents coupled to the different new vectors are also written. Unless otherwise stated in the tables, $F = l_L, q_L$, $f = e_R, u_R, d_R$ and $\psi = F, f$ run over all the possibilities. As stressed in Section 4.1, in order to apply our results the heavy vectors must be in the basis with diagonal mass and kinetic terms. Then, the contributions from several extra vectors are summed independently in the coefficients.

For only one of the SM replicas $\mathcal{B}$, $\mathcal{W}$ and $\mathcal{G}$, we can easily recover the effect of kinetic mixing with the SM fields. Since the rescaling of the heavy vector field $\mathcal{A}$ in Eq. (4.6) affects in the same way the current $J^{\mathcal{A}}$ and the heavy mass $M_{\mathcal{A}}$, we only need to perform the following replacements in the formulas in Tables 4.7, 4.8 and 4.9:

$$\begin{aligned}
(g_{\mathcal{B}}^{\psi,\phi})_{ij} &\to (g_{\mathcal{B}}^{\psi,\phi})_{ij} + g' g_{\mathcal{B}}^{B} Y_{\psi,\phi} \delta_{ij}, \\
(g_{\mathcal{W}}^{F,\phi})_{ij} &\to (g_{\mathcal{W}}^{F,\phi})_{ij} + g g_{\mathcal{W}}^{W} \delta_{ij}, \\
(g_{\mathcal{G}}^{\psi})_{ij} &\to (g_{\mathcal{G}}^{\psi})_{ij} + g_s g_{\mathcal{G}}^{G} \delta_{ij}.
\end{aligned} \tag{4.16}$$

$\mathcal{B}_\mu \sim (1,1)_0$

$$J^{\mathcal{B}}_\mu = (g^l_{\mathcal{B}})_{ij}\overline{l^i_L}\gamma_\mu l^j_L + (g^q_{\mathcal{B}})_{ij}\overline{q^i_L}\gamma_\mu q^i_L + (g^e_{\mathcal{B}})_{ij}\overline{e^i_R}\gamma_\mu e^j_R + (g^u_{\mathcal{B}})_{ij}\overline{u^i_R}\gamma_\mu u^j_R + (g^d_{\mathcal{B}})_{ij}\overline{d^i_R}\gamma_\mu d^j_R + (g^\phi_{\mathcal{B}}\ \phi^\dagger i D_\mu \phi + \text{h.c.})$$

Four-Fermion Operators

- **LLLL**

$$\frac{\left(\alpha^{(1(,1))}_{FF'}\right)_{ijkl}}{\Lambda^2} = -\frac{\left(g^F_{\mathcal{B}}\right)_{ij}\left(g^{F'}_{\mathcal{B}}\right)_{kl}}{M^2_{\mathcal{B}}}$$

- **RRRR**

$$\frac{\left(\alpha^{(1)}_{ff'}\right)_{ijkl}}{\Lambda^2} = -\frac{\left(g^f_{\mathcal{B}}\right)_{ij}\left(g^{f'}_{\mathcal{B}}\right)_{kl} + \left(g^f_{\mathcal{B}}\right)_{il}\left(g^{f'}_{\mathcal{B}}\right)_{kj}\delta_{ff',ee}}{\left(1+\delta_{ff',ee}\right)M^2_{\mathcal{B}}}$$

- **LRRL**

$$\frac{\left(\alpha_{Ff}\right)_{ijkl}}{\Lambda^2} = \frac{2\left(g^F_{\mathcal{B}}\right)_{il}\left(g^f_{\mathcal{B}}\right)_{kj}}{M^2_{\mathcal{B}}}$$

$$\frac{\left(\alpha^{(1)}_{qf}\right)_{ijkl}}{\Lambda^2} = \frac{2\left(g^q_{\mathcal{B}}\right)_{il}\left(g^f_{\mathcal{B}}\right)_{kj}}{3M^2_{\mathcal{B}}}$$

$$\frac{\left(\alpha^{(8)}_{qf}\right)_{ijkl}}{\Lambda^2} = \frac{\left(g^q_{\mathcal{B}}\right)_{il}\left(g^f_{\mathcal{B}}\right)_{kj}}{M^2_{\mathcal{B}}}$$

SVF and SF Operators

$$\frac{\left(\alpha^{(1)}_{\phi\psi}\right)_{ij}}{\Lambda^2} = -\frac{\left(g^\psi_{\mathcal{B}}\right)_{ij}g^\phi_{\mathcal{B}}}{M^2_{\mathcal{B}}}$$

$$\frac{\left(\alpha_{u\phi}\right)_{ij}}{\Lambda^2} = \frac{\left(g^\phi_{\mathcal{B}}\right)^2}{2M^2_{\mathcal{B}}}V^\dagger_{ij}y^u_{jj}$$

$$\frac{\left(\alpha_{f\phi}\right)_{ij}}{\Lambda^2} = \frac{\left(\alpha^\dagger_{u\phi}\right)_{ij}}{\Lambda^2}\frac{y^f_{ii}\delta_{ij}}{V_{ij}y^u_{jj}} \quad (f = e, d)$$

Oblique Operators

$$\frac{\alpha^{(1)}_\phi}{\Lambda^2} = -\frac{\text{Re}\left[\left(g^\phi_{\mathcal{B}}\right)^2\right]}{M^2_{\mathcal{B}}}$$

$$\frac{\alpha^{(3)}_\phi}{\Lambda^2} = -\frac{2\text{Re}\left[g^\phi_{\mathcal{B}}\right]^2}{M^2_{\mathcal{B}}}$$

$$\frac{\alpha_{\phi 6}}{\Lambda^2} = \frac{6\lambda_\phi \text{Re}\left[\left(g^\phi_{\mathcal{B}}\right)^2\right]}{M^2_{\mathcal{B}}}$$

$$\frac{\alpha_{\phi 4}}{\Lambda^2} = -\frac{\mu^2_\phi}{6\lambda_\phi}\frac{\alpha_{\phi 6}}{\Lambda^2}$$

Table 4.7: Operators arising from the integration of a $\mathcal{B}$ vector field.

$\mathcal{W}_\mu \sim (1, \text{Adj})_0$

$$J^{\mathcal{W}}_{a\ \mu} = (g^l_{\mathcal{W}})_{ij}\overline{l^i_L}\gamma_\mu\frac{\sigma_a}{2}l^j_L + (g^q_{\mathcal{W}})_{ij}\overline{q^i_L}\gamma_\mu\frac{\sigma_a}{2}q^j_L + (g^\phi_{\mathcal{W}}\ \phi^\dagger\frac{\sigma_a}{2}iD_\mu\phi + \text{h.c.})$$

Four-Fermion Operators

- **LLLL**

$$\frac{\left(\alpha^{((1),3)}_{FF'}\right)_{ijkl}}{\Lambda^2} = -\frac{\left(g^F_{\mathcal{W}}\right)_{ij}\left(g^{F'}_{\mathcal{W}}\right)_{kl}}{4M^2_{\mathcal{W}}}$$

SVF and SF Operators

$$\frac{\left(\alpha^{(3)}_{\phi F}\right)_{ij}}{\Lambda^2} = -\frac{\left(g^F_{\mathcal{W}}\right)_{ij}g^\phi_{\mathcal{W}}}{4M^2_{\mathcal{W}}}$$

$$\frac{\left(\alpha_{u\phi}\right)_{ij}}{\Lambda^2} = \frac{\left(g^\phi_{\mathcal{W}}\right)^2}{8M^2_{\mathcal{W}}}V^\dagger_{ij}y^u_{jj}$$

$$\frac{\left(\alpha_{f\phi}\right)_{ij}}{\Lambda^2} = \frac{\left(\alpha^\dagger_{u\phi}\right)_{ij}}{\Lambda^2}\frac{y^f_{ii}\delta_{ij}}{V_{ij}y^u_{jj}} \quad (f = e, d)$$

Oblique Operators

$$\frac{\alpha^{(1)}_\phi}{\Lambda^2} = -\frac{\text{Re}\left[\left(g^\phi_{\mathcal{W}}\right)^2\right] + 2\left|g^\phi_{\mathcal{W}}\right|^2}{4M^2_{\mathcal{W}}}$$

$$\frac{\alpha^{(3)}_\phi}{\Lambda^2} = \frac{\text{Im}\left[g^\phi_{\mathcal{W}}\right]^2}{2M^2_{\mathcal{W}}}$$

$$\frac{\alpha_{\phi 6}}{\Lambda^2} = 6\lambda_\phi\frac{\text{Re}\left[\left(g^\phi_{\mathcal{W}}\right)^2\right]}{4M^2_{\mathcal{W}}}$$

$$\frac{\alpha_{\phi 4}}{\Lambda^2} = -\frac{\mu^2_\phi}{6\lambda_\phi}\frac{\alpha_{\phi 6}}{\Lambda^2}$$

Table 4.8: Operators arising from the integration of a $\mathcal{W}$ vector field.

$$\boldsymbol{\mathcal{G}_\mu \sim (\mathrm{Adj},1)_0}$$

$$J^{\mathcal{G}}_{A\ \mu} = (g^q_{\mathcal{G}})_{ij}\overline{q^i_L}\gamma_\mu\tfrac{\lambda_A}{2}q^j_L + (g^u_{\mathcal{G}})_{ij}\overline{u^i_R}\gamma_\mu\tfrac{\lambda_A}{2}u^j_R + (g^d_{\mathcal{G}})_{ij}\overline{d^i_R}\gamma_\mu\tfrac{\lambda_A}{2}d^j_R$$

Four-Fermion Operators

- **LLLL**

$$\frac{\left(\alpha^{(8,1)}_{qq}\right)_{ijkl}}{\Lambda^2} = -\frac{\left(g^q_{\mathcal{G}}\right)_{ij}\left(g^q_{\mathcal{G}}\right)_{kl}}{4M^2_{\mathcal{G}}}$$

- **LRRL**

$$\frac{\left(\alpha^{(1)}_{qf}\right)_{ijkl}}{\Lambda^2} = \frac{8\left(g^q_{\mathcal{G}}\right)_{il}\left(g^f_{\mathcal{G}}\right)_{kj}}{9M^2_{\mathcal{G}}} \qquad (f=u,d)$$

$$\frac{\left(\alpha^{(8)}_{qf}\right)_{ijkl}}{\Lambda^2} = -\frac{\left(g^q_{\mathcal{G}}\right)_{il}\left(g^f_{\mathcal{G}}\right)_{kj}}{3M^2_{\mathcal{G}}}$$

- **RRRR**

$$\frac{\left(\alpha^{(8)}_{ff'}\right)_{ijkl}}{\Lambda^2} = -\frac{\left(g^f_{\mathcal{G}}\right)_{ij}\left(g^{f'}_{\mathcal{G}}\right)_{kl}}{4M^2_{\mathcal{G}}} \qquad (ff' = uu, dd, ud)$$

Table 4.9: Operators arising from the integration of a $\mathcal{G}$ vector field.

$$\boldsymbol{\mathcal{H}_\mu \sim (\mathrm{Adj},\mathrm{Adj})_0}$$

$$J^{\mathcal{H}}_{a,A\ \mu} = (g^q_{\mathcal{G}})_{ij}\overline{q^i_L}\gamma_\mu\tfrac{\sigma_a}{2}\tfrac{\lambda_A}{2}q^j_L$$

Four-Fermion Operators

- **LLLL**

$$\frac{\left(\alpha^{(8,3)}_{qq}\right)_{ijkl}}{\Lambda^2} = -\frac{\left(g^q_{\mathcal{H}}\right)_{ij}\left(g^q_{\mathcal{H}}\right)_{kl}}{16M^2_{\mathcal{H}}}$$

Table 4.10: Operators arising from the integration of a $\mathcal{H}$ vector field.

$$\boldsymbol{\mathcal{B}^1_\mu \sim (1,1)_1}$$

$$J^{\mathcal{B}^1}_\mu = \left(g^{du}_{\mathcal{B}^1}\right)_{ij}\overline{d^i_R}\gamma_\mu u^j_R + g^\phi_{\mathcal{B}^1} iD_\mu\phi^T i\sigma_2\phi$$

Four-Fermion Operators

- **RRRR**

$$\frac{\left(\alpha^{(1)}_{ud}\right)_{ijkl}}{\Lambda^2} = -\frac{\left(g^{du}_{\mathcal{B}^1}\right)^\dagger_{ij}\left(g^{du}_{\mathcal{B}^1}\right)_{kl}}{3M^2_{\mathcal{B}^1}} \qquad \frac{\left(\alpha^{(8)}_{ud}\right)_{ijkl}}{\Lambda^2} = -\frac{\left(g^{du}_{\mathcal{B}^1}\right)^\dagger_{ij}\left(g^{du}_{\mathcal{B}^1}\right)_{kl}}{2M^2_{\mathcal{B}^1}}$$

SVF Operators

$$\frac{\alpha_{\phi ud}}{\Lambda^2} = \frac{g^\phi_{\mathcal{B}^1}\left(g^{du}_{\mathcal{B}^1}\right)^\dagger_{ij}}{M^2_{\mathcal{B}^1}}$$

Oblique Operators

$$\frac{\alpha^{(1)}_\phi}{\Lambda^2} = -\frac{3\left|g^\phi_{\mathcal{B}^1}\right|^2}{2M^2_{\mathcal{B}^1}}$$

$$\frac{\alpha^{(3)}_\phi}{\Lambda^2} = \frac{\left|g^\phi_{\mathcal{B}^1}\right|^2}{M^2_{\mathcal{B}^1}}$$

Table 4.11: Operators arising from the integration of a $\mathcal{B}^1$ vector field.

$\mathcal{W}^1_\mu \sim (1, \mathrm{Adj})_1$	
$J^{\mathcal{W}^1}_\mu = g^\phi_{\mathcal{W}^1} i D_\mu \phi^T i\sigma_2 \frac{\sigma_a}{2} \phi$	
Oblique Operators	
$\frac{\alpha^{(1)}_\phi}{\Lambda^2} = -\frac{\left\lvert g^\phi_{\mathcal{W}^1}\right\rvert^2}{4M^2_{\mathcal{W}^1}}$	$\frac{\alpha^{(3)}_\phi}{\Lambda^2} = -\frac{\left\lvert g^\phi_{\mathcal{W}^1}\right\rvert^2}{4M^2_{\mathcal{W}^1}}$

Table 4.12: Operators arising from the integration of a $\mathcal{W}^1$ vector field.

$\mathcal{G}^1_\mu \sim (\mathrm{Adj}, 1)_1$	
$J^{\mathcal{G}^1}_\mu = \left(g^{du}_{\mathcal{G}^1}\right)_{ij} \overline{d^i_R} \frac{\lambda_A}{2} \gamma_\mu u^j_R$	
Four-Fermion Operators	
• **RRRR**	
$\frac{\left(\alpha^{(1)}_{ud}\right)_{ijkl}}{\Lambda^2} = -\frac{4\left(g^{du}_{\mathcal{G}^1}\right)^\dagger_{il}\left(g^{du}_{\mathcal{G}^1}\right)_{kj}}{9M^2_{\mathcal{G}^1}}$	$\frac{\left(\alpha^{(8)}_{ud}\right)_{ijkl}}{\Lambda^2} = \frac{\left(g^{du}_{\mathcal{G}^1}\right)^\dagger_{il}\left(g^{du}_{\mathcal{G}^1}\right)_{kj}}{6M^2_{\mathcal{G}^1}}$

Table 4.13: Operators arising from the integration of a $\mathcal{G}^1$ vector field.

$\mathcal{L}_\mu \sim (1, 2)_{-\frac{3}{2}}$
$J^{\mathcal{L}}_\mu = \left(g^{el}_{\mathcal{L}}\right)_{ij} \overline{e^{c\ i}_R} \gamma_\mu l^j_L$
Four-Fermion Operators
• **LRRL**
$\frac{(\alpha_{le})_{ijkl}}{\Lambda^2} = -\frac{2\left(g^{el}_{\mathcal{L}}\right)^\dagger_{ik}\left(g^{el}_{\mathcal{L}}\right)_{jl}}{M^2_{\mathcal{L}}}$

Table 4.14: Operators arising from the integration of a $\mathcal{L}$ vector field.

$$\mathcal{U}_\mu^2 \sim (3,1)_{\frac{2}{3}}$$

$$J_\mu^{\mathcal{U}^2} = \left(g_{\mathcal{U}^2}^{ed}\right)_{ij} \overline{e_R^i}\gamma_\mu d_R^j + (g_{\mathcal{U}^2}^{lq})_{ij}\overline{l_L^i}\gamma_\mu q_L^j$$

Four-Fermion Operators

- **LLLL**

$$\frac{\left(\alpha_{lq}^{(1)}\right)_{ijkl}}{\Lambda^2} = -\frac{\left(g_{\mathcal{U}^2}^{lq}\right)^\dagger_{kj}\left(g_{\mathcal{U}^2}^{lq}\right)_{il}}{2M_{\mathcal{U}^2}^2} \qquad \frac{\left(\alpha_{lq}^{(3)}\right)_{ijkl}}{\Lambda^2} = \frac{\left(\alpha_{lq}^{(1)}\right)_{ijkl}}{\Lambda^2}$$

- **RRRR**

$$\frac{(\alpha_{ed})_{ijkl}}{\Lambda^2} = -\frac{\left(g_{\mathcal{U}^2}^{ed}\right)^\dagger_{kj}\left(g_{\mathcal{U}^2}^{ed}\right)_{il}}{M_{\mathcal{U}^2}^2}$$

- **LRRL**

$$\frac{\left(\alpha_{qde}\right)_{ijkl}}{\Lambda^2} = \frac{2\left(g_{\mathcal{U}^2}^{ed}\right)^\dagger_{kj}\left(g_{\mathcal{U}^2}^{lq}\right)_{il}}{M_{\mathcal{U}^2}^2}$$

Table 4.15: Operators arising from the integration of a $\mathcal{U}^2$ vector field.

$$\mathcal{U}_\mu^5 \sim (3,1)_{\frac{5}{3}}$$

$$J_\mu^{\mathcal{U}^5} = \left(g_{\mathcal{U}^5}^{eu}\right)_{ij} \overline{e_R^i}\gamma_\mu u_R^j$$

Four-Fermion Operators

- **RRRR**

$$\frac{(\alpha_{eu})_{ijkl}}{\Lambda^2} = -\frac{\left(g_{\mathcal{U}^5}^{eu}\right)^\dagger_{kj}\left(g_{\mathcal{U}^5}^{eu}\right)_{il}}{M_{\mathcal{U}^5}^2}$$

Table 4.16: Operators arising from the integration of a $\mathcal{U}^5$ vector field.

$$\mathcal{Q}_\mu^1 \sim (3,2)_{\frac{1}{6}}$$

$$J_\mu^{\mathcal{Q}^1} = \left(g_{\mathcal{Q}^1}^{ul}\right)_{ij} \overline{u_R^{c\,i}}\gamma_\mu l_L^j + \left(g_{\mathcal{Q}^1}^{dq}\right)_{ij} \epsilon_{ABC}\overline{d_R^{i\,B}}\gamma_\mu i\sigma_2 q_L^{c\,j\,C}$$

Four-Fermion Operators

- **LRRL**

$$\frac{(\alpha_{lu})_{ijkl}}{\Lambda^2} = -\frac{2\left(g_{\mathcal{Q}^1}^{ul}\right)^\dagger_{ik}\left(g_{\mathcal{Q}^1}^{ul}\right)_{jl}}{M_{\mathcal{Q}^1}^2}$$

$$\frac{\left(\alpha_{qd}^{(1)}\right)_{ijkl}}{\Lambda^2} = \frac{4\left(g_{\mathcal{Q}^1}^{dq}\right)^\dagger_{lj}\left(g_{\mathcal{Q}^1}^{dq}\right)_{ki}}{3M_{\mathcal{Q}^1}^2} \qquad \frac{\left(\alpha_{qd}^{(8)}\right)_{ijkl}}{\Lambda^2} = -\frac{\left(g_{\mathcal{Q}^1}^{dq}\right)^\dagger_{lj}\left(g_{\mathcal{Q}^1}^{dq}\right)_{ki}}{M_{\mathcal{Q}^1}^2}$$

- **LRRL: B−L**

$$\frac{\left(\alpha_{lqdu}\right)_{ijkl}}{\Lambda^2} = \frac{2\left(g_{\mathcal{Q}^1}^{ul}\right)^\dagger_{il}\left(g_{\mathcal{Q}^1}^{dq}\right)_{kj}}{M_{\mathcal{Q}^1}^2}$$

Table 4.17: Operators arising from the integration of a $\mathcal{Q}^1$ vector field.

$$\boldsymbol{\mathcal{Q}^5_\mu \sim (3,2)_{-\frac{5}{6}}}$$

$$J_\mu^{\mathcal{Q}^5} = \left(g^{dl}_{\mathcal{Q}^5}\right)_{ij} \overline{d_R^{c\,i}}\gamma_\mu l_L^j + \left(g^{eq}_{\mathcal{Q}^5}\right)_{ij} \overline{e_R^{c\,i}}\gamma_\mu q_L^j + \left(g^{uq}_{\mathcal{Q}^5}\right)_{ij} \epsilon_{ABC}\overline{u_R^{i\,B}}\gamma_\mu i\sigma_2 q_L^{c\,j\,C}$$

Four-Fermion Operators

- **LRRL**

$$\frac{(\alpha_{ld})_{ijkl}}{\Lambda^2} = -\frac{2\left(g^{dl}_{\mathcal{Q}^5}\right)^\dagger_{ik}\left(g^{dl}_{\mathcal{Q}^5}\right)_{jl}}{M^2_{\mathcal{Q}^5}} \qquad \frac{(\alpha_{qe})_{ijkl}}{\Lambda^2} = -\frac{2\left(g^{eq}_{\mathcal{Q}^5}\right)^\dagger_{ik}\left(g^{eq}_{\mathcal{Q}^5}\right)_{jl}}{M^2_{\mathcal{Q}^5}}$$

$$\frac{\left(\alpha_{qde}\right)_{ijkl}}{\Lambda^2} = -\frac{2\left(g^{dl}_{\mathcal{Q}^5}\right)^\dagger_{ik}\left(g^{eq}_{\mathcal{Q}^5}\right)_{jl}}{M^2_{\mathcal{Q}^5}}$$

$$\frac{\left(\alpha^{(1)}_{qu}\right)_{ijkl}}{\Lambda^2} = \frac{4\left(g^{uq}_{\mathcal{Q}^5}\right)^\dagger_{lj}\left(g^{uq}_{\mathcal{Q}^5}\right)_{ki}}{3M^2_{\mathcal{Q}^5}} \qquad \frac{\left(\alpha^{(8)}_{qu}\right)_{ijkl}}{\Lambda^2} = -\frac{\left(g^{uq}_{\mathcal{Q}^5}\right)^\dagger_{lj}\left(g^{uq}_{\mathcal{Q}^5}\right)_{ki}}{M^2_{\mathcal{Q}^5}}$$

- **LRRL: B−L**

$$\frac{\left(\alpha_{lqdu}\right)_{ijkl}}{\Lambda^2} = \frac{2\left(g^{dl}_{\mathcal{Q}^5}\right)^\dagger_{ik}\left(g^{uq}_{\mathcal{Q}^5}\right)_{lj}}{M^2_{\mathcal{Q}^5}} \qquad \frac{\left(\alpha_{qqeu}\right)_{ijkl}}{\Lambda^2} = -\frac{2\left(g^{eq}_{\mathcal{Q}^5}\right)^\dagger_{ik}\left(g^{uq}_{\mathcal{Q}^5}\right)_{lj}}{M^2_{\mathcal{Q}^5}}$$

Table 4.18: Operators arising from the integration of a $\mathcal{Q}^5$ vector field.

$$\boldsymbol{\mathcal{X}_\mu \sim (3,\mathrm{Adj})_{\frac{2}{3}}}$$

$$J_\mu^{\mathcal{X}} = \left(g^{lq}_{\mathcal{X}}\right)_{ij} \overline{l_L^i}\gamma_\mu \tfrac{\sigma_a}{2} q_L^j$$

Four-Fermion Operators

- **LLLL**

$$\frac{\left(\alpha^{(1)}_{lq}\right)_{ijkl}}{\Lambda^2} = -\frac{3\left(g^{lq}_{\mathcal{X}}\right)^\dagger_{kj}\left(g^{lq}_{\mathcal{X}}\right)_{il}}{8M^2_{\mathcal{X}}} \qquad \frac{\left(\alpha^{(3)}_{lq}\right)_{ijkl}}{\Lambda^2} = \frac{\left(g^{lq}_{\mathcal{X}}\right)^\dagger_{kj}\left(g^{lq}_{\mathcal{X}}\right)_{il}}{8M^2_{\mathcal{X}}}$$

Table 4.19: Operators arising from the integration of a $\mathcal{X}$ vector field.

$$\boldsymbol{\mathcal{Y}^1_\mu \sim (\overline{6},2)_{\frac{1}{6}}}$$

$$J_\mu^{\mathcal{Y}^1} = \left(g^{dq}_{\mathcal{Y}^1}\right)_{ij} \overline{d_R^{i(A|}}\gamma_\mu i\sigma_2 q_L^{c\,j|B)}$$

Four-Fermion Operators

- **LRRL**

$$\frac{\left(\alpha^{(1)}_{qd}\right)_{ijkl}}{\Lambda^2} = -\frac{4\left(g^{dq}_{\mathcal{Y}^1}\right)^\dagger_{lj}\left(g^{dq}_{\mathcal{Y}^1}\right)_{ki}}{3M^2_{\mathcal{Y}^1}} \qquad \frac{\left(\alpha^{(8)}_{qd}\right)_{ijkl}}{\Lambda^2} = -\frac{\left(g^{dq}_{\mathcal{Y}^1}\right)^\dagger_{lj}\left(g^{dq}_{\mathcal{Y}^1}\right)_{ki}}{2M^2_{\mathcal{Y}^1}}$$

Table 4.20: Operators arising from the integration of a $\mathcal{Y}^1$ vector field. $(A|\cdots|B) = \frac{1}{2}(AB+BA)$ stands for the symmetric combination of color indices.

$$\boldsymbol{\mathcal{Y}^5_\mu \sim \left(\overline{6}, 2\right)_{-\frac{5}{6}}}$$

$$J^{\mathcal{Y}^5}_\mu = \left(g^{uq}_{\mathcal{Y}^5}\right)_{ij} \overline{u^{i(A|}_R} \gamma_\mu i\sigma_2 q^{c\ j|B)}_L$$

Four-Fermion Operators

• **LRRL**

$$\frac{\left(\alpha^{(1)}_{qu}\right)_{ijkl}}{\Lambda^2} = -\frac{4\left(g^{uq}_{\mathcal{Y}^5}\right)^\dagger_{lj}\left(g^{uq}_{\mathcal{Y}^5}\right)_{ki}}{3M^2_{\mathcal{Y}^5}} \qquad \frac{\left(\alpha^{(8)}_{qu}\right)_{ijkl}}{\Lambda^2} = -\frac{\left(g^{uq}_{\mathcal{Y}^5}\right)^\dagger_{lj}\left(g^{uq}_{\mathcal{Y}^5}\right)_{ki}}{2M^2_{\mathcal{Y}^5}}$$

Table 4.21: Operators arising from the integration of a $\mathcal{Y}^5$ vector field.

Chapter 5

Beyond the Standard Model dimension-six effective Lagrangian

Despite its generality, the basis of dimension five and six operators introduced in Chapter 1 and used throughout the subsequent chapters is not sufficient if there are new light particles that can be produced on their mass shell. It is easy to adapt the effective method to that situation. As only the light degrees of freedom of the theory as well as its symmetries are required in order to build the most general effective Lagrangian, we simply need to add more fields and maybe to impose additional symmetry requirements. The only limitations we have in doing so is that the SM particles and symmetries must be incorporated to the final effective Lagrangian. On the other hand, additional light particles are ruled out by current observations, unless they have escaped direct detection, either because their interactions are too small, or because we lack precision in measuring those processes where they may be involved.

In the previous chapters we have examined the available EWPD, looking for some space to accommodate the existence of new heavy particles. We have been checking the consistency of such extensions with observations, which ultimately reveals that to understand the data the best choice is probably the SM. But we did not consider the only observational evidence we have of physics beyond the SM: neutrino oscillations. The observed neutrino properties are in agreement with the minimal extension of the SM resulting from the sole addition of neutrino masses [18, 167, 168]. Neutrinos are massless within the SM because there are not neutrino singlet counterparts, Higgs fields transform as an electroweak doublet, and the theory is renormalizable. However, neutrino masses are generated relaxing any of these conditions. Within the effective Lagrangian approach we have been using up to now, which assumes the minimal SM fermion content, neutrino masses can be explained since we allow for higher-dimensional operators. This is the case of the lepton number violating dimension-five Weinberg operator $\mathcal{O}_5$ [60]. As we saw in Chapter 2, after EWSB $\mathcal{O}_5$ generates Majorana mass terms for the SM neutrinos

$$\frac{(\alpha_5)_{ij}}{\Lambda}\,(\mathcal{O}_5)_{ij} = \frac{(\alpha_5)_{ij}}{\Lambda}\overline{l_L^{i\,c}}\tilde{\phi}^*\tilde{\phi}^\dagger l_L^j \overset{\text{EWSB}}{\longrightarrow} \frac{(\alpha_5)_{ij}}{\Lambda}\frac{v^2}{2}\overline{\nu_L^{i\,c}}\nu_L^j\,, \quad m_i^\nu = -(\mathcal{U}_L^{\nu\,T})_{ik}\frac{(\alpha_5)_{kl}}{\Lambda}v^2(\mathcal{U}_L^\nu)_{li}\,, \tag{5.1}$$

with $\mathcal{U}_L^\nu$ the corresponding unitary transformation diagonalizing the mass matrix. Assuming l_L^i in the charged lepton mass eigenstate basis, this gives the charged current mixing upon diagonalization

$$\mathcal{L}_{\text{CC}} = -\frac{g}{\sqrt{2}}U_{ij}W_\mu^-\overline{e_L^i}\gamma^\mu\nu_L^j + \text{h.c.}, \quad U = \mathcal{U}_L^\nu\,. \tag{5.2}$$

The tiny neutrino masses require very small values for the coefficients $(\alpha_5)_{ij}/\Lambda$ multiplying $(\mathcal{O}_5)_{ij}$, which are so minuscule because $(\alpha_5)_{ij}$ are extremely small ($\sim 10^{-12}$ for $\Lambda \sim v$) or Λ is very large ($\sim 10^{14}$ GeV for $(\alpha_5)_{ij} \sim 1$).

On the other hand, Dirac masses cannot be described within this minimal realization as there are no singlet RH neutrinos in the light spectrum. Indeed, the addition of three RH neutrinos ν_R^i allows for arbitrary Dirac neutrino masses after EWSB,

$$-y^\nu_{ij}\overline{l^i_L}\tilde{\phi}\nu^j_R + \text{h.c.} \overset{\text{EWSB}}{\longrightarrow} -y^\nu_{ij}\frac{v}{\sqrt{2}}\overline{\nu^i_L}\nu^j_R + \text{h.c.}\,, \quad m^\nu_i = (\mathcal{U}^{\nu\,\dagger}_L)_{ik}y^\nu_{kl}\frac{v}{\sqrt{2}}(\mathcal{U}^\nu_R)_{li}\,, \tag{5.3}$$

similarly as for up quarks but with much smaller Yukawa couplings y^ν_{ij}. This lepton number conserving term and the corresponding neutrino mass matrix then can also provide the observed neutrino masses and charged current mixing.

Neutrino oscillations, which are the only manifestation of neutrino masses and mixing up to now, are well described by two mass splitings $\Delta m^2_{ij} \equiv m^{\nu\,2}_i - m^{\nu\,2}_j$ and the PMNS mixing matrix [63] U in Eq. (5.2). Therefore, these experiments cannot distinguish between Dirac and Majorana masses because in both cases the charged gauge interactions are given by $\mathcal{U}^\nu_L$, and neutral gauge interactions also only involve LH neutrinos and are universal at lowest order [169] (see also [170]). Note also that neutrino masses, bounded to be less than 0.1 eV [171] and then very small compared to other mass parameters in the theory, and in particular to the electroweak scale $v \approx 246$ GeV, are unobservable in laboratory experiments where the relevant energies are much larger, and generically in experiments sensitive to electroweak interactions ranging from muon decay to particle collisions at LHC. Thus, the question is whether light neutrinos have further observable interactions beyond their masses. This can be answered considering the corresponding effective Lagrangian and fitting it to present data. In this regard, though the standard effective Lagrangian suffices to describe non-standard LH neutrino interactions, answering the previous question in the most general scenario requires to extend the formalism to the case where we consider also light RH neutrinos within the fermionic spectrum. On the other hand, as the neutrino mass scale is so small, it is appropriate to assume that new physics parameterized by dimension-six operators involving only SM fields or light RH neutrinos is lepton number conserving. Limits on those operators for LH neutrinos can be found in [102, 172, 173, 174], being typically at the per cent level in definite models and near the expected sensitivity in neutrino oscillation experiments. Model-independent bounds can be one order of magnitude larger. In the present chapter, however, we would like to turn our attention to the interactions of the RH counterparts, since if some of them are large enough to give any observable effect they could guide us in the determination of the existence of these extra neutral fermions. Therefore, we devote the first section of this chapter to introduce the corresponding effective Lagrangian extension. We then comment on the new interactions effects at the Lagrangian level after EWSB, and whether they have any observable impact on the EWPD used in our fits. In the second section we emphasize that a muon based neutrino factory could show the existence of light RH neutrinos, if a deficit in the number of detected events is observed at a near detector. We find that this could be as large as $\sim 10\%$ if the size of the new interactions saturate the present limits from EWPD. This is not excluded by the oscillation experiments performed up to now. We also present a simple model realizing such a scenario, obtained by adding RH neutrinos to the minimal SM, together with an extra scalar doublet and a triplet of hypercharge 1. In this case, however, the possible deficit is reduced by a factor of ~ 3, and the Yukawa couplings must be adequately chosen. This is also generically required if lepton flavor violation must be below present bounds.

5.1 The dimension-six effective Lagrangian with light right-handed neutrinos

Describing light RH neutrino interactions within the effective Lagrangian only requires to complete the basis of tree-level generated operators introduced in Table 1.1 with those in Table 5.1. For the complete set including also operators that may arise at the loop order see Ref. [175], although in that reference the RH neutrinos are assumed to have masses of few hundreds of GeV (Note that the operators $\mathcal{O}'_{NN}$ in Eq. (6) and $\mathcal{O}_{QNdQ}$ in Eq. (7) in that reference are redundant and therefore do not appear in Table 5.1.). The extended basis of tree-level operators has one more operator of dimension five, sixteen four-fermion interactions, and two SVF and one SF operators. We have also included the few new dimension-six interactions violating B and L, but preserving $B-L$, that can be built if we include the RH neutrinos. As we argued in Chapter 1, these last interactions involve three quarks and one lepton, and the quark combination must carry zero hypercharge in order to preserve $U(1)_Y$ gauge invariance. This leaves only two possible combinations of quarks: $d_R q_L q_L$ and $u_R d_R d_R$, and the latter can be combined in two different ways with the ν_R. Finally, in this case it is also possible to construct a dimension-six operator violating $B-L$. This is the operator we call $\mathcal{O}_{\nu^c\nu}$, and is built from four neutrino singlets, so it violates L in four units.

	Operator	Notation	Operator	Notation
	$\left(\phi^\dagger\phi\right)\left(\overline{\nu_R}\nu_R^c\right)$	$\mathcal{O}_{5\nu}$		
RRRR	$\frac{1}{2}\left(\overline{\nu_R}\gamma_\mu\nu_R\right)\left(\overline{\nu_R}\gamma^\mu\nu_R\right)$	$\mathcal{O}_{\nu\nu}$	$\left(\overline{e_R}\gamma_\mu e_R\right)\left(\overline{\nu_R}\gamma^\mu\nu_R\right)$	$\mathcal{O}_{e\nu}$
	$\left(\overline{u_R}\gamma_\mu u_R\right)\left(\overline{\nu_R}\gamma^\mu\nu_R\right)$	$\mathcal{O}_{u\nu}$	$\left(\overline{d_R}\gamma_\mu d_R\right)\left(\overline{\nu_R}\gamma^\mu\nu_R\right)$	$\mathcal{O}_{d\nu}$
	$\left(\overline{u_R}\gamma_\mu d_R\right)\left(\overline{e_R}\gamma^\mu\nu_R\right)$	$\mathcal{O}_{ud\nu}$		
LRRL	$\left(\overline{l_L}\nu_R\right)\left(\overline{\nu_R}l_L\right)$	$\mathcal{O}_{l\nu}$	$\left(\overline{q_L}\nu_R\right)\left(\overline{\nu_R}q_L\right)$	$\mathcal{O}_{q\nu}$
	$\left(\overline{l_L}\nu_R\right)\left(\overline{u_R}q_L\right)$	$\mathcal{O}_{l\nu u}$	$\left(\overline{q_L}u_R\right)\left(\overline{\nu_R}l_L\right)$	$\mathcal{O}_{qu\nu l}$
	$\epsilon_{ABC}\left(\overline{q_L^A}i\sigma_2 q_L^{c\,B}\right)\left(\overline{\nu_R}d_R^{c\,C}\right)$	$\mathcal{O}_{qq\nu d}$		
LRLR	$\left(\overline{l_L}e_R\right)i\sigma_2\left(\overline{l_L}\nu_R\right)$	$\mathcal{O}_{ll}$	$\left(\overline{l_L}\nu_R\right)i\sigma_2\left(\overline{q_L}d_R\right)$	$\mathcal{O}_{ql}$
	$\left(\overline{l_L}d_R\right)i\sigma_2\left(\overline{q_L}\nu_R\right)$	$\mathcal{O}_{ql'}$		
	$\epsilon_{ABC}\left(\overline{u_R^{c\,A}}d_R^B\right)\left(\overline{d_R^{c\,C}}\nu_R\right)$	$\mathcal{O}_{udd\nu}$	$\epsilon_{ABC}\left(\overline{u_R^{c\,A}}\nu_R\right)\left(\overline{d_R^{c\,B}}d_R^C\right)$	$\mathcal{O}_{u\nu dd}$
	$\left(\overline{\nu_R^c}\nu_R\right)\left(\overline{\nu_R^c}\nu_R\right)$	$\mathcal{O}_{\nu^c\nu}$		
SVF	$\left(\phi^\dagger iD_\mu\phi\right)\left(\overline{\nu_R}\gamma^\mu\nu_R\right)$	$\mathcal{O}^{(1)}_{\phi\nu}$	$\left(\phi^T i\sigma_2 iD_\mu\phi\right)\left(\overline{\nu_R}\gamma^\mu e_R\right)$	$\mathcal{O}_{\phi\nu e}$
SF	$\left(\phi^\dagger\phi\right)\left(\overline{l_L}i\sigma_2\phi^*\nu_R\right)$	$\mathcal{O}_{\nu\phi}$		

Table 5.1: Dimension five and six operators completing Table 1.1, in the case that RH neutrinos are light. Transposition of the second $SU(2)_L$ doublet is understood in the LRLR four-fermion operators.

Following the discussion in Chapter 2, after EWSB some of the new operators will correct neutrino masses and interactions. Thus, whereas the Weinberg operator $\mathcal{O}_5$ gives Majorana masses to the SM neutrinos, the corresponding corrections to the SM neutrino Dirac masses are introduced by $\mathcal{O}_{\nu\phi}$. The extra neutral singlets can also receive extra Majorana masses from $\mathcal{O}_{5\nu}$. Both

operators, $\mathcal{O}_{\nu\phi}$ and $\mathcal{O}_{5\nu}$, also generate additional Yukawa interactions with the Higgs boson:

$$\begin{aligned}
\Delta\mathcal{L}_H &= -\frac{1}{\sqrt{2}} H \left(1+\delta^U y\right) \left[\left(y^\nu_{ii}\delta_{ij} + \delta y^\nu_{ij}\right) \overline{\nu^i_L} \nu^j_R + \delta y^{\nu^c}_{ij} \overline{\nu^i_R} \nu^{jc}_R + \text{h.c.}\right], \\
\delta y^\nu_{ij} &= -\left((U\alpha_{\nu\phi})_{ij} + \frac{1}{4}\left(U\alpha_{\nu\phi} + \text{h.c.}\right)_{ii} \delta_{ij} \right) \frac{v^2}{\Lambda^2}, \\
\delta y^{\nu^c}_{ij} &= -\sqrt{2}\left(\alpha_{5\nu}\right)_{ij} \frac{v}{\Lambda},
\end{aligned} \tag{5.4}$$

where $\delta^U y$ is given by Eq. (2.74) and we have assumed, as we did for the other fermions, that the RH singlets are chosen in the basis of mass eigenstates in absence of higher-dimensional operators. As we saw, Yukawa interactions for the SM fermions had no effect in the electroweak precision observables included in our fits but may be constrained by FCNC processes. In this case, however, the strongest bound comes from the tiny neutrino masses, which make the above interactions unobservable. Other dimension-six operators are not bounded by neutrino masses and could eventually yield sizable effects. This might be the case of $\mathcal{O}^{(1)}_{\phi\nu}$ which induces neutrino RH neutral currents as well as derivative couplings with the Higgs boson, or $\mathcal{O}_{\phi\nu e}$ which introduces RH leptonic charged current interactions:

$$\Delta\mathcal{L}_{\text{NC}} = -\frac{e}{sc}\left(\delta^D g^\nu_R\right)_{ij} Z_\mu \, \overline{\nu^i_R}\gamma^\mu \nu^j_R, \qquad \delta^D g^\nu_R = -\frac{1}{4}\left(\alpha^{(1)}_{\phi\nu} + \text{h.c.}\right)\frac{v^2}{\Lambda^2},$$

$$\Delta\mathcal{L}_{\text{CC}} = -\frac{e}{\sqrt{2}s} W^+_\mu \left(\delta U^\dagger_R\right)_{ij} \overline{\nu^i_R}\gamma^\mu e^j_R + \text{h.c.}, \qquad \delta U_R = -\frac{1}{2}\alpha^\dagger_{\phi\nu e}\frac{v^2}{\Lambda^2}, \tag{5.5}$$

$$\Delta\mathcal{L}_H = i h^{\nu_R}_{ij} \, \partial_\mu H \, \overline{\nu^i_R}\gamma^\mu \nu^j_R, \qquad h^{\nu_R} = \frac{1}{2}\left(\alpha^{(1)}_{\phi\nu} - \text{h.c.}\right)\frac{v}{\Lambda^2},$$

where we have directly written the global factors in the gauge couplings using the input values for the SM parameters, for the above interactions are generated starting at order $1/\Lambda^2$.

5.1.1 Contributions to precision observables

The first thing to note when analyzing the implications of the RH neutrino interactions is that, as none of them are present at order 1, for whatever observable one may consider the corresponding corrections always enter at order $1/\Lambda^4$. Then, as we expect that only $1/\Lambda^2$ effects are relevant for the precision of current data, this means that only relatively weak bounds can be derived for these interactions. From a computational point of view we must also note that, for consistency and in order to compare with any other sources of new physics, one should work out the effective Lagrangian up to dimension eight for all interactions except for those involving RH neutrinos when the effects of the latter are considered. This is so because contributions from dimension-eight operators interfering with the SM amplitudes are comparable to the quadratic new dimension-six operators contributions. In the same way, it is also required to extend the formulae in Chapter 2 to include quadratic effects from all the other dimension-six interactions. Including dimension-eight effects is however beyond the scope of this thesis and, when necessary for the observables and interactions of our interest, we will simply work out the quadratic effects of the dimension-six operators.

There are very few places where the new neutrino interactions introduced in Table 5.1 may have a direct observable effect. Processes such as neutrino scattering with electrons or nuclei at

low energies should be in principle sensitive to them but only if the incoming neutrino has the adequate helicity. However, as mentioned in Chapter 2, in these processes the incident (muon) neutrinos are produced at accelerator facilities where they originate from pion and kaon decays, and these are known to be LH [176, 177]. In particular, the helicity of the neutrino coming from pion decay, which is the dominant source in the beams[1], has been measured with very high precision: $\left|h_{\nu_\mu}\right| > 0.9959$ at 90% C.L. [176]. Other precision observables where the RH neutrinos may appear as final states can be directly sensitive to new interactions. This is the case of the Z invisible width and the W leptonic width, which can be affected by the neutral and charged current couplings in Eq. (5.5), and also of muon decay where the polarization of the final neutrinos is unknown. This last example will play a crucial rôle in the discussion in the next section, where we deal with the implications that new physics correcting muon decay and its inverse process may have in order to test the existence of RH neutrinos at a neutrino factory. Let us review the form of these corrections. The inverse muon decay (IMD) reaction $\nu e \to \nu\mu$ was not considered in Chapter 2, for in the discussion presented there it essentially receives the same corrections as the muon decay process. However, if RH neutrino interactions are present in nature this is not necessarily true. This is so because whereas in IMD experiments [178] we are blind to such interactions since the initial neutrino is produced at the laboratory and is LH as argued above, in muon decays, as we also have stressed, we do not know what is the helicity of the final neutrinos. Therefore, these two processes could distinguish the presence of RH neutrino interactions if they contributed to muon decay. In particular, if we assume that new physics is lepton flavor conserving, as we will do in next section, we only need to consider the standard decay channel[2]. The relation between the muon decay constant and the SM G_F is modified

$$\frac{G_\mu^2}{G_F^2} = \left|1 + \left(\alpha_{\phi l}^{(3)}\right)_{22} \frac{v^2}{\Lambda^2} + \left(\alpha_{\phi l}^{(3)}\right)^\dagger_{11} \frac{v^2}{\Lambda^2} - (\alpha_{ll})_{2211} \frac{v^2}{\Lambda^2}\right|^2 + \frac{1}{16} \left|(\alpha_{l\nu})_{1122}\right|^2 \frac{v^4}{\Lambda^4}, \tag{5.6}$$

where for simplicity we have only included the extra corrections from the operator $\mathcal{O}_{l\nu}$ since, as will be discussed below, other interactions entering in muon decay are strongly bounded to small values. We have also omitted in Eq. (5.6) the corrections from the operators $\mathcal{O}_\phi^{(1)}$ and $\mathcal{O}_{\phi 6}$ because they have no impact in our fits, as explained in Chapter 2.

On the other hand, the IMD cross section, normalized to the SM value, is only affected by new physics involving LH neutrinos. With the same considerations as above:

$$S_{\rm IMD} \equiv \frac{\sigma\left(\nu e \to \nu\mu\right)}{\sigma_{\rm SM}\left(\nu e \to \nu\mu\right)} = \frac{G_F^2}{G_\mu^2} \left|1 + \left(\alpha_{\phi l}^{(3)}\right)_{22} \frac{v^2}{\Lambda^2} + \left(\alpha_{\phi l}^{(3)}\right)^\dagger_{11} \frac{v^2}{\Lambda^2} - (\alpha_{ll})_{2211} \frac{v^2}{\Lambda^2}\right|^2. \tag{5.7}$$

As we did for the other observables, we normalize all the new effects so the muon decay rate is exactly reproduced by (5.6):

$$S_{\rm IMD} = 1 - \frac{1}{16} \left|(\alpha_{l\nu})_{1122}\right|^2 \frac{v^4}{\Lambda^4}, \tag{5.8}$$

which is the expression that will enter in the fits. In the same way, the coefficient $(\alpha_{l\nu})_{1122}$ will now enter in all the other electroweak precision observables in the form of indirect corrections, which can be constrained in the global fit to data.

[1] The kaon to pion ratios measured for instance by the CHARM collaboration are: $K^+/\pi^+ = 0.1282 \pm 0.0028$ and $K^-/\pi^- = 0.0630 \pm 0.0033$ [73].

[2] It is straightforward to generalize the formula to include lepton flavor violating contributions by summing over all the possible channels with the different neutrino flavors. At order $1/\Lambda^4$ there are contributions from genuine four-fermion interactions and from amplitudes exchanging W and Z vector bosons where only one of the vertices violate flavor.

5.2 Looking for right-handed neutrino signals at neutrino factories

As emphasized in the introduction of this chapter, neutrino oscillations provide the only observational evidence of new physics beyond the minimal SM. These observations, however, cannot distinguish between Dirac or Majorana neutrinos, nor they require new interactions [3]. The obvious question is then, where do we have to look in order to determine the neutrino character and/or to observe possible new interactions involving light neutrinos? This will become especially relevant when we face the need to interpret new data with higher statistics and precision, as foreseen at a neutrino factory [180]. In the following we show that present experimental constraints leave room for observing new interactions involving light RH neutrinos, corresponding to a $\sim 10\%$ deficit in the expected number of events in appropriate processes. Such a scenario can be easily realized with a mild extension of the SM, through the addition of additional scalar weak isodoublet (to be denoted by η), and a scalar iso-triplet of hypercharge 1, (denoted by Δ), besides three RH neutrinos, ν_R^i. But it requires an adequate choice of Yukawa couplings to suppress lepton flavor violation; moreover, for this particular model, the deficit allowed by current EWPD is reduced by a factor of ~ 3 compared to the general case above, where arbitrary new interactions are parameterized by gauge-invariant dimension-six operators with unrelated coefficients.

Within the SM muons only decay into LH neutrinos. Even if the spectrum is enlarged to include their RH counterparts, these are not produced in such decays because they have no gauge interactions, and neutrino masses are negligible. On the other hand, if other interactions are present in nature, a muon based neutrino factory could inject an admixture of neutrinos with both chiralities. We will show below that the limits on new interactions involving RH neutrinos are to a large extent those derived from (inverse) muon decay, and therefore relatively weak. This is then a promising reaction to look for new physics effects in the neutrino system.

Let us first, however, describe our setup. We assume that the three light neutrinos are of Dirac type, i.e. that there are three light neutrino singlets beyond the minimal SM, and that lepton number is conserved. In practice this is not a restriction on the light neutrino character, but on the type of new interactions. As it was also noted at the beginning of the chapter, neutrino masses are negligible in all experiments performed up to now, except in neutrino oscillations (and eventually in neutrino-less double β decay, $0\nu\beta\beta$). Thus, we can assume that all interactions conserve lepton number because neutrino masses are much smaller than the energy relevant in the processes considered and/or the experimental precision is much lower than the size of the effects proportional to them, as it is the case for all foreseen experiments not involving neutrino oscillations and excluding $0\nu\beta\beta$. Though we could consider lepton number violating new interactions, their effects can be ignored in our analysis [4], as can be the lepton number violating effects from neutrino masses.

Hence, the new interactions effects we are interested in will be relatively large and lepton number conserving, whereas neutrino masses will be safely taken to vanish. The effective Lagrangian

[3] In what follows we will ignore the LSND data [179].

[4] In an effective theory only involving the light SM fields and invariant under the SM gauge group the only dimension-five operator violating L, the Weinberg operator $\mathcal{O}_5$, is negligible because of the smallness of neutrino masses. There is no dimension-six operator violating B-L [61]. Thus, any lepton number violating dimension-six operator violates B at the same time, and then involve quarks and will play no rôle in our analysis. If the effective theory also includes RH neutrinos, as in our case, there are two additional dimension five lepton number violating operators [175]. One of them arises at the loop level, generates a magnetic coupling for the RH neutrinos and is very strongly constrained when the ν_R are light [181]. The other, the operator $\mathcal{O}_{5\nu}$, generates a correction to the ν_R Majorana mass term and is therefore also negligible. There is only one dimension-six operator violating B-L (and L), the operator $\mathcal{O}_{\nu^c\nu}$, but involves four RH neutrinos, and then is uninteresting for us. The other dimension-six operators violating L also violate B, and can be also ignored.

describing such a scenario will not distinguish between (*i.e.* approximates equally well) the case of exact lepton number conservation with very small Dirac masses for the three light neutrinos, and the case of negligible Majorana masses for the six light neutral fermions, the only vestige of the very slightly broken lepton number in this case. This was explicitly proved in [182] for (inverse) muon decay assuming no additional constraints on new interactions. Note that by similar arguments we can also neglect lepton flavor violation induced by light neutrino mixing (to a very good approximation).

The most general four-fermion effective Hamiltonian describing muon decay reads

$$\mathcal{H}_{\mu\to\nu\overline{\nu}e} = \frac{4G_F}{\sqrt{2}} \sum_{\substack{a,\,b\,=\,L,\,R \\ \gamma\,=\,S,\,V,\,T}} g^{\gamma}_{ab}(\overline{e}\;\Gamma^{\gamma}\;\nu^{e}_{a})(\overline{\nu^{\mu}_{b}}\;\Gamma^{\gamma}\;\mu) + \text{h.c.}\;, \tag{5.9}$$

where a, b label the chirality of the neutrinos, while γ refers to the Lorentz character of the interaction (scalar, vector and tensor). The present limits on the size of the various coefficients will be discussed in the following section. Here we merely remark that the two couplings g^{V}_{LL}, g^{S}_{RR} are also associated with the largest departure from the SM predictions for the number of events to be detected by a neutrino factory.

There are many other available EWPD that can be used to indirectly constrain the Hamiltonian (5.9), and in particular those two couplings. To derive such restrictions one can take two routes. The first one consists in re-writing (5.9) as a linear combination of higher-dimensional operators invariant under $SU(3)_c \otimes SU(2)_L \otimes U(1)_Y$, and adding these operators to the SM Lagrangian [173]; the coefficients of the resulting effective theory can then be bound using experimental data at all available energies. In this approach the physics responsible for generating these operators is left unspecified, except for the requirement that its characteristic scale lie beyond the electroweak scale. The advantage of this approach is its generality, since it is not tied to any specific assumption about the physics beyond the SM, its disadvantage is the proliferation of coefficients, and the fact that more than one gauge-invariant operator contributes to each term in (5.9).

The second route is to extend the SM by adding a specific set of new fields (such as the η and Δ mentioned previously) and interactions. This has the advantage of providing a specific scenario for the physics beyond the SM, but the results obtained are often specific to the assumptions made in constructing the model. At scales below those of the heavy particles this model will reduce to an effective theory of the type mentioned above, except that the effective-operator coefficients are all expressed in terms of a smaller number of parameters and can be constrained more tightly.

In the following we will examine both of these possibilities. In the next section we consider the effective Lagrangian approach, which we denote by E1, where we choose a set of four-fermion effective operators that generate (5.9) at low energies and have little impact on other electroweak observables. In Section 5.2.2 we will also consider a specific extension of the SM, which we denote by E2, based on an extended scalar sector. Finally, in the last two sections we discuss the implications of these SM extensions for neutrino oscillations and other experiments, respectively.

5.2.1 Electroweak precision data constraints on right-handed neutrino interactions

One effective-Lagrangian extension of the SM, which we denote by E1, consists in adding to the SM the following set of effective operators

$$\begin{aligned}\Delta\mathcal{L}_{\rm E1} = &-\frac{4G_F}{\sqrt{2}}\Big[g^S_{LL}(\overline{l^\mu_L}\mu_R)(\overline{e_R}l^e_L)+g^S_{RR}(\overline{l^e_L}\nu^e_R)(\overline{\nu^\mu_R}l^\mu_L)+g^S_{LR}(\overline{e_R}l^e_L)i\sigma_2(\overline{\nu^\mu_R}l^\mu_L)-g^S_{RL}(\overline{l^e_L}\nu^e_R)i\sigma_2(\overline{l^\mu_L}\mu_R)+\\ &+\frac{\delta g^V_{LL}}{2}(\overline{l^e_L}\gamma^\alpha l^\mu_L)(\overline{l^\mu_L}\gamma_\alpha l^e_L)+g^V_{RR}(\overline{e_R}\gamma^\alpha\nu^e_R)(\overline{\nu^\mu_R}\gamma_\alpha\mu_R)-\frac{g^V_{LR}}{v^2}(\overline{l^e_L}\sigma_a\gamma^\alpha l^e_L)(\phi^T i\sigma_2\sigma_a\phi)(\overline{\nu^\mu_R}\gamma_\alpha\mu_R)+\\ &+\frac{g^V_{RL}}{v^2}(\overline{e_R}\gamma^\alpha\nu^e_R)(\phi^\dagger\sigma_a i\sigma_2\phi^*)(\overline{l^\mu_L}\sigma_a\gamma_\alpha l^\mu_L)+g^T_{LR}(\overline{e_R}\sigma^{\alpha\beta}l^e_L)i\sigma_2(\overline{\nu^\mu_R}\sigma_{\alpha\beta}l^\mu_L)-\\ &-g^T_{RL}(\overline{l^e_L}\sigma^{\alpha\beta}\nu^e_R)i\sigma_2(\overline{l^\mu_L}\sigma_{\alpha\beta}\mu_R)\Big]+\text{h.c.}\,,\end{aligned} \tag{5.10}$$

where the adequate $SU(2)_L$ transposed are understood in order to render the operators with an $i\sigma_2$ gauge invariant. The dimension-six operators in the above Lagrangian can be readily related to those in the basis presented in Chapter 1 and extended in the first section of this one. We choose to write them in this way in order to directly compare this extension with the standard muon decay effective Hamiltonian in Eq. (5.9). For the same reason we label the operator coefficients as g^γ_{ab}, instead of using the notation employed till now in this thesis. E1 is manifestly invariant under $SU(3)_c \otimes SU(2)_L \otimes U(1)_Y$, and lepton flavor (and lepton number) conserving. Note that g^V_{LR} and g^V_{RL} are associated with operators of dimension eight: $\overline{\nu^\mu_R}\gamma^\alpha\mu_R$ and $\overline{e_R}\gamma^\alpha\nu^e_R$ have hypercharges $Y=-1$ and 1, respectively, and we cannot construct a gauge invariant vector with opposite hypercharge using only $\overline{l_L}$ and l_L; at low energies (5.10) reduces to (5.9) with the definition $g^V_{LL}\equiv 1+\delta g^V_{LL}$.

In (5.10) we have chosen to write all dimensional coefficients in terms of v. This implies that the natural size for the coefficients is

$$g^\gamma_{ab}\sim\begin{cases}(v/\Lambda)^4 & \text{for } g^V_{LR,\,RL}\,,\\ (v/\Lambda)^2 & \text{otherwise}\,,\end{cases} \tag{5.11}$$

where Λ denotes the heavy scale of the physics responsible for generating the corresponding operator.

A characteristic feature of this particular extension is that, except for the effect on the muon decay constant and IMD, EWPD are blind to the operators in Eq. (5.10). For instance, although g^S_{LR} and g^T_{LR} contribute to $e^+e^-\to\overline{\nu^\mu}\nu^\mu$ and affect the Z invisible width, as was emphasized in Chapter 2 the effects from four-fermion interactions are negligible compared to the Z pole contribution. E1 does not contribute to lepton flavor violating processes either, because it does not include lepton flavor violating operators. Similarly, universality is preserved since the gauge couplings to leptons remain the same as in the SM.

It must be emphasized, however, that in specific models (such as E2, described in Section 5.2.2 below) the various coefficients in Eq. (5.9) are written in terms of the fundamental parameters of the theory, these parameters appear in all other interactions, and in general will contribute to other observables, which in turn can be used to stringently constrain g^γ_{ab}. In fact, it is non-trivial to find models where these limits are not so strict that they exclude further observable effects from (5.9).

As we argue below the largest departure from the SM predictions is parameterised by g^V_{LL} and g^S_{RR}. Constraints on these two operators $(\overline{l^e_L}\nu^e_R)(\overline{\nu^\mu_R}l^\mu_L)$ and $(\overline{l^e_L}\gamma^\alpha l^\mu_L)(\overline{l^\mu_L}\gamma_\alpha l^e_L)$ in Eq. (5.10) can be

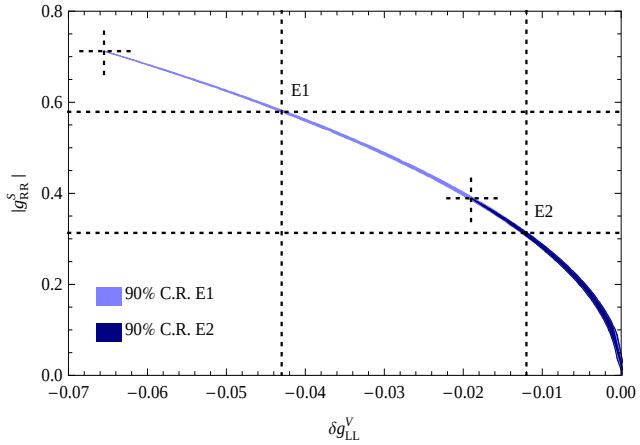

Figure 5.1: 90% C.L. bounds for E1 case (b) in Eq. (5.12); and the same for the SM extension E2 in next section. The narrow bands between the origin and the crosses define the 90% confidence region for the global fit to the two parameters for E1 (left cross) and E2 (right cross) respectively.

obtained using current data. At 90% C.L. we find

$$\begin{array}{lll} \text{case} & \left|g^V_{LL} \equiv 1 + \delta g^V_{LL}\right| & \left|g^S_{RR}\right| \\ (a) & > 0.960 & < 0.550 \\ (b) & > 0.957 & < 0.579 \\ (c) & > 0.9998 & < 0.054 \end{array} \tag{5.12}$$

where the limits in case (a) are obtained directly from (5.9) using muon decay and $\nu e \to \nu\mu$ data [18, 183]; in case (b) from a global fit using the precision data in Appendix A to the operator coefficients with the SM parameters fixed at their best-fit values [5]; in case (c) as in case (b) but taking one effective-operator coefficient to be non-zero at a time. This last possibility, though often adopted for simplicity is seldom realistic: as noted previously one must expect the heavy physics to generate several operators with related coefficients, so that fits allowing for several non-zero interactions become compulsory. Even more, if the new physics is to have sizable indirect effects, then it must also *conspire* to preserve the excellent fit of the SM to the EWPD at the 1‰ level [18]. In Fig. 5.1 we plot the bounds for case (b). The results in (5.12) indicate that the two parameters in the fit are highly correlated. This is expected since the fit is dominated by the constraint on the strength of the muon decay constant G_μ, which is proportional to the SM Fermi constant G_F in Eq. (5.9):

$$\begin{aligned} G_\mu = G_F \Big[& \left|1 + \delta g^V_{LL}\right|^2 + \left|g^V_{RR}\right|^2 + \left|g^V_{LR}\right|^2 + \left|g^V_{RL}\right|^2 + \\ & + \frac{1}{4}\left(\left|g^S_{LL}\right|^2 + \left|g^S_{RR}\right|^2 + \left|g^S_{LR}\right|^2 + \left|g^S_{RL}\right|^2\right) + \\ & + 4\left(\left|g^T_{RL}\right|^2 + \left|g^T_{LR}\right|^2\right)\Big]^{\frac{1}{2}} \equiv G_F A \ , \end{aligned} \tag{5.13}$$

with the proportionality constant A restricted by the global fit to the interval

$$0.9997 < A < 1.0004 \quad \text{at } 90\% \text{ C.L.} \ . \tag{5.14}$$

[5] These limits stay mainly unchanged if the SM parameters are also left free in the global fit.

This bound alone constrains the coefficients to a narrow band in the $\delta g_{LL}^V - \left|g_{RR}^S\right|$ plane

$$|g_{RR}^S|^2 \simeq -8\ \delta g_{LL}^V\ , \tag{5.15}$$

as depicted in Fig. 5.1.

Using the bounds above we can derive limits on the scale of new physics responsible for the two operators being considered. Using (5.11) and assuming the underlying physics is weakly coupled ($g_{ab}^\gamma \sim g^2v^2/\Lambda^2$ for the dimension-six coefficients) we find the weak constraints $\Lambda > 200$ GeV for g_{RR}^S and $\Lambda > 800$ GeV for δg_{LL}^V.

As already stressed, we are interested in those interactions in the muon decay effective Hamiltonian that could allow for the largest deviation from the SM prediction of the number of events that may be eventually detected at a neutrino factory. In general, while it is clear that a negative δg_{LL}^V is strongly favored for this to be possible (see Eqs. (5.13, 5.14)), one may wonder whether any of the other interactions involving a RH neutrino may play the role of g_{RR}^S. This could be the case for g_{RR}^V or the LR and RL operators in Eq. (5.10). However, unlike for g_{RR}^S, which cannot be separated from δg_{LL}^V in muon decay experiments since we do not measure the polarization of the final neutrinos, all the other interactions are constrained by the absence of any significant deviation from the V−A prediction in the spectrum of the outgoing electrons. In particular, $\left|g_{RR}^V\right| < 0.034$. On the other hand, the bounds for some of the LR and RL interactions are relatively weak, but they also generate radiative corrections to the neutrino masses and, assuming naturality, are constrained by the associated upper limits [184]: $\left|g_{LR}^S\right|, \left|g_{RL}^V\right|, \left|g_{LR}^T\right| < 10^{-2}$ and $\left|g_{RL}^S\right|, \left|g_{LR}^V\right|, \left|g_{RL}^T\right| < 10^{-4}$. Therefore, when we consider the data from IMD, where the incident neutrinos come from pion decays and then are LH, and derive a relatively weak bound on δg_{LL}^V, this can be only compensated by g_{RR}^S in order to satisfy (5.14), but in contrast with the remaining operators in Eq. (5.10) has no further constraints.

5.2.2 A simple Standard Model extension

Let us discuss a simple model realizing the former scenario. It extends the SM including besides three RH neutrinos ν_R^i with zero lepton number, a second scalar doublet η with lepton number equal to -1, and a scalar triplet Δ with hypercharge 1 and lepton number equal to -2,

$$\eta = \begin{pmatrix} \eta^+ \\ \eta^0 \end{pmatrix}, \quad \Delta = \begin{pmatrix} \Delta^+ & \sqrt{2}\Delta^{++} \\ \sqrt{2}\Delta^0 & -\Delta^+ \end{pmatrix}, \tag{5.16}$$

as in [185] and [2, 3, 102, 186], respectively. They both can acquire a vacuum expectation value through very small lepton number violating couplings to the SM Higgs (which carries zero lepton number), and provide masses and mixings to the light neutrinos, which must be then fit the observed spectrum in oscillation experiments [6]. But, these couplings, as the neutrino masses, can be safely neglected in our analysis: we can assume that light neutrinos are massless, and that lepton number and lepton flavor are both conserved. Thus, besides the kinetic term for the RH neutrinos, the SM fermionic Lagrangian acquires only two more terms

$$-f_{ij}\overline{\nu_R^i} l_L^{jT} i\sigma_2 \eta - \lambda_{ij} l_L^{iT} C i\sigma_2 \Delta l_L^j + \text{h.c.}\ , \tag{5.17}$$

with only $f_{ee,\mu\mu}$ and $\lambda_{e\mu} = \lambda_{\mu e}$ potentially large enough to produce measurable effects in current and near-future experiments. The integration of the extra scalars results, in particular, in the following contributions to the muon decay effective Hamiltonian:

$$\frac{4G_F}{\sqrt{2}}\left[g_{RR}^S\ (\overline{l_L^e}\nu_R^e)(\overline{\nu_R^\mu} l_L^\mu) + \frac{\delta g_{LL}^V}{2}(\overline{l_L^e}\gamma^\alpha l_L^\mu)(\overline{l_L^\mu}\gamma_\alpha l_L^e)\right] + \text{h.c.}\ , \tag{5.18}$$

[6] There can be also tiny RH neutrino mass terms.

Process	E1	E2
ν-N	8.5% (5.0%)	2.5% (2.5%)
IMD	15.4% (9.3%)	4.8% (4.8%)

Table 5.2: Maximum deficit in the number of observed events in a near detector sensitive to neutrino-nucleon collisions (ν-N) and IMD for the two SM extensions discussed in the text. In parentheses we show the deficits expected in the case that the precision on the measurement of IMD is improved by a factor of 2.

with coefficients

$$g^S_{RR} = -\frac{1}{2\sqrt{2}G_F}\frac{f^\dagger_{ee} f_{\mu\mu}}{M^2_\eta} \quad \text{and} \quad \delta g^V_{LL} = -\frac{1}{\sqrt{2}G_F}\frac{\lambda^\dagger_{\mu e}\lambda_{\mu e}}{M^2_\Delta} \ , \tag{5.19}$$

respectively, where $M_{\eta,\Delta}$ stand for the scalar masses. The full set of dimension-six operators arising from the integration of the scalar triplet Δ is given in [2, 3, 102].

In this case, named E2 in the former section, the EWPD analysis implies more stringent bounds on δg^V_{LL} and g^S_{RR} than for E1:

$$\left|1 + \delta g^V_{LL}\right| > 0.988, \text{ and } |g^S_{RR}| < 0.313 \ . \tag{5.20}$$

The corresponding band is plotted in Fig. 5.1. The bounds obtained are tighter because, as emphasized previously, the integration of definite new physics also gives, in general, operators contributing to other processes, further restricting the model. In the present case the integration of the Δ generates also the operator $(\overline{l^e_L}\gamma^\alpha l^e_L)(\overline{l^\mu_L}\gamma_\alpha l^\mu_L)$, which has the same coefficient δg^V_{LL} as $(\overline{l^e_L}\gamma^\alpha l^\mu_L)(\overline{l^\mu_L}\gamma_\alpha l^e_L)$, and contributes to $\nu^\mu e \to \nu^\mu e$, further restricting the allowed deviation from the SM predictions [7].

Lepton flavor violation is below experimental bounds because similarly to the E1 case the only non-negligible couplings in Eq. (5.17) are $f_{ee,\mu\mu}$ and $\lambda_{e\mu} = \lambda_{\mu e}$, and because the scalar doublets and triplet mix very little, as required by approximate lepton number conservation. The absence of new τ couplings and that the SM gauge couplings stay unchanged guarantee the agreement with universality constraints on the lepton sector.

5.2.3 Neutrino factory predictions

The relevant phenomenological question is where could the RH neutrinos be eventually observed if the δg^V_{LL} and g^S_{RR} four-fermion interactions are non-zero. Obviously, they can be probed in a more precise IMD experiment: a more precise measurement of this process could give evidence for those new interactions (or reduce the allowed deviation from the SM in Eqs. (5.12,5.20) and Fig. 5.1). But a muon-based neutrino factory will also be sensitive to them. Indeed, if a substantial amount of the neutrinos produced in muon decay are RH, a near-detector sensitive to neutrino-hadron collisions will observe a deficit in the same proportion, and this deficit would be twice as large if the detector could also measure the IMD process. In Table 5.2 we give the maximum deficits expected in the case that the new interactions saturate the 90% C.L. bounds obtained in the previous sections. Whereas in Fig. 5.2 we show the predicted deficit as a function of δg^V_{LL} for the SM completions considered.

[7] In our approximation (implying negligible lepton number violation in the scalar sector) there are no tree-level contributions to the oblique parameters.

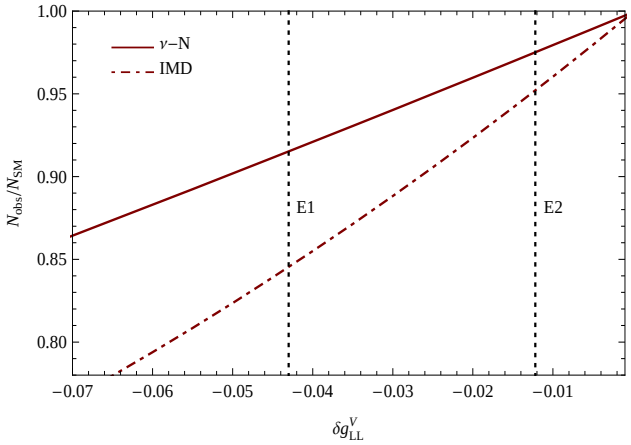

Figure 5.2: Percentage of detected events in a near detector at a neutrino factory compared to the predicted number by the SM, as a function of the new interactions strength δg^V_{LL}. The solid (dotted-dashed) curve corresponds to neutrino-nucleon (IMD) collisions. The vertical lines stand for the E1 and E2 limits on δg^V_{LL} in the text.

If the precision in the measurement of the IMD is improved by a factor of 2 without modifying the central value, the limits on the new interactions would be strengthened and the allowed deficit of observed events at a neutrino factory reduced; the corresponding percentages in such a case are given in parentheses in Table 5.2. For the E1 extension the deficit would be reduced to $\sim 5\%$, being the 90% C.L. bounds in this case $\left|1+\delta g^V_{LL}\right| > 0.975$ and $|g^S_{RR}| < 0.442$. In the E2 case the improvement in the precision of IMD would have no appreciable effect because this constraint would be weaker than the one derived from $e\nu$ elastic scattering.

For a neutrino factory to be sensitive to a deficit $< 3\%$ (the smallest value listed in Table 5.2), the neutrino flux must be known with enough precision. Besides, large fluxes are also required to have a large number of events at a near detector in order to keep the statistical error small. For a detailed study about future neutrino factories see [180]. Assuming 10^{21} muon decays in one year of operation, the number of expected ν-N events at a near detector (such as the one described in Table 1 of [180]) is of the order of 10^9; while the number of IMD events range from 10^4 to 10^6, depending on the energy and polarization of the decaying muon. Then, deficits even smaller than few per mille due to the injection of RH neutrinos could be eventually testable for such a large statistics. However, per mille deficits may be too small because the highest achievable precision in the determination of the flux is expected to be at most of $\sim 1‰$. But being conservative, it could be up to a factor ten times larger, and then of the same order as the largest possible deficit for the E2 extension.

At this point one may wonder about the consistency of these large deficits with the interpretation of present neutrino oscillation experiments summarized in Table 5.3. As we will argue, these seem to be largely insensitive to new four-fermion interactions involving an electron, a muon and the corresponding neutrinos. Reactor experiments are initiated by electron antineutrinos from β decay, they are then LH and fully described by the SM. Similarly, solar neutrinos have electronic flavor, are also LH and produced by SM reactions. Atmospheric neutrinos are decay products of pions and muons from cosmic rays, and may include RH neutrinos. However, since the flux of cosmic rays is isotropic, and atmospheric neutrino oscillation experiments only compare fluxes of muon

ν source	Experiment	Detection
Reactor (β decay)	Palo Verde [187], CHOOZ [188] KamLAND [189]	$\overline{\nu^e} \not\to \overline{\nu^\mu}$ $\overline{\nu^e} \to \overline{\nu^x}$
Solar	SNO [190], Borexino [191]	$\nu^e \to \nu^\mu$
Atmospheric (π & μ decays)	Super Kamiokande [192]	$\nu^\mu \to \nu^\tau$
Accelerator (π & K decays)	K2K [193], MINOS [194], CHORUS [195], NOMAD [196] MiniBooNE [197]	$\nu^\mu \to \nu^\tau$ $\overline{\nu^\mu} \not\to \overline{\nu^e}$
Accelerator (μ decays)	LSND [179] KARMEN [198]	$\overline{\nu^\mu} \to \overline{\nu^e}$ $\overline{\nu^\mu} \not\to \overline{\nu^e}$

Table 5.3: Neutrino source for the different oscillation experiments and search process.

neutrinos coming from different directions, they are not sensitive to a possible deficit in the *total* number of initial LH neutrinos from muon decays. On the other hand, in accelerator experiments looking for $\nu^\mu \to \nu^\tau$ or $\nu^\mu \to \nu^e$, neutrino beams are mainly formed by muon neutrinos originating from pion decays (with a fairly small contamination) [193], and then LH and with the SM oscillation pattern. Finally, in accelerator experiments looking for $\overline{\nu^\mu} \to \overline{\nu^e}$, the muon antineutrinos are produced in μ^+ decays, and therefore they are sensitive to the new interactions we are interested in. However, what they measure is the number of positrons produced by inverse β decay, looking for an excess of electron anti-neutrinos instead of looking for a deficit in the observed number of muon anti-neutrinos. (The excess reported by the LSND experiment [179] has no explanation in this setup.) Hence, there appears not to be any contradiction between the significant deficit predicted by the new interactions considered here and the interpretation of current oscillation experiments.

5.2.4 Further phenomenological implications

In specific models that contain new fields and interactions there are in general further observable effects, as for instance the production of the new particles at large colliders. This is the case of the simple model E2 discussed in Section 5.2.2. If this type of new interactions saturates the EWPD limits,

$$\left| \frac{\lambda_{\mu e}}{M_\Delta \, [\text{TeV}]} \right| \simeq 0.4 \ , \tag{5.21}$$

implying a relatively large $\lambda_{\mu e}$ and a light Δ. The LHC will be able to uncover such a scalar triplet for Δ masses up to 900 GeV and an integrated luminosity of 30 fb^{-1} [199] [8].

For this model the relation in Eq. (5.15) translates into a correlation between the scalar masses $M_{\eta,\Delta}$ and/or the Yukawa couplings $f_{ee,\mu\mu}, \lambda_{\mu e}$, namely

$$\left| \frac{f_{ee}^\dagger f_{\mu\mu}}{M_\eta^2} \right|^2 \simeq 32\sqrt{2} G_F \ \frac{\lambda_{\mu e}^\dagger \lambda_{\mu e}}{M_\Delta^2} \ . \tag{5.22}$$

This implies that for these new interactions to have sizable effects at a neutrino factory we must have relatively large $f_{ee,\mu\mu}$ and light η. The main signals in this case are missing energy plus one

[8] This estimate is larger than those quoted in [199] for in this model the scalar triplet only couples to e and μ but not to taus, which are more difficult to identify and have larger backgrounds. In contrast with type II see-saw models, this triplet is not the only source of neutrino masses, and light neutrino masses and mixings can be reproduced even when the Δ-τ conplings vanish.

or two leptons $\ell = e, \mu$ because a charged (neutral) η has only sizable decays into $\ell\nu$ ($\nu\nu$) [9]. Thus, W, WZ and WW production can provide too large irreducible backgrounds for observing these scalars. Other SM processes like $t\bar{t}$ production can also give large backgrounds. The search for this scalar doublet is similar to left slepton searches assuming that they only decay into a LH charged lepton and the lightest supersymmetric particle [201]. (Although in general sleptons can also have cascade decays and be decay products of other supersymmetric particles [202].) In this case the LHC discovery limit is ~ 300 GeV for an integrated luminosity of 30 fb^{-1} [203], but this is assuming that the slepton doublets coupling to the first two families are degenerate. However, in our model there is only one scalar doublet, scaling the corresponding limit to 250 GeV after correcting by the factor of 2. It may also happen that though the Δ and η may be too heavy to be directly observed at the LHC (*e.g.* $M_\Delta \gtrsim 1$ TeV and $M_\eta \gtrsim 250$ GeV), their effects can still be observable at a neutrino factory provided f and λ fulfill Eqs. (5.21) and (5.22): $f_{ee,\mu\mu} \simeq 2\lambda_{\mu e} \gtrsim 0.8$. Obviously, large enough lepton colliders are better suited for searching these scalars, since they couple mainly to leptons, and these colliders allow for a better kinematical reconstruction. On the other hand, the relation in Eq. (5.22), as the cancellation of other possible lepton flavor violating couplings, does not appear to be natural in this simple model, but they could be in more complicated frameworks.

Finally, we note that one might consider other SM additions/extensions generating δg^V_{LL}, as for instance, heavy neutrino singlets or triplets mixing with the electron or muon. In theses cases, however, the relatively small mixings allowed by EWPD (see Table 3.11 in Chapter 3) are too small to produce a sizable deficit.

[9] See [200] for alternative scalar doublet models.

Conclusions

The SM has proved to be an excellent phenomenological description of nature at energies of the order of a few hundred GeV. Nevertheless, there are several reasons to believe that it is an incomplete theory, which needs to be extended if we aim to understand phenomena at even higher energies. The nature of such an extension is unknown, and we hope the LHC will help in providing some hints about which road to follow. In the meantime indirect searches, looking for new effects in available EWPD, may give hints of physics beyond the SM. We have no clue of what the right SM extension may be, but we know it must be characterized by a rather heavy mass scale. This makes the use of an effective Lagrangian approach very convenient for the analysis of the implications of new physics. This is what we have done in this work. Its main results and conclusions are the following:

- Based on a dimension-six effective Lagrangian approach, we have performed a model-independent description of new physics. We have computed the leading corrections from the new operators to all electroweak precision observables, providing explicit formulae for the new contributions. Though less precisely measured, we also consider LEP 2 cross sections and asymmetries. These are relevant in constraining four-fermion interactions.

  We have discussed the main experimental constraints on each of the dimension-six operators that can arise at tree level, as well as their interplay with the determination of the Higgs mass.

- Using the effective Lagrangian approach we have described the effects of extra matter fields [1] and new vector bosons [5] for arbitrary SM extensions. We have classified all such particles that may mix with the SM fields and give an observable effect in current precision observables. For each case, we have computed the corresponding operator coefficients in the dimension-six effective Lagrangian, integrating the heavy particles out of the theory.

- Our phenomenological analysis of new fermions has been focussed on the effects of heavy vector-like leptons [1, 2, 3, 4]. The results show that, even in the best case, the improvement in the χ^2 with respect to the SM fit is mild. In those cases the quality of the fit is similar to the one of the SM fit.

  We have derived upper bounds on the mixing of extra leptons with the SM fermions. They are relevant for the production and decay of heavy resonances at large colliders. At 95% C.L. the bounds range from 0.01 to 0.08. Our results improve existing limits, and provide a significant reduction of the parameter space regions allowed by EWPD. In particular, the new limits further reduce the possibility of producing heavy Majorana neutrino singlets at the LHC in minimal models. In addition, we provide limits for cases not considered previously in the literature.

It is also noteworthy that mixing with extra neutrino singlets can help in accommodating a relatively heavy Higgs. In particular, mixing with electron neutrinos allows to raise the preferred value for M_H above the LEP 2 direct limit, and place it right in the region were some excess events were found in direct Higgs search experiments at LEP 2 and Tevatron. The upper indirect limit is also relaxed $M_H < 228$ GeV at 95% C.L.. The EWPD constraints on extra vector-like quarks have received more attention in these years, especially for extra doublets and singlets and in the cases where they are coupled to the third family.

- SM extensions with extra vector bosons are also considered [5]. This includes the cases of Z' and W' vector bosons, as well as more exotic possibilities such as vector leptoquarks and a few vector particles not considered previously. EWPD are blind to those new vector bosons that couple to quarks only, but they may be relevant for LHC.

  From the global fit, only the ratios between couplings and masses of the new vectors can be constrained. We find that LEP 2 data are relevant for two reasons. On the one hand, they strengthen the constraints on leptonic couplings. On the other, they favor interactions that raise the prediction for the hadronic cross section above the Z pole. The discrepancy with the bottom Z-pole forward-backward asymmetry, A_{FB}^b, can be also relaxed in the case of extra neutral singlets although this requires pretty large couplings. These can be avoided combining several vector bosons.

  Assuming that the fermionic couplings of the new vectors have the same strength as the massive gauge bosons in the SM, we can estimate for new vector boson masses $M > 1$ TeV at 95% C.L. for extra neutral singlets and $M > 2.5$ TeV for new charged vectors coming from hypercharge 0 triplets. This is well within the LHC reach. Limits on vector leptoquarks are also derived and range from 70 GeV to 830 GeV at 95% C.L., assuming couplings ~ 0.1. However, some protection to avoid FCNC is required in order to saturate the bounds.

  Finally, we point out that besides the known case with an extra neutral vector boson, there is an "exotic" representation also allowing for a heavy Higgs mass, with the same effect as a fermiophobic Z'.

- The effective Lagrangian approach can be easily adapted to more general scenarios with extra light particles and/or additional symmetry requirements. In this thesis we have considered the case of light RH neutrinos. To illustrate its interest we have analyzed the possibility that they have observable effects at a muon based neutrino factory. We observe that sizable RH neutrino interactions correcting muon decay can agree with EWPD if a cancellation with non-standard LH neutrino interactions takes place. In such a case we expect a deficit $\lesssim 10\%$ in the number of events observed at a near detector [6, 7]. This is compatible with the existing results from neutrino oscillation experiments. We provide an explicit model realizing such a scenario, but in this case the deficit is reduced to $\lesssim 3\%$.

Conclusiones

El Modelo Estándar (ME) ha demostrado ser una excelente descripción fenomenológica de la naturaleza hasta energías del orden de unos pocos cientos de GeV. No obstante, hay varias razones para creer que es una teoría incompleta y que necesita ser extendida para entender los fenómenos a energías más altas. La naturaleza de dicha extensión es desconocida aunque esperamos que los resultados de los experimentos en el LHC nos ayudarán a discernir que camino seguir. Mientras tanto las búsquedas indirectas, investigando nuevos efectos en los datos electrodébiles de precisión disponibles, pueden darnos indicios de nueva física más allá del ME. Puesto que desconocemos cuál podría ser la extensión del ME correcta, pero sabemos que debe estar caracterizada por una escala de masas bastante pesada, el uso del formalismo de Lagrangianos efectivos resulta conveniente para el análisis de las implicaciones de la nueva física. Este es el camino que hemos seguido en esta tesis. Los principales resultados y conclusiones de la misma son los siguientes:

- Usando una aproximación de Lagrangiano efectivo hasta dimensión seis hemos realizado una descripción de nueva física independiente de modelo. Hemos calculado las correcciones dominantes de los nuevos operadores a los observables electrodébiles de precisión, proporcionando fórmulas explícitas para las nuevas contribuciones. Aunque con una precisión menor, también consideramos secciones eficaces y asimetrías medidas en LEP 2. Estas son relevantes para restringir efectos de nueva física en forma de interacciones de cuatro fermiones.

  Hemos discutido las principales restricciones experimentales sobre cada uno de los operadores de dimensión seis que pueden surgir a nivel árbol, así como su influencia en la determinación de la masa del Higgs.

- Hemos utilizado técnicas de Lagrangianos efectivos para describir los efectos de campos de materia adicionales [1] y nuevos bosones vectoriales [5] en una extensión arbitraria del ME. Hemos clasificado todas aquellas partículas que puedan mezclarse con los campos del ME y dar un efecto observable en los observables de precisión actuales. Para cada caso se han calculado los correspondientes coeficientes de los operadores en el Lagrangiano efectivo de dimensión seis, integrando las partículas pesadas de la teoría.

- Nuestro análisis fenomenológico de nuevos fermiones del Capítulo 3 se centra en los efectos de nuevos leptones pesados no quirales [1, 2, 3, 4]. Los resultados obtenidos muestran que, incluso en el mejor de los casos, la mejora en el valor de la χ^2 respecto al ajuste del ME es leve. En esos casos la calidad del ajuste es también similar a la del ME.

  Los límites obtenidos sobre la mezcla de los leptones extra con los fermiones ligeros varían entre 0.01 y 0.08, con un nivel de confianza del 95%. Nuestros resultados mejoran los límites existentes en la literatura, encontrándose una reducción significativa de las regiones del espacio de parámetros permitidas por los datos electrodébiles de precisión. En particular, los nuevos límites reducen la posibilidad de producir en el LHC neutrinos singlete de Majorana

pesados en modelos minimales. Además, proporcionamos límites sobre casos no considerados previamente en la literatura.

Es también digno de mención que la mezcla con neutrinos singlete podría ayudar a acomodar un Higgs relativamente pesado. En particular, la mezcla con neutrinos electrónicos permite aumentar el valor preferido de la masa del Higgs por encima del límite de exclusión directo de LEP 2, colocándola justo en la región donde los experimentos de búsquedas directas del Higgs en LEP 2 y Tevatron han observado un cierto exceso de eventos. El límite indirecto también se relaja en este caso, $M_H < 228$ GeV con un nivel de confianza del 95%.

- El análisis de bosones vectoriales adicionales [5] incluye los casos de bosones Z' y W', así como otras casos más "exóticos" tales como leptoquarks vectoriales y unas cuantas representaciones no consideradas hasta ahora. Los datos electrodébiles de precisión, sin embargo, no son sensibles a algunos de estos casos, debido a que los nuevos vectores se acoplan sólo a quarks.

  Del ajuste a los datos sólo los cocientes entre los acoplamientos y las masas de los nuevos vectores pueden ser determinados. Encontramos que los datos de LEP 2 son relevantes por dos razones. En primer lugar fortalecen las restricciones sobre acoplamientos leptónicos. Por otro lado, favorecen interacciones que pudieran aumentar la predicción de la sección eficaz $e^+e^- \to$ hadrones por encima del polo de la Z. La discrepancia con la asimetría angular del quark b medida en el polo de la Z también puede disminuirse en el caso de singletes neutros adicionales, aunque esto requiere de acoplamientos relativamente grandes. Estos pueden evitarse si combinamos varios tipos de vectores.

  Suponiendo que los acoplamientos fermiónicos de los nuevos vectores tienen la misma fuerza que los de los bosones gauge del ME podemos estimar límites sobre las masas de los nuevos vectores. Encontramos $M >1$ TeV con un nivel de confianza del 95% para nuevos singletes neutros y $M >2.5$ TeV para nuevos bosones cargados que vengan de tripletes de hipercarga nula. Los límites sobre las masas de los leptoquarks vectoriales varían entre 70 GeV y 830 GeV, suponiendo acoplamientos ~ 0.1. Sin embargo, para poder saturar estos, es necesario algún mecanismo que proteja de la presencia de corrientes neutras que mezclen sabor.

  El efecto sobre la masa del Higgs también es estudiado e indicamos cómo, a parte del caso bien conocido de un singlete neutro adicional, una de las representaciones "exóticas" también hace compatible los datos con un Higgs pesado, pues tiene el mismo efecto que una Z' sin acoplamientos fermiónicos.

- El formalismo de Lagrangianos efectivos puede adaptarse fácilmente a escenarios con nuevas partículas ligeras o requisitos adicionales sobre las simetrías de la teoría. En esta tesis hemos considerado el caso de neutrinos ligeros singlete con quiralidad positiva. Para ilustrar el interés de dicha extensión hemos explorado la posibilidad de encontrar evidencia de la existencia de estas partículas en factorías de neutrinos donde estos se producen a través de la desintegración del muón. Esto es así si los nuevos neutrinos vienen acompañados de interacciones que corrijan dicho proceso, las cuales están permitidas por los datos si tiene lugar una cancelación con nuevas interacciones de los neutrinos del ME. En tal caso, sería de esperar un déficit $\lesssim 10\%$ en el número de eventos observados en un detector cercano [6, 7]. Esto es compatible con las observaciones existentes de los experimentos de oscilaciones de neutrinos. Finalmente, proporcionamos un modelo explícito de dicho escenario, aunque en este caso el déficit se reduce a $\lesssim 3\%$.

Appendix A

Experimental data and fit methodology

The method used in our analyses is the standard global least squares fit. In order to determine the values of the free parameters θ in a given model, we test its predictions against the available experimental data. For that purpose we construct the χ^2 function,

$$\chi^2(\theta) = \left[\mathrm{O}_{\mathrm{exp}} - \mathrm{O}_{\mathrm{th}}(\theta)\right]^T U_{\mathrm{exp}}^{-1} \left[\mathrm{O}_{\mathrm{exp}} - \mathrm{O}_{\mathrm{th}}(\theta)\right], \tag{A.1}$$

where $(U_{\mathrm{exp}})_{ij} = \sigma_i \rho_{ij} \sigma_j$ is the covariance matrix, with σ the experimental errors and ρ the correlation matrix. In U_{exp} we include both statistical and systematic errors. We also include the most significant theoretical uncertainties. $\mathrm{O}_{\mathrm{exp}}$ are the experimental values for the observables included in the fit. We introduce them below. $\mathrm{O}_{\mathrm{th}}(\theta)$ on the other hand are the theoretical predictions depending on the free parameters θ. For the computation of the SM predictions we have used the `FORTRAN` package `ZFITTER 6.43` [204], which includes the effects of higher-order radiative corrections. Some of the low-energy observables introduced below, however, are not available in that code. In those cases we use our own routines based on the SM computations in [205, 206, 207, 208, 209]. For $e^+e^- \to e^+e^-$ at LEP 2 energies, the SM predictions have been computed using `BHWIDE` [210]. To the SM contribution we add the corresponding new physics effects from the dimension-six effective Lagrangian, using the results of Chapter 2. As stressed there, we restrict to tree-level corrections and, unless otherwise is stated, we keep only the leading order in $1/\Lambda^2$. This is consistent with the effective Lagrangian expansion we are using.

The quantity in Eq. (A.1) is directly related to the probability of the predictions to be consistent with the experimental measurements: $\mathcal{P} \sim e^{-\frac{1}{2}\chi^2}$. Therefore, minimizing (maximizing) the χ^2 ($\mathcal{P}$) we obtain the set of parameters best suited to describe data. For the determination of the minima we use the package `MINUIT` [211]. This is also used in the computation of contours of constant probability delimiting the confidence regions shown in our studies. For a detailed description of the method and the statistical meaning of these analyses see Ref. [212].

In what follows we introduce the experimental values for the observables introduced in our fits. After the brief review we comment on the results of the SM fit.

A.1 Experimental data

The experimental data included in our analyses are gathered in Tables A.1 to A.6. There we only provide the central values and experimental errors. The experimental correlation matrices can be

obtained from the references given for each data set. We also include the SM predictions for the different observables for comparison, as well as the pulls to quantify the level of agreement between theory and data. These are obtained from the fits presented below. We include:

- Precision measurements at the Z lineshape. As discussed in Chapter 2, these include Z decay partial widths and branching ratios, cross sections and left-right and forward-backward asymmetries. We also include the determination of the hadronic charge asymmetry (instead of the value of $\sin^2\theta^{\rm lept}_{\rm eff}$ derived from it). These measurements were performed during the first run of LEP and also at SLC [70]. Let us note first that several of these measurements are reported twice by the experimental groups, depending on whether they were derived imposing lepton universality or not in the fits to the measured cross sections and asymmetries. For this reason we include Table A.2, which is analogous to Table A.1 but with the experimental measurements reported with the assumption of lepton universality. (The corresponding SM predictions from the fit including these data are also given.) These are used in our analysis of extra heavy leptons in Chapter 3. Z-pole data comprises some of the most precise measurements available, with relative errors that range from the very few percent to even below the per mille level in some cases. In particular, the precision of the Z mass around $2\cdot10^{-2}$ ‰ allows to fix the corresponding input of the fits to the experimental value, as we have done in some cases. In general, there is a very good agreement between these data and the SM predictions. The exception is the measurement of the forward-backward asymmetry for the bottom quark, which is more than 2.5 σ below the theoretical prediction.

- LEP 2 and Tevatron precision data. These include the top mass [117] as well as the W mass, decay widths [71] and branching ratios [18]. There is also a determination of the effective leptonic weak angle from Tevatron [121], with precision comparable to the one derived from the LEP hadronic charge asymmetry. Although an order of magnitude less precise than the Z counterpart, the W mass is measured also with great precision, below the per mille level. The experimental value turns out to be above the SM prediction by more than 1 σ. Though it is a small deviation, it suffices to strengthen the fit preference for a light Higgs, given the remarkable sensitivity of M_W to M_H. The top mass measurement is also very accurate, with a relative error slightly below the one percent, imposing a strong direct constraint on the corresponding SM input parameter. The total W decay width as well as the branching ratios into leptons are less precise, with relative errors at the few percent. As in the case of some of the Z-pole measurements, the leptonic branching ratios are also reported twice, with and without assuming lepton universality. The latter are given in Table A.2.

- The latest determinations of the Z-pole strong coupling constant, $\alpha_s\left(M_Z^2\right)$, [118] and five-flavor hadronic contribution to the running of α, $\Delta\alpha^{(5)}_{\rm had}(M_Z^2)$. The world average for the former includes the result from the EWPD data fit. For consistency, this should be excluded from the average if it is going to be used in our fits. This yields no significant variation neither in the central value nor in the error. For the value of $\Delta\alpha^{(5)}_{\rm had}(M_Z^2)$ we have combined the recent result in [120] with the previous determination from [119]. It is noteworthy the precision achieved for the determination of $\alpha_s\left(M_Z^2\right)$, at the few per mille level. The precision of $\Delta\alpha^{(5)}_{\rm had}(M_Z^2)$ has been also improved [120]. The error is at the same level as the one for the strong couplings constant. These two determinations directly constrain the values of the corresponding SM input free parameters.

- Low-energy data. In order to constrain most types of new physics we also need to include measurements sensitive to new interactions not contributing at the Z pole. Thus, we also consider observables determined at low Q^2, and then sensitive to four-fermion interactions. These

include the low-energy effective couplings discussed in Chapter 2, from neutrino-nucleon and neutrino-electron scattering experiments, as well as parity violation measurements in atoms and in Møller scattering. Deep inelastic neutrino-nucleon scattering data from NuTeV [75] are also taken into account. These were originally in disagreement with the SM by almost 3 σ, with the discrepancy coming entirely from the low-energy effective coupling g_L^2. Part of such discrepancy, though, has been accounted for by incorporating the effects of the quark-antiquark asymmetry in strange sea quarks [38]. Currently the departure is $\sim 2\,\sigma$. The values for the neutrino-nucleon scattering presented in Table A.1 have been obtained from [38] and, together with the NuTeV results, include older measurements from CDHS [72], CHARM [73] and CCFR [74]. Neutrino-electron scattering data are dominated by CHARM II [76] results and they are in perfect agreement with the SM [38]. Results from atomic parity violation experiments are given in the form of atomic weak charges for Cesium and Thallium. The value of the Cesium weak charge, the more precise among the APV measurements, which was slightly above 1 σ with respect to the SM prediction, is now in almost perfect agreement, after including the latest improvements in the atomic structure calculations [78]. The value for Thallium is from [79]. We also include the determination of the C_{1u} and C_{1d} combinations[1] included in the analysis of [144]. The electron's weak charge has been extracted from the parity violating asymmetry in Møller scattering $A_{PV} = (-1.31 \pm 0.17) \cdot 10^{-7}$ [80], using $A_{PV} = \mathcal{A}\, Q_W\,(e)$ with $\mathcal{A} = (3.25 \pm 0.05) \cdot 10^{-6}$ as determined from Monte Carlo simulation also in [80]. Finally, we include the inverse muon decay experimental results from [178], which are only relevant for the analysis in the last chapter.

- CKM unitarity constraints. We include the experimental determination of the combination $|V_{ud}|^2 + |V_{us}|^2 + |V_{ub}|^2$, which serves to test the unitarity of the first row of the CKM matrix. This has been measured to high precision, with a relative error of 0.6‰ [68], and agrees with the SM at less than 0.2 σ. Thus, it imposes strong restrictions on new physics contributing to CC processes involved in the determination of these CKM matrix elements.

- $e^+e^- \to \bar{f}f$ data above the Z pole. Apart from the observables described above, we also gather in Table A.3 the values for several cross sections and forward-backward asymmetries measured at LEP 2 [81]. We include measurements of cross sections and asymmetries for $e^+e^- \to \mu^+\mu^-$ and $e^+e^- \to \tau^+\tau^-$, as well as the inclusive hadronic cross section $e^+e^- \to$ hadrons, with energies varying from 130 to 209 GeV. We also include in the fits the OPAL results for the differential cross-section $e^+e^- \to e^+e^-$ [213]. These are given in Table A.4. The precision of these LEP 2 measurements is low, in general, compared to the previous observables. They range from around ten percent in the worst cases for leptonic cross sections and asymmetries to very few percent for the, more precise, hadronic data. On general grounds these data are in agreement with the SM. The exception is the total hadronic cross section, which in many energy bins is around 1 σ above the SM prediction. However, when taking into account the correlations this translates only into a global 1.7 σ discrepancy. Although often excluded from the fits [38, 71, 214], the large number of measurements makes LEP 2 data relevant when testing some specific types of new physics since, as for the low-energy observables, they are sensitive to four-fermion interactions.

  We do not include in our fits the heavy flavor data in [81]. As explained there, R_b and R_c data are strongly correlated, and each one is obtained assuming the other is given by the SM prediction. Thus, these data should not in general be used for new physics analyses, except in cases where this only affects the corresponding quark generation. We have checked, anyway,

[1] $\cos\gamma\; C_{1d} - \sin\gamma\; C_{1u}$ and $\sin\gamma\; C_{1d} + \cos\gamma\; C_{1u}$, with $\gamma \approx \arctan 0.445$.

that the inclusion of these data has no impact in our conclusions. This is explained by the poor precision of these measurements, in particular for the forward-backward asymmetries.

- Higgs direct searches limits. Finally, we also consider in our analyses the results of the Higgs boson direct searches at LEP 2 [39] and Tevatron [40]. These are expressed in terms of the log-likelihood ratio

$$\mathrm{LLR} \equiv -2 \ln \frac{p\,(\mathrm{data}|H_1)}{p\,(\mathrm{data}|H_0)}, \tag{A.2}$$

  where p are the probabilities of the data according to the hypothesis of SM background, H_0, and SM background plus Higgs signal, H_1. This can be used to compute several types of different p-values, which lead to the determination of the regions in the M_H parameter space where the Higgs is excluded at a given confidence level. This log-likelihood directly contributes to the total χ^2 function, $\Delta\chi^2 = \mathrm{LLR}$ [215], thus contraining directly the values of M_H in the fit. The values for the observed log-likelihood ($\mathrm{LLR}_{\mathrm{obs}}$) to be added to the χ^2 have been extracted from Figure 1 in Ref. [39] and read from Table XIX in Ref. [40]. They are shown in Tables A.5 and A.6. The individual and total contributions to the χ^2 are given in Fig. 1.2 (left) in Chapter 1.

We do not include explicitly in the fits to new physics the anomalous magnetic moment of the muon or other one-loop order observables because we are only considering beyond the SM effects at tree-level.

A.2 The Standard Model fit

Unless otherwise stated, the SM parameters that we allow to float in the fits are the Higgs mass M_H, the top mass m_t, the Z mass M_Z, the strong coupling constant at the Z pole $\alpha_s\left(M_Z^2\right)$, and the five-flavor hadronic contribution to the running of the electromagnetic coupling constant at the Z pole $\Delta\alpha^{(5)}_{\mathrm{had}}\left(M_Z^2\right)$. The other fermion masses and the mixings are fixed for simplicity. These, as well as the value of the QED coupling constant at $q^2 = 0$,

$$\alpha^{-1} = 137.035999679(94), \tag{A.3}$$

and the muon decay constant G_μ,

$$G_\mu = 1.16637(1) \cdot 10^{-5}\ \mathrm{GeV}^{-2}, \tag{A.4}$$

have been taken from the Particle Data Group [18].

We have performed several SM fits changing the experimental data included. The results in the form of the best fit values and errors of the parameters, the minimum value of the χ^2, χ^2_{min}, as well as its ratio with the number of degrees of freedom[2], χ^2_{min}/d.o.f., are given in Table A.7. The different fits correspond to the use of data with and without lepton universality ("Standard" and "LU" fits, respectively) and including or not the limits from Higgs direct searches. The results from both the standard and the LU fits are very similar, though the latter gives a marginally better χ^2_{min}/d.o.f.. Apart from confirming the good agreement between data and the SM, the most significant information we can obtain is the indirect determination of the Higgs mass. From the standard fit (without Higgs direct searches) we get $M_H = 101^{+32}_{-26}$ GeV. This is slightly below the

[2]The number of degrees of freedom is given by the number of observables included in the fit minus the number of free parameters.

direct LEP 2 limit $M_H \geq 114.4$ GeV at 95% C.L., but it is consistent with it at less than 1 σ as we comment below. At 90% C.L. the confidence interval for M_H (95% C.L. upper and lower limits) is

$$62 \text{ GeV} \leq M_H \leq 159 \text{ GeV}. \tag{A.5}$$

It is also noteworthy that there are significant correlations at the minimum between M_H and m_t ($\approx 37\%$), $\Delta\alpha^{(5)}_{\rm had}\left(M_Z^2\right)$ ($\approx -27\%$) and, to a lesser extent, with M_Z ($\approx 13\%$).

As stressed in Chapter 1, the indirect determination of the Higgs mass results from the rather different preferences of M_W and the Z-pole leptonic asymmetries on the one hand, and the hadronic asymmetries on the other. While the former prefer a light Higgs, the latter favors a heavy one. In order to illustrate this, we have performed a fit to each of the previous observables independently, allowing only M_H to vary (with all the other parameters fixed to the best fit values in Table A.7). On the other hand, we also consider the cases where each of them is excluded from the global fit, in order to quantify their impact in the final determination of M_H. In this way we obtain:

- Fit to only (excluding) M_W: $M_H = 59^{+35}_{-26}$ GeV ($M_H = 133^{+52}_{-39}$ GeV).
- Fit to only (excluding) $A_{e,\mu,\tau}$ (SLD): $M_H = 37^{+31}_{-19}$ GeV ($M_H = 127^{+42}_{-33}$ GeV).
- Fit to only (excluding) A^b_{FB}: $M_H = 488^{+388}_{-210}$ GeV ($M_H = 73^{+28}_{-22}$ GeV).

Removing both the W mass and the leptonic asymmetries the preferred Higgs mass raises up to $M_H = 219^{+91}_{-29}$ GeV. In this last case and in the one removing A^b_{FB} we get a noticeable (but small) improvement in the quality of the fit: $\chi^2_{\rm min}/\text{d.o.f.} = 0.93$ and 0.91, respectively.

Including Higgs direct searches shifts the best fit value obtained for M_H to 115.5 GeV. There are also small shifts in the values for the top mass, $\Delta\alpha^{(5)}_{\rm had}\left(M_Z^2\right)$ and M_Z which follow from the correlations above. Because of the Tevatron exclusion limits, the upper bound in (A.5) is reduced to

$$M_H \leq 138 \text{ GeV}, \quad \text{at } 95\% \text{ C.L.} . \tag{A.6}$$

We must also mention that the value of the χ^2 at the minimum in the case we include direct searches data must been renormalized to account for the negative contributions coming from the $\text{LLR}_{\rm obs}$, for the χ^2 must be positive-definite. This is also required in order to compare the results from the fits with and without direct searches. In such a case we observe how the impact of forcing M_H above the direct LEP 2 bound is around 0.2 σ, so there is no conflict with this direct limit.

Finally, in order to compare the results of Chapter 4, where the $e^+e^- \to \bar{f}f$ LEP 2 data are taken into account, with the SM ones, we have also performed a SM fit including LEP 2 data. The results for the best fit values are unchanged with respect to the other cases. At the minimum we find

$$\chi^2_{\rm min} = 162.30, \qquad \frac{\chi^2_{\rm min}}{\text{d.o.f.}} = 0.78, \tag{A.7}$$

where the improvement in the quality of the fit is simply because we are including many more data points in good agreement with the SM predictions. Since, as we have checked, the effect of the variation of the SM parameters in the predictions for the LEP 2 data is small, they have been fixed for these observables in our fits to new physics. We have included, however, the leading oblique correction from the variation of the Higgs mass, as this is the parameter with the largest uncertainty.

Observable		Experimental Value	Standard Model	Pull	Standard Model +Higgs Searches	Pull
m_t [GeV]	[117]	173.1 ± 1.3	173.2	-0.1	173.4	-0.3
$\Delta\alpha^{(5)}_{\rm had}\left(M_Z^2\right)$	[119, 120]	0.02760 ± 0.00014	0.02762	-0.2	0.02760	0
$\alpha_s\left(M_Z^2\right)$	[118]	0.1184 ± 0.0007	0.1184	0	0.1184	0
M_W [GeV]	[71]	80.399 ± 0.023	80.372	$+1.2$	80.367	$+1.4$
Γ_W [GeV]		2.098 ± 0.048	2.091	$+0.1$	2.091	$+0.1$
Br $(W \to e\nu)$	[18]	0.1075 ± 0.0013	0.1083	-0.6	0.1083	-0.6
Br $(W \to \mu\nu)$		0.1057 ± 0.0015		-1.7		-1.7
Br $(W \to \tau\nu)$		0.1125 ± 0.0020		$+2.1$		$+2.1$
M_Z [GeV]	[70]	91.1876 ± 0.0021	91.1875	$+0.1$	91.1876	0
Γ_Z [GeV]		2.4952 ± 0.0023	2.4957	-0.2	2.4955	-0.1
$\sigma_{\rm had}$ [nb]		41.541 ± 0.037	41.479	$+1.7$	41.479	$+1.7$
R_e		20.804 ± 0.050	20.741	$+1.3$	20.740	$+1.3$
R_μ		20.785 ± 0.033	20.741	$+1.4$	20.740	$+1.4$
R_τ		20.764 ± 0.045	20.788	-0.5	20.787	-0.5
$A^e_{\rm FB}$		0.0145 ± 0.0025	0.0164	-0.8	0.0163	-0.7
$A^\mu_{\rm FB}$		0.0169 ± 0.0013		$+0.4$		$+0.5$
$A^\tau_{\rm FB}$		0.0188 ± 0.0017		$+1.4$		$+1.5$
A_e (SLD)	[70]	0.1516 ± 0.0021	0.1477	$+1.8$	0.1474	$+2.0$
A_μ (SLD)		0.142 ± 0.015		-0.4		-0.4
A_τ (SLD)		0.136 ± 0.015		-0.8		-0.8
$A_e\left(P_\tau\right)$	[70]	0.1498 ± 0.0049		$+0.4$		$+0.5$
$A_\tau\left(P_\tau\right)$		0.1439 ± 0.0043		-0.9		-0.8
R_b	[70]	0.21629 ± 0.00066	0.21580	$+0.7$	0.21580	$+0.7$
R_c		0.1721 ± 0.0030	0.1722	-0.1	0.1722	-0.1
$A^b_{\rm FB}$		0.0992 ± 0.0016	0.1036	-2.7	0.1033	-2.6
$A^c_{\rm FB}$		0.0707 ± 0.0035	0.0740	-1.0	0.738	-0.9
A_b		0.923 ± 0.020	0.935	-0.6	0.935	-0.6
A_c		0.670 ± 0.027	0.668	$+0.1$	0.668	$+0.1$
$A^s_{\rm FB}$	[70]	0.098 ± 0.011	0.1037	-0.5	0.1034	-0.5
A_s		0.895 ± 0.091	0.936	-0.5	0.936	-0.5
R_u/R_{u+d+s}		0.258 ± 0.045	0.282	-0.5	0.282	-0.5
$Q^{\rm had}_{\rm FB}$	[70]	0.0403 ± 0.0026	0.0424	-0.8	0.0423	-0.8
$\sin^2\theta^{\rm lept}_{\rm eff}$	[121]	0.2315 ± 0.0018	0.2314	0	0.2315	0
g^2_L	[38]	0.3012 ± 0.0013	0.3039	-2.0	0.3039	-2.0
g^2_R		0.0310 ± 0.0010	0.03012	$+0.9$	0.03013	$+0.9$
θ_L		2.500 ± 0.033	2.46	$+1.1$	2.46	$+1.1$
θ_R		4.58 ± 0.41	5.18	-1.5	5.18	-1.5
$g^{\nu e}_V$	[38]	-0.040 ± 0.015	-0.0399	0	-0.0398	0
$g^{\nu e}_A$		-0.507 ± 0.014	-0.507	0	0.507	0
$Q_W\left({}^{133}_{55}{\rm Cs}\right)$	[78]	-73.16 ± 0.35	-73.13	-0.1	-73.14	-0.1
$Q_W\left({}^{205}_{81}{\rm Tl}\right)$	[79]	-116.4 ± 3.6	-116.7	$+0.1$	-116.7	$+0.1$
$\cos\gamma C_{1d} - \sin\gamma C_{1u}$	[144]	0.342 ± 0.063	0.388	-0.7	0.388	-0.7
$\sin\gamma C_{1d} + \cos\gamma C_{1u}$		-0.0285 ± 0.0043	-0.0335	$+1.2$	-0.0335	$+1.2$
$Q_W\left(e\right)$ (Møller)	[80]	-0.0403 ± 0.0053	-0.0473	$+1.3$	-0.0471	$+1.3$
$\sum_i \lvert V_{ui}\rvert^2$	[68]	0.9999 ± 0.0006	1	-0.2	1	-0.2
$\sigma^{\nu e\to\nu\mu}/\sigma^{\nu e\to\nu\mu}_{\rm SM}$	[178]	0.981 ± 0.057	1	-0.3	1	-0.3

Table A.1: Measurements of the observables included in our fits, compared with the best-fit values in the SM. We give the predictions from the fits including and excluding the results from Higgs direct searches.

Observable		Experimental Value	Standard Model	Pull	Standard Model +Higgs Searches	Pull
m_t [GeV]	[117]	173.1 ± 1.3	173.2	-0.1	173.4	-0.3
$\Delta\alpha^{(5)}_{\rm had}\left(M_Z^2\right)$	[119, 120]	0.02760 ± 0.00014	0.02762	-0.2	0.02760	0
$\alpha_s\left(M_Z^2\right)$	[118]	0.1184 ± 0.0007	0.1184	0	0.1184	0
M_W [GeV]	[71]	80.399 ± 0.023	80.372	$+1.2$	80.367	$+1.4$
Γ_W [GeV]		2.098 ± 0.048	2.091	$+0.1$	2.091	$+0.1$
Br $(W \to l\nu)$	[18]	0.1080 ± 0.0009	0.1083	-0.3	0.1083	-0.3
M_Z [GeV]	[70]	91.1875 ± 0.0021	91.1875	0	91.1876	-0.1
Γ_Z [GeV]		2.4952 ± 0.0023	2.4957	-0.2	2.4955	-0.4
$\sigma_{\rm had}$ [nb]		41.540 ± 0.037	41.479	$+1.7$	41.479	$+1.7$
R_l		20.767 ± 0.025	20.741	$+1.0$	20.740	$+1.1$
$A^l_{\rm FB}$		0.0171 ± 0.0010	0.01636	$+0.7$	0.01628	$+0.8$
A_l (SLD)	[70]	0.1513 ± 0.0021	0.1477	$+1.7$	0.1473	$+1.9$
$A_l\,(P_\tau)$	[70]	0.1465 ± 0.0033	0.1477	-0.4	0.1473	-0.3
R_b	[70]	0.21629 ± 0.00066	0.2158	$+0.7$	0.2158	$+0.7$
R_c		0.1721 ± 0.0030	0.1722	-0.1	0.1722	-0.1
$A^b_{\rm FB}$		0.0992 ± 0.0016	0.1035	-2.7	0.1033	-2.6
$A^c_{\rm FB}$		0.0707 ± 0.0035	0.0740	-1.0	0.0738	-0.9
A_b		0.923 ± 0.020	0.9346	-0.6	0.9346	-0.6
A_c		0.670 ± 0.027	0.668	$+0.1$	0.668	$+0.1$
$A^s_{\rm FB}$	[70]	0.098 ± 0.011	0.1037	-0.5	0.1034	-0.5
A_s		0.895 ± 0.091	0.9357	-0.5	0.9357	-0.5
R_u/R_{u+d+s}		0.258 ± 0.045	0.2815	-0.5	0.2815	-0.5
$Q^{\rm had}_{\rm FB}$	[70]	0.0403 ± 0.0026	0.0424	-0.8	0.0423	-0.8
$\sin^2\theta^{\rm lept}_{\rm eff}$	[121]	0.2315 ± 0.0018	0.2314	0	0.2315	0
g_L^2	[38]	0.3005 ± 0.0012	0.30391	-2.1	0.30385	-2.0
g_R^2		0.0311 ± 0.0010	0.03012	$+0.9$	0.03013	$+0.9$
θ_L		2.500 ± 0.033	2.46	$+1.1$	2.46	$+1.1$
θ_R		4.59 ± 0.41	5.18	-1.5	5.17	-1.5
$g_V^{\nu e}$	[38]	-0.040 ± 0.015	-0.0399	0	-0.0398	0
$g_A^{\nu e}$		-0.507 ± 0.014	-0.507	0	-0.507	0
$Q_W\left({}^{133}_{55}{\rm Cs}\right)$	[78]	-73.16 ± 0.35	-73.13	-0.1	-73.14	-0.1
$Q_W\left({}^{205}_{81}{\rm Tl}\right)$	[79]	-116.4 ± 3.6	-116.7	$+0.1$	-116.7	$+0.1$
$\cos\gamma C_{1d} - \sin\gamma C_{1u}$	[144]	0.342 ± 0.063	0.389	-0.7	0.388	-0.7
$\sin\gamma C_{1d} + \cos\gamma C_{1u}$		-0.0285 ± 0.0043	-0.0335	$+1.2$	-0.0335	$+1.2$
$Q_W\,(e)$ (Møller)	[80]	-0.0403 ± 0.0053	-0.0473	$+1.3$	-0.0471	$+1.3$
$\sum_i \lvert V_{ui}\rvert^2$	[68]	0.9999 ± 0.0006	1	-0.2	1	-0.2
$\sigma^{\nu e\to\nu\mu}/\sigma^{\nu e\to\nu\mu}_{\rm SM}$	[178]	0.981 ± 0.057	1	-0.3	1	-0.3

Table A.2: Measurements of the observables included in our fits assuming lepton universality, compared with the best-fit values in the SM. We give the predictions from the fits including and excluding the results from Higgs direct searches.

$\sqrt{s}$ [GeV]	$\sigma(\mu^+\mu^-)$ [pb]	$A_{\rm FB}^{\mu^+\mu^-}$ $(\times 10^{-3})$	$\sigma(\tau^+\tau^-)$ [pb]	$A_{\rm FB}^{\tau^+\tau^-}$ $(\times 10^{-3})$	σ (had) [pb]
130	8.62 ± 0.68	694 ± 60	9.02 ± 0.93	663 ± 76	82.1 ± 2.2
	[8.44(0.3)]	[0.705(−0.2)]	[8.44(0.6)]	[0.704(−0.5)]	[82.8(−0.3)]
136	8.27 ± 0.67	708 ± 60	7.078 ± 0.820	753 ± 88	66.7 ± 2.0
	[7.28(1.5)]	[0.684(0.4)]	[7.279(−0.3)]	[0.683(0.8)]	[66.6(0.1)]
161	4.61 ± 0.36	538 ± 67	5.67 ± 0.54	646 ± 77	37.0 ± 1.1
	[4.61(0)]	[0.609(−1.1)]	[4.61(2)]	[0.609(0.5)]	[35.2(1.6)]
172	3.57 ± 0.32	675 ± 77	4.01 ± 0.45	342 ± 94	29.23 ± 0.99
	[3.95(−1.2)]	[0.591(1.1)]	[3.95(0.1)]	[0.591(−2.7)]	[28.74(0.5)]
183	3.49 ± 0.15	559 ± 35	3.37 ± 0.17	608 ± 45	24.59 ± 0.42
	[3.45(0.3)]	[0.576(−0.5)]	[3.45(−0.5)]	[0.576(0.7)]	[24.20(0.9)]
189	3.123 ± 0.076	569 ± 21	3.20 ± 0.10	596 ± 26	22.47 ± 0.24
	[3.207(−1.1)]	[0.569(0)]	[3.20(0)]	[0.569(1)]	[22.156(1.3)]
192	2.92 ± 0.18	553 ± 51	2.81 ± 0.23	615 ± 69	22.05 ± 0.53
	[3.10(−1)]	[0.566(−0.3)]	[3.10(−1.3)]	[0.566(0.7)]	[21.24(1.5)]
196	2.94 ± 0.11	581 ± 31	2.94 ± 0.14	505 ± 44	20.53 ± 0.34
	[2.96(−0.2)]	[0.562(0.61)]	[2.96(−0.1)]	[0.562(−1.3)]	[20.13(1.2)]
200	3.02 ± 0.11	524 ± 31	2.90 ± 0.14	539 ± 42	19.25 ± 0.32
	[2.83(1.7)]	[0.558(−1.1)]	[2.83(0.5)]	[0.558(−0.5)]	[19.09(0.5)]
202	2.58 ± 0.14	547 ± 47	2.79 ± 0.20	589 ± 59	19.07 ± 0.44
	[2.77(−1.4)]	[0.556(−0.2)]	[2.77(0.1)]	[0.556(0.6)]	[18.57(1.1)]
205	2.45 ± 0.10	565 ± 35	2.78 ± 0.14	571 ± 42	18.17 ± 0.31
	[2.67(−2.2)]	[0.553(0.3)]	[2.67(0.8)]	[0.553(0.4)]	[17.81(1.2)]
207	2.595 ± 0.088	542 ± 27	2.53 ± 0.11	564 ± 37	17.49 ± 0.26
	[2.623(−0.3)]	[0.552(−0.4)]	[2.62(−0.8)]	[0.551(0.4)]	[17.42(0.3)]

Table A.3: LEP 2 results for $e^+e^- \to f\bar{f}$ (first line), together with the SM predictions in the brackets and the pulls in parentheses (second line).

$\cos\theta$	$d\sigma\,(e^+e^- \to e^+e^-)\,/d\cos\theta$ [pb]						
	189 GeV	**192 GeV**	**196 GeV**	**200 GeV**	**202 GeV**	**205 GeV**	**207 GeV**
$[-0.90, -0.72]$	1.3 ± 0.2 [1.65(−1.8)]	1.4 ± 0.7 [1.60(−0.3)]	1.3 ± 0.4 [1.52(−0.6)]	1.5 ± 0.3 [1.45(0.2)]	2.2 ± 0.7 [1.44(1.1)]	0.8 ± 0.3 [1.38(−1.9)]	1.4 ± 0.2 [1.37(0.2)]
$[-0.72, -0.54]$	2.1 ± 0.3 [1.82(0.9)]	2.5 ± 0.9 [1.76(0.8)]	1.5 ± 0.3 [1.70(−0.7)]	1.8 ± 0.4 [1.63(0.4)]	1.3 ± 0.6 [1.58(−0.5)]	1.7 ± 0.4 [1.52(0.44)]	1.7 ± 0.3 [1.50(0.7)]
$[-0.54, -0.36]$	2.4 ± 0.3 [2.15(0.8)]	1.5 ± 0.8 [2.06(−0.7)]	2.2 ± 0.4 [1.96(0.6)]	2.0 ± 0.4 [1.88(0.3)]	2.8 ± 0.8 [1.83(1.2)]	2.3 ± 0.4 [1.78(1.3)]	1.7 ± 0.3 [1.76(−0.2)]
$[-0.36, -0.18]$	2.5 ± 0.3 [2.75(−0.8)]	2.4 ± 0.9 [2.63(−0.3)]	2.9 ± 0.5 [2.52(0.8)]	2.5 ± 0.4 [2.42(0.2)]	3.8 ± 0.8 [2.37(1.8)]	2.3 ± 0.4 [2.31(0)]	2.8 ± 0.3 [2.28(1.7)]
$[-0.18, \ 0.00]$	3.8 ± 0.4 [3.98(−0.5)]	2.9 ± 1.0 [3.85(−1)]	3.5 ± 0.5 [3.65(−0.3)]	3.9 ± 0.5 [3.49(0.8)]	2.2 ± 0.8 [3.42(−1.5)]	3.8 ± 0.5 [3.29(1)]	2.8 ± 0.4 [3.23(−1.1)]
$[\ 0.00, \ 0.09]$	4.5 ± 0.5 [5.32(−1.7)]	6.5 ± 2.0 [5.14(0.7)]	5.1 ± 0.9 [4.95(0.2)]	5.1 ± 0.9 [4.70(0.4)]	5.0 ± 1.6 [4.68(0.2)]	5.7 ± 0.9 [4.48(1.4)]	3.9 ± 0.6 [4.40(−0.8)]
$[\ 0.09, \ 0.18]$	6.3 ± 0.6 [6.94(−1.1)]	6.6 ± 2.1 [6.74(−0.1)]	5.6 ± 0.9 [6.45(−0.9)]	6.2 ± 1.0 [6.14(0.1)]	8.2 ± 1.6 [6.03(1.4)]	6.9 ± 1.0 [5.84(1.1)]	6.4 ± 0.7 [5.73(1)]
$[\ 0.18, \ 0.27]$	9.2 ± 0.8 [9.46(−0.3)]	9.2 ± 1.9 [9.13(0)]	8.4 ± 1.1 [8.69(−0.3)]	9.7 ± 1.2 [8.36(1.1)]	8.9 ± 1.6 [8.18(0.5)]	7.2 ± 1.0 [7.86(−0.7)]	7.4 ± 0.8 [7.71(−0.4)]
$[\ 0.27, \ 0.36]$	12.3 ± 0.9 [13.2(−1)]	13.7 ± 2.3 [12.7(0.4)]	12.7 ± 1.4 [12.3(0.3)]	10.0 ± 1.2 [11.6(−1.5)]	10.8 ± 1.8 [11.5(−0.4)]	11.2 ± 1.3 [11.1(0.1)]	11.9 ± 1.0 [11.0(0.9)]
$[\ 0.36, \ 0.45]$	19.7 ± 1.1 [19.5(0.2)]	21.2 ± 2.9 [18.8(0.8)]	14.9 ± 1.5 [18.0(−2)]	15.6 ± 1.5 [17.2(−1.1)]	14.6 ± 2.1 [16.9(−1.1)]	14.2 ± 1.4 [16.4(−1.6)]	17.1 ± 1.2 [16.1(0.8)]
$[\ 0.45, \ 0.54]$	31.9 ± 1.4 [30.1(1.2)]	31.0 ± 3.5 [29.2(0.5)]	26.7 ± 2.0 [28.0(−0.6)]	28.8 ± 2.1 [26.9(0.9)]	24.5 ± 2.7 [26.3(−0.7)]	27.2 ± 2.0 [25.6(0.8)]	25.1 ± 1.5 [25.2(−0.1)]
$[\ 0.54, \ 0.63]$	51.6 ± 1.8 [50.6(0.5)]	45.2 ± 4.3 [49.2(−0.9)]	50.1 ± 2.8 [47.2(1)]	48.4 ± 2.7 [45.3(1.1)]	45.4 ± 3.8 [44.4(0.3)]	43.8 ± 2.5 [42.9(0.4)]	41.9 ± 1.9 [42.2(−0.2)]
$[\ 0.63, \ 0.72]$	94.9 ± 2.4 [95.6(−0.3)]	91.6 ± 5.9 [92.8(−0.2)]	90.5 ± 3.6 [89.0(0.4)]	87.1 ± 3.5 [85.5(0.44)]	84.4 ± 5.0 [83.7(0.1)]	79.0 ± 3.3 [81.1(−0.6)]	77.3 ± 2.5 [79.8(−1)]
$[\ 0.72, \ 0.81]$	215 ± 4 [213(0.5)]	206 ± 9 [206(−0.1)]	199 ± 6 [199(0.1)]	194 ± 5 [191(0.7)]	184 ± 8 [187(−0.4)]	173 ± 5 [181(−1.5)]	174 ± 4 [178(−0.9)]
$[\ 0.81, \ 0.90]$	684 ± 7 [686(−0.2)]	663 ± 16 [665(−0.1)]	640 ± 10 [639(0.1)]	606 ± 10 [614(−0.7)]	606 ± 14 [601(0.3)]	578 ± 9 [583(−0.5)]	565 ± 7 [573(−1)]

Table A.4: LEP 2 results for the differential cross section of $e^+e^- \to e^+e^-$ from the OPAL collaboration [213](first line), together with the SM predictions in the brackets and the pulls in parentheses (second line).

M_H [GeV]	100	101	102	103	104	105	106	107	108	109	110
$\mathrm{LLR_{obs}}$	113.5	105.3	97.1	88.9	80.8	72.6	64.4	56.3	48.1	41.8	34.9
M_H [GeV]	111	112	113	114	115	116	117	118	119	120	
$\mathrm{LLR_{obs}}$	24.9	18.7	11.3	4.54	-0.71	-1.42	-1.73	-0.95	-0.31	-0.11	

Table A.5: Values of $\mathrm{LLR_{obs}}$ obtained from Higgs direct searches at LEP 2. Extracted from Fig. 1 in Ref. [39].

M_H [GeV]	100	105	110	115	120	125	130	135	140	145	150
$\mathrm{LLR_{obs}}$	-0.99	-1.41	-0.55	-2.58	-0.99	-1.62	-1.61	-2.22	-1.94	-0.07	-0.15
M_H [GeV]	155	160	165	170	175	180	185	190	195	200	
$\mathrm{LLR_{obs}}$	-0.29	3.23	5.04	2.24	3.64	2.79	0.90	1.28	-0.98	-0.48	

Table A.6: Values of $\mathrm{LLR_{obs}}$ obtained from Higgs direct searches at Tevatron [40].

Fit	M_H [GeV]	m_t [GeV]	M_Z [GeV]	$\alpha_s\left(M_Z^2\right)$	$\Delta\alpha^5_{\mathrm{had}}\left(M_Z^2\right)$	χ^2	χ^2/d.o.f
Standard	101^{+32}_{-26}	173.2 ± 1.3	91.1875(21)	0.1184(7)	0.02762(14)	44.1	1.08
+ Higgs DS	115.5	173.4 ± 1.2	91.1876(21)	0.1184(7)	0.02760(13)	44.32	1.06
LU	102^{+34}_{-26}	173.2 ± 1.3	91.1875(21)	0.1184(7)	0.02762(14)	30.04	0.94
+ Higgs DS	115.5	173.4 ± 1.2	91.1876(21)	0.1184(7)	0.02760(13)	30.23	0.92

Table A.7: Best fit values for the SM parameters for the different global fits discussed.

List of figures

1.1 Pulls for the SM theoretical predictions for some of the most representative observables included in the fit. 14

1.2 (Left) Higgs direct searches results from LEP 2 (red dotted line), Tevatron (blue dashed line), and the total combined contribution (black solid line) to the observed log-likelihood ($\mathrm{LLR}_{\mathrm{obs}}$). (Right) Minimum of the χ^2 in the SM as a function on the Higgs mass for the "standard" fit (blue dotted line) described in Appendix A and the fit including the Higgs direct searches results (black solid line). Note that the latter has been normalized to agree with the former for large M_H. 17

1.3 For an S-matrix element involving only light particles (thin lines) in the initial and final states, the effect of the exchange of the heavy ($M \sim \Lambda$) particles (thick lines) is mimicked in the effective theory by the presence of new interactions and/or corrections to the existing vertex and propagators. The exact correspondence between both theories is performed by matching their results at the threshold $E \sim \Lambda$. . . . 21

2.1 (Left) χ^2 profile as a function of M_H from the global fit excluding Higgs direct searches for the operator coefficients $\alpha_{ll}^{(3)}$, $\alpha_{\phi l}^{(3)}$, $\alpha_{\phi}^{(3)}$ and α_{WB}. (Right) 95% C.L. regions in the $\alpha_{\phi}^{(3)}$- α_{WB} plane for $M_H = 116, 300$ and 1000 GeV. 58

3.1 95% confidence region in the $\left|U_L^{eN}\right| - M_H$ parameter space for the N singlet coupled to the first, second and third family (blue, green and orange solid regions, respectively). The last plot corresponds to the universal case (gray solid region). In all cases the corresponding 95% confidence region excluding Higgs direct searches from the fit is delimited by the solid line. 75

3.2 95% confidence region in the $\left|U_L^{E\nu}\right| - M_H$ parameter space for the E singlet coupled to the first, second and third family (blue, green and orange solid regions, respectively). The last plot corresponds to the universal case (gray solid region). In all cases the corresponding 95% confidence region excluding Higgs direct searches from the fit is delimited by the solid line. 76

3.3 95% confidence region in the $\left|U_R^{eN}\right| - M_H$ parameter space for the Δ_1 doublet coupled to the first, second and third family (blue, green and orange solid regions, respectively). The last plot corresponds to the universal case (gray solid region). In all cases the corresponding 95% confidence region excluding Higgs direct searches from the fit is delimited by the solid line. 77

3.4 95% confidence region in the $\left|U_R^{E^{--}e}\right| - M_H$ parameter space for the Δ_3 doublet coupled to the first, second and third family (blue, green and orange solid regions, respectively). The last plot corresponds to the universal case (gray solid region). In all cases the corresponding 95% confidence region excluding Higgs direct searches from the fit is delimited by the solid line. 78

3.5 95% confidence region in the $\left|U_L^{eN}\right| - M_H$ parameter space for the Σ_0 triplet coupled to the first, second and third family (blue, green and orange solid regions, respectively). The last plot corresponds to the universal case (gray solid region). In all cases the corresponding 95% confidence region excluding Higgs direct searches from the fit is delimited by the solid line. 79

3.6 95% confidence region in the $\left|U_L^{E\nu}\right| - M_H$ parameter space for the Σ_1 triplet coupled to the first, second and third family (blue, green and orange solid regions, respectively). The last plot corresponds to the universal case (gray solid region). In all cases the corresponding 95% confidence region excluding Higgs direct searches from the fit is delimited by the solid line. 80

4.1 Feynman diagrams relevant for the dimension-six effective Lagrangian. 88

4.2 From darker to lighter, confidence regions with $\Delta\chi^2 \leq 2$ (blue), 4 (orange) and 6 (95% C.L.) (green), respectively, for the $\mathcal{B}$ couplings to leptons assuming no couplings to quarks. The region in the left plot results from the fit to EWPD without LEP 2 data. This is further constrained into the smaller region in the right plot by adding the LEP 2 cross sections and asymmetries to the fit. 93

4.3 From darker to lighter, confidence regions with $\Delta\chi^2 \leq 2$(blue), 4 (orange) and 6 (95% C.L.) (green), respectively, for the $\mathcal{B}$ couplings to the Higgs and LH leptons assuming no couplings to quarks. The regions in the plot on the left are obtained from a fit to EWPD without LEP 2 data. They are reduced to smaller regions when the LEP 2 cross sections and asymmetries are added to the fit, as shown in the plot on the right. 94

4.4 95% C.L. contour in the $M_{Z'}$ - $\sin\theta_{ZZ'}$ plane for the Z'_R model (left) and Z'_ψ (right). The different contours correspond to the fit to EWPD without LEP 2 cross sections and asymmetries (solid line), to LEP 2 cross sections and asymmetries (dashed line), and to all data (solid region). 96

4.5 From darker to lighter, confidence regions with $\Delta\chi^2 \leq 2$ (blue), 4 (orange) and 6 (95% C.L.) (green), respectively, for the $\mathcal{W}$ couplings to LH leptons and to the Higgs boson. Notice the flat direction along the Higgs coupling axis when the lepton charge vanishes. 97

4.6 From darker to lighter, confidence regions with $\Delta\chi^2 \leq 2$ (blue), 4 (orange) and 6 (95% C.L.) (green), respectively, in the $G^l_{\mathcal{W}_1}$ - $G^\phi_{\mathcal{W}_1}$ plane of an extension with two mirror left-handed triplets, $\mathcal{W}_1$ and $\mathcal{W}_2$. 100

4.7 Allowed regions of the $\mathcal{B}$ couplings to the RH bottom and to the Higgs at 1 σ (solid regions) and at 95% C.L. (regions between lines) from the nonuniversal $\mathcal{B}$ fit (blue, dotted) and the $\mathcal{B} + \mathcal{B}^1$ fit (orange, solid). 103

4.8 Confidence regions at 1 σ (blue, dark) and 95% C.L. (orange, light) on the plane determined by the corrections to the $Z\bar{b}_L b_L$ coming from a singlet $\mathcal{B}$ and a triplet $\mathcal{W}$.103

4.9 *Left:* Minimum of the χ^2 as a function of the Higgs mass for the SM fit, the $\mathcal{W}^1$ fit and the $\mathcal{B}$ fit. Higgs direct searches data are available up to $M_H = 200$ GeV. Above that value the effect of neutral-boson mixing flattens the curve. *Right:* From darker to lighter, confidence regions with $\Delta\chi^2 \leq 2$ (blue), 4 (orange) and 6 (95% C.L.) (green), in the plane parametrized by the Higgs mass and the $\mathcal{W}^1$ coupling to the Higgs. 105

5.1 90% C.L. bounds for E1 case (b) in Eq. (5.12); and the same for the SM extension E2 in next section. The narrow bands between the origin and the crosses define the 90% confidence region for the global fit to the two parameters for E1 (left cross) and E2 (right cross) respectively. 123

5.2 Percentage of detected events in a near detector at a neutrino factory compared to the predicted number by the SM, as a function of the new interactions strength δg^V_{LL}. The solid (dotted-dashed) curve corresponds to neutrino-nucleon (IMD) collisions. The vertical lines stand for the E1 and E2 limits on δg^V_{LL} in the text. 126

List of tables

1.1 Dimension five and six operators arising from the integration of heavy scalars, vector bosons or fermions at tree level. We also include the dimension-four operator $\mathcal{O}_{\phi 4}$ and the loop-level generated dimension-six operator $\mathcal{O}_{WB}$ for notational purposes. Transposition of the second $SU(2)_L$ doublet is understood in the first four LRLR operators. σ_a and λ_A stand for the Pauli and Gell-Mann matrices, respectively, and ϵ_{ABC} is the totally antisymmetric tensor for color indices ($A, B, \cdots = 1, 2, 3$ in this case). 25

2.1 Dimension-six operators contributing (directly or indirectly) to the different observables included in the fits. 54
2.2 95% C.L. limits on (90% central confidence interval of) the operator coefficients in Table 4.3, considering only one operator at a time and for each data set. Limits are in units of TeV^{-2}. The different columns show the results for different fits depending on the observables included. 55
2.3 Correlation (ρ_{ij}) between the operator coefficients and $\log M_H$ at the global minimum, and without Higgs direct searches data. The corresponding 95% C.L. limits for the coefficients and M_H are also given. 58

3.1 Lepton multiplets mixing with the SM leptons through Yukawa couplings to the SM Higgs. 63
3.2 Quark multiplets mixing with the SM leptons through Yukawa couplings to the SM Higgs. In this case the spinor field describing the fermions can be only of Dirac type. 63
3.3 Form of the scalar doublet required to make the operators $\overline{\Psi_L}\Phi\Psi'_R$, $\overline{\Psi_R}\Phi\psi_L$ and $\overline{\Psi_L}\Phi\psi_R$ gauge invariant, in terms of the quantum numbers of the fermions appearing in the operator. 64
3.4 First order expressions in $\frac{yv}{M}$ of the mixing between one SM lepton of a given flavor and one extra lepton. Family indices are implicit and "negligible" stands for higher order contributions. 65
3.5 Resulting first order expressions of a complete subset of independent charged current couplings $-\frac{g}{\sqrt{2}}U_\alpha^{ff'}W_\mu^-\overline{f_\alpha}\gamma^\mu f'_\alpha$, $\alpha = L, R$, as a function of the lepton mixing. . . . 65
3.6 Coefficients of the operators arising from the integration of heavy leptons. The dimension-five operator entry, $\frac{\alpha_5}{\Lambda}$, only appears when the singlet N and/or the triplet Σ_0 are Majorana fermions. 68
3.7 Coefficients of the operators arising from the integration of heavy quarks. 69
3.8 Combined contribution to $\alpha_{e\phi}$ from the simultaneous integration of different mixed lepton multiplets. Even if the corresponding operator does not affect our fits, we include the values of the coefficient for completeness. 70

3.9 Combined contribution to $\alpha_{u\phi}$ and $\alpha_{d\phi}$ from the simultaneous integration of different mixed quark multiplets. 71
3.10 Decrease in $\chi^2_{\rm min}$ with respect to the SM minimum, $\chi^2_{\rm SM} = 44.32$ ($\chi^2_{\rm SM} = 30.23$ with lepton universality), obtained by adding to the SM the different leptons. The number of degrees of freedom is obtained as $\mathcal{N} - 5 - n^{\rm new}_{\rm par}$, where n^{new}_{par} is the number of independent lepton mixings and $\mathcal{N} = 47$ is the number of observables ($\mathcal{N} = 38$ for the universal case). In parenthesis we write the value of $\chi^2_{\rm min}$/d.o.f., which for the SM is 1.06 (0.92 with lepton universality). 72
3.11 Upper limit at 95 % C.L. on the absolute value of the mixings in Table 3.5 and their value at the minimum. The first three rows are obtained by coupling each new lepton with only one SM family. The last one corresponds to the case of lepton universality. All numbers are computed including the M_H constraints from Higgs direct searches at LEP 2 and Tevatron. 73
3.12 Upper limit at 95 % C.L. on the Higgs mass (in GeV). The first three rows are obtained by coupling each new lepton with only one SM family. The last one correspond to the case of lepton universality. All numbers are computed taking into account the M_H constraints from Higgs direct searches at LEP 2 and Tevatron. . . 74

4.1 Vector bosons contributing to the dimension-six effective Lagrangian. 85
4.2 Examples of symmetry breaking patterns giving rise to each type of vectors bosons in Table 4.1 [134]. Generating the right Weinberg angle and accommodating the matter fields requires, in some cases, an extension of the gauge groups in this table and a more involved pattern of symmetry breaking. 86
4.3 Experimental data constraining (directly or indirectly) the couplings of the vector bosons. 90
4.4 Results of the fit to EWPD for the extra vector bosons. We give $\Delta\chi^2_{\rm min} = \chi^2_{\rm min} - \chi^2_{\rm SM}$ values, together with the best fit values and bounds on the interactions of the new vectors. The results for the last six representations are obtained from a fit to each of the entries of the coupling matrices at a time. $[i, j]$ refers to the entries in the family matrices that give the best fit. See text for more details. 92
4.5 Comparison of 95% C.L. limits on $\sin\theta_{ZZ'}$ and $M_{Z'}$ obtained for several popular Z' models from a fit to standard EWPD without LEP 2, to LEP 2 cross sections and asymmetries, and to all data. The gauge coupling constants are taken equal to the GUT-inspired value, $\sqrt{5/3}\, g' \approx 0.46$. 95
4.6 Effect of the SM singlets on the forward-backward asymmetry for the b quark from the nonuniveral fit. The improvement in the χ^2 for the cases of $M_H = 200, 500$ GeV is given with respect to the SM with the same values of the Higgs mass. The last two columns correspond to different points along a flat direction. 102
4.7 Operators arising from the integration of a $\mathcal{B}$ vector field. 108
4.8 Operators arising from the integration of a $\mathcal{W}$ vector field. 108
4.9 Operators arising from the integration of a $\mathcal{G}$ vector field. 109
4.10 Operators arising from the integration of a $\mathcal{H}$ vector field. 109
4.11 Operators arising from the integration of a $\mathcal{B}^1$ vector field. 109
4.12 Operators arising from the integration of a $\mathcal{W}^1$ vector field. 110
4.13 Operators arising from the integration of a $\mathcal{G}^1$ vector field. 110
4.14 Operators arising from the integration of a $\mathcal{L}$ vector field. 110
4.15 Operators arising from the integration of a $\mathcal{U}^2$ vector field. 111
4.16 Operators arising from the integration of a $\mathcal{U}^5$ vector field. 111
4.17 Operators arising from the integration of a $\mathcal{Q}^1$ vector field. 111

4.18 Operators arising from the integration of a $\mathcal{Q}^5$ vector field. 112
4.19 Operators arising from the integration of a $\mathcal{X}$ vector field. 112
4.20 Operators arising from the integration of a $\mathcal{Y}^1$ vector field. $(A|\cdots|B) = \frac{1}{2}(AB+BA)$ stands for the symmetric combination of color indices. 112
4.21 Operators arising from the integration of a $\mathcal{Y}^5$ vector field. 113

5.1 Dimension five and six operators completing Table 1.1, in the case that RH neutrinos are light. Transposition of the second $SU(2)_L$ doublet is understood in the LRLR four-fermion operators. 117
5.2 Maximum deficit in the number of observed events in a near detector sensitive to neutrino-nucleon collisions (ν-N) and IMD for the two SM extensions discussed in the text. In parentheses we show the deficits expected in the case that the precision on the measurement of IMD is improved by a factor of 2. 125
5.3 Neutrino source for the different oscillation experiments and search process. . . . 127

A.1 Measurements of the observables included in our fits, compared with the best-fit values in the SM. We give the predictions from the fits including and excluding the results from Higgs direct searches. 138
A.2 Measurements of the observables included in our fits assuming lepton universality, compared with the best-fit values in the SM. We give the predictions from the fits including and excluding the results from Higgs direct searches. 139
A.3 LEP 2 results for $e^+e^- \to f\bar{f}$ (first line), together with the SM predictions in the brackets and the pulls in parentheses (second line). 140
A.4 LEP 2 results for the differential cross section of $e^+e^- \to e^+e^-$ from the OPAL collaboration [213](first line), together with the SM predictions in the brackets and the pulls in parentheses (second line). 141
A.5 Values of $\mathrm{LLR}_{\mathrm{obs}}$ obtained from Higgs direct searches at LEP 2. Extracted from Fig. 1 in Ref. [39]. 142
A.6 Values of $\mathrm{LLR}_{\mathrm{obs}}$ obtained from Higgs direct searches at Tevatron [40]. 142
A.7 Best fit values for the SM parameters for the different global fits discussed. 142

Bibliography

[1] F. del Aguila, J. de Blas and M. Perez-Victoria, Phys. Rev. D **78** (2008) 013010 [arXiv:0803.4008 [hep-ph]].

[2] F. del Aguila, J. A. Aguilar-Saavedra, J. de Blas and M. Zralek, Acta Phys. Polon. B **38** (2007) 3339 [arXiv:0710.2923 [hep-ph]].

[3] F. del Aguila, J. A. Aguilar-Saavedra, J. de Blas and M. Perez-Victoria, arXiv:0806.1023 [hep-ph].

[4] F. del Aguila, J. A. Aguilar-Saavedra and J. de Blas, Acta Phys. Polon. B **40** (2009) 2901 [arXiv:0910.2720 [hep-ph]].

[5] F. del Aguila, J. de Blas and M. Perez-Victoria, arXiv:1005.3998 [hep-ph].

[6] F. del Aguila, J. de Blas, R. Szafron, J. Wudka and M. Zralek, Phys. Lett. B **683** (2010) 282 [arXiv:0911.3158 [hep-ph]].

[7] F. del Aguila, J. de Blas, A. Carmona and J. Santiago, arXiv:1003.5799 [hep-ph].

[8] J. de Blas, A. Falkowski, M. Perez-Victoria and S. Pokorski, JHEP **0608** (2006) 061 [arXiv:hep-th/0605150].

[9] J. de Blas, P. Langacker, G. Paz and L. T. Wang, JHEP **1001** (2010) 037 [arXiv:0911.1996 [hep-ph]].

[10] S. L. Glashow, Nucl. Phys. **22** (1961) 579.

[11] S. Weinberg, Phys. Rev. Lett. **19** (1967) 1264.

[12] A. Salam, *Originally printed in *Svartholm: Elementary Particle Theory, Proceedings Of The Nobel Symposium Held 1968 At Lerum, Sweden*, Stockholm 1968, 367-377.*

[13] S. F. Novaes, arXiv:hep-ph/0001283.

[14] S. Pokorski, arXiv:hep-ph/0502132.

[15] W. Hollik, J. Phys. Conf. Ser. **53** (2006) 7.

[16] A. Pich, arXiv:0705.4264 [hep-ph].

[17] P. Langacker, arXiv:0901.0241 [hep-ph]; P. Langacker, *Boca Raton, USA: CRC Pr. (2010) 663 p.*

[18] C. Amsler *et al.* [Particle Data Group], Phys. Lett. B **667**, 1 (2008) and 2009 partial update for the 2010 edition.

[19] H. Georgi, Ann. Rev. Nucl. Part. Sci. **43** (1993) 209.

[20] A. V. Manohar, arXiv:hep-ph/9606222.

[21] A. Pich, arXiv:hep-ph/9806303.

[22] I. Z. Rothstein, arXiv:hep-ph/0308266.

[23] C. P. Burgess, Ann. Rev. Nucl. Part. Sci. **57** (2007) 329 [arXiv:hep-th/0701053].

[24] W. D. Goldberger, arXiv:hep-ph/0701129.

[25] P. W. Higgs, Phys. Lett. **12** (1964) 132.

[26] F. Englert and R. Brout, Phys. Rev. Lett. **13** (1964) 321.

[27] G. S. Guralnik, C. R. Hagen and T. W. B. Kibble, Phys. Rev. Lett. **13** (1964) 585.

[28] T. W. B. Kibble, Phys. Rev. **155** (1967) 1554.

[29] Y. Nambu, Phys. Rev. Lett. **4** (1960) 380.

[30] J. Goldstone, Nuovo Cim. **19** (1961) 154.

[31] N. Cabibbo, Phys. Rev. Lett. **10** (1963) 531.

[32] M. Kobayashi and T. Maskawa, Prog. Theor. Phys. **49** (1973) 652.

[33] B. Aubert *et al.* [BABAR Collaboration], Phys. Rev. Lett. **103** (2009) 231801 [arXiv:0908.3589 [hep-ex]].

[34] B. L. Roberts, arXiv:1001.2898 [hep-ex]; G. W. Bennett *et al.* [Muon G-2 Collaboration], Phys. Rev. D **73** (2006) 072003 [arXiv:hep-ex/0602035]; G. W. Bennett *et al.* [Muon g-2 Collaboration], Phys. Rev. Lett. **92** (2004) 161802 [arXiv:hep-ex/0401008].

[35] M. Davier, S. Eidelman, A. Hocker and Z. Zhang, Eur. Phys. J. C **31** (2003) 503 [arXiv:hep-ph/0308213].

[36] M. W. Grunewald, arXiv:0710.2838 [hep-ex].

[37] LEP Electroweak Working Group, `http://lepewwg.web.cern.ch`.

[38] See J. Erler and P. Langacker in [18].

[39] R. Barate *et al.* [LEP Working Group for Higgs boson searches and ALEPH, DELPHI, L3 and OPAL Collaborations], Phys. Lett. B **565** (2003) 61 [arXiv:hep-ex/0306033].

[40] The CDF Collaboration, the DØ Collaboration, the Tevatron New Physics and Higgs Working Group, arXiv:0911.3930 [hep-ex].

[41] J. Baglio and A. Djouadi, arXiv:1003.4266 [hep-ph].

[42] M. S. Chanowitz, Phys. Rev. D **66** (2002) 073002 [arXiv:hep-ph/0207123].

[43] M. S. Chanowitz, arXiv:hep-ph/0304199.

[44] B. W. Lee, C. Quigg and H. B. Thacker, Phys. Rev. D **16** (1977) 1519.

[45] J. Erler, arXiv:1002.1320 [hep-ph].

[46] T. Hambye and K. Riesselmann, arXiv:hep-ph/9708416.

[47] R. D. Peccei, Adv. Ser. Direct. High Energy Phys. **3** (1989) 503.

[48] T. Appelquist and J. Carazzone, Phys. Rev. D **11** (1975) 2856.

[49] S. Weinberg, Physica A **96** (1979) 327.

[50] A. Dobado, D. Espriu and M. J. Herrero, Phys. Lett. B **255** (1991) 405.

[51] C. P. Burgess, S. Godfrey, H. Konig, D. London and I. Maksymyk, Phys. Rev. D **49** (1994) 6115 [arXiv:hep-ph/9312291].

[52] Z. Han and W. Skiba, Phys. Rev. D **71** (2005) 075009 [arXiv:hep-ph/0412166]; Z. Han, Phys. Rev. D **73** (2006) 015005 [arXiv:hep-ph/0510125].

[53] G. Cacciapaglia, C. Csaki, G. Marandella and A. Strumia, Phys. Rev. D **74** (2006) 033011 [arXiv:hep-ph/0604111].

[54] H. C. Cheng and I. Low, JHEP **0309** (2003) 051 [arXiv:hep-ph/0308199]; H. C. Cheng and I. Low, JHEP **0408** (2004) 061 [arXiv:hep-ph/0405243].

[55] H. C. Cheng, K. T. Matchev and M. Schmaltz, Phys. Rev. D **66** (2002) 036005 [arXiv:hep-ph/0204342].

[56] H. Lehmann, K. Symanzik and W. Zimmermann, Nuovo Cim. **1** (1955) 205.

[57] W. Buchmuller and D. Wyler, Nucl. Phys. B **268** (1986) 621.

[58] C. Arzt, M. B. Einhorn and J. Wudka, Nucl. Phys. B **433** (1995) 41 [arXiv:hep-ph/9405214].

[59] B. Grzadkowski, Z. Hioki, K. Ohkuma and J. Wudka, Nucl. Phys. B **689** (2004) 108 [arXiv:hep-ph/0310159]; J. A. Aguilar-Saavedra, Nucl. Phys. B **812** (2009) 181 [arXiv:0811.3842 [hep-ph]]; D. Nomura, JHEP **1002** (2010) 061 [arXiv:0911.1941 [hep-ph]].

[60] S. Weinberg, Phys. Rev. Lett. **43** (1979) 1566.

[61] A. de Gouvea and J. Jenkins, Phys. Rev. D **77** (2008) 013008 [arXiv:0708.1344 [hep-ph]].

[62] M. E. Peskin and T. Takeuchi, Phys. Rev. D **46** (1992) 381.

[63] B. Pontecorvo, Sov. Phys. JETP **6** (1957) 429 [Zh. Eksp. Teor. Fiz. **33** (1957) 549]; Z. Maki, M. Nakagawa and S. Sakata, Prog. Theor. Phys. **28** (1962) 870.

[64] D. Hanneke, S. Fogwell and G. Gabrielse, Phys. Rev. Lett. **100** (2008) 120801 [arXiv:0801.1134 [physics.atom-ph]].

[65] D. B. Chitwood *et al.* [MuLan Collaboration], Phys. Rev. Lett. **99** (2007) 032001 [arXiv:0704.1981 [hep-ex]].

[66] A. Barczyk *et al.* [FAST Collaboration], Phys. Lett. B **663** (2008) 172 [arXiv:0707.3904 [hep-ex]].

[67] J. C. Hardy and I. S. Towner, Phys. Rev. C **79** (2009) 055502 [arXiv:0812.1202 [nucl-ex]].

[68] See E. Blucher and W.J. Marciano in [18].

[69] J. A. Aguilar-Saavedra, Nucl. Phys. B **821** (2009) 215 [arXiv:0904.2387 [hep-ph]].

[70] [The ALEPH, DELPHI, L3, OPAL, SLD Collaborations, the LEP Electroweak Working Group, the SLD Electroweak and Heavy Flavor Groups], Phys. Rept. **427** (2006) 257 [arXiv:hep-ex/0509008].

[71] J. Alcaraz [The ALEPH, CDF, DØ, DELPHI, L3, OPAL, SLD Collaborations, the LEP Electroweak Working Group, the Tevatron Electroweak Working Group, and the SLD Electroweak and Heavy Flavor Groups], arXiv:0911.2604 [hep-ex].

[72] H. Abramowicz *et al.*, Phys. Rev. Lett. **57** (1986) 298; A. Blondel *et al.*, Z. Phys. C **45** (1990) 361.

[73] J. V. Allaby *et al.* [CHARM Collaboration], Phys. Lett. B **177** (1986) 446; J. V. Allaby *et al.* [CHARM Collaboration], Z. Phys. C **36** (1987) 611.

[74] C. Arroyo *et al.* [CCFR Collaboration], Phys. Rev. Lett. **72** (1994) 3452 [arXiv:hep-ex/9405008]; K. S. McFarland *et al.* [CCFR Collaboration and The E744 Collaboration and The E770 Collaboration], Eur. Phys. J. C **1** (1998) 509 [arXiv:hep-ex/9701010].

[75] G. P. Zeller *et al.* [NuTeV Collaboration], Phys. Rev. Lett. **88** (2002) 091802 [Erratum-ibid. **90** (2003) 239902] [arXiv:hep-ex/0110059].

[76] P. Vilain *et al.* [CHARM-II Collaboration], Phys. Lett. B **335** (1994) 246.

[77] C. S. Wood, S. C. Bennett, D. Cho, B. P. Masterson, J. L. Roberts, C. E. Tanner and C. E. Wieman, Science **275** (1997) 1759; J. Guena, M. Lintz and M. A. Bouchiat, arXiv:physics/0412017.

[78] S. G. Porsev, K. Beloy and A. Derevianko, Phys. Rev. Lett. **102** (2009) 181601 [arXiv:0902.0335 [hep-ph]].

[79] P. A. Vetter, D. M. Meekhof, P. K. Majumder, S. K. Lamoreaux and E. N. Fortson, Phys. Rev. Lett. **74** (1995) 2658.

[80] P. L. Anthony *et al.* [SLAC E158 Collaboration], Phys. Rev. Lett. **95** (2005) 081601 [arXiv:hep-ex/0504049].

[81] J. Alcaraz *et al.* [The LEP Collaborations ALEPH, DELPHI, L3, OPAL, and the LEP Electroweak Working Group], arXiv:hep-ex/0612034.

[82] E. Eichten, K. D. Lane and M. E. Peskin, Phys. Rev. Lett. **50** (1983) 811; H. Kroha, Phys. Rev. D **46** (1992) 58.

[83] R. Barbieri and A. Strumia, Phys. Lett. B **462** (1999) 144 [arXiv:hep-ph/9905281].

[84] W. Loinaz, N. Okamura, T. Takeuchi and L. C. R. Wijewardhana, Phys. Rev. D **67** (2003) 073012 [arXiv:hep-ph/0210193].

[85] A. Sirlin, Phys. Rev. D **22** (1980) 971.

[86] H. Georgi and S. L. Glashow, Phys. Rev. Lett. **32** (1974) 438; H. Georgi, H. R. Quinn and S. Weinberg, Phys. Rev. Lett. **33** (1974) 451; J. C. Pati and A. Salam, Phys. Rev. D **10** (1974) 275 [Erratum-ibid. D **11** (1975) 703]; M. Gell-Mann, P. Ramond and R. Slansky, Rev. Mod. Phys. **50** (1978) 721; P. Langacker, Phys. Rept. **72** (1981) 185; J. L. Hewett and T. G. Rizzo, Phys. Rept. **183** (1989) 193.

[87] F. del Aguila and M. J. Bowick, Nucl. Phys. B **224** (1983) 107.

[88] N. Arkani-Hamed, A. G. Cohen and H. Georgi, Phys. Lett. B **513**, 232 (2001) [arXiv:hep-ph/0105239]; N. Arkani-Hamed, A. G. Cohen, E. Katz and A. E. Nelson, JHEP **0207** (2002) 034 [arXiv:hep-ph/0206021]; M. Perelstein, Prog. Part. Nucl. Phys. **58**, 247 (2007) [arXiv:hep-ph/0512128].

[89] I. Antoniadis, Phys. Lett. B **246** (1990) 377; N. Arkani-Hamed, S. Dimopoulos and G. R. Dvali, Phys. Lett. B **429** (1998) 263 [arXiv:hep-ph/9803315]; C. Csaki, arXiv:hep-ph/0404096.

[90] J. Erler and P. Langacker, arXiv:1003.3211 [hep-ph].

[91] M. Bander, Phys. Lett. B **277** (1992) 509.

[92] D. Chang, W. F. Chang and E. Ma, Phys. Rev. D **61** (2000) 037301 [arXiv:hep-ph/9909537].

[93] D. Choudhury, T. M. P. Tait and C. E. M. Wagner, Phys. Rev. D **65** (2002) 053002 [arXiv:hep-ph/0109097].

[94] G. Cynolter and E. Lendvai, Eur. Phys. J. C **58** (2008) 463 [arXiv:0804.4080 [hep-ph]].

[95] P. Lodone, JHEP **0812** (2008) 029 [arXiv:0806.1472 [hep-ph]].

[96] S. Mert Aybat and J. Santiago, Phys. Rev. D **80** (2009) 035005 [arXiv:0905.3032 [hep-ph]].

[97] F. del Aguila, J. de Blas and M. Perez-Victoria, in preparation.

[98] P. Langacker and D. London, Phys. Rev. D **38** (1988) 886; P. Langacker and D. London, Phys. Rev. D **39** (1989) 266; P. Langacker, M. x. Luo and A. K. Mann, Rev. Mod. Phys. **64** (1992) 87; D. London, arXiv:hep-ph/9303290.

[99] E. Nardi, E. Roulet and D. Tommasini, Phys. Lett. B **327**, 319 (1994) [arXiv:hep-ph/9402224]; E. Nardi, E. Roulet and D. Tommasini, Nucl. Phys. B **386**, 239 (1992).

[100] S. Bergmann and A. Kagan, Nucl. Phys. B **538** (1999) 368 [arXiv:hep-ph/9803305]; B. Bekman, J. Gluza, J. Holeczek, J. Syska and M. Zralek, Phys. Rev. D **66** (2002) 093004 [arXiv:hep-ph/0207015]; see also F. del Aguila, G. L. Kane, J. M. Moreno and M. Quiros, Phys. Rev. Lett. **66** (1991) 2943.

[101] D. Tommasini, G. Barenboim, J. Bernabeu and C. Jarlskog, Nucl. Phys. B **444** (1995) 451 [arXiv:hep-ph/9503228].

[102] A. Abada, C. Biggio, F. Bonnet, M. B. Gavela and T. Hambye, JHEP **0712** (2007) 061 [arXiv:0707.4058 [hep-ph]].

[103] A. Abada, C. Biggio, F. Bonnet, M. B. Gavela and T. Hambye, arXiv:0803.0481 [hep-ph].

[104] M. Raidal *et al.*, arXiv:0801.1826 [hep-ph].

[105] R. N. Mohapatra, Nucl. Phys. Proc. Suppl. **77** (1999) 376 [arXiv:hep-ph/9808284]; C. Aalseth *et al.*, arXiv:hep-ph/0412300.

[106] G. Ingelman and J. Rathsman, Z. Phys. C **60** (1993) 243; F. del Aguila, J. A. Aguilar-Saavedra, A. Martinez de la Ossa and D. Meloni, Phys. Lett. B **613** (2005) 170 [arXiv:hep-ph/0502189].

[107] J. Kersten and A. Y. Smirnov, Phys. Rev. D **76** (2007) 073005 [arXiv:0705.3221 [hep-ph]].

[108] P. Minkowski, Phys. Lett. B **67** (1977) 421; T. Yanagida, Proceedings of the *Workshop on Unified Theories and Baryon Number in the Universe*, Tsukuba, 1979, eds. A. Sawada and A. Sugamoto; S. Glashow, in *Cargese 1979, Proceedings, Quarks and Leptons* (1979); M. Gell-Mann, P. Ramond and R. Slansky, Proceedings of the *Supergravity Stony Brook Workshop*, New York, 1979, eds. P. Van Niewenhuizen and D. Freedman; R. Mohapatra and G. Senjanović, Phys. Rev. Lett. **44** (1980) 912.

[109] R. Foot, H. Lew, X. G. He and G. C. Joshi, Z. Phys. C **44** (1989) 441; see also for recent work B. Bajc and G. Senjanovic, JHEP **0708** (2007) 014 [arXiv:hep-ph/0612029]; B. Bajc, M. Nemevsek and G. Senjanovic, Phys. Rev. D **76** (2007) 055011 [arXiv:hep-ph/0703080].

[110] S. Bray, J. S. Lee and A. Pilaftsis, Nucl. Phys. B **786** (2007) 95 [arXiv:hep-ph/0702294].

[111] T. Han and B. Zhang, Phys. Rev. Lett. **97** (2006) 171804 [arXiv:hep-ph/0604064]; F. del Aguila, J. A. Aguilar-Saavedra and R. Pittau, JHEP **0710** (2007) 047 [arXiv:hep-ph/0703261].

[112] F. del Aguila, L. Ametller, G. L. Kane and J. Vidal, Nucl. Phys. B **334** (1990) 1.

[113] F. del Aguila and J. A. Aguilar-Saavedra, JHEP **0505** (2005) 026 [arXiv:hep-ph/0503026].

[114] A. Bandyopadhyay *et al.* [ISS Physics Working Group], arXiv:0710.4947 [hep-ph]; T. Adams *et al.*, arXiv:0803.0354 [hep-ph].

[115] F. del Aguila, M. Perez-Victoria and J. Santiago, JHEP **0009** (2000) 011 [arXiv:hep-ph/0007316].

[116] F. del Aguila, M. Masip and J. L. Padilla, Phys. Lett. B **627** (2005) 131 [arXiv:hep-ph/0506063].

[117] [The Tevatron Electroweak Working Group for the CDF and DØ Collaborations], arXiv:0903.2503 [hep-ex].

[118] S. Bethke, Eur. Phys. J. C **64** (2009) 689 [arXiv:0908.1135 [hep-ph]]; See also G. Dissertori and G. P. Salam in [18].

[119] H. Burkhardt and B. Pietrzyk, Phys. Rev. D **72** (2005) 057501 [arXiv:hep-ph/0506323].

[120] T. Teubner, K. Hagiwara, R. Liao, A. D. Martin and D. Nomura, arXiv:1001.5401 [hep-ph].

[121] D. E. Acosta *et al.* [CDF Collaboration], Phys. Rev. D **71** (2005) 052002 [arXiv:hep-ex/0411059]; V. M. Abazov *et al.* [DØ Collaboration], Phys. Rev. Lett. **101** (2008) 191801 [arXiv:0804.3220 [hep-ex]].

[122] R. Barbieri, A. Pomarol, R. Rattazzi and A. Strumia, Nucl. Phys. B **703** (2004) 127 [arXiv:hep-ph/0405040].

[123] M. Passera, W. J. Marciano and A. Sirlin, arXiv:0804.1142 [hep-ph].

[124] A. Datta, M. Guchait and D. P. Roy, Phys. Rev. D **47** (1993) 961 [arXiv:hep-ph/9208228].

[125] F. del Aguila *et al.*, arXiv:0801.1800 [hep-ph].

[126] B. Bekman, J. Gluza, J. Holeczek, J. Syska and M. Zralek, Phys. Rev. D **66** (2002) 093004 [arXiv:hep-ph/0207015].

[127] F. del Aguila, J. de Blas, P. Langacker and M. Perez-Victoria, in preparation.

[128] I. Antoniadis, K. Benakli and M. Quiros, Phys. Lett. B **460** (1999) 176 [arXiv:hep-ph/9905311].

[129] S. Weinberg, Phys. Rev. D **13** (1976) 974; S. Weinberg, Phys. Rev. D **19** (1979) 1277; L. Susskind, Phys. Rev. D **20** (1979) 2619; E. Farhi and L. Susskind, Phys. Rept. **74** (1981) 277.

[130] M. Bando, T. Kugo, S. Uehara, K. Yamawaki and T. Yanagida, Phys. Rev. Lett. **54** (1985) 1215.

[131] J. M. Maldacena, Adv. Theor. Math. Phys. **2** (1998) 231 [Int. J. Theor. Phys. **38** (1999) 1113] [arXiv:hep-th/9711200].

[132] N. Arkani-Hamed, M. Porrati and L. Randall, JHEP **0108** (2001) 017 [arXiv:hep-th/0012148]; R. Rattazzi and A. Zaffaroni, JHEP **0104** (2001) 021 [arXiv:hep-th/0012248]; M. Perez-Victoria, JHEP **0105** (2001) 064 [arXiv:hep-th/0105048].

[133] P. Langacker, Rev. Mod. Phys. **81** (2008) 1199 [arXiv:0801.1345 [hep-ph]].

[134] R. Slansky, Phys. Rept. **79** (1981) 1.

[135] N. Arkani-Hamed, A. G. Cohen and H. Georgi, Phys. Rev. Lett. **86** (2001) 4757 [arXiv:hep-th/0104005]; C. T. Hill, S. Pokorski and J. Wang, Phys. Rev. D **64** (2001) 105005 [arXiv:hep-th/0104035].

[136] W. Buchmuller, R. Ruckl and D. Wyler, Phys. Lett. B **191** (1987) 442 [Erratum-ibid. B **448** (1999) 320].

[137] F. del Aguila, G. D. Coughlan and M. Quiros, Nucl. Phys. B **307** (1988) 633 [Erratum-ibid. B **312** (1989) 751]; B. Holdom, Phys. Lett. B **259** (1991) 329; F. del Aguila, M. Masip and M. Perez-Victoria, Nucl. Phys. B **456** (1995) 531 [arXiv:hep-ph/9507455].

[138] K. Agashe, G. Perez and A. Soni, Phys. Rev. D **71** (2005) 016002 [arXiv:hep-ph/0408134].

[139] L. S. Durkin and P. Langacker, Phys. Lett. B **166** (1986) 436; F. del Aguila, J. M. Moreno and M. Quiros, Phys. Rev. D **40** (1989) 2481; M. C. Gonzalez-Garcia and J. W. F. Valle, Phys. Lett. B **236** (1990) 360; F. del Aguila, J. M. Moreno and M. Quiros, Phys. Lett. B **254** (1991) 497; M. C. Gonzalez-Garcia and J. W. F. Valle, Nucl. Phys. B **345** (1990) 312; F. del Aguila, J. M. Moreno and M. Quiros, Nucl. Phys. B **361** (1991) 45; F. del Aguila, W. Hollik, J. M. Moreno and M. Quiros, Nucl. Phys. B **372** (1992) 3; P. Langacker and M. x. Luo, Phys. Rev. D **45** (1992) 278; J. Erler and P. Langacker, Phys. Lett. B **456**

(1999) 68 [arXiv:hep-ph/9903476]; J. Erler and P. Langacker, Phys. Rev. Lett. **84** (2000) 212 [arXiv:hep-ph/9910315].

[140] E. Salvioni, G. Villadoro and F. Zwirner, JHEP **0911** (2009) 068 [arXiv:0909.1320 [hep-ph]].

[141] E. Salvioni, A. Strumia, G. Villadoro and F. Zwirner, arXiv:0911.1450 [hep-ph].

[142] F. Del Aguila, M. Cvetic and P. Langacker, Phys. Rev. D **52** (1995) 37 [arXiv:hep-ph/9501390]; A. Leike, Phys. Rept. **317** (1999) 143 [arXiv:hep-ph/9805494]; M. S. Carena, A. Daleo, B. A. Dobrescu and T. M. P. Tait, Phys. Rev. D **70** (2004) 093009 [arXiv:hep-ph/0408098]; For the Particle Data Group review see M.-C. Chen and B.A. Dobrescu in [18].

[143] F. del Aguila, M. Quiros and F. Zwirner, Nucl. Phys. B **287** (1987) 419. K. S. Babu, C. F. Kolda and J. March-Russell, Phys. Rev. D **54** (1996) 4635 [arXiv:hep-ph/9603212].

[144] J. Erler, P. Langacker, S. Munir and E. R. Pena, JHEP **0908** (2009) 017 [arXiv:0906.2435 [hep-ph]].

[145] F. del Aguila, M. Quiros and F. Zwirner, Nucl. Phys. B **284** (1987) 530.

[146] V. Bernard, M. Oertel, E. Passemar and J. Stern, Phys. Lett. B **638** (2006) 480 [arXiv:hep-ph/0603202].

[147] F. del Aguila, G. A. Blair, M. Daniel and G. G. Ross, Nucl. Phys. B **283** (1987) 50.

[148] A. Djouadi, G. Moreau and F. Richard, Nucl. Phys. B **773** (2007) 43 [arXiv:hep-ph/0610173].

[149] F. del Aguila, M. Perez-Victoria and J. Santiago, Phys. Lett. B **492** (2000) 98 [arXiv:hep-ph/0007160].

[150] K. Agashe, R. Contino, L. Da Rold and A. Pomarol, Phys. Lett. B **641** (2006) 62 [arXiv:hep-ph/0605341].

[151] M. S. Carena, E. Ponton, J. Santiago and C. E. M. Wagner, Nucl. Phys. B **759** (2006) 202 [arXiv:hep-ph/0607106].

[152] E. L. Berger, Q. H. Cao and I. Low, Phys. Rev. D **80** (2009) 074020 [arXiv:0907.2191 [hep-ph]].

[153] M. E. Peskin and J. D. Wells, Phys. Rev. D **64** (2001) 093003 [arXiv:hep-ph/0101342].

[154] M. S. Chanowitz, arXiv:0806.0890 [hep-ph].

[155] F. del Aguila and J. A. Aguilar-Saavedra, JHEP **0711** (2007) 072 [arXiv:0705.4117 [hep-ph]]; F. del Aguila, J. A. Aguilar-Saavedra, M. Moretti, F. Piccinini, R. Pittau and M. Treccani, Phys. Lett. B **685** (2010) 302 [arXiv:0912.3799 [hep-ph]].

[156] S. Godfrey and T. A. W. Martin, Phys. Rev. Lett. **101** (2008) 151803 [arXiv:0807.1080 [hep-ph]].

[157] T. Aaltonen *et al.* [CDF Collaboration], Phys. Rev. Lett. **102** (2009) 091805 [arXiv:0811.0053 [hep-ex]].

[158] R. Diener, S. Godfrey and T. A. W. Martin, arXiv:0910.1334 [hep-ph]; P. Langacker, arXiv:0911.4294 [hep-ph].

[159] S. N. Gninenko, M. M. Kirsanov, N. V. Krasnikov and V. A. Matveev, Atom. Nucl. **70** (2007) 441; F. del Aguila, J. A. Aguilar-Saavedra and J. de Blas, Acta Phys. Polon. B **40** (2009) 2901 [arXiv:0910.2720 [hep-ph]].

[160] T. Aaltonen *et al.* [CDF Collaboration], Phys. Rev. Lett. **103** (2009) 041801 [arXiv:0902.3276 [hep-ex]]; V. M. Abazov *et al.* [D0 Collaboration], Phys. Rev. Lett. **100** (2008) 031804 [arXiv:0710.2966 [hep-ex]].

[161] G. Aad *et al.* [The ATLAS Collaboration], arXiv:0901.0512 [hep-ex].

[162] T. Aaltonen *et al.* [CDF Collaboration], Phys. Rev. D **79** (2009) 112002 [arXiv:0812.4036 [hep-ex]].

[163] G. Weiglein *et al.* [LHC/LC Study Group], Phys. Rept. **426** (2006) 47 [arXiv:hep-ph/0410364].

[164] J. L. Hewett and S. Pakvasa, Phys. Rev. D **37** (1988) 3165; O. J. P. Eboli and A. V. Olinto, Phys. Rev. D **38** (1988) 3461; A. Dobado, M. J. Herrero and C. Munoz, Phys. Lett. **207B** (1988) 97; V. D. Barger, K. Hagiwara, T. Han and D. Zeppenfeld, Phys. Lett. B **220** (1989) 464; M. De Montigny and L. Marleau, Phys. Rev. D **40** (1989) 2869 [Erratum-ibid. D **56** (1997) 3156].

[165] D. E. Acosta *et al.* [CDF Collaboration], Phys. Rev. D **72** (2005) 051107 [arXiv:hep-ex/0506074]; V. M. Abazov *et al.* [D0 Collaboration], Phys. Rev. D **71** (2005) 071104 [arXiv:hep-ex/0412029]; A. Abulencia *et al.* [CDF Collaboration], Phys. Rev. D **73** (2006) 051102 [arXiv:hep-ex/0512055]; V. M. Abazov *et al.* [D0 Collaboration], Phys. Lett. B **636** (2006) 183 [arXiv:hep-ex/0601047].

[166] S. Chekanov *et al.* [ZEUS Collaboration], Phys. Rev. D **68** (2003) 052004 [arXiv:hep-ex/0304008].

[167] M. C. Gonzalez-Garcia and M. Maltoni, Phys. Rept. **460** (2008) 1 [arXiv:0704.1800 [hep-ph]].

[168] For monographs see: R. N. Mohapatra and P. B. Pal, World Sci. Lect. Notes Phys. **60** (1998) 1 [World Sci. Lect. Notes Phys. **72** (2004) 1]; M. Fukugita and T. Yanagida, Physics of neutrinos and applications to astrophysics (Springer-Verlag, Heidelberg, 2003), 593 pp; G. C. Branco, L. Lavoura and J. P. Silva, Int. Ser. Monogr. Phys. **103** (1999) 1.

[169] F. del Aguila, J. Syska and M. Zralek, Phys. Rev. D **76** (2007) 013007 [arXiv:hep-ph/0702182].

[170] J. W. F. Valle, Phys. Lett. B **199** (1987) 432; M. C. Gonzalez-Garcia *et al.*, Phys. Rev. Lett. **82** (1999) 3202 [arXiv:hep-ph/9809531]; S. Bergmann, Y. Grossman and E. Nardi, Phys. Rev. D **60** (1999) 093008 [arXiv:hep-ph/9903517]; N. Fornengo, M. Maltoni, R. Tomas and J. W. F. Valle, Phys. Rev. D **65** (2002) 013010 [arXiv:hep-ph/0108043]; M. Blennow, T. Ohlsson and W. Winter, Eur. Phys. J. C **49** (2007) 1023 [arXiv:hep-ph/0508175]; J. Kopp, M. Lindner, T. Ota and J. Sato, Phys. Rev. D **77** (2008) 013007 [arXiv:0708.0152 [hep-ph]].

[171] U. Seljak, A. Slosar and P. McDonald, JCAP **0610** (2006) 014 [arXiv:astro-ph/0604335]; see also A. Osipowicz *et al.* [KATRIN Collaboration], arXiv:hep-ex/0109033.

[172] S. Antusch, C. Biggio, E. Fernandez-Martinez, M. B. Gavela and J. Lopez-Pavon, JHEP **0610** (2006) 084 [arXiv:hep-ph/0607020].

[173] M. B. Gavela, D. Hernandez, T. Ota and W. Winter, Phys. Rev. D **79** (2009) 013007 [arXiv:0809.3451 [hep-ph]].

[174] C. Biggio, M. Blennow and E. Fernandez-Martinez, JHEP **0908** (2009) 090 [arXiv:0907.0097 [hep-ph]].

[175] F. del Aguila, S. Bar-Shalom, A. Soni and J. Wudka, Phys. Lett. B **670** (2009) 399 [arXiv:0806.0876 [hep-ph]].

[176] W. Fetscher, Phys. Lett. B **140** (1984) 117.

[177] R. Abela, G. Backenstoss, W. Kunold, L. m. Simons and R. Metzner, Nucl. Phys. A **395** (1983) 413.

[178] S. R. Mishra *et al.*, Phys. Lett. B **252** (1990) 170.

[179] A. Aguilar *et al.* [LSND Collaboration], Phys. Rev. D **64** (2001) 112007 [arXiv:hep-ex/0104049].

[180] T. Abe *et al.* [ISS Detector Working Group], JINST **4** (2009) T05001 [arXiv:0712.4129 [physics.ins-det]]; for a recent review on muon factories see D. M. Kaplan, arXiv:0910.3154 [physics.acc-ph].

[181] A. Aparici, K. Kim, A. Santamaria and J. Wudka, Phys. Rev. D **80** (2009) 013010 [arXiv:0904.3244 [hep-ph]].

[182] P. Langacker and D. London, Phys. Rev. D **39** (1989) 266.

[183] W. Fetscher, H. J. Gerber and K. F. Johnson, Phys. Lett. B **173** (1986) 102; C. A. Gagliardi, R. E. Tribble and N. J. Williams, Phys. Rev. D **72** (2005) 073002 [arXiv:hep-ph/0509069].

[184] G. Prezeau and A. Kurylov, Phys. Rev. Lett. **95** (2005) 101802 [arXiv:hep-ph/0409193].

[185] E. Ma, Phys. Rev. Lett. **86** (2001) 2502 [arXiv:hep-ph/0011121].

[186] See also T. Ohlsson, T. Schwetz and H. Zhang, arXiv:0909.0455 [hep-ph].

[187] F. Boehm *et al.*, Phys. Rev. D **64** (2001) 112001 [arXiv:hep-ex/0107009].

[188] M. Apollonio *et al.* [CHOOZ Collaboration], Eur. Phys. J. C **27** (2003) 331 [arXiv:hep-ex/0301017].

[189] S. Abe *et al.* [KamLAND Collaboration], Phys. Rev. Lett. **100** (2008) 221803 [arXiv:0801.4589 [hep-ex]].

[190] B. Aharmim *et al.* [SNO Collaboration], Phys. Rev. C **72** (2005) 055502 [arXiv:nucl-ex/0502021].

[191] C. Arpesella *et al.* [Borexino Collaboration], Phys. Lett. B **658** (2008) 101 [arXiv:0708.2251 [astro-ph]].

[192] Y. Ashie *et al.* [Super-Kamiokande Collaboration], Phys. Rev. D **71** (2005) 112005 [arXiv:hep-ex/0501064].

[193] M. H. Ahn *et al.* [K2K Collaboration], Phys. Rev. D **74** (2006) 072003 [arXiv:hep-ex/0606032].

[194] D. G. Michael *et al.* [MINOS Collaboration], Phys. Rev. Lett. **97** (2006) 191801 [arXiv:hep-ex/0607088].

[195] E. Eskut *et al.* [CHORUS Collaboration], Nucl. Phys. B **793** (2008) 326 [arXiv:0710.3361 [hep-ex]].

[196] P. Astier *et al.* [NOMAD Collaboration], Nucl. Phys. B **611** (2001) 3 [arXiv:hep-ex/0106102].

[197] A. A. Aguilar-Arevalo *et al.* [The MiniBooNE Collaboration], Phys. Rev. Lett. **98** (2007) 231801 [arXiv:0704.1500 [hep-ex]].

[198] B. Armbruster *et al.* [KARMEN Collaboration], Phys. Rev. D **65** (2002) 112001 [arXiv:hep-ex/0203021].

[199] F. del Aguila and J. A. Aguilar-Saavedra, Nucl. Phys. B **813** (2009) 22 [arXiv:0808.2468 [hep-ph]]; see also K. Huitu, J. Maalampi, A. Pietila and M. Raidal, Nucl. Phys. B **487** (1997) 27 [arXiv:hep-ph/9606311]; J. F. Gunion, C. Loomis and K. T. Pitts, *In the Proceedings of 1996 DPF / DPB Summer Study on New Directions for High-Energy Physics (Snowmass 96), Snowmass, Colorado, 25 Jun - 12 Jul 1996, pp LTH096* [arXiv:hep-ph/9610237]; A. G. Akeroyd and M. Aoki, Phys. Rev. D **72** (2005) 035011 [arXiv:hep-ph/0506176]; A. Hektor, M. Kadastik, M. Muntel, M. Raidal and L. Rebane, Nucl. Phys. B **787** (2007) 198 [arXiv:0705.1495 [hep-ph]]; P. Fileviez Perez, T. Han, G. Y. Huang, T. Li and K. Wang, Phys. Rev. D **78** (2008) 071301 [arXiv:0803.3450 [hep-ph]]; P. Fileviez Perez, T. Han, G. y. Huang, T. Li and K. Wang, Phys. Rev. D **78** (2008) 015018 [arXiv:0805.3536 [hep-ph]].

[200] T. Aaltonen *et al.* [CDF Collaboration], Phys. Rev. Lett. **102** (2009) 041801 [arXiv:0809.4903 [hep-ex]], and references there in.

[201] F. del Aguila and L. Ametller, Phys. Lett. B **261** (1991) 326.

[202] H. Baer, C. h. Chen, F. Paige and X. Tata, Phys. Rev. D **49** (1994) 3283 [arXiv:hep-ph/9311248]; H. Baer, B. W. Harris and M. H. Reno, Phys. Rev. D **57** (1998) 5871 [arXiv:hep-ph/9712315].

[203] Yu. M. Andreev, S. I. Bityukov and N. V. Krasnikov, Phys. Atom. Nucl. **68** (2005) 340 [Yad. Fiz. **68** (2005) 366] [arXiv:hep-ph/0402229]; see for a review F. del Aguila *et al.*, Eur. Phys. J. C **57** (2008) 183 [arXiv:0801.1800 [hep-ph]].

[204] A. B. Arbuzov *et al.*, Comput. Phys. Commun. **174** (2006) 728 [arXiv:hep-ph/0507146].

[205] J. Erler and M. J. Ramsey-Musolf, Phys. Rev. D **72** (2005) 073003 [arXiv:hep-ph/0409169].

[206] W. J. Marciano and A. Sirlin, Phys. Rev. D **22** (1980) 2695 [Erratum-ibid. D **31** (1985) 213].

[207] A. Czarnecki and W. J. Marciano, Phys. Rev. D **53** (1996) 1066 [arXiv:hep-ph/9507420]; A. Czarnecki and W. J. Marciano, Int. J. Mod. Phys. A **15** (2000) 2365 [arXiv:hep-ph/0003049].

[208] W. J. Marciano and A. Sirlin, Phys. Rev. D **27** (1983) 552; W. J. Marciano and A. Sirlin, Phys. Rev. D **29** (1984) 75 [Erratum-ibid. D **31** (1985) 213]; J. Erler, A. Kurylov and M. J. Ramsey-Musolf, Phys. Rev. D **68** (2003) 016006 [arXiv:hep-ph/0302149].

[209] S. Sarantakos, A. Sirlin and W. J. Marciano, Nucl. Phys. B **217** (1983) 84.

[210] S. Jadach, W. Placzek and B. F. L. Ward, Phys. Lett. B **390** (1997) 298 [arXiv:hep-ph/9608412].

[211] F. James and M. Roos, Comput. Phys. Commun. **10** (1975) 343.

[212] G. Cowan, *Oxford, UK: Clarendon (1998) 197 p.*

[213] G. Abbiendi *et al.* [OPAL Collaboration], Eur. Phys. J. C **33** (2004) 173 [arXiv:hep-ex/0309053].

[214] H. Flacher, M. Goebel, J. Haller, A. Hocker, K. Moenig and J. Stelzer, Eur. Phys. J. C **60** (2009) 543 [arXiv:0811.0009 [hep-ph]].

[215] J. Erler, Phys. Rev. D **63** (2001) 071301 [arXiv:hep-ph/0010153].